Charles University in Prague
Faculty of Science

Study programme: Organic chemistry

Mgr. Jan Nekvinda

Carborane structural blocks in medicinal chemistry
Karboranové strukturní bloky v medicinální chemii

Doctoral Thesis

Supervisor: RNDr. Bohumír Grüner, CSc.

Prague 2018

ACKNOWLEDGMENTS

This work was supported by Grant Agency of the Academy of Sciences of the Czech Republic, Project No.: 15-05677S and 16-01618s, and by the Research Plan RVO 61388980 awarded by the Academy of Sciences of the Czech Republic and in part by research projects DAAD 57316638 and National Science Centre, Poland, Grant No. 2014/14/E/ST5/00577.

PRONOUNCEMENT

I thereby declare that this thesis was written independently and under supervising by Dr. Bohumír Grüner. I cited all used information sources and literature. This Thesis or its any part was not introduced to claim another or same academic title.

In Prague 21st June 2018 ….……..

Jan Nekvinda

PERSONAL ACKNOWLEDGMENTS

First of all, I would like to express my gratitude to my supervisor Dr. Bohumír Grüner for his patience and kindness during my PhD study. Big thank belongs also to all my colleagues from Department of Synthesis, especially to Michael G. S. Londesborough, Ph.D. and Jiří Dolanský, not only for the creating a good lab environment, but also for solving everyday struggles.

Furthermore, I would like to thank to Prof. Detlef Gabel, Ph.D. for his guidance during my internship in his group at Jacobs University. Also, many thanks belong to Khaleel Assaf, Ph.D. for DFT calculations and help with NMR titrations and UV-Vis measurments.

Next, my thanks go to Prof. Agnieszka B. Olejniczak, Ph.D. who led me during my internship at the Institute of Medical Biology of the Polish Academy of Sciences in Lodz.

I would like to acknowledge also Prof. Aleš Růžička, Ph.D. from University in Pardubice and Dr. Ivana Císařová from Charles University for their X-ray measurements, Pavlína Řezáčová, Ph.D. and Jiří Brynda, Ph.D. from IOCB for *in vitro* tests, enzyme crystallography and their kind cooperation, to Marián Hajdůch, Ph.D. and his group at IMTM at Palacký University in Olomouc for *in vitro*, *in vivo*, ADME and pharmacokinetic tests.

Finally, I am glad to thank my family for supporting me during my final stage of my studies. To my friends, who made time off work fun and last, but not least, to my love Aneta, simply for everything.

ABSTRACT

This work deals with carborane and metallacarborane clusters, in terms of their fundamental chemistry and complexation with cyclodextrins, and in the context of emerging pharmacophores applicable in medicinal chemistry.

The most important part of this work is the preparation of cobalt bis(dicarbollide) sulfamide derivatives. The sulfamido group is attached to the metallacarborane carbon vertex by an alkyl chain that may be modified in its length. This was accomplished by, firstly, the abstraction of the acidic hydrogen, located on the {CH}-vertex from the metallacarborane, by reaction with lithium base, followed by, secondly, reaction with electrophilic agents (paraformaldehyde, oxirane and oxetane), which leads to a cascade of reactions to give the desired sulfamide derivatives. These compounds were then tested by collaborators in other institutes for *in vitro* and *in vivo* activity towards Carbonic Anhydrase IX (CA IX), which is an enzyme associated with tumour growth. *In vivo* tests on mice have shown that these types of substances are able to effectively reduce tumour size by 30%. The synthetic research continued with the preparation of sulfonamide compounds of the isomers of the carborane series. The reactions began exclusively with propylhydroxy carborane starting materials, which provide optimum linker length, and have then been converted to the corresponding sulfonamides by a 4-step transformation cascade. These compounds were then tested *in vitro* to confirm their low nanomolar CA IX inhibitory activity and excellent selectivity.

The work here also details the preparation of new types of DNA intercalators and marker molecules. This type of molecule is based on a combination of amino metallacarborane clusters with 1,8-naphthalic anhydride. The resulting metallacarborane naphthalimides are entirely new types of biologically active compounds, and their biological studies are currently underway in Poland.

The chemistry of carborane cluster compounds was then extended by a new method to the direct alkylation of the cluster boron vertices on the open face of *nido*-tricarbollides. In addition to the skeletal alkylcarbonation reactions and the complexation of the *nido*-tricarbollides with cyclopentadienes, a third method to derivatize this type of cluster compounds, which could be useful in the preparation of further inhibitors, was developed.

The last topic of this work is the study of the complexation of carborane acids with cyclodextrins. Using several methods, the binding constants of these carborane acids with cyclodextrins were determined.

ABSTRAKT

Tato práce se zabývá karboranovými a metalakarboranovými klastry jako vhodnými molekulami pro medicinální chemii, základní chemií karboranových klastrů a v neposlední řadě jejich komplexaci do cyklodextrinů.

Nejdůležitější část této práce je příprava sulfamidových derivátů kobalt bis(dikarbolidu). Sulfamidová skupina je připojena k metalakarboranovému uhlíku pomocí různě dlouhého alkylového řetězce. Tohoto bylo dosaženo abstrakcí kyselého vodíku z metalakarboranu působením lithné báze a následnou reakcí s elktrofilními činidly (paraformaldehyd, oxiran a oxetan). Kaskádou organických reakcí jsme docílili požadovaného sulfamidu. Tyto látky byly pak testovány na spolupracujících pracovištích *in vitro* a *in vivo* na aktivitu vůči enzymu Karbonická Anhydrasa IX (CA IX), který je spjatý s růstem tumoru. *In vivo* testy na myších ukázali, že tento typ látek je schopen efektivně snížit velikost tumoru v krátkém čase až o 30%. Tento výzkum pak pokračoval přípravou sulfonamidových látek odvozených z izomerní série karboranů. Ta spočívala v identické první reakci jako v předchozím případě až na jeden rozdíl, kdy byl použit výhradně oxetan jako elektrofil. Tím se docílilo přípravy propylhydroxy karboranů, které pak byly další kaskádou organických transformací převedeny na příslušné sulfonamidy. Tyto látky byly pak testovány *in vitro*, kde potvrdili velice dobrou inhibiční aktivitu a selektivitu vůči CA IX.

Dále tato práce také zahrnuje přípravu nového typu DNA interkalátorů a značících molekul. Tento typ molekul je založen na kombinaci amino karboranových klastrů s 1,8-naftal anhydridem. Vznikající metalakarboranový naftalimid je tak zcela novým typem biologicky aktivních látek. Biologické studie této problematiky jsou aktuálně kompletovány na pracovišti v Polsku, kde byla tato problematika vypracována.

Chemie klastrových látek byla pak rozšířena o novou metodu umožňující přímou alkylaci borových vrcholů na otevřené straně v *nido*-trikarbolidech. Kromě skeletálních alkylkarbonilacčních reakcí a komplexace *nido*-trikarbolidů s cyklopentadieny tak existuje třetí metoda, jak derivatizovat tento typ klastrů, což by mohlo být užitečné v přípravě dalších inhibitorů.

Poslední téma, jímž se zabývá tato práce, je studium komplexace karboranových kyselin do cyklodextrinů. Pomocí několika metod byly stanoveny vazebné konstanty těchto kyselin v cyklodextrinech.

KEY WORDS

carboranes, metallacarboranes, tricarbollides, carbonic anhydrase, DNA intercalators, cyclodextrins, synthesis

KLÍČOVÁ SLOVA

karborany, metalakarborany, trikarbolidy, karbonická anhydrasa, DNA interkalátory, cyklodextriny, syntéza

CONTENT

LIST OF PUBLICATIONS

Nekvinda, J.; Švehla, J.; Císařová, I.; Grüner, B.; **Chemistry of cobalt bis(1,2-dicarbollide) ion; the synthesis of carbon substituted alkylamino derivatives from hydroxyalkyl derivatives via methylsulfonyl or p-toluenesulfonyl esters.** *J. Organomet. Chem.* **2015**, *798/1*, 112-120.

Bakardjiev, M.; Holub, J.; Tok, O.; Štíbr, B.; Hnyk, D.; Nekvinda, J.; Růžička, A.; Růžičková, Z.; **Open-face alkylation of the 8-R-*nido*-7,8,9-$C_3B_8H_{11}$ tricarbollides.** *J. Organomet. Chem.* **2016**, 822, 80-84.

Nekvinda, J.; Grüner, B.; Gabel, D.; Nau, W. M.; Assaf, K. I. **Host-Guest Chemistry of Carboranes: Synthesis of Carboxylate Derivatives and Their Binding to Cyclodextrins**, *Chem. Eur. J.* **2018***,* doi:10.1002/chem.201802134

Nekvinda, J.; Różycka, D.; Rykowski, S.; Wyszko, E.; Gurda, D.; Orlicka-Płocka, M.; Wojcieszak, J.; Bachorz, R.; Grüner, B.; Olejniczak, A. B. **Naphthalimide derivatives modified with boron clusters and their biological propierties**, *In preparation*.

Grüner, B.; Šícha, V.; Nekvinda, J.; Pospíšilová, K.; Fábry, M.; Pachl, P.; Král, V.; Kugler, M.; Das, V.; Mašek, V.; Michalová, M.; Nová, A.; Lišková, B.; Gurská, S.; Džubák, P.; Štěpánková, J.; Brynda, J.; Hajdůch, M.; Řezáčová, P. **Metallacarborane sulfamides as unconventional, specific, and highly selective inhibitors of Carbonic Anhydrase IX,** *MS prepared for submission to PNAS.*

Holub, J.; Šícha, V.; Nekvinda, J.; Cígler, P.; Pospíšilová, K.; Fábry, M.; Pachl, P.; Král, V.; Štěpánková, J.; Hajdůch, M.; Brynda, J.; Grüner, B.; Řezáčová, P.; **Sulfonamido carboranes, highly selective inhibitors of cancer specific carbonic Anhydrase IX,** *MS in final stages of preparation.*

Nekvinda, J.; Holub, J.; Růžička, A.; Brynda, J.; Řezáčová, P.; Grüner, B.; **Direct intruduction of alkylsulfonamido group on C-sites of three isomeric carboranes; the influence of stereochemistry on inhibitory activity against cancer-associated Carbonic Anhydrase IX isoenzyme**. *In preparation.*

Fojt, L; Fojta, M.; Grüner, B.; Nekvinda, J.; Šícha, V.; Vespalec R. **Electrochemistry of icosahedral metal bis(dicarbollide) ions and some of their carbon and boron substituted derivatives in aqueous phosphate buffers**. *MS prepared for submission to Anal Chem in June 2018.*

"An expert is a person who has made all the mistakes that can be made in a very narrow field."

– Niels Bohr

PREFACE

This thesis is concerned with carborane structural blocks in medicinal chemistry, and has been developed at the Institute of Inorganic Chemistry of the Czech Academy of Sciences at the Department of Synthesis. This department belongs to a group of well-established and well-recognised international teams in the field of carborane and metallacarborane chemistries. One leading focus of the department is the development of borane/carborane-based biologically active compounds. I started my contribution to this subject in 2012 as an undergraduate student and I have continued here for my postgraduate study to extend my abilities and knowledge in organic and medicinal chemistry as well as carborane chemistry.

In Chapter One – Introduction, the basic properties of carboranes and metallacarboranes are reviewed as well as their applicability in medicinal chemistry. This account is, however, concise and brief and the carboranes and metallacarboranes were discussed previously in my Diploma Thesis[1] at greater length and detail. Instead, more focus is placed on another type of carborane cluster – the tricarbollides. In particular, an emphasis has been given to their chemical versatility and the scope for their functionalisation. Following the carboranes, the Chapter pays attention to the enzyme carbonic anhydrase, whose cancer associated isoform IX is indeed the major focus in this thesis. The Introduction provides an up-to-date assessment of carbonic anhydrase inhibition, describes its mechanism of action, trends, and surveys the latest results on combining carboranes with the inhibition of this enzyme. The Chapter then continues with a summary on DNA intercalators, which alongside CA IX inhibition. 1,8-naphthalimide is one such intercalator and is discussed more thoroughly. Finally, the basic properties of cyclodextrins and their combination with carboranes and metallacarboranes are discussed.

In Chapter Two – Results and Discussion, new experimental information and insights are applied to the problems discussed in Chapter One. The main thrust is dedicated to a preparation of novel carborane and metallacarborane inhibitors of carbonic anhydrase IX and their biological tests. It should be noted here that, for a better understanding, the Lexicon of biological terms is included at the end of this thesis. The preparation of novel DNA intercalators based on the naphthalimide moiety combined with metallacarboranes is presented. A new study on the facile alkylation of tricarbollides is included. Last, a new study on the behaviour between carborane acid derivatives and cyclodextrins in water solution is described.

The Thesis ends with Chapter Three, the Conclusion, in addition to a number of Appendices containing full experimental details and literature references.

CHAPTER ONE

INTRODUCTION

1.1 CARBORANES

1.1.1. ICOSAHEDRAL CARBORANES AND METALLACARBORANES

Dicarba dodecahydro dodecaboranes or *closo*-dicarbadodecaboranes(12) usually referred to more simply as carboranes are twelve vertex cage molecules of three-dimensional icosahedral geometry constructed of ten boron-hydrogen and two carbon-hydrogen vertices. We distinguish between three different isomers of carboranes, namely *ortho*- (1,2-$C_2B_{10}H_{12}$) (**1o**), *meta*-(1,7-$C_2B_{10}H_{12}$) (**1m**) and *para*-carboranes (1,12-$C_2B_{10}H_{12}$) (**1p**) as they differ in the respective positions of their two carbon vertices (Figure 1).[2]

These molecules are chemically and thermally stable. *Ortho*-carborane is thermally stable up to 300°C. Heating of **1o** between 400°C and 500°C leads to isomerization to give *meta*-carborane **1m**. Further isomerization occurs when **1m** is heated to temperatures over 600°C, which results in *para*-carborane **1p**.[2] Treatment of **1o** by some strong nucleophiles such as alkoxides or fluoride ions results in the removal of one of symmetrically equivalent boron vertices B(3 or 6).[3] This reaction produces the dicarbollide *nido* $C_2B_9H_{12}^{1-}$ systematically named 7,8-dicarba-*nido*-undecaborate(12)(1-) (**2**) ion, which after *in situ* deprotonation behaves as a η^5 coordinating ligand. Thus, these ligands are capable of sandwiching a central metal atom to form another important type of compound – the icosahedral metallacarborane ions. The central metal atom in these molecules are most commonly cobalt, iron, nickel or chromium.[4] The systematic nomenclature for these univalent anionic species with 3D aromaticity is quite complex: 3,3′-*commo*-bis[closo-1,2-undecahydro-dicarba-3-metalladodecaborate(11)](1-) ions (current IUPAC nomenclature recommendations. The nomenclature for asymmetrically substituted ions is even more complicated. Thus, the common name, cobalt bis(dicarbollide), has been ascribed as a generic designation along with fully abbreviated term COSAN, derived from CObalt Sandwich ANnion) (**3**) that are frequently used in the literature.[2] Concordantly, these names are used throughout this thesis.

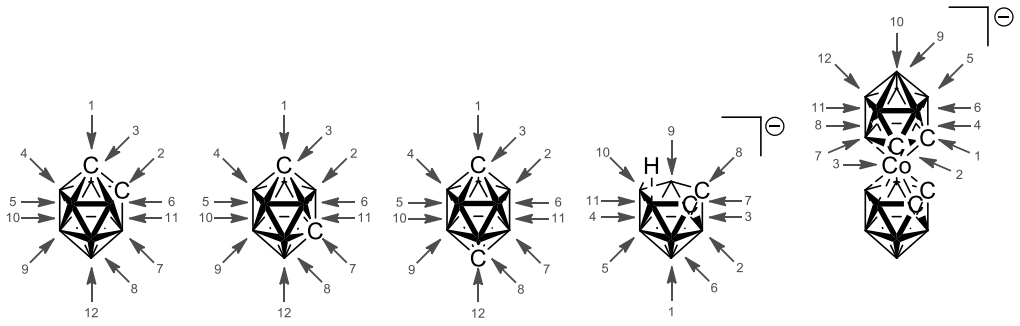

Figure 1 *All three carborane isomers (**1o,m,p**), dicarbollide ligand (**2**) and metallacarborane COSAN (**3**) where all hydrogen atoms have been omitted and unlabelled vertices represent boron atoms.*

Salts of these ions are hydrophobic solids due to a partial polarization of B-H bonds causing a hydridic character to the hydrogen atoms. On the contrary, the partial positive charge on the C-H hydrogen atoms allows to abstract these hydrogen atoms with organolithium bases, which is a method developed at the Institute of Inorganic Chemistry of the CAS[5–7] and used in recent years for the substitution of the carbon sites in COSAN with various organic residues. This lithiation reaction step thus enables the preparation of designed molecules with unique chemical properties[6,8–10] and forms the basic approach to many of the syntheses covered in this Thesis.

1.1.2. USE OF BORON CAGE COMPOUNDS IN MEDICINE

From the standpoint of structural and substitution chemistry, the variety of known structural types featured in the boranes, heteroboranes and metallaboranes (polyhedral and quasi-aromatic cluster molecules) represents an interesting counterpart to organic compounds, especially to aromatic rings.[2,11,12] Previously, the sole focus of boron-containing compounds in medicine was the use of ^{10}B-isotope labelled cage compounds as carriers of boron in Boron Neutron Capture Therapy (BNCT).[13–17] During the last two decades, however, boron cages have been intensively exploited as pharmacologically relevant species. In particular, the icosahedral carboranes have been successfully incorporated into structures of a number of biologically active compounds. The three isomers of the 12-vertex carborane, **1o,m,p** , and, to a lesser extent, the 11-vertex *nido*-[7,8-$C_2B_9H_{12}$]$^-$ (**2**) anion, have found applications as newly emerging types of three-dimensional pharmacophores. These carborane species not only act as hydrophobic space-filling fragments, but are also able to increase the interaction energy, *in vivo* stability, and bioavailability of the biologically active compounds. [2,18–22]

Despite the successful exploitation of icosahedral carboranes as hydrophobic pharmacophores in drug design, relatively little attention has been directed to other chemically and thermally stable boron cluster compounds *i.e.* icosahedral boranes, smaller carboranes and metallacarboranes.[23,24] Such species offer variety in terms of molecular size, geometry, dipole moment and charge density over the cluster surface area. Indeed, although currently rare, there are examples of biological activity for such species; for instance the cytostatic effect of smaller metallacarboranes.[25] Cobalt bis(dicarbollides) have been shown to serve as potent and specific inhibitors of the HIV protease.[26,27] Studies on the cytotoxicity, antiviral properties against a

panel of DNA and RNA viruses, penetration through artificial lipid bilayers and cellular membranes, of cobalt bis(dicarbollide) have also been published.[16] Recently, the antifungal and antibacterial activity of the cobalt bis(dicarbollide) ion bearing particular substitutions has also been demonstrated.[28,29]

1.1.3. TRICARBOLLIDES

Tricarbollides (or less preferentially tricarbaboranes), belong to the carborane family of molecules; the known examples being composed of seven or eight boron-hydrogen and three carbon-hydrogen vertices to form ten or eleven vertex polyhedral cages. The empirical chemical formula of the latter class of neutral 11-vertex tricarbollide species is *nido*-$C_3B_8H_{12}$, whereas systematic nomenclature is 7,8,9-tricarba-*nido*-undecaborate(12) Their chemistry demonstrates all properties of the dicarbollides mentioned above and therefore undergo facile alkylation[30] or, upon deprotonation also complexation reactions.[31–33] Indeed, the acidic bridging hydrogen atoms (that participate in B-H-B three-centre/two-electron bonding) in the tricarbollides are readily removed by base to form their respective anions. As presented on the next pages, tricarbollides are versatile compounds with wide range of utilization.

Tricarbollides are usually prepared by the insertion of one carbon atom into the structure of 10-vertex open-cage dicarbaborate anions such as Na[1,10-*arachno*-$C_2B_8H_{13}$].[34] Previously, a polar ^{t}Bu-isonitrile was typically used for carbon insertion followed by the cleavage of the ^{t}Bu group from the resulting N-^{t}Bu by $AlCl_3$.[35] In 2011 a simpler and more convenient synthesis of the carbon-substituted eleven vertex *nido*-tricarbollides was developed[36] that involved the insertion of the C-R (R = alkyl, cycle, aromatic) vertex into *in situ* deprotonated *arachno*-6,9-$C_2B_8H_{14}$ (**4**) *via* the acyl chloride -C=OCl group, which results in an effective cross-coupling between R and the tricarbollide cage.

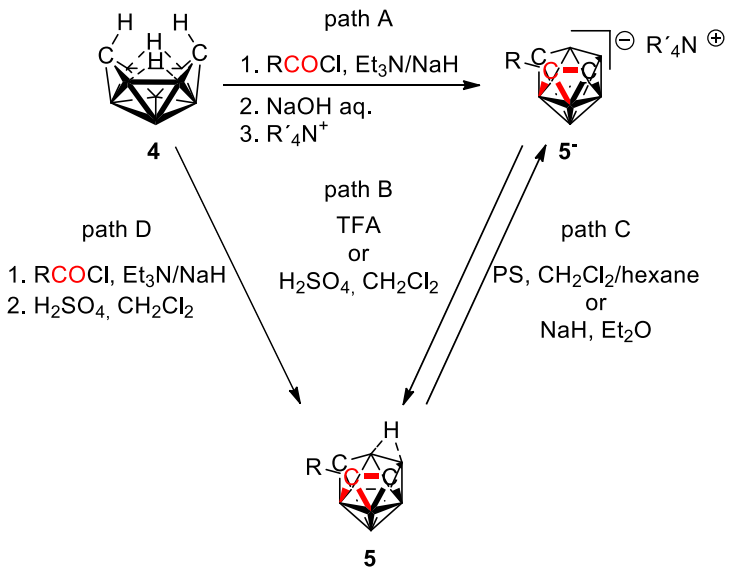

Scheme 1 *Synthetic pathways for alkylated tricarollides* ***5***$^{-}$ *and* ***5****.*

Scheme 1 shows a reaction involving the *arachno*-6,9-$C_2B_8H_{14}$ (**4**) dicarbaborane,[37] two equivalents of Et_3N (*in situ* generator of **4** and HCl scavenger), NaH (H_2O scavenger), and acyl chlorides RCOCl (R = Me, Ph and Naph), followed by treatment with aqueous NaOH, and precipitation with R'_4NCl (R´=Me or Et) that lead to the isolation of a series of monoanionic [8-R-*nido*-7,8,9-$C_3B_8H_{10}$]$^{-}$ compounds (**5**$^{-}$) (R = Me, Ph, Naph), which were isolated in yields of up to 85% (Path A). The skeletal alkylcarbonation (SAC) reactions are consistent with a regiospecific net insertion of the three-electron carbine RC≡ unit into the *endo*-skeletal site of **4** under elimination of three extra hydrogen atoms as H_2O and HCl. The anion **5**$^{-}$ can be protonated by treatment with concentrated H_2SO_4 (or TFA) (Path B). This reaction proceeds quantitatively and generates product **5** with a bridging hydrogen atom between B10 and B11. Deprotonation of this neutral product **5** with PS or NaH (Path C) simply leads back to the anionic compound **5**$^{-}$. Alternatively, compound **5** is available directly through pathway D in Scheme 1 by careful treatment with concentrated H_2SO_4 in CH_2Cl_2 while cooling, followed by filtration of the CH_2Cl_2 layer through a silica-gel pad, and removal of the solvent by evaporation.

Due to the presence of the pentagonal open face and single negative charge, the known 11-vertex *nido*-tricarbollide anions [*nido*-7,8,9-$C_3B_8H_{11}$]$^{-}$(**6a**) and [*nido*-7,8,10-$C_3B_8H_{11}$]$^{-}$(**6b**) along with their hypothetical congener [*nido*-2,8,10-$C_3B_8H_{11}$]$^{-}$(**6c**) (Figure 2) can be considered as close analogues of the Cp-anion, which can be used to prepare tricarbollide complexes analogous to metallocenes.[38,39]

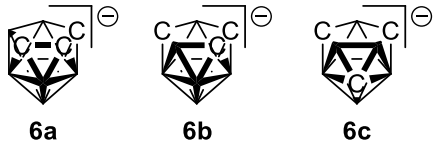

Figure 2 *Three tricarbollide anion isomers **6a-c**.*

The synthetic pathways for three isomeric $Cp^*FeC_3B_8H_{11}$ compounds, **7a-c**, and their rearrangements were published in 2005 (Scheme 2).[31] The photochemical reaction of **6a** with $[Cp^*Fe(C_5H_5)]^+$ in CH_2Cl_2 at room temperature gives red complex **7a** in good 60% yield. **7a** then undergoes cluster rearrangement in refluxing toluene to give the isomeric dark red compound **7b** (71% yield) and further rearrangement in refluxing mesitylene results in orange isomer **7c** (96%).

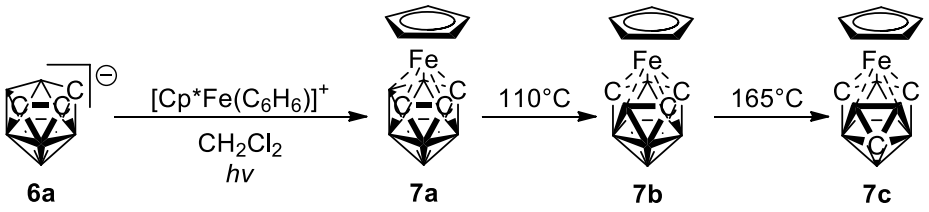

Scheme 2 *Complexation between nido anion **6a** and iron complex leads to a sandwich compound **7a** which isomerises by heating into **7b** and further into **7c**.*

Another interesting phenomenon was observed for the zwitterionic compound 7-RR´NH-7,8,9-$C_3B_8H_{10}$ (R, R´= H, H; H, ^{t}Bu; Me, Me; Me, ^{t}Bu). This compound exhibits tautomerism (rare in the chemistry of boron clusters). The tautomerisation equilibrium is in all cases mediated by a common anion.[40] In Scheme 3 are shown tautomeric conversions between all species (**8**$^-$, **8N** and **8Z**). Dissolution of the zwitterionic compound (**8Z**) in proton nontransferring (PNT) solvents ($CHCl_3$, CH_2Cl_2, benzene etc.) surprisingly leads to quantitative tautomeric conversion to **8N** with no sign of equilibrium between **8Z** and **8N** (step 1). The reverse reaction is also quantitative where is **8N** crystallized from proton transferring (PT) solvents (such as EtOH/H_2O, acetone/H_2O) (step 2). The anion **8**$^-$ could be obtained from both **8Z** and **8N** by treating those molecules with NaH in Et_2O or with PS in CH_2Cl_2/hexane (step 3). On the other hand, acidification (HCl, TFA) of the sodium salt of **8**$^-$ in PT solvents generates **8Z** (step 4), while treating PS^+ salts of **6**$^-$ with H_2SO_4 in PNT leads exclusively to tautomers **8N** (step 5).

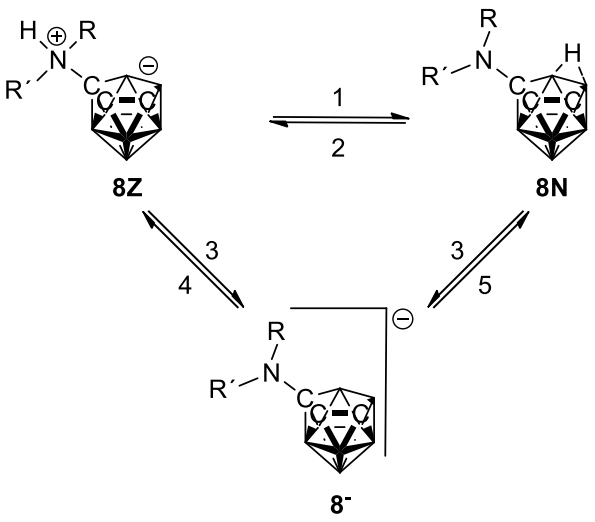

Scheme 3 *Reaction scheme showing tautomerism between anionic* ***8***$^{-}$*, zwitterionic* ***8Z*** *and neutral* ***8N*** *compounds.*

1.2 CARBONIC ANHYDRASE

Carbonic anhydrases (CAs) are zinc metalloenzymes found in all animals and photosynthetizing organisms as well as in some nonphotosynthetic bacteria. The CAs family could be divided into three main, evolutionary unrelated, lines. These are often referred to as α-, β- and γ-CA.[41] All known CAs from the animal kingdom are of the α-type.

1.2.1 IMPORTANCE AND MECHANISM OF ACTION

CAs catalyse the reversible hydration of carbon dioxide to bicarbonate and a proton (Scheme 4).

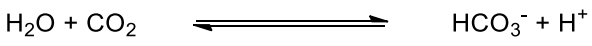

Scheme 4 *Reversible hydration by zinc-containing CA enzyme.*

The mechanism of action is proposed to be centred around the interaction of the metallic zinc ion of the enzyme, which was found by X-ray crystallography measurements to be at the bottom of a 15 Å deep active-site cleft and is coordinated by three histidine residues (His94, His96 and His119) and a water molecule/hydroxide ion. (Scheme 5).[42–48]

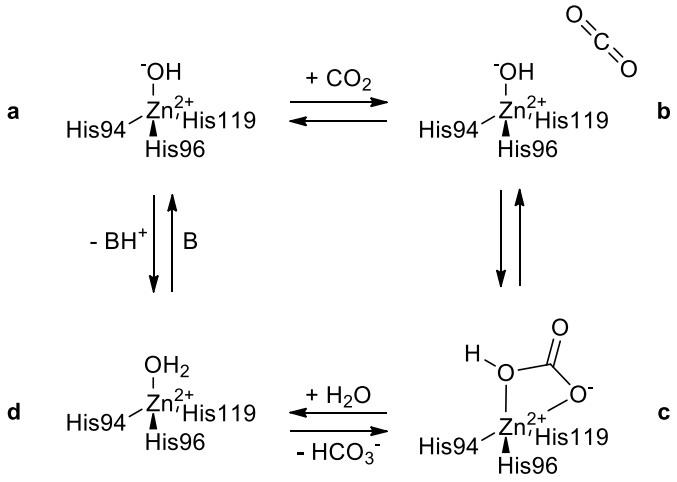

Scheme 5 *The active form of the enzyme requires basic conditions, with a hydroxide bound to* Zn^{2+} ***(a)****. This strong nucleophile then attacks the* CO_2 *molecule incorporated within a hydrophobic pocket in close proximity* ***(b)****, leading to the formation of a bicarbonate ion coordinated to* Zn^{2+} ***(c)****. The bicarbonate ion is then displaced by a water molecule and liberated into solution, leading to the acid form of the enzyme, with water coordinated to* Zn^{2+} ***(d)****, which is catalytically inactive.*[49]

This equilibrium is essential for many physiological processes. including respiration and transportation of CO_2 and bicarbonate between metabolizing tissues and the lungs; pH and CO_2 homeostasis; electrolyte secretion in various tissues and organs; biosynthetic reactions (such as gluconeogenesis, lipogenesis and ureagenesis); bone resorption; calcification; and tumourigenicity.[15,22–25]

1.2.2 Carbonic Anhydrase Inhibitors

Many of the CA isozymes involved in the biological processes mentioned above have been validated as important therapeutic targets, their effective inhibition used to treat a range of disorders including glaucoma, obesity, cancer, epilepsy and osteoporosis.[49] Two main classes of CA inhibitors (CAIs) are known: metal-complexing anions and unsubstituted sulfonamides and their bioisosteres – for example, sulfamates and sulfamides compounds **9-14** (Figure 4). These inhibitors bind to the Zn^{2+} ion of the enzyme either by substituting the non-protein zinc ligand to generate a tetrahedral adduct or by addition to the metal coordination sphere to generate a trigonal-bipyramidal species (Figure 3).[44–48] At least 25 clinically used drugs have been reported to possess significant CA inhibitory properties, in addition to many other derivatives belonging to the sulfonamide, sulfamate or sulfamide families.[21–31]

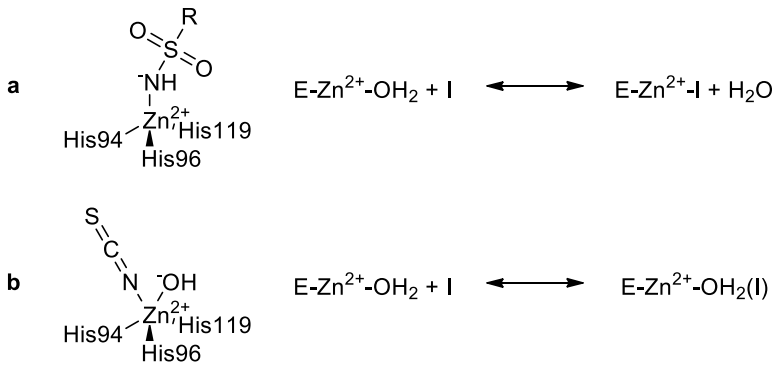

Figure 3 *Mechanism of inhibition of CA.* ***a)*** *Unsubstituted sulfonamides and their bioesters bind to the Zn^{2+} ion of the enzyme by substituting the non-protein zinc ligand to generate a tetrahedral adduct;* ***b)*** *Anionic inhibitors add to the metal coordination sphere, generating trigonal bipyramidal species.*

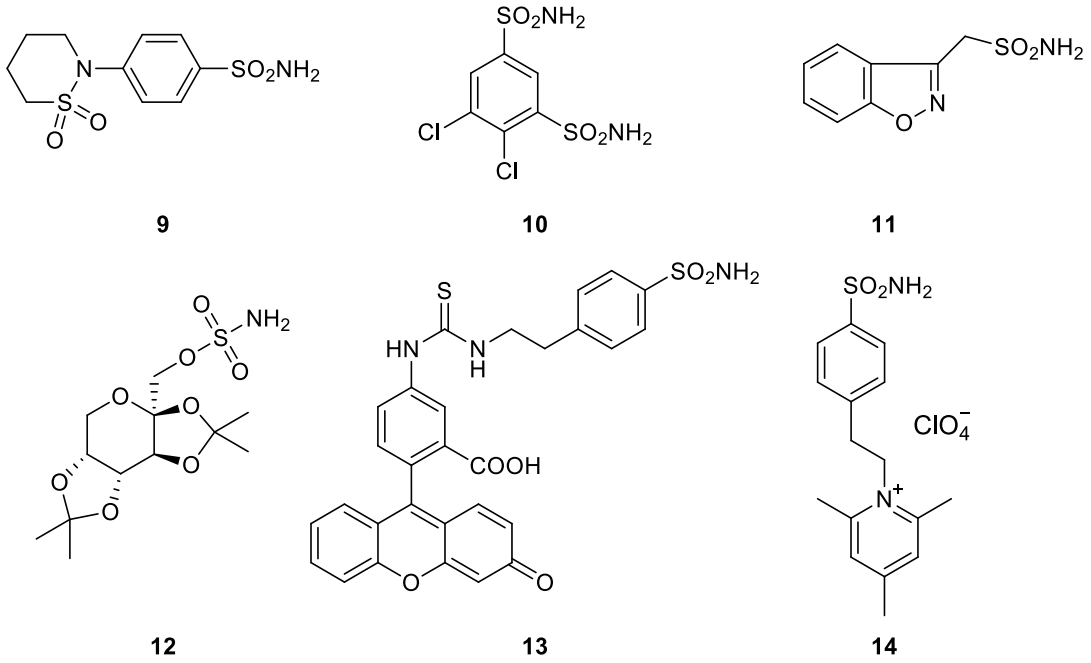

Figure 4 *Typical structures of organic CA inhibitors* ***9-14****.*

Many of these compounds were initially developed years ago, during the search for diuretics.[46,54] However, some of these enzyme inhibitors were found also to be useful for the systemic treatment of glaucoma, and more recently, some derivatives have been discovered that have the potential as anticancer, antiobesity or antiinflammatory drugs.[22–32] The inhibitory effects of some of these clinically used drugs (**9-14**) against the mammalian isoforms CA II and CA IX of human or mouse origin are shown in Table 1. It is noteworthy here that several CA isoforms, such as CA II, VII, IX, show low nanomolar affinities towards inhibitors containing sulfonamide and sulfamate groups. There are a number of crucial problems in the design of CAIs. These include (*i*) the high number of CA isoforms, (*ii*) their diffuse localization in many

tissues and organs (Table 1), and (*iii*) the lack of selectivity of traditional inhibitors towards individual isoforms.

Table 1 *Isozymes of CA and their localization in cell tissue alongside their inhibitory constants K_i measured for compounds* ***9-14***.

subcellular localization	cytosol	membrane-bound	transmembrane	cytosol
tissue/organ localization	erythrocytes, eye, GI tract, kidney	brain, lung, pancreas	tumours, GI mucosa	kidney, brain, lung, reproductive tract
***K_i* [nM]**	**Isozyme**			
	hCA II‡	**hCA IV‡**	**hCA VII‡**	**hCA IX***
9	9	95	6	43
10	38	15000	26	50
11	35	8590	117	5.1
12	10	4900	0.9	58
13	45	650	18	24
14	21	60	15	14

‡ Full-length enzyme; * Catalytic domain; h, human.

In recent years, significant progress in the design of CA-selective and isozyme-specific CAIs has been made. Owing to the extracellular location of some CA isozymes, such as CA IV and IX (Table 1), it is possible to design membrane-impairment CAIs that specifically inhibit membrane-associated CAs without interacting with the cytosolic or mitochondrial isoforms. This possibility has been explored through the design of positively charged sulfonamides that generally incorporate pyridinium moieties, of which compound **14** is a representative example (Figure 4). Such sulfonamide inhibitors showed nanomolar affinities for CA II as well as CA IV and CA IX, and, more importantly, they were unable to cross the plasma membranes *in vivo*. This new class of potent, positively charged CAIs, was able to discriminate between the membrane-bound and the cytosolic isozymes, selectively inhibiting only CA IV, in two model systems.[55–57]

1.2.3 TRANSMEMBRANE ISOZYME CA IX ASSOCIATED WITH SOLID TUMOURS

A key feature of many tumours is hypoxia,[58–60] primarily a pathophysiological consequence of structurally and functionally disturbed microcirculation and deteriorated oxygen diffusion processes. CA IX appears to be strongly associated with tumour propagation, malignant progression, and resistance to chemotherapy and radiotherapy.[58–61] Hypoxia regulates the expression of several genes, including a CA IX, through the hypoxia inducible factor 1 (HIF1) cascade.[58–63] The expression of CA IX is strongly upregulated by hypoxia and is downregulated by the wild-type von Hippel-Lindau tumour suppressor protein (VHL). CA IX expression is strongly increased in many types of tumours, such as gliomas/ependymomas,[58] mesotheliomas,[58] papillary/follicular carcinomas,[58] carcinomas of the bladder,[64] uterine cervix,[65] head and neck,[66] breast,[67] lungs,[68] brain,[58] vulva,[58] squamous/basal cell carcinomas[58] and kidney[69] tumours. In some cancer cells, the VHL gene is mutated leading to the strong upregulation of CA IX (up to 150-fold) as a consequence of constitutive HIF activation.[58,61,67]

CA IX belongs to the highly active human α-CAs. Its catalytic properties for the CO_2 hydration reaction being comparable with those of the highly-evolved catalyst CA II.[58,61] As for all α-CAs, CA IX is susceptible to inhibition by anions and sulfonamides and sulfamates,[47,48,53,61,70–72] with the inhibitors coordinating directly to the zinc ion within the active-site cavity and participating in various other favourable interactions with amino-acid residues that are situated in the hydrophobic and hydrophilic halves of the active site. Studies of such inhibitory compounds also evidenced that they are membrane impermeable (and thus specifically inhibit CA IX *in vivo*)[73,74] or act as dual CA IX–COX2 (cyclooxygenase 2) inhibitors.[70,74] Both heterocyclic[75] and aromatic sulfonamides,[76] as well as aliphatic sulfonamides/sulfamates/sulfamides[77,78] possessing low nanomolar inhibitory activity against CA IX have been detected so far. Some sulfonamides incorporating various sugar moieties were also reported,[79] but up until now the most useful CAIs for understanding the function of this protein *in vivo* were the fluorescent compounds (such as **13**).[71,75,80]

A further approach for selectively inhibiting the tumour-associated isoforms CA IX (and XII) present in hypoxic tumour tissues envisaged bioreductive prodrugs that are activated by hypoxia. The chosen strategy was to use the disulfide bond as a bioreducible function. The reducing conditions present in hypoxic tumours, in combination with the presence of the redox protein thioredoxin 1, mediates the reduction of the disulfide bond with the formation of thiols. The reduced compounds (thiols) are less bulky and show excellent CA inhibitory activity (in the low nanomolar range) compared with the corresponding sterically hindered disulfides, which have difficulty entering the limited space of the enzyme active site.[81,82]

As described previously, hypoxia, through the HIF cascade, leads to a strong overexpression of CA IX in many tumours. The overall consequence of this is a pH imbalance, with most hypoxic tumours having acidic pH values around 6, in contrast to normal tissue, which has characteristic pH values around 7.4.[71,72,80] Constitutive expression of human CA IX was recently shown to decrease extracellular pH (pH_e) in Madin-Darby canine kidney epithelial cells. CA IX-selective sulfonamide inhibitors (of type **13** and **14**) reduced the medium acidity by inhibiting the catalytic activity of the enzyme, and thus the generation of H^+ ions, binding specifically only to hypoxic cells expressing CA IX. Deletion of the CA active site was also shown to reduce the acidity of the medium, but a sulfonamide inhibitor did not bind to the active site of such mutant proteins. Therefore, tumour cells decrease their pH_e both by production of lactic acid (due to the high glycolysis rates), and by CO_2 hydration catalysed by the tumour-associated CA IX, possessing an extracellular catalytic domain.[61,71,80] Low pH_e has been associated with tumourigenic transformation, chromosomal rearrangements, extracellular matrix breakdown, migration and invasion, induction of the expression of cell growth factors and protease activation. CA IX probably also plays a role in providing bicarbonate to be used as a substrate for cell growth, as it is established that bicarbonate is required in the synthesis of pyrimidine nucleotides.[58,61,80]

Indisulam (compound **11**), a sulfonamide derivative (originally called E7070) with powerful anticancer activity, was recently shown to act as a nanomolar inhibitor of CA IX (Table 1). Indisulam showed *in vivo* efficacy against human tumour xenografts in nude mice, exhibiting a significant anticancer effect and progressing to Phase I and II clinical trials for the treatment of solid tumours.[83,84] Among other interesting potent inhibitors so far are compounds **13** and **14**. Compound **13** is a fluorescent sulfonamide that binds only to CA IX under hypoxic conditions *in vivo*.[71,72,80] Thus, this compound can be used as a fluorescent probe in hypoxic tumour imaging. Compound **14** belongs to a class of positively charged, membrane-impermeable compounds. Therefore, as such compounds do not inhibit intracellular CAs, they may exhibit fewer side effects as compared with the presently available compounds, which indiscriminately inhibit all CAs.[85,86] The positively charged pyridinium derivative **14** favourably binds within the enzyme active site, coordinating with the deprotonated sulfonamide moiety to the catalytically critical Zn^{2+} ion. Therefore, such structures can be used in the rational drug design of more selective and potent isozyme IX inhibitors. Currently, a single-crystal X-ray diffraction structure of CA IX is available, although there is no structure of CA IX with inhibitor due to difficulties in crystallization. Most crystallographic studies have therefore used inhibitor complex structures with the cytosolic CA II isoform. More recently, an artificial CA

IX-mimic was introduced successfully as an alternative to crystallographic studies.[87] The CA-IX-mimic enzyme has an active site analogous to CA IX thanks to site directed mutagenesis of CA II and thus behaves as CA II, which tends to crystallize very well. The structures are further used for computational modelling studies and in the design of CA IX inhibitors.

In summary, biochemical, physiological and pharmacological data indicate that inhibition of the tumour-associated CA IX may be useful in the treatment of hypoxic tumours that do not respond to classical chemotherapy or radiotherapy, possibly in combination therapy with other cytostatics. Therefore, the use of the CAIs described above provide possibilities of developing both diagnostic tools for the non-invasive imaging of these tumours, as well as therapeutic agents that probably perturb the extratumoural acidification pathways in which CA IX is involved.[58,61,71,80] Many types of highly effective *in vitro* CA IX inhibitors have been developed and evaluated *in vitro*.[71,75,77,80,83–86]

1.2.4 CAIs BASED ON CARBORANES

Although the conical active-site clefts of different human CA isozymes are conserved, variations exist in the amino acid residues at the entrance to the active site. As a result of their differing in shape and hydrophobicity, these surface pockets can be exploited to design specific inhibitors.[88] Carboranes (as defined and described in Section 1.1 of this Thesis) are bulky pharmacophores used to replace various hydrophobic structures in biologically active molecules.[89,90] The 12-vertex carboranes are an abiotic species that are very stable towards catabolism and degradation by enzymes, there is an increasing use of boron clusters as components of new pharmacological agents.[19,26,91]

Most of the currently used CAIs lack selectivity, and their use causes numerous unwanted side effects. Results published by our team in 2013[92] suggest that carborane-based compounds are promising lead structures for the development of inhibitors of CA isozymes. Pilot experiments presented in this paper showed that various types of hydrophobic carborane clusters could be accommodated in the CA active site and that substitution with an appropriately attached sulfamide group leads to compounds with activity in low micromolar range and moderate selectivity for the tumour-associated CA IX isozyme over the more ubiquitous CA II isozyme. It was also confirmed by crystal structures of enzyme-inhibitor complexes that carborane inhibitors bind to the Zn^{2+} atom in the active site by the sulfamide group and the carborane cage occupies the adjacent hydrophobic pocket. The structural studies provided information that could be further applied to the structure-based rational design of specific CA IX inhibitors.

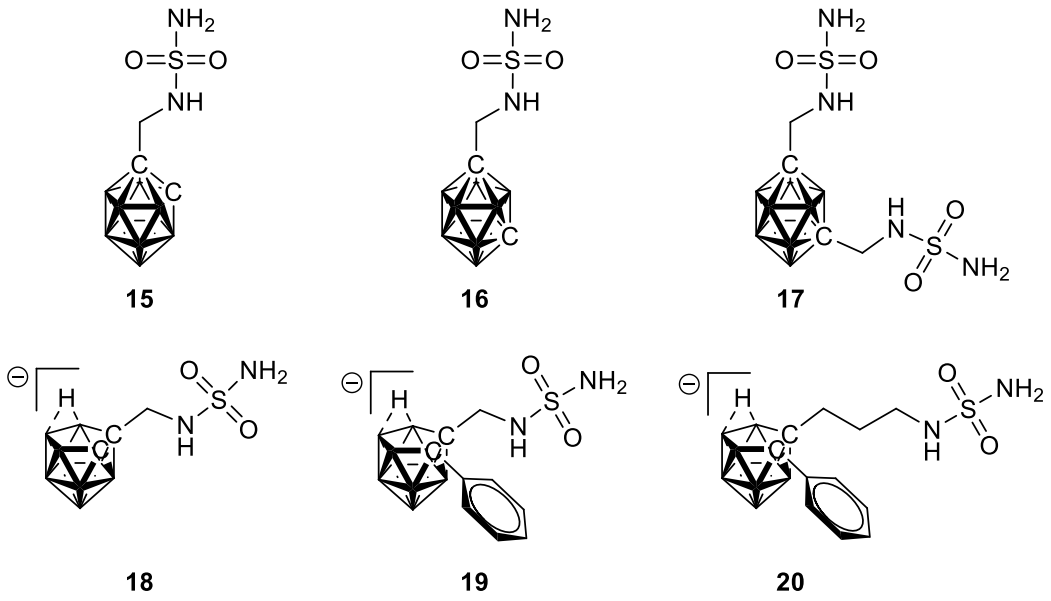

Figure 5 *Chosen carborane CAIs.*

For the initial series, the optimal length of the linker between the sulfamide group and carborane cluster was assumed to be one methylene group, which followed from the comparisons with the structures of isoquinoline sulfonamide inhibitors.[93] Nevertheless, it corresponded to limitations of the synthetic tools available at that time. Data for compounds **15-20** (Figure 5) are summarised in the Table 2.[92] This pilot series showed promising micromolar activity and selectivity between two isozymes CA II and CA IX and also indicated that a longer linker and an introduction of more sterically demanding fragments might lead to improvements.

Table 2 *Selectivity index between CA II and CA IX with their inhibitory constants for compounds* ***15-20****.*

compound	CA II K_i [μM]	CA IX K_i [μM]	selectivity index‣
15	0.70	0.38	1.8
16	1.16	1.12	1.0
17	0.38	0.23	1.7
18	6.79	5.09	1.3
19	9.00	2.32	3.9
20	2.71	0.15	18.1

‣ ratio between CA II a CA IX

Several crystal structures of CA II in complex with carboranes have been published. The sulfamide moiety in the structurally most simple derivative **15** proved to be the anchoring group that completes the coordination sphere of Zn^{2+} in the active site and makes the polar interactions with Thr199 that are typical of other CAIs.[94] An additional polar interaction is a hydrogen bond between a linker NH group and the side chain Oγ of Thr200 (Figure 6a). Further interactions of the inhibitor with the active site cavity are mediated through van der Waals interactions between the carborane cluster and amino acid residues Gln92, His94, Phe131, Leu198, and Thr200. Compound **15** fills the proximal active site cavity of CA II, but some side pockets at the entrance of the active site could potentially be targeted by cluster substituents (Figure 6b).[92]

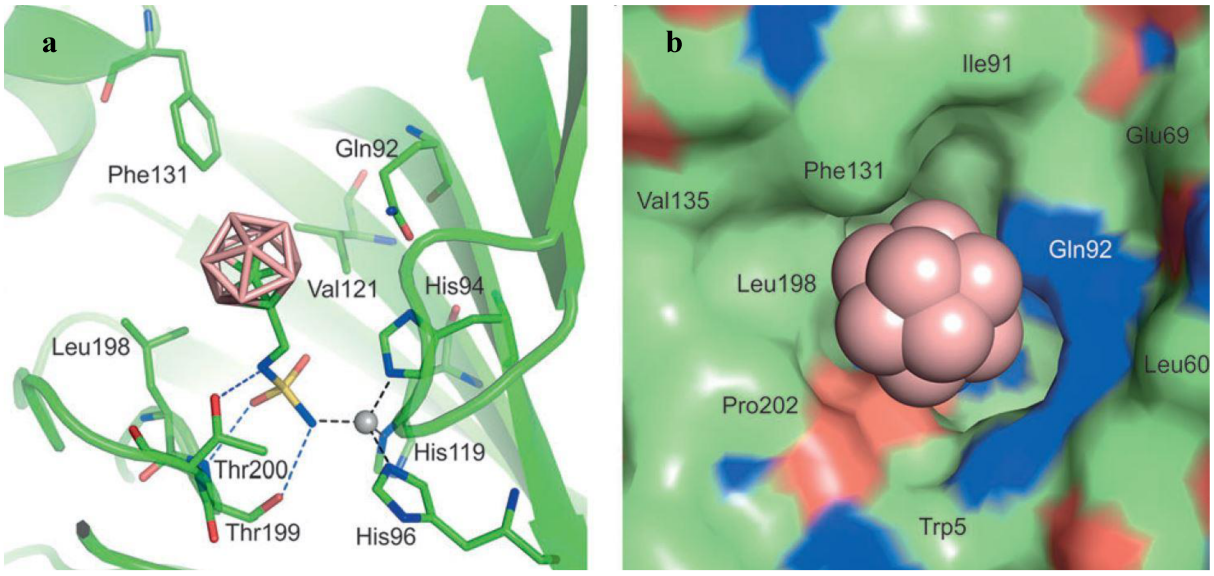

Figure 6 *Crystal structure of CA II in complex with* ***15****.* ***a)*** *The protein is shown as a ribbon diagram; residues involved in interactions with the* Zn^{2+} *ion (gray sphere) and* ***15*** *are shown*

as stick representations. C green, B pink, S yellow, O red, and N blue atoms are shown. Polar interactions are represented by blue dashed lines; Zn^{2+} ion coordination is shown as black dashed lines. ***b)*** *Top view into the active site, shown as a surface representation.* ***15*** *is shown as a space filling model.*

1.3 DNA INTERCALATORS

Deoxyribonucleic acid (DNA) binders are molecules that can interact with DNA in several possible ways; *i.* external binding, *ii.* groove binding, and *iii.* intercalation.[95] Particular interest is often paid to DNA binders with stronger modes of binding, increased regioselectivity and greater specificity.[96] Intercalation is a phenomenon whereby molecules, especially aromatic chromophores, of appropriate size and chemical nature are inserted in between two adjacent planar base pairs of DNA. This phenomenon was first described by Lerman in 1961.[97] Usually, these agents are characterized by the presence of a tri- or tetracyclic annulated planar and aromatic ring, capable of inserting in between nucleic acid bases.[98] Moreover, these molecules have one or two flexible amino side chains for promoting DNA affinity through electrostatic or hydrophobic interactions[99] *via* electron-deficient planar chromophores with flexible side chains.[100] This complex formation is usually non-covalent and reversible, involving van der Waals forces with the base pairs. The binding of intercalators induces unwinding, lengthening and stiffening of the double helix, thus introducing structural changes, which affect both condensation of chromatin and interaction of DNA with associated enzymes.[101] These specially designed groups could also confer DNA sequence selectivity and allow aromatic heterocycles to position at appropriate sites or interact with topoisomerases so as to interfere with DNA replication and transcription.[102] DNA topoisomerase II regulates DNA topology during replication, transcription, recombination and reparation and chromosome segregation. This enzyme catalyses a DNA breakage-reunion reaction coupled to a strand passage event. Mammalian topoisomerase II is recognized as the primary cellular target of several drugs such as anthracyclines, acridness and antitumour.[103] These drugs interfere with the breakage-reunion activity of the enzyme by freezing a covalent intermediate of the enzymatic reaction, thus resulting in the enhancement of DNA cleavage. Thus, the intercalation studies of appropriate molecules can lead to the rational design and development of molecules having anticancer activity. The structural basis as well as intercalation studies of various types of molecules like daunorubicin (**21**),[104] berberine (**22**)[105] and phenanthrene (**23**)[106] derivatives have been explored and are well-documented in literature (Figure 7).

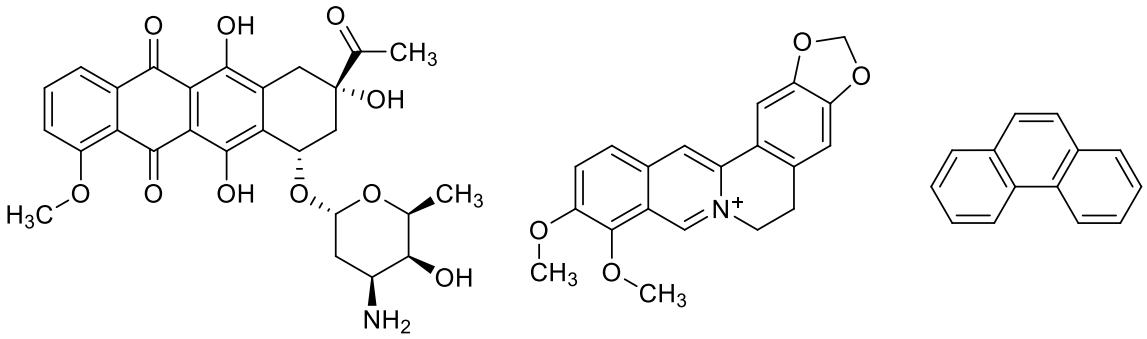

21 **22** **23**

Figure 7 *DNA intercalators **21-23** used in medicinal applications.*

1.3.1. 1,8-NAPHTHALIMIDE

Naphthalimides (**24**) are a class of polycyclic imides consisting of π-deficient flat aromatic or heteroaromatic ring systems (Figure 8). These are generally characterized by the presence of a planar tri- or tetracyclic aromatic chromophore and one or two flexible basic side chains. Most of the naphthalimide derivatives are fluorescent in their nature and possess many biological activities like anticancer activity against murine and human tumour cells,[107] antiviral,[108] analgesic,[109] and local anaesthetics.[110] 1,8-Naphthalimides are a category of substances exhibiting high anticancer activities based on an effective intercalation into DNA and other effects such as apoptosis induction.[111] Naphthalimide was first recognized as intercalating cytotoxic agent in the early 1980's and since then many derivatives has been evaluated for antitumour activity, with two examples of this class of compound (mitonafide **25** and amonafide **26**) entering clinical trials.[112] As the first compound reaching the clinical trial stage, amonafide showed very good anticancer activity,[99,112] but its CNS neurotoxicity and hematotoxicity limited its further applications.[99,112–114] It has been proved that linker arms containing at least one amino group and 1,8-naphthalimide moiety with at least one 3-nitro group are beneficial to enhance cytotoxic activity in the naphthalimide series.[115,116] Since then, significant numbers of efforts have been spent to synthesize novel naphthalimide derivatives as anticancer agents.

Braña *et al.* reported a series of biologically active naphthalimide derivatives that showed substantial cytotoxic activity against HeLa and KB cell lines. Compounds **27** and **28** exhibit enhanced cytotoxic activity that is 0.5-1.0 μM compared to compound **25** (Figure 8). SAR studies showed the increase in the basicity of the terminal nitrogen is the most important structural factor regarding the cytotoxic activity of these derivatives.[115,116]

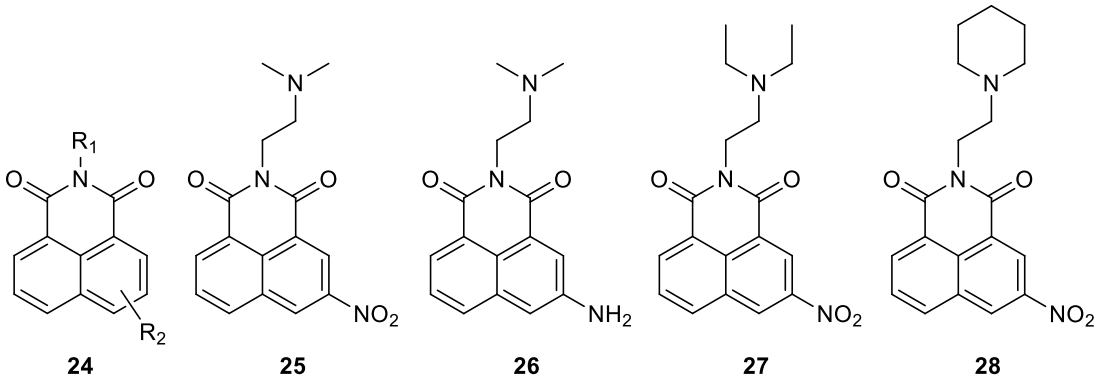

Figure 8 *Naphthalimide DNA intercalators **24-28**.*

1.3.2. MODIFICATION OF 1,8-NAPHTHALIMIDE

Johnson and co-workers studied the effect of substitution on the intercalation behaviour of 3-substituted naphthalimide derivatives (**25**, **26**, **29-32**; Figure 9) with different DNA and RNA.[117]

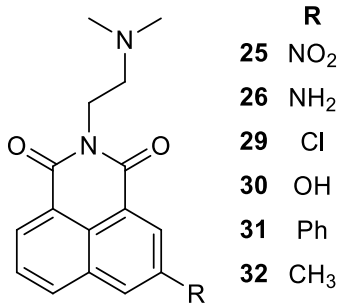

Figure 9 *Graphical representation of different DNA intercalators.*

It was revealed that the substituents on the naphthalimide backbone had remarkable effects on its anticancer activity, DNA binding properties, and spectroscopic chracteristics.[99,112–114] Generally, naphthalimide derivatives modified at the 3-position have typical absorption bands within the range of 300 to 430 nm, and fluorescent emission bands ranging from 390 to 550 nm, limiting their application as imaging agents because of auto-fluorescence and light scattering in biological environments.[113] In contrast, naphthalimide derivatives modified at the 4-position showed very good spectroscopic properties with absorption bands in 350 – 550 nm and emission bands within 490 –700 nm, which provided potential application in fluorescence sensing (Figure 10)[118] and imaging.[119] However, the binding interactions between naphthalimide derivatives and DNA molecules usually causes the quenching of any fluorescence, which impedes their applications in biological imaging.[120,121]

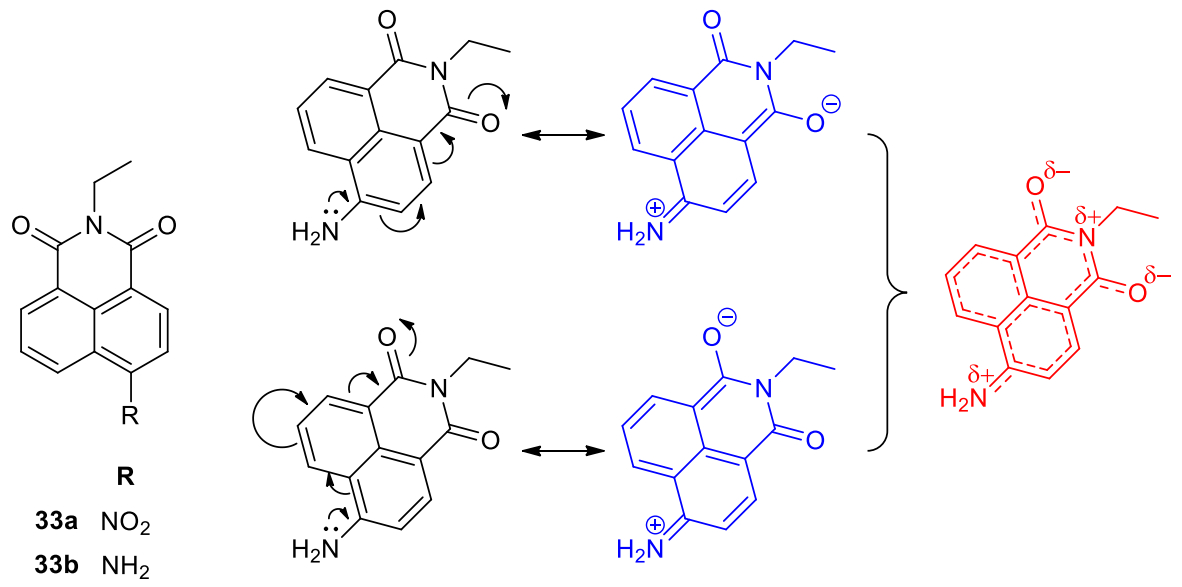

Figure 10 *4-Nitro-, **33a**, and 4-amino-1,8-naphthalimide **33b**, structures, and schematic representation of the internal charge transfer excited state within the 4-amino-1,8-naphthalimide fluorophore caused by a 'push–pull' action.*

The average change in the melting temperature of DNA in the presence of naphthalimide derivatives containing electron withdrawing groups (**25** and **29**) was found to be 6.5°C whereas it was 4.8°C in case of electron releasing substituents (**26**, **30-32**). The stabilization of a higher melting temperature of DNA in the presence of nitro substituted naphthalimide (**25**), as compared to methyl substitution (**32**), could also be attributed to the co-planarity of the nitro group with the aromatic ring system, which further facilitates a stacking interaction between individual molecules.

1.4 CYCLODEXTRINS

Cyclodextrins (CDs) are natural cyclic oligosaccharides that were discovered more than 100 years ago,[122] but only recently became available as pharmaceutical excipients. They are composed from (α-1,4)-linked α-D-glucopyranose units. These natural products are formed during bacterial degradation of starch and contain lipophilic inner cavity and a hydrophilic outer surface. The natural α-, β- and γ-cyclodextrin consist of six, seven, and eight glucopyranose units, respectively. Due to the chair conformation of the glucopyranose units, the cyclodextrins are shaped like a truncated cone rather than perfect cylinders. The hydroxyl functions are orientated to the cone exterior with the primary hydroxyl groups of the sugar residues at the narrow edge of the cone and the secondary hydroxyl groups at the wider edge (Figure 11). The central cavity is lined by the skeletal carbon atoms and ethereal oxygen atoms of the glucose

residues, which gives it a lipophilic character. The aqueous solubility of natural cyclodextrins is much lower than that of comparable acyclic saccharides. This is thought to be due to relatively strong intermolecular hydrogen bonding in the crystal state.[123] The low solubility of β-cyclodextrin, when compared to α- and γ-cyclodextrins presents a puzzle. It appears that the stronger crystal structure (i.e. relatively high crystal lattice energy[124]), due to better placed intramolecular hydrogen bonding, together with a similarly better fit with the structure of water, and consequential low entropy of hydration, are responsible (Table 3).

1.4.1 Fundamental Properties and Behaviour

Cyclodextrin cavities have different diameters dependent on the number of their constituent glucose units (α = 0.56 nm, β = 0.70 nm, γ = 0.88 nm). In aqueous solution, these hydrophobic cavities contain about 3 (α-CD), 7 (β-CD) or 9 (γ-CD) poorly held (but low entropy) and easily displaceable water molecules. The water in these cavities has low-density as the cavities are large enough to accommodate several more molecules. Thus, the otherwise hydrophilic CD molecules may bind non-polar suitably-sized aliphatic or aromatic compounds and lipophilic drugs.[125] The binding is driven by the enthalpic and entropic gain on the reduction in the hydrophobe-aqueous surface and the release of water molecules from the cavity to the bulk phase. Such binding also allows cyclodextrins to be used to increase the water solubility of normally hydrophobic compounds or minimize undesirable properties such as bad odour or taste in certain food additives.[126]

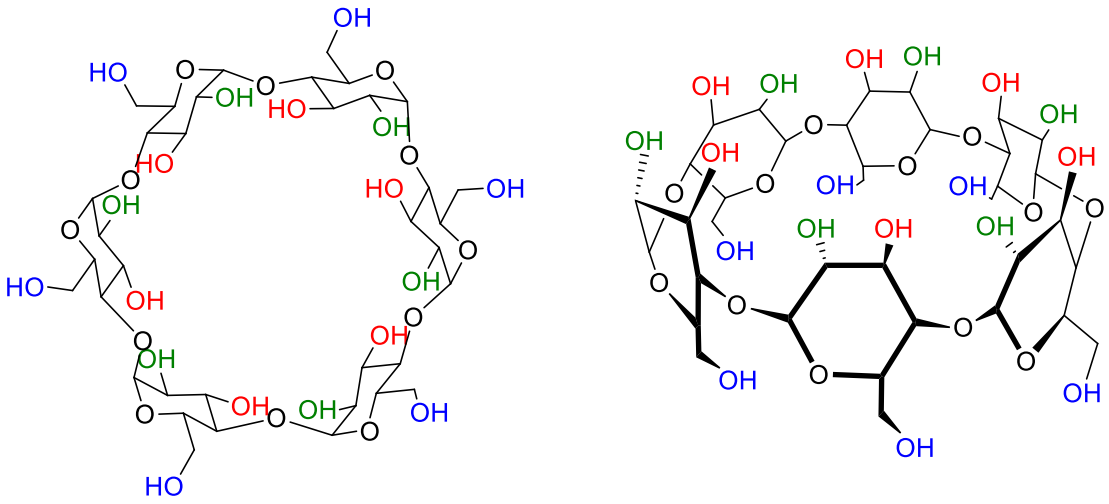

Figure 11 *Representation of α-CD highlighting secondary hydroxyl functions 2-OH and 3-OH and primary 6-OH (left) and conic shaped model with representation of primary hydroxyl groups on the narrow edge and the secondary hydroxyl groups on the wider edge (right).*

Table 3 *Cyclodextrins that can be found in pharmaceutical products.*

Cyclodextrin	Substitution*	MW (Da)	Solubility in water (mg/ml)‡
α-CD	-	972	145
β-CD	-	1135	19
2-hydroxypropyl-β-CD	0.65	1400	> 600
randomly methylated β-CD	1.80	1312	> 500
γ-CD	-	1297	232
2-hydroxypropyl-γ-CD	0.60	1576	> 500

* Average number of substituents per glucopyranose unit. ‡ Solubility in pure water at ~ 25°C. MW: molecular weight.

Random substitution of the hydroxy groups, even by hydrophobic moieties, result in dramatic improvements in their solubility (Table 3). The 6-OH groups are the most easily derivatized, not only because they are less sterically hindered but also because they are primary hydroxyls.

The main reason for the solubility enhancement is that the random substitution transforms the crystalline cyclodextrins into amorphous mixtures of isomeric derivatives. Cyclodextrin molecules are relatively large in size with a large number of hydrogen donors and acceptors, and are consequently poorly absorbed through biological membranes. The natural α- and β-cyclodextrin, unlike γ-cyclodextrin, cannot be hydrolysed by human salivary and pancreatic amylases,[127,128] but all three are subjected to fermentation by intestinal microflora.

1.4.2 CYCLODEXTRINS IN DRUG DEVELOPMENT

Cyclodextrins are useful functional excipients and, are being increasingly used to camouflage and surpass undesirable pharmaceutical characteristics, especially poor aqueous solubility. Studies in both humans and animals have shown that cyclodextrins can be used to improve drug delivery from almost any type of drug molecule. Currently, there are over 30 different pharmaceutical products composed of a drug/CD complex on the market.[129] In the pharmaceutical industry cyclodextrins have been mainly used as complexing agents, not only to increase aqueous solubility of poorly soluble drugs, but also to increase their bioavailability and stability. In addition, cyclodextrins can, for example, be used to reduce gastrointestinal drug irritation, convert liquid drugs into microcrystalline or amorphous powders, and prevent drug-drug and drug-excipient interactions. A number of books and review articles have been published on the pharmaceutical applications of cyclodextrins.[130–133]

The chemical structure of cyclodextrins (the large number of hydrogen donors and acceptors), their molecular weight (> 970 Da) and their very low octanol/water partition coefficient (approximately $\log P_{o/w}$ between -3 and 0) are all characteristics of compounds that do not readily permeate biological membranes.[134] In fact, experiments have shown that only negligible amounts of hydrophilic cyclodextrins and drug/cyclodextrin complexes are able to permeate lipophilic membranes such as skin and gastrointestinal mucosa.[135,136] Only the free form of the drug, which is in equilibrium with the drug/cyclodextrin complex, is capable of penetrating lipophilic membranes.[137] In other words, cyclodextrins will enhance drug delivery through aqueous diffusion-controlled barriers, but can hamper drug delivery through lipophilic membrane-controlled barriers (Figure 12).[129] However, there is one exception: lipophilic cyclodextrins, such as the methylated β-cyclodextrins, are able to permeate mucosa and are known to enhance drug delivery through biological membranes, such as through the nasal mucosa, by reducing the barrier function of the membranes.

Cyclodextrins can, at least in theory, enhance drug bioavailability by stabilisation of drug molecules at the biomembrane surface. For example, cyclodextrins have been shown to prevent insulin aggregation and to enhance insulin stability at the nasal mucosa. It has been suggested that cyclodextrin-enhanced insulin bioavailability after nasal administration is partly due to this stabilising effect.[138] In general, drug stabilisation associated with cyclodextrin complexation plays only a very minor role when it comes to drug delivery through biological membranes. It is their solubilising effect that is usually related to improved drug delivery. However, as cyclodextrins can both enhance and hamper drug delivery through biological membranes it is of utmost importance to optimise cyclodextrin-containing drug formulations with regard to drug delivery from the formulations.[139] Too much or too little cyclodextrin can result in less than optimum drug bioavailability.[140,141]

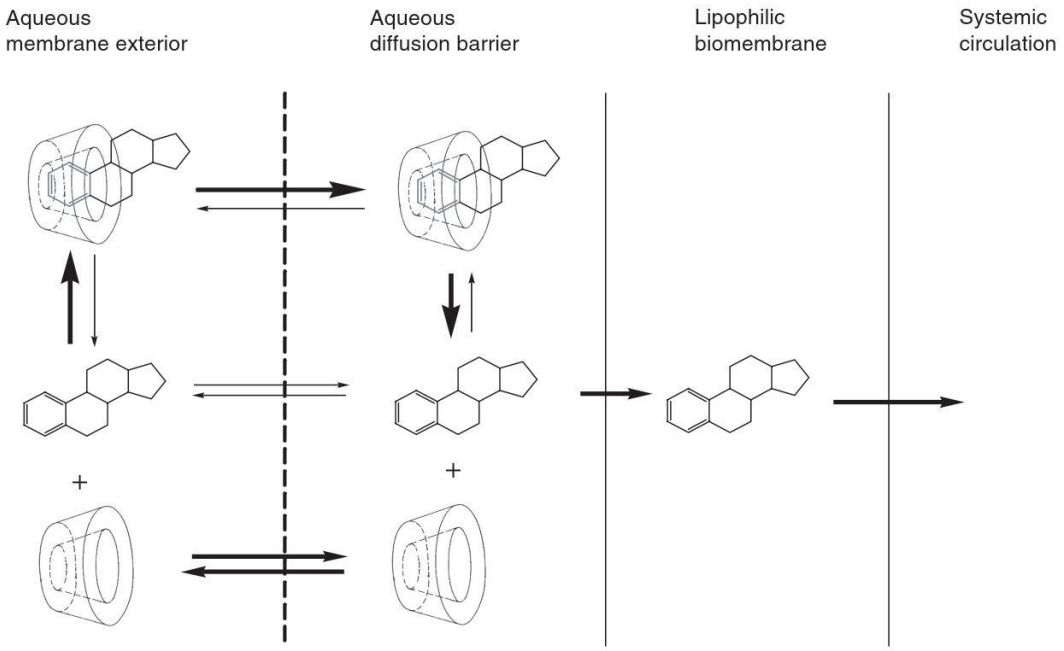

Figure 12 *The effect of cyclodextrin complexation on drug bioavailability after non-parental administration.*

1.4.3 PHYSICOCHEMICAL PROPERTIES OF CYCLODEXTRINS COMPLEX

As previously mentioned, in aqueous solutions CDs can encapsulate lipophilic moieties, most commonly drug molecules, into the central cavity. The polarity of the cavity has been estimated to be similar to that of an aqueous ethanolic solution (40% EtOH).[130] No covalent bonds are formed or broken during complex formation, and drug molecules in the complex are in rapid equilibrium with free molecules in the solution. The driving forces for the complex formation include release of enthalpy-rich water molecules from the cavity (i.e., water molecules that cannot have a full complement of hydrogen bonds), electrostatic interactions, van der Waals interactions, hydrophobic interactions, hydrogen bonding, release of conformational strain and charge-transfer interactions.[142] The physicochemical properties of free drug molecules are different from those bound to the cyclodextrin molecules. Likewise, the physicochemical properties of free cyclodextrin molecules are different from those in the complex. In theory, any methodology that can be used to observe these changes in additive physicochemical properties may be utilised to determine the stoichiometry of the complexes formed and the numerical values of their stability constants.[143–145] These include changes in solubility, chemical reactivity, UV/VIS absorbance, fluorescence, drug retention (e.g., in liquid chromatography), pK_a values, potentiometric measurements and chemical stability, NMR chemical shifts and effects on drug permeability through artificial membranes.

In aqueous cyclodextrin solution, free drug molecules are in equilibrium with molecules bound to cyclodextrin molecules. The two most important characteristics of the complexes are their stoichiometry and the numerical values of their stability constants. If *m* drug molecules (D) associate with *n* cyclodextrin molecules (CD) to form a complex ($D_m \cdot CD_n$), the following overall equilibrium is attained:

$$mD + nCD \xleftrightarrow{K_{m:n}} D_m \cdot CD_n$$

where $K_{m:n}$ is the stability constant of the drug/cyclodextrin complex. In general, the physicochemical properties of free drug molecules are different from those bound to the cyclodextrin molecules.

Stability issues can limit the feasibility of a pharmaceutical formulation. This is especially true for aqueous formulations of drugs that are prone to hydrolysis or oxidation. The reaction rates can be affected by inclusion of the drug, and especially inclusion of its chemically labile moiety, into the cyclodextrin cavity.

Cyclodextrins can sometimes have a destabilising effect on drugs through direct catalysis or, for example, by enhancing drug solubility in aqueous drug suspensions.[142] Frequently, the catalytic effect is associated with deprotonisation of the hydroxy groups located at the rim of the cyclodextrin cavity.[146,147] In this way cyclodextrins behave like carbohydrates and other polyhydric alcohols with adjacent hydroxy groups.[146] In this case the catalytic effect will mainly be observed under basic conditions and will increase with increasing pH.

1.4.4 CARBORANE INTERCALATIONS INTO CYCLODEXTRINS

Highly hydrophobic adamantyl or ferrocenyl residues, as carboxylate or ammonium salts, present well-known gold standards in the CD field and have been extensively studied.[148–150] The binding affinities measured for adamantane, diamantane, and triamantane with CDs are in the range of 10^3-10^5 M^{-1}, with the highest affinity being for triamantane carboxylic acid with γ-CD ($K_a = 3 \times 10^5$ M^{-1}).[148] Recently, it was reported that dodecaborate anions, which are hydrophilic guest molecules, form very stable complexes ($K_a > 1 \times 10^6$ M^{-1}) with CDs (γ-, ε-, and δ-CD) in aqueous solution.[151,152] The high-affinity of dodecaborate anions to CDs can be explained by: (*i*) their icosahedral (truncated-spherical) structure, which enables a good fit inside the CD cavity, (*ii*) the clusters have a double negative charge and display very high polarizabilities, which enables them to undergo ionic electrostatic and dispersion interactions (in comparison with adamantane, a well-known dispersion-energy donor, the polarizability of $[B_{12}H_{12}]^{2-}$ is significantly higher, although the two molecular species are comparable in shape,

size (152 *versus* 147 Å^3), and number of valence electrons (50 *versus* 26)), and (*iii*) dodecaborate clusters are highly water-soluble anions, and as such the hydrophobic effect is not the operative driving force to complexation in water as is the case for the adamantane binding, but rather a new effect, which was termed the chaotropic effect.[151,152] Salting-in experiments revealed that dodecaborate anions are superchaotropes, and water-structure breaking agents, therefore their complexation by CDs faciliates recovery of the water structure. This process involves the restoration of hydrogen-bonding network. The chaotropic effect as a driving force showed a distinct thermodynamic signature: highly negative enthalpies and entropies, which position these guests at the bottom end of the well-known enthalpy-entropy correlation for CDs.[151,152] Differently, from hydrophobic moieties, such as adamantane or triamantane residues, the complexation with borane clusters is entropically driven.[148] Metallacarboranes were investigated in this matter as well. NMR alongside with isothermal titration calorimetry (ITC) was performed and these results confirmed that metallacarboranes are suitable guests to cyclodextrins.[153] It is also known that mellacarboranes tend to aggregate in aqueous media.[154,155] It was found that metallacarboranes in the blood stream are stabilized by human serum albumins (HSA).[156] This unwanted stabilization in blood is challenged by the introduction of metallacarboranes complexed in cyclodextrins.[153,157]

Hydrophobic and neutral carborane clusters fit very well inside the cavity of β-CD.[158–160] The association constants (K_a) of unsubstituted *o*-, *m*-, and *p*-carborane with mono- and disubstituted hydroxy derivatives (**34o,m,p**) of these species, as well as that of adamantane (**35**), with β-cyclodextrin (Figure 13) were reported using displacement binding in an aqueous solution.[158] Their K_a's are summarised in Table 4. Although hydrophobicity plays a major role in the association with β-CD, unsubstituted *o*-carborane, which is the least hydrophobic of the carborane derivatives, exhibits the highest $K_a^{'}$ of 2.69×10^3 M^{-1}. The K_a values for the *m*- and *p*-carborane isomers decrease with decreasing dipole moment (1.83×10^3 M^{-1} and 1.56×10^3 M^{-1} respectively). Unsubstituted adamantane exhibits a K_a value lower than each of the three carborane isomers at 1.41×10^3 M^{-1}.

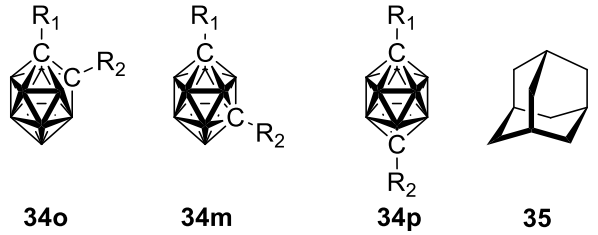

Figure 13 *o-, m-, p-carboranes (**34o,m,p**) with adamantane (**35**) and β-cyclodextrin as a host-guest molecule complex.*

Table 4 *Association constant K_a (M^{-1}) of carborane derivatives (**34o,m,p**) and adamantane (**35**) with β-CD at 22°C in 4 mM Na_2CO_3 buffer (pH 10.65).*

R_1	R_2	**34o**	**34m**	**34p**	**35**
H	H	2.69×10^3	1.83×10^3	1.56×10^3	1.41×10^3
H	OH	1.53×10^3	8.59×10^2	-	1.52×10^3
OH	OH	1.66×10^3	1.52×10^2	-	-
H	CH_2OH	1.80×10^3	2.34×10^3	-	1.91×10^3
CH_2OH	CH_2OH	1.59×10^3	1.47×10^3	-	-
H	$(CH_2)_2OH$	2.28×10^3	-	-	-
$(CH_2)_2OH$	$(CH_2)_2OH$	2.40×10^3	-	-	-

Cyclodextrins are therefore very useful excipients of hydrophobic metallacarboranes and carboranes. Not only that they stabilize these clusters and prevent their aggregations in aqueous media, but also challenge and limit unwanted interactions with other excipients, such a HSA.[157]

AIMS OF THIS THESIS

The Introductory Chapter to this Thesis has reviewed the state-of-the-art regarding the functionalization of carboranes and metallacarboranes as pharmaceutical structural blocks and covered the contemporary strategies of inhibition of the enzyme carbonic anhydrase IX, DNA intercalators and cyclodextrins. From this survey of the literature, and on the foundation of the expertise developed at our Institute, four objectives for the submitted Doctoral thesis have been defined as follows:

1) to find a suitable method for preparation of amino derivatives of cobalt bis(dicarbollide) derived from alkylhydroxy derivatives of this metallacarborane and subsequently, to prepare sulfamides from this amine derivatives. Furthermore, to develop a suitable methodology for the preparation of isomeric *closo*- and *nido*-carborane sulfonamides. Then, these sulfamide and sulfonamide derivatives should be passed on to *in vitro* and *in vivo* assays as inhibitors of the CA IX enzyme;
2) to prepare a new type of DNA intercalator based on a combination of carboranes and metallacarboranes with 1,8-naphthlic anhydride and to pass these derivatives to biological assays;
3) to find new possibilities for derivatization of carborane clusters, namely alkylation of boron vertices of *nido*-tricarbolides;
4) to prepare and fully characterize the isomeric series of carborane acid derivatives and to determine their association constants in cyclodextrins as potential carborane excipients.

CHAPTER TWO

RESULTS AND DISCUSSION

2.1 CARBONIC ANHYDRASE IX INHIBITORS

2.1.1 COBALT BIS(DICARBOLLIDE) INHIBITORS

Recently it has been shown that reaction of the C-lithiated cobalt bis(dicarbollide) anion **3** with PFA, oxirane and oxetane produces a series of mono- and disubstituted alkylhydroxyderivatives, **36a-c** and **37a-c** respectively (Scheme 6).[5] Prior this reaction is essential to remove all moisture from the Cs salt of anion **3**. This is accomplished by drying at temperature 180°C or higher under reduced pressure for a minimum of one day. The reaction is then carried out at low temperature, typically in a dry ice-acetone bath (approx. -80°C) in dry non-polar etheric solvents, such as dimethoxyethane (DME), and under an inert atmosphere (N_2 or preferably Ar). In this procedure we observed rapid colour changes, which varied from yellow-light orange (unsubstituted parent anion **3**) to black-red (lithiated species), to a dark orange-red which revert back after the addition of an electrophilic reagent (PFA, oxirane or oxetane). The negatively charged carbon atom(s) attacks the partially positive carbon atom of electrophile next to the oxygen of an electrophilic reagent. This leads to the formation of a new σ-bond between the cluster carbon(s) and the electrophile carbon and forms an open-ring alkyl chain with an oxygen anionic end. That is later protonated to form a hydroxy functional group. The resulting mixture always contains several components – starting material **3**, mono- [(1-HO-$(CH_2)_n$-1,2-$C_2B_9H_{10}$)(1',2'-$C_2B_9H_{11}$)-3,3'-Co)]$^-$ (n = 1-3, **36a-c**) and isomeric disubstituted *anti*-[(HO-$(CH_2)_n$-1,2-$C_2B_9H_{10}$)$_2$-3,3'-Co)]$^-$ (n = 1,2, **37a,b**) and *syn*-[(HO-$(CH_2)_3$-1,2-$C_2B_9H_{10}$)$_2$-3,3'-Co)]$^-$ (**37c**) products. The mono- and disubstituted compounds can then be easily separated by column chromatography. Obviously, the ratio between products depends on the amount of base used. The addition of 1.1 equivalents of base favours monosubstituted derivatives whereas two or more equivalents favour the formation of mixtures of diastereoisomers corresponding to the disubstituted derivatives.

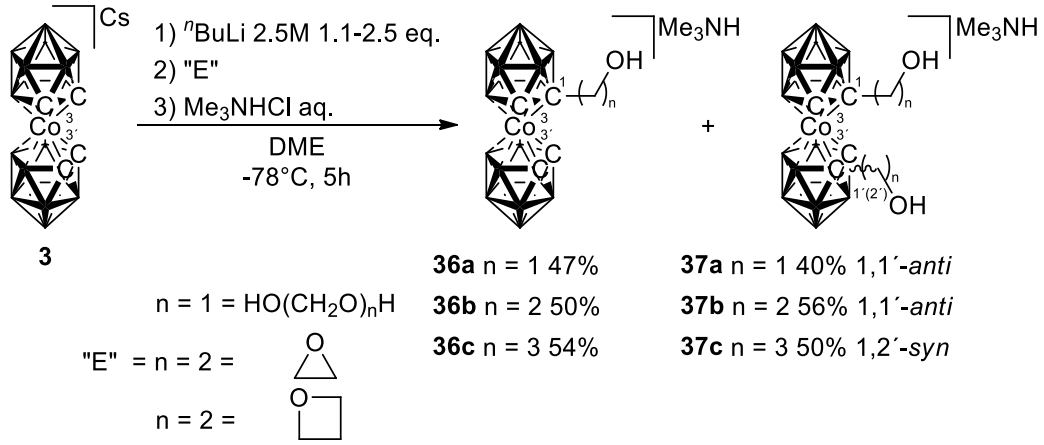

Scheme 6 *The initial step of substituting cobalt bis(dicarbollide) (**3**) with functional group attached to an alkyl chain providing mono- (**36a-c**) and dialkylhydroxy (**37a-c**) derivatives.*

Isomeric purity seems essential in any prospective biomedicinal use of the latter class of disubstituted species (Figure 14). It was found that the main species present in the fraction of disubstituted products, denoted previously[5] as *anti*-diastreoisomer, could be simply isolated, (for n = 1 and 2), on a preparative scale by multiple (6-fold in average as proved by HPLC analysis and NMR) crystallizations of their Me_3NH^+ salts from CH_2Cl_2–hexane. When n = 3, the *syn* isomer slightly predominates and its crystallizations have to be repeated several times more in combination with column chromatography (using only very little polar mobile phase, e.g. CH_2Cl_2:CH_3CN 10:1 to achieve good purity). Following this procedure, the *syn*-isomer could also be separated. The *anti*-isomer corresponds to racemic compound whether *syn* and *vicinal* represent *meso* forms.[5] Whether the racemic form is truly optically active or not depends upon the averaging of the substituent orientations due to rotation of ligand planes. Until the rotation around the cobalt in solution is fast, we can observe *pseudo*-symmetry. This is apparent, for example, on the relatively slow NMR time scale, where the racemic forms, with two identical substituents, show only one set of 6 boron signals in ^{11}B NMR. The optical activity is only apparent when the rotation is completely stopped, possibly, for example, in the case of bridge amines **48** and **49** (later in the text) or if both substituents are fixed in stable positions, for example, by interactions with enzyme. All reactions with dialkylhydroxy derivatives were carried out using either of the isomerically pure, *anti*- or *syn*-diastereoisomers of the disubstituted derivatives.

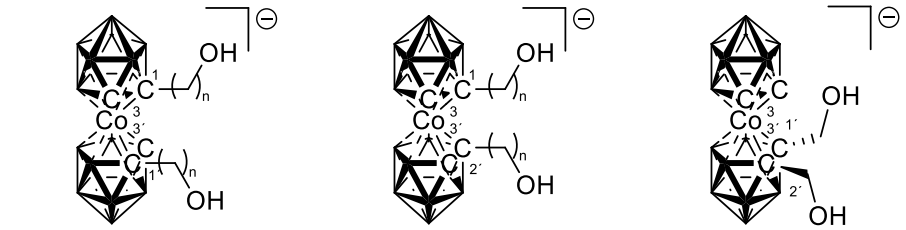

Figure 14 *Diastereoisomers of disubstituted compound **37**. The anti-isomer forms preferentially probably because the convenient sterical demands. The vicinal-isomer is formed only when the n = 3.*

Since other substitutions at C-sites of the metallacarboranes remain a challenge, the hydroxyalkyl compounds represent the only starting materials, which are currently available for the introduction of various functional groups at the cage carbon atoms. As shown here, those substituents are accessible by using modified procedures known from organic chemistry. In organic chemistry, alkylhalides are usually used for reaction with various nitrogen nucleophiles to produce amines.[161] However, the synthesis of the corresponding iodides from recently available alkylhydroxy derivatives and iodic acid led to incomplete conversions and difficulties in separation of the resultant alkyliodides from the parent compounds. Known alternatives for replacing halogenoalkyl compounds in these reactions are *p*-toluenesulfonyl (tosyl, Ts), methanesulfonyl (mesyl, Ms) and trifluormethylsulfonyl (triflate, Tf) esters.[161,162]

The ionic hydroxyalkyl cobalt bis(dicarbollides) (**36,37a-c**) react easily with the respective *p*-toluenesulfonyl and methanesulfonyl chlorides, producing the corresponding monosubstituted esters of formula [(1-X-O-$(CH_2)_n$-1,2-$C_2B_9H_{10}$)(1',2'-$C_2B_9H_{11}$)-3,3'-Co)]Me_4N (n = 1-3, X = -SO_2(-C_6H_4-4-CH_3), -SO_2CH_3, –$COCH_3$) (**38a-c**; **39a-c**; **40**), the corresponding diesters *anti*-[(1,1'-X-O-$(CH_2)_n$-1,2-$C_2B_9H_{10}$)$_2$-3,3'-Co)]Me_4N (**41a,b, 42**), *syn*-[(1,1'-MsO-$(CH_2)_3$-1,2-$C_2B_9H_{10}$)$_2$-3,3'-Co)]Me_4N (**41c**) or even half-way reacted semi-ester-hydroxyl [(1-MsO-$(CH_2)_3$-1,2-$C_2B_9H_{10}$)(1'-HO-$(CH_2)_3$-1',2'-$C_2B_9H_{11}$)-3,3'-Co)]Me_4N (**41-**) (Scheme 7). These species are formed in almost quantitative yields when the ethylhydroxy, propylhydroxy or diethylhydroxy compounds are allowed to react as their trimethylamonium salts in dry acetonitrile in the presence of Cs_2CO_3 or K_2CO_3 as the base.

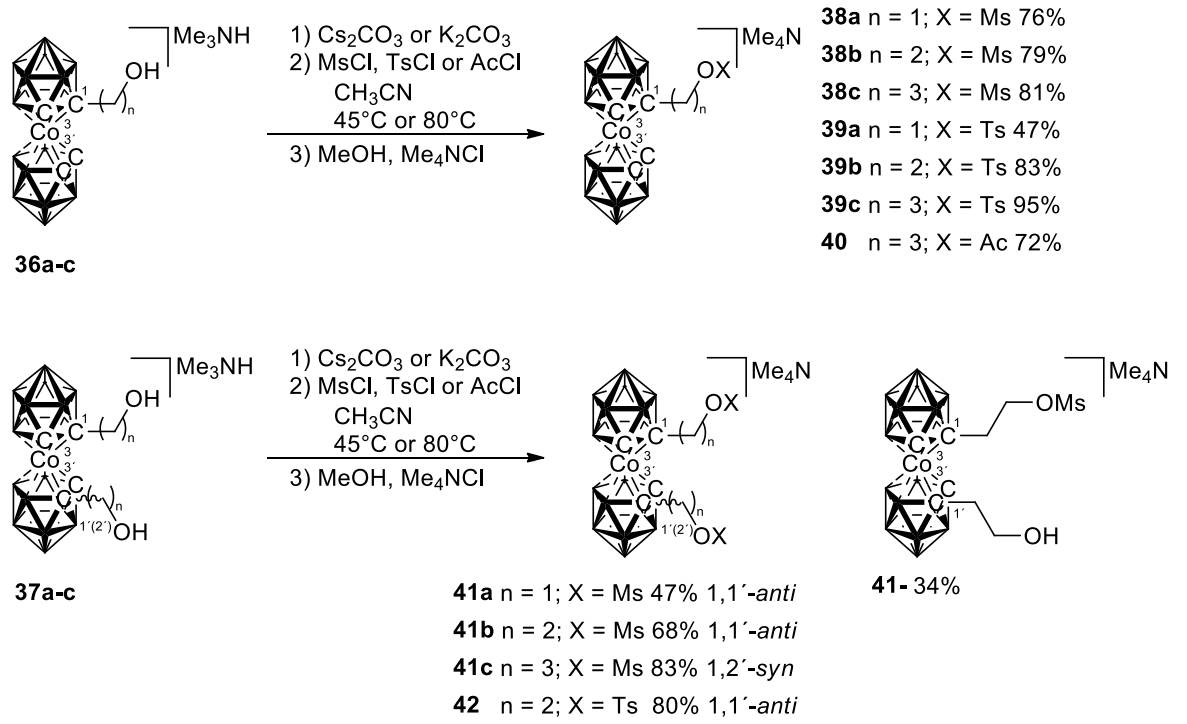

Scheme 7 *Synthesis of mono- and distubstituted mesyl and tosyl esters of cobalt bis(dicarbollide) from the reaction of hydroxyalkyl derivatives with methanesulfonyl, p-toluenesulfonyl or acyl chloride.*

The essential condition for good yields is the presence of the trimethylammonium or triethylammonium cation in the starting salt or in the reaction mixture. Indeed, triethylamine is known to act as promotor of tosylation reactions in organic chemistry. When caesium salts were used, the yields significantly drop. It should be noted that the corresponding reactions with triflic chloride resulted, in our hands, in rich mixtures of products and these have not been further studied in detail. The course of the reaction was monitored by MS and HPLC. This monitoring was particularly essential when the reactant is the disubstituted isomer. For example, we used this monitoring to quench the reaction of **37b** with MsCl when MS had indicated that the reaction mixture contained mainly the diester **41b** and only the *semi*-ester-hydroxy derivative **41-** and that all the starting material **37b** had disappeared. This *semi*-ester-compound **41-** based on *anti*-isomer is inherently asymmetric. When the *meso*-form of the starting alcohol was used, the presence of two different substituents causes the plane of symmetry to be lost, leading to an asymmetric molecule.

Nevertheless, other esters are available from reactions of acyl chlorides, which are exemplified here by X-ray structure of acetyl ester **40** prepared as a model compound (Figure 15).

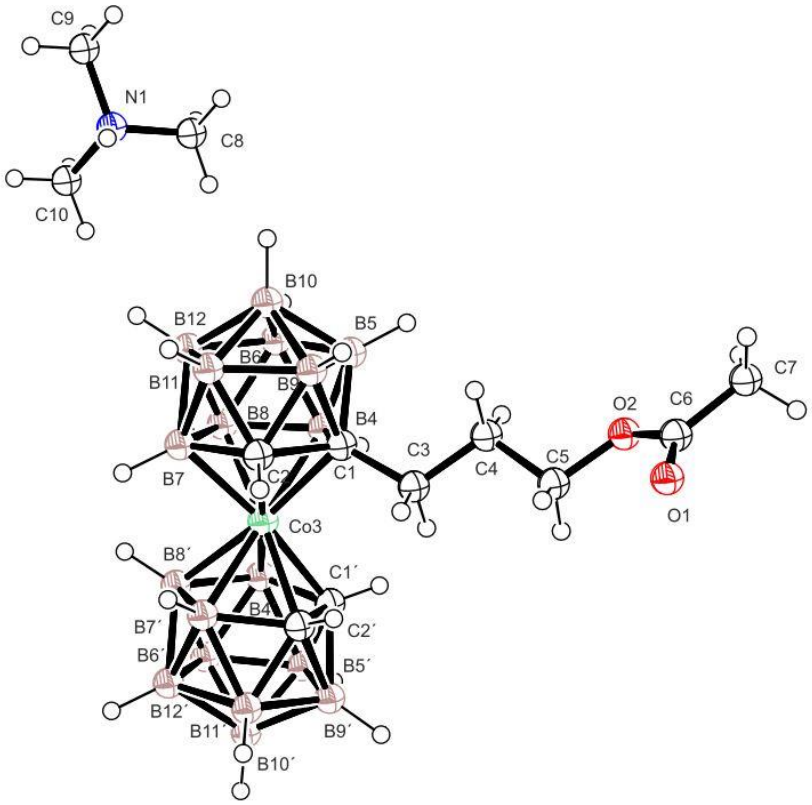

Figure 15 *The molecular structure of the acetyl ester **40** (trimethylammonium salt) (ORTEP view, 30% probability level). Selected interatomic distances [Å] and angles [°]: Co3-C1 2.107(1), Co3-B8 2.099(1), C1-C2 1.639(1), C1-C3 1.537(1), C3-C4 1.530(1), C4-C5 1.511(1), C5-O2 1.458(1), C6-O1 1.207(1), C3-C1-C2 118.63 (10), C3-C1-B4 125.5(1), O1-C6-O2 122.9(1).*

The crude sulfonyl esters (Ts or Ms) were, after removal of the organic solvents, rapidly precipitated as their respective Me_4N^+ salts dissolved in aqueous methanol, which was followed by fast filtration or decantation and drying under vacuum followed by crystallization from CH_2Cl_2-hexane. This procedure gives the esters in essentially quantitative yields and in a purity sufficient for synthetic purposes (ca. 95% according to HPLC and NMR analyses). It may be also noted that the tetramethylammonium salts of these esters with ethylene and propylene linkers' **38b,c, 39b,c** and also the diesters **41a-c, 42** are reasonably stable compounds, which could be further purified by a flash chromatography on silica gel. The methanesulfonyl ester with ethylene connector **38b** was characterized crystallographically (Figure 16).

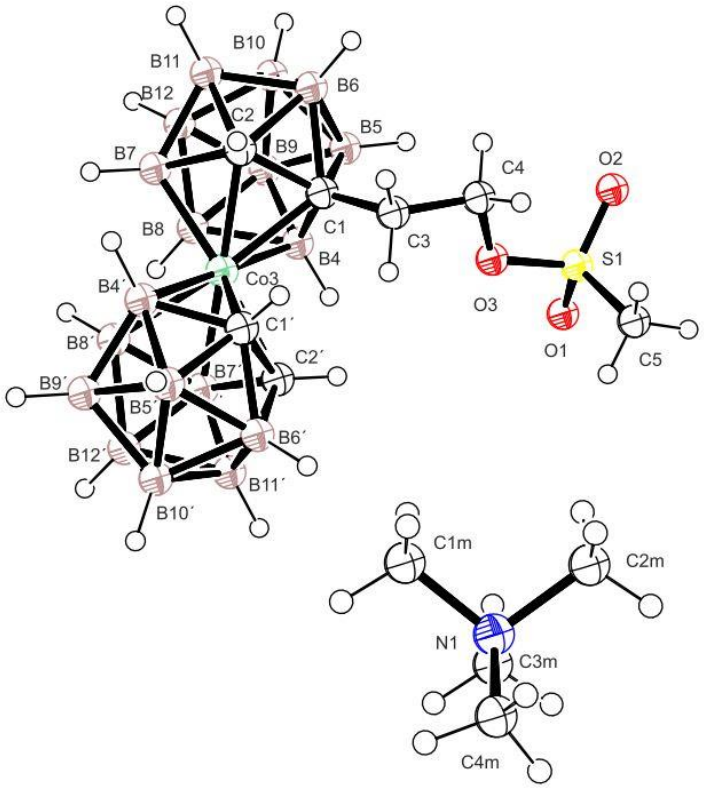

Figure 16 *The molecular structure of the ion* ***38b*** *(ORTEP view, 30% probability level). Selected interatomic distances [Å] and angles [°]: Co3-C1 2.095(3), Co3-B82.090 (3), C1-C2 1.630(4), C3-C4 1.530(1), C4-O3 1.460 (4), S1-O3 1.569 (3), S1-C51.731(4), C3-C1-C2 117.3 (2), C3-C1-B4 126.7(2), O3-S1-C5 103.1(1).*

Differences in reactivity were observed for the methylene hydroxy derivatives, which, under identical reaction conditions, reacted less readily and their conversions to their respective methanesulfonyl esters were generally lower, ranging for monosubstituted species **38a** between 60-85% (according to HPLC analysis of samples from repeated runs) and around 40-50% for di(methanesulfonyl) ester **41a**. The reaction with *p*-toluenesulfonyl chloride under these conditions led to only 20-30% conversion to the monosubstituted ester **39a**. This *p*-toluenesulfonyl ester could be prepared in 47% yield under alternative conditions when the trimethylammonium salt of hydroxy derivative **36a** and *p*-toluenesulfonyl chloride were stirred in biphasic system consisting of ether and a small volume of concentrated aqueous caesium hydroxide. The esters containing the methylene linker between the cage and the ester group are quite reactive species, and are sensitive to humidity and should be rapidly precipitated, dried and stored at low temperature. Nevertheless, even the di(methanesulfonyl) ester could be isolated by flash chromatography on silica gel from the unreacted dihydroxy derivative and a species containing only one esterified hydroxy group site as the main side product. However,

the mono methanesulfonyl ester **38a** decomposes during chromatography and thus could not be fully purified and completely characterized. Therefore, for reactions with amines, its crude form was used. The amine could then be purified by column chromatography.

It has been found that *p*-toluenesulfonyl and methanesulfonyl ester groups in these compounds used in form of their tetramethylammonium salts react readily with ammonia, primary and secondary amines acting as the nitrogen nucleophiles producing the corresponding alkylamine derivatives. The amine was typically used in a large excess such that no other base or promotor was necessary to accomplish these reactions. Thus, the reactions of the esters **38a,c, 39a-c** (Scheme 8) and **41a,b** (Scheme 9) with excess ammonia, performed by heating in dry toluene-acetonitrile solvent (1:1) in a Kimberly-Clark glass pressure tube or flask, or in a Teflon lined stainless steel pressure vessel, provided very good yield of the respective primary alkylamines $[(1\text{-}H_2N\text{-}(CH_2)_n\text{-}1,2\text{-}C_2B_9H_{10})(1',2'\text{-}C_2B_9H_{11})\text{-}3,3'\text{-}Co)]^-$ (where n = 1-3 and ^1R = ^2R = H) (**43a-c**) and the diamines of formula *anti*-$[(1,1'\text{-}NH_2\text{-}(CH_2)_n\text{-}1,2\text{-}C_2B_9H_{10})_2\text{-}3,3'\text{-}Co)]^-$ (n = 1,2, **44a,b**) and *syn*-$[(1,2'\text{-}NH_2\text{-}(CH_2)_3\text{-}1,2\text{-}C_2B_9H_{10})_2\text{-}3,3'\text{-}Co)]^-$ (**44c**). These were then purified by column chromatography and crystallization. Other primary and secondary amines, ^{n}BuNH$_2$ or Et$_2$NH and BnNH$_2$, selected as basic representatives of aliphatic and aromatic amines, were heated with the esters in acetonitrile providing good yields of their respective secondary or tertiary amines with the general formulation $[(1\text{-}^1R^2RN\text{-}(CH_2)_n\text{-}1,2\text{-}C_2B_9H_{10})(1',2'\text{-}C_2B_9H_{11})\text{-}3,3'\text{-}Co)]^-$ (^1R = ^{n}Bu, ^2R = H, ^1R = Bn, ^2R = H and ^1R = ^2R = Et) (**45a-c, 46a-c, 47b,c**). No reaction was observed after prolonged heating with tertiary amines such as triethylamine and pyridine.

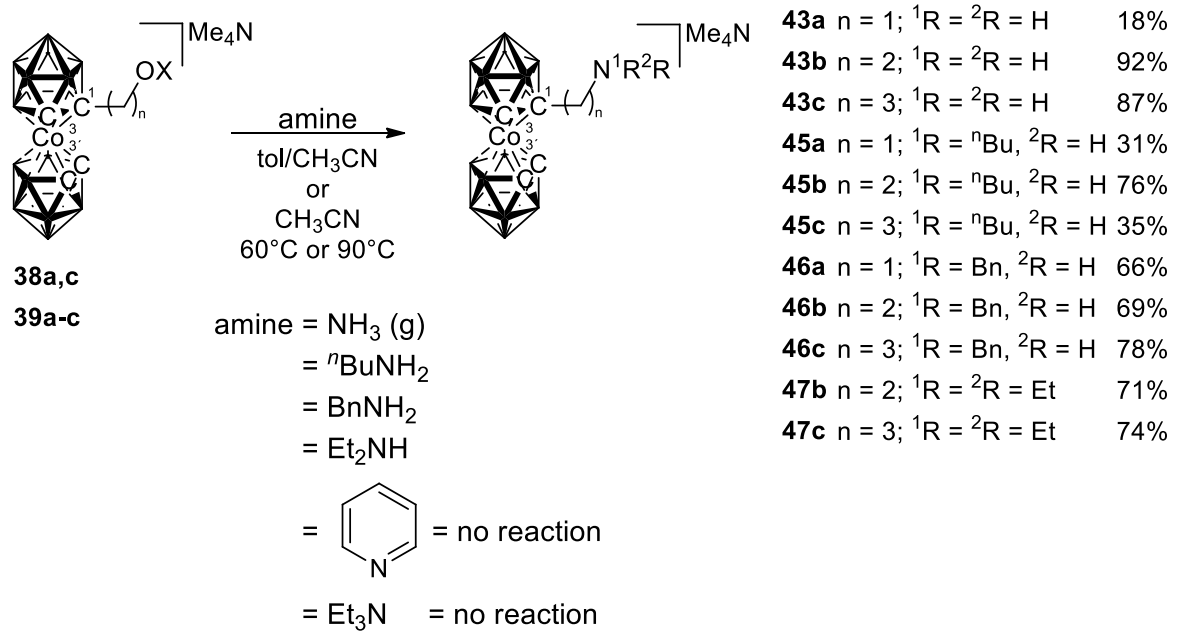

Scheme 8 *Synthesis of alkylamine substituted cobalt bis(dicarbollide) from the reaction of monosubstituted methanesulfonyl or p-toluenesulfonyl esters* ***38a,c, 39a-c*** *with ammonia, primary and secondary amines.*

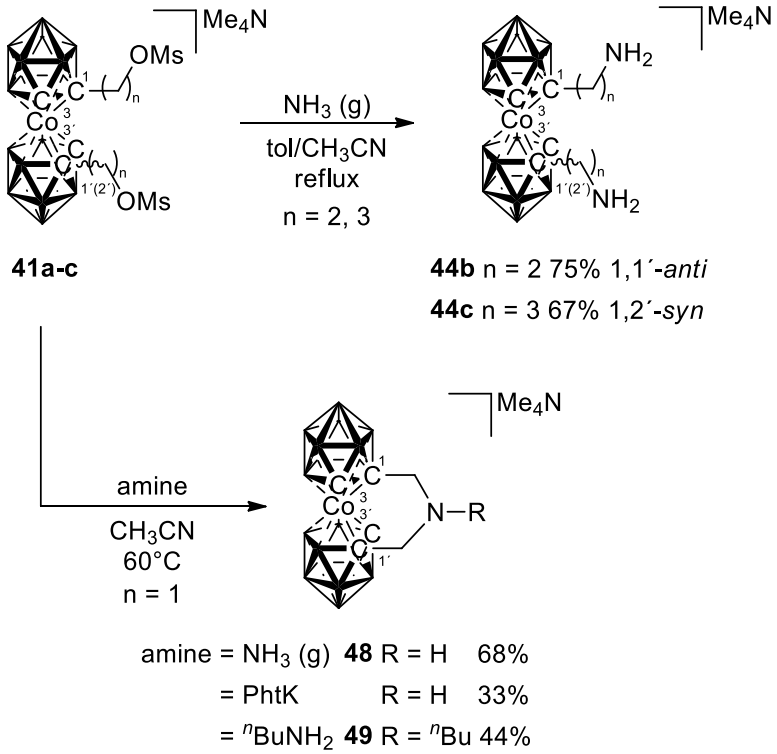

Scheme 9 *Diethylamine substituted (44) and bridge (48, 49) derivatives of cobalt bis(dicarbollide).*

It was apparent that steric and electronic effects due to the close proximity of the bulky and ionic cage in the ester **38a**, resulted in a different reactivity. Typically, the formation of

several side products was observed, often accompanied by partial degradation of the cage, which was indicated by the green colour of the reaction mixture. Nevertheless, the respective amines **43a**, **45a** and **46a** could be isolated, but in significantly lower yields.

A clear difference in the reaction pathways was observed in case of the disubstituted ester **41a** (Scheme 8). Its reaction with ammonia, ^{n}butyl amine and even with potassium phthalimide (PhtK) resulted, according to spectral data, in the formation of a species of the formula [1,1'-μ-(CH_2-NR-CH_2-)-1,2-$C_2B_9H_{10}$)$_2$-3,3'-Co)]Me_4N (R = H, **48**) (R = ^{n}Bu, **49**) containing a triatomic bridge structure attached to carbon atoms present in both ligand planes. This can probably be ascribed to the strong tendency of the cobalt bis(dicarbollide) ion to form structures bridging both dicarbollide planes around the cobalt atom.

Thhe amination of *semi*-ester-hydroxy derivative **41-** using the gaseous ammonia was also performed. The reaction proceeds as expected to produce a *semi*-amine-hydroxy compound **44-** (Scheme 10).

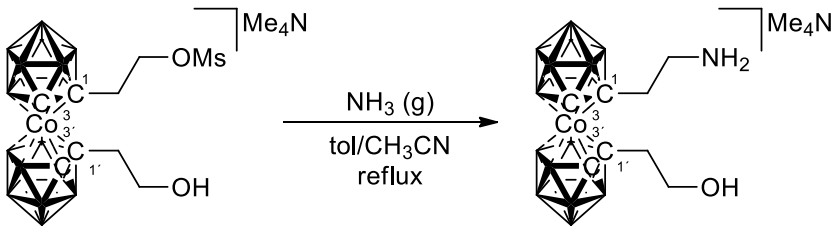

41- **44-** 79%

Scheme 10 *Semi-amine-hydroxy derivative **44-** was prepared using the same condition as previous mono- or diamines.*

To illustrate better the limits of direct substitutions, a well-known direct alkylamination using *N*-bromoalkyl phthalimide with lithiated cobalt bis(dicarbollide) (**3**) led to the desired product using only *N*-(2-bromomethyl) phthalimide. This reaction results to the derivative **43a** in low yields. Other experiments showed unexpected products **50a,b** of intramolecular cyclization reactions which led to five or six membered rings (Scheme 11).[163]

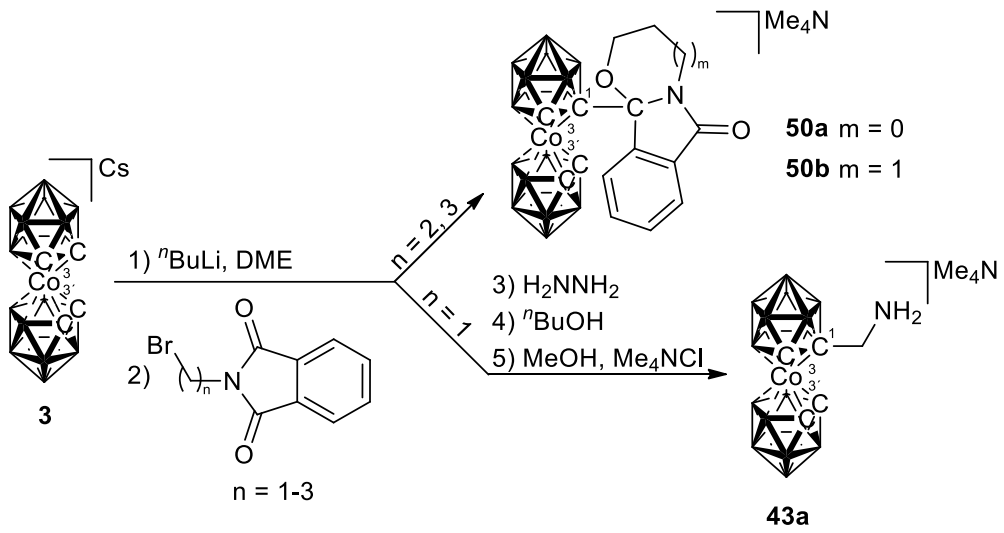

Scheme 11 *Direct alkylamination of cobalt bis(dicarbollide) using phthalimide N-alkylamines.*

The presented reaction sequence leading to primary amines is a very useful tool in the introduction of a variety of functional groups into the metallacarborane moiety and this work was published in 2015.[6] In this article we aimed mainly at the primary amine derivatives **43a-c** of monosubstituted species and **44b,c** of *anti*-disubstituted species. These represented our main interest for biomedicinal use and will be discussed later in the text. Other amine derivatives, such as *n*-butyl, benzyl and diethyl were synthesized only as a pilot series to demonstrate the ease with which they may be prepared. On the other hand, reaction with heterocyclic compounds such as pyridine does not lead to the desired product. We also found out that the reaction between amines and the shortest alkyl linker possible leads to the triatomic bridged compounds **48** and **49**.

An additional reaction outlined in previous text (Section 1.2.4) is an exchange reaction between amine derivatives (**43a-c**, **44b,c** and **44-**) and sulfamide (Scheme 12) similar to previously reported carborane inhibitors.[92] The new compounds were designed to vary the length of the linker between the sulfamide group and metallacarborane cluster and the number of the groups attached to the cage. The resultant alkylaminess were subsequently converted to their respective sulfamides of general formulation $[(1\text{-}NH_2SO_2NH\text{-}(CH_2)_n\text{-}1,2\text{-}C_2B_9H_{10})(1',2'\text{-}C_2B_9H_{11})\text{-}3,3'\text{-}Co]^-$ (n = 1-3) (**51a-c**). The compounds **51b** and **51c** were prepared in gram quantities for *in vivo* tests.

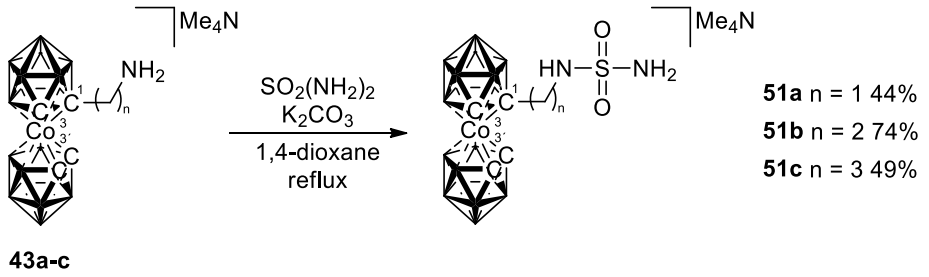

Scheme 12 *Preparation of inhibitors **51a-c** with sulfamide group.*

The series of compounds substituted by a single sulfamide group has been augmented by compounds containing two identical substituents on the cluster carbon atoms. As has been described previously, disusbstitutions at carbon atoms can lead, in principle, to the presence of two or three diastereoisomers.[5] In the case of sulfamide substituted compounds, only two compounds could be isolated in the form of pure diastereoisomers: *anti*-[1,1'-(NH_2SO_2NH-$(CH_2)_2$-1,2-$C_2B_9H_{10}$)$_2$-3,3'-Co]$^-$ (**52b**) and *syn*-[1,2'-(NH_2SO_2NH-$(CH_2)_3$-1,2-$C_2B_9H_{10}$)$_2$-3,3'-Co]$^-$ (**52c**) (Scheme 13). The former substitution is asymmetric corresponding to the racemic form, the latter is symmetric provided that both of the carbon atoms in the ligand planes are in an eclipsed *cisoidal* arrangement, and this corresponds to the *meso*-form. Isomers **52b** and **52c** were separated after the initial step of the reaction sequence as their alkylhydroxy derivatives. This was because it was easier to separate the alkylhydroxy derivatives rather than their amine and sulfamide derivatives due to their poor crystallization properties and unsuitability for chromatographic separation.

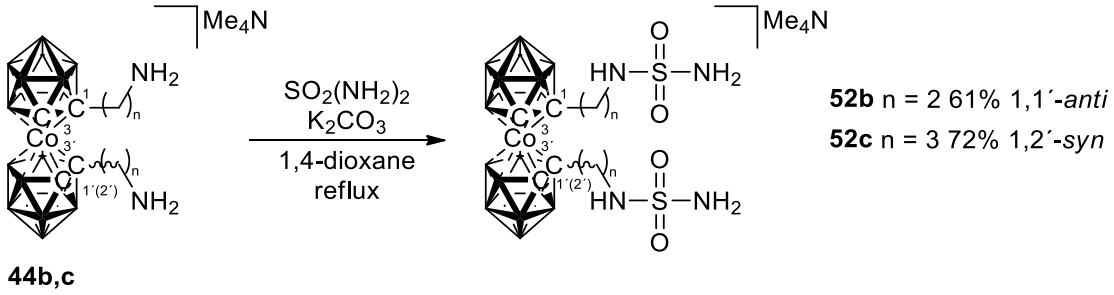

Scheme 13 *Preparation of inhibitors **52b,c** with sulfamide group.*

The same reaction was also performed for the *semi*-amine-hydroxy derivative (Scheme 14) with the expected formation of a *semi*-sulfamido-hydroxy derivative **52-**.

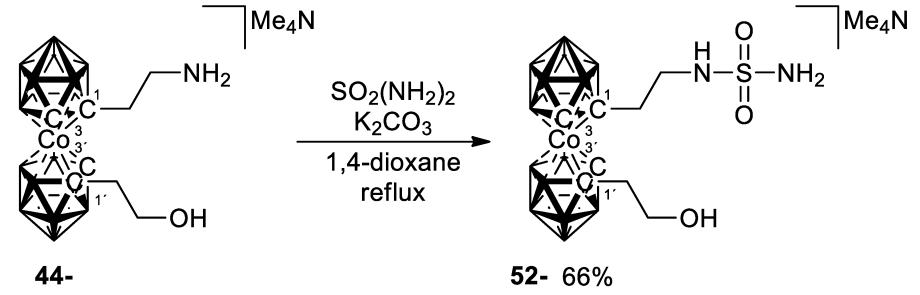

44- **52-** 66%

Scheme 14 *Preparation of inhibitors **52-** with sulfamide head group.*

These metallacarborane sulfamides are the targeted structures in our search for specific inhibitors of the tumour associated isozyme CA IX and their *in vitro* and *in vivo* studies will be discussed in Section 2.1.4.

2.1.2 CARBORANE INHIBITORS

The general methods to substituted *ortho*-carboranes (**54**) usually proceed either by incorporation of substituted alkynes into ten-vertex open-cage precursors (typically to bis(ligando) derivatives of decaborane(14) *arachno*-6,9-$(Me_2S)_2$-$B_{10}H_{12}$ (**53**)) or by lithiation of the CH groups in the carborane cage (**1**) following by reaction with numerous reagents (alkyl halides or cyclic ethers) in a non-polar solvents at low temperatures (0°C to -78°C) (Scheme 15).[18,90]

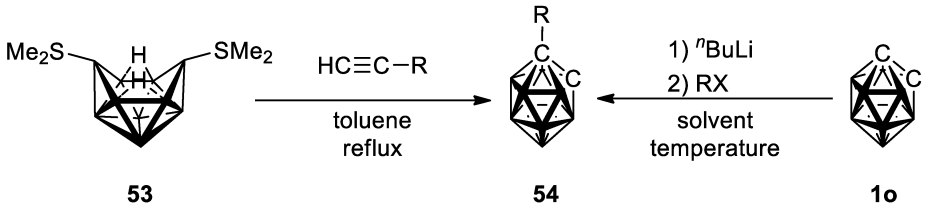

53 **54** **1o**

Scheme 15 *General overview on the two possible ways of the preparation of substituted ortho-carborane derivative **54**.*

However, as far as we are aware, no carborane derivatives holding sulfonamide groups in their structure had been prepared to date. A still-limited availability of alkynes bearing terminal sulfonamide groups for insertion reactions may account for absence of such derivatives within the otherwise broad series of substituted carboranes. It may have also been assumed that the presence of polar sulfonamide groups in the starting reagents could prove to be a troublesome and discouraging point for the synthesis, as it might, in principle, lead to degradations of the cage. My colleagues proved experimentally that the latter considerations are groundless by the insertion of sulfonamide alkynes of the general formulation $NH_2SO_2(CH_2)_nC{\equiv}C$ (n = 1-4) into the open-cage ten vertex *arachno*-6,9-$(Me_2S)_2$-$B_{10}H_{12}$

derivative **53**. The reactions carried out in toluene at high temperature proceeded easily, with high conversions and the respective sulfonamide *closo*-carboranes of general formula $NH_2SO_2(CH_2)_n$-$C_2B_{10}H_{11}$ (n = 1-4) (**54a-d**) (Scheme 16) were isolated in good yields (around 60%) after a simple work up.[165]

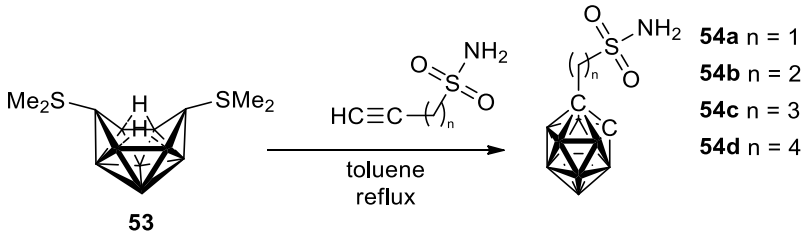

Scheme 16 *Insertion of an alkyne sulfamide into an arachno species **53** is one way how to prepare desired closo-carborane derivatives.*

This approach using insertion of acetylenes could, however, provide only *ortho*-isomer of the *closo*-carboranes. Nevertheless, we were strongly interested in inspecting the effect of the isomeric nature of compounds on their activity. Similarly to the pathways described in Scheme 6 on cobalt bis(dicarbollide) ion (**3**), the lithiations followed by reaction with cyclic ethers could be much more easily performed on twelve-vertex *closo*-carborane isomers (**1o,m,p**).[8,92,166] This approach was performed with an oxetane ring to produce a mono-propylhydroxy derivative of *ortho*-carborane **55o** (Scheme 17). The conversion of the reaction was improved by elevating the temperature from -78°C to 0°C and by the use of low polar *n*-hexane as a solvent, in which the monosubstituted derivative **55o** is only slightly soluble and it precipitates from the reaction mixture. A propyl linker was chosen based on current biological studies as the best fit into the CA IX active site.

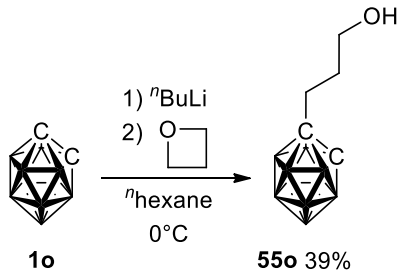

Scheme 17 *Ring-opening reaction after initial lithiation forms a hydroxy derivative **55o**.*

The successful introduction of the hydroxypropyl group represented the first step in the overall sequence to sulfonamide. For the next step, i.e. the synthesis of the triflate ester (applicable in the case of carboranes, not metallacarborane anions), the reaction conditions could be found in the literature for a triflate ester with a shorter methylene connector.[145] Thus, reaction between hydroxy derivative **55o** and a triflate anhydride in the presence of pyridine as

a base was carried out. However, the isolated final product did not corresponded to the expected triflate ester, instead a pyridinium salt **56** (Scheme 18) was formed in a high yield due to the fast alkylation of the nitrogen atom in pyridine.

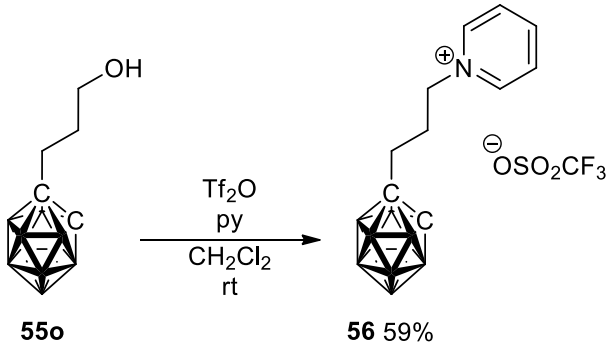

Scheme 18 *Pyridinium salt from esterification with triflate anhydride.*

The possibility of formation of pyridinium salt was described previously by Hey-Hawkins *et al.* for the compound with a methylene linker.[145] However, it was believed that this cation forms only when an excess of pyridine is used. This reaction should be thus eliminated by allowing the components to react in a 1:1:1 molar ratio. Nevertheless, at least in our case, the formation of triflate salts of pyridinium derivative was **56** could not be avoided and this product always resulted in a high yields. This undesired product was characterised by X-ray crystallography (Figure 17).

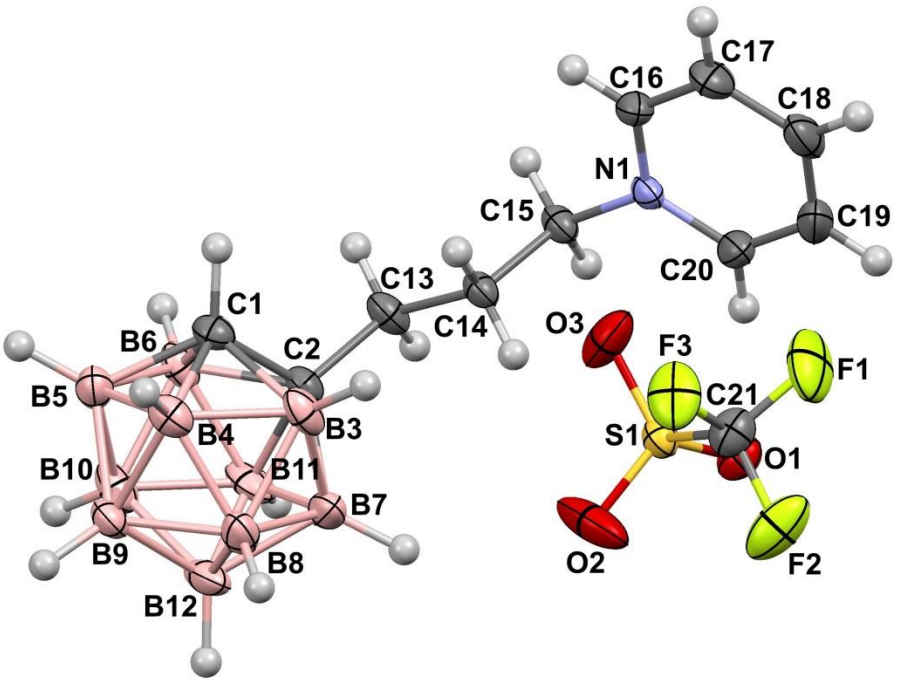

Figure 17 *The compound **56** crystallizes in the monoclinic space group $P2_1/c$ with four molecules within the unit cell. The structure of **56** contains positional static disorder of CF_3*

group, this disorder was treated by standard procedures implemented in SHELXL software[167] *and atoms were split into two positions with occupancy of about 68:32. The molecular structure (ORTEP 40% probability level) of* ***56****, disorder of CF_3 group is omitted for clarity. Interatomic distances [Å] and angles [°] in the carborane cage: C1-B5 1.690(4), C1-B4 1.693(4), C1-B6 1.700(4), C1-B3 1.699(5), C2-C1 1.635(4), C2-B7 1.697(4), C2-B11 1.706(4), C2-B3 1.718(4), C2-B6 1.727(4), B3-B8 1.754(5), B4-B8 1.757(5), B4-B3 1.756(5), B5-B4 1.760(5), B5-B10 1.767(5), B6-B10 1.760(5), B6-B11 1.761(5), B6-B5 1.774(5), B7-B3 1.760(6), B7-B12 1.771(5), B7-B8 1.775(5), B7-B11 1.777(6), B9-B5 1.767(5), B9-B4 1.768(5), B9-B12 1.774(5), B9-B10 1.776(5), B9-B8 1.777(5), B10-B11 1.767(5), B10-B12 1.780(6), B12-B11 1.774(6), B12-B8 1.774(6).*

We found that reaction proceeds well in nonpolar solvents at room temperature without any base being necessary and gives a triflate ester, CF_3SO_2-$O(CH_2)_3$-$C_2B_{10}H_{11}$ **57o**, in good yield with no need for further purification. Alternatively, a good yield is also provided by analogous reaction with mesyl chloride following a protocol known from previous experience with metallacarborane mesyl esters. In this case the presence of base (Et_3N) is necessary to give CH_3SO_2-$O(CH_2)_3$-$C_2B_{10}H_{11}$ **58** (Scheme 19). Nevertheless, for the subsequent steps to sulfonamide and other derivatives, the triflate ester **57o** was considered as a better solution due to its higher reactivity.

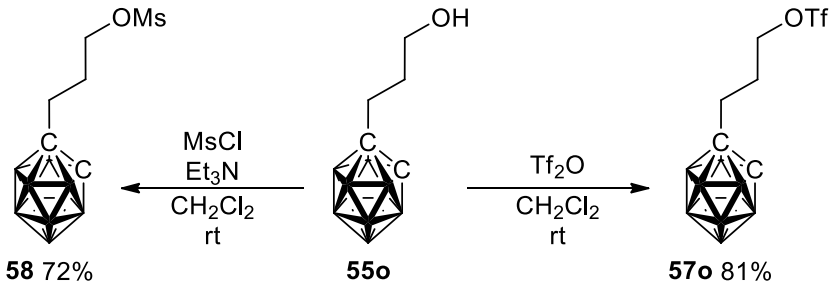

Scheme 19 *Two different esterifications giving products* ***57o*** *and* ***58*** *in very good yields.*

The ester groups in **57o** and **58** can be easily transformed to other functional groups. As a next step to sulfonamides, the thiocyanate group was selected. The introduction of new carbon-sulfur bond was achieved by an S_N2 substitution of **57o** with potassium thiocyanate in polar solvent.[168] The reaction is rapid, as indicated by a colour change; the slightly pink solution of **57o** immediately turns yellow. This reaction was monitored by proton NMR and was quenched when no trace of the starting compound was present in spectra. The new thiocyanate derivative NCS-$(CH_2)_3$-$C_2B_{10}H_{11}$ **59o** doesn't need any further purification and is obtained in almost quantitative yield (Scheme 20).

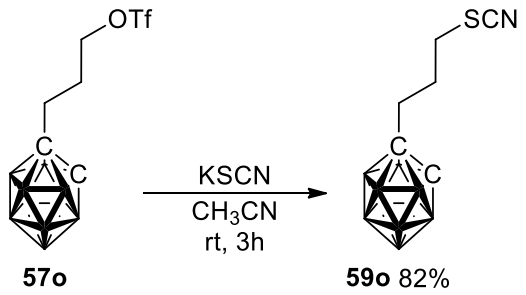

Scheme 20 *Thiocynate **59o** is prepared by simple substitution of triflate ester **57o**.*

The next step was the reaction between thiocyanate derivative **59o** and sulfuryl chloride in a mixture of water/acetic acid under mild conditions. The use of a large excess of SO_2Cl_2 (10 equivalents) and a CH_3COOH-H_2O ratio of 3:1 at 50°C were found to be the best conditions. The presence of water is essential for accomplishing the oxidisation of the sulfur atom in the thiocyanate group. Under these conditions, the reaction proceeded smoothly and with no trace of starting compound after 3 hours of heating. We obtained the sulfonyl chloride derivative $ClSO_2$-$(CH_2)_3$-$C_2B_{10}H_{11}$ **60o** in good yield (Scheme 21).[169]

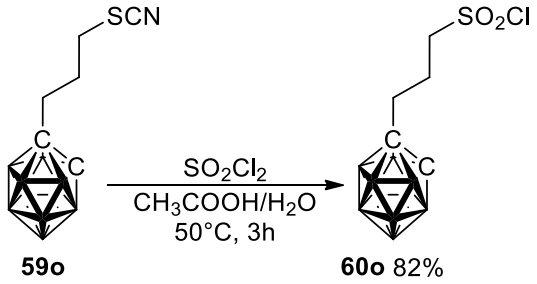

Scheme 21 *Oxidation and chlorination is done in one step in very good yields.*

To finalize this synthetic sequence and to obtain a carborane derivative with the desired sulfonamide group, we used the well-known[170,171] reaction between sulfonyl chloride and aqueous ammonia at low temperature. The reaction has been carried out in acetonitrile and the expected product NH_2SO_2-$(CH_2)_3$-$C_2B_{10}H_{11}$ **61o** was obtained in 72% yield (Scheme 22).

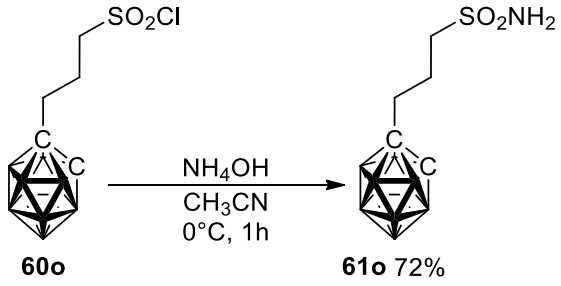

Scheme 22 *Standard procedure to get sulfamides from sulfonyl chlorides is simple reaction with any source of amine.*

The direct pathway leading to sulfonamide developed on the better accessible *ortho*-carborane (**1o**) was then applied to the synthesis of the still missing *meta*- (**1m**), and *para*-carborane isomers (**1p**). In this case, we also focused on disubstituted products which might provide additional interactions around the active site. The protocol described above was successfully applied over the whole group of compounds from the *m*-carborane series using either 1.2 or 2.2 equivalents of ^{n}BuLi and thus, the mono- (**55m**) or disubstituted (**62m**) hydroxypropyl derivatives were isolated (Scheme 23).

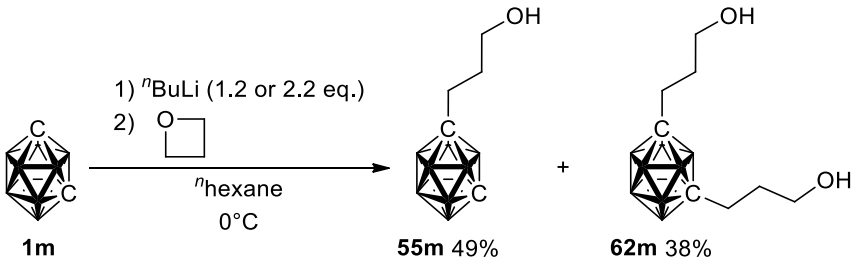

Scheme 23 *Ring-opening reaction performed on lithiated meta-carborane.*

After a successful separation of the initial products shown in Scheme 24, we proceeded with the subsequent steps summarised in Scheme 24.

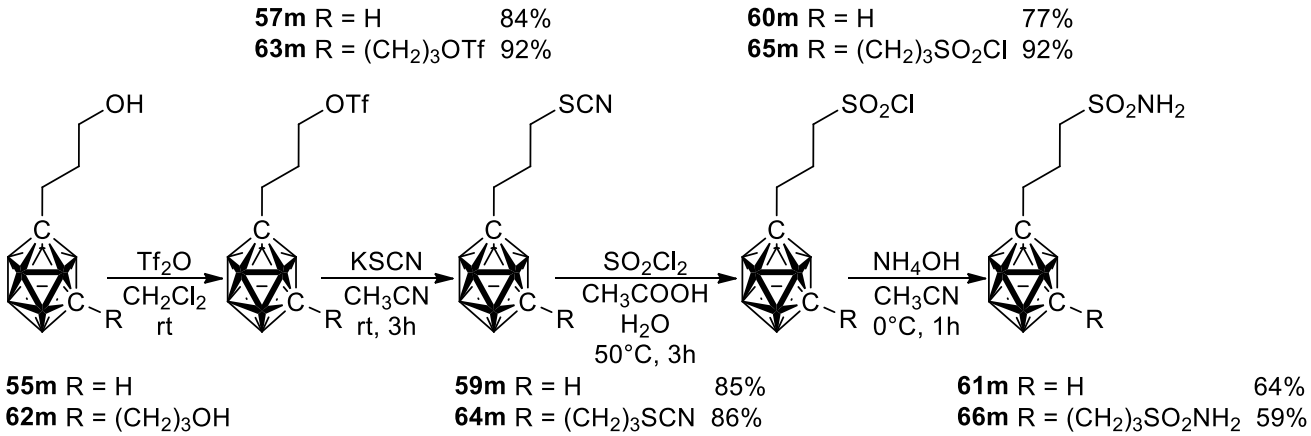

Scheme 24 *Synthetic protocol providing sulfonamides **61m** and **66m** in good yields.*

Finally, a five-step reaction sequence leading to the last remaining *para*-isomer was carried out: the initial lithiation and ring opening, the separation of the products obtained by using 1.2 (**55p**) and 2.2 equivalents (**62p**) of base (Scheme 25), and a sequence of transformations providing sulfonamides *para*-carboranes **61p** and **66p** (Scheme 26).

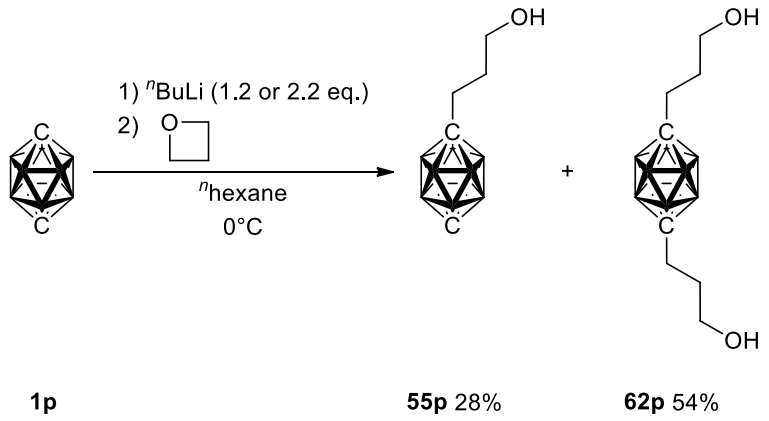

1p **55p** 28% **62p** 54%

Scheme 25 *Ring-opening reaction performed on lithiated para-carborane.*

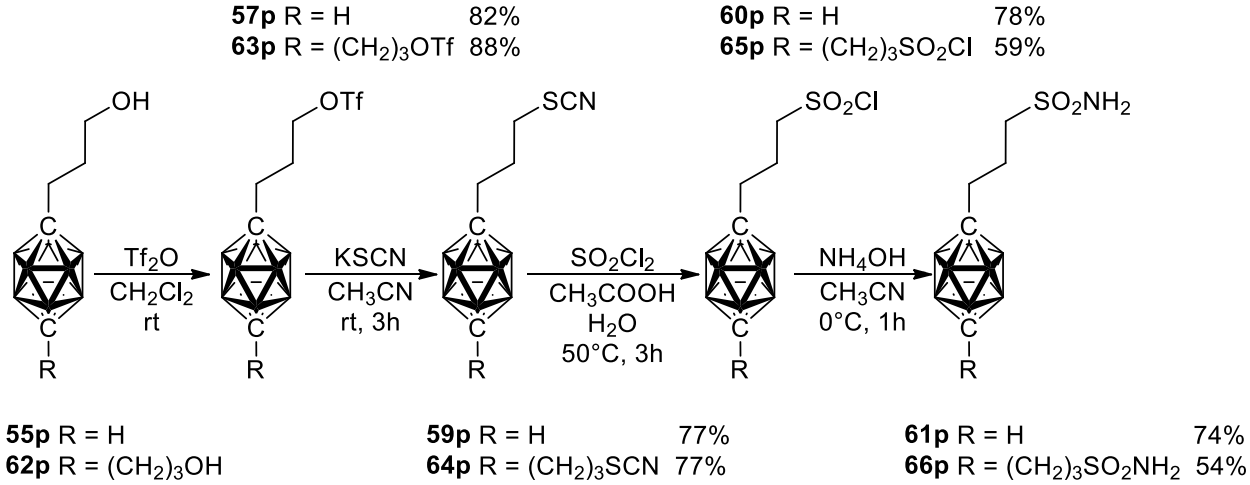

Scheme 26 *Synthetic protocol providing sulfonamides **61p** and **66p** in respective good yields.*

For comparison and summary, see Table 5 from which is evident that the initial reaction with cyclic ether is the main limiting step. Mixtures with unreacted starting material were typically obtained. However, the starting material could be regenerated and reused. This is very important since the price of *meta*-, and in particular *para*-carborane in particular, is high and steadily increasing. Starting from the second step, the reactions provided products in good yields. The triflate derivatives of *meta*- and *para*-isomers did not crystallize (as in *ortho* isomer) and were used in crude isolated forms. Nevertheless, NMR spectra showed no additional peaks and these products also provided the expected products in good yields in next steps. The triflate corresponds to labile functional group and decomposes during column chromatography. All thiocyanates were obtained in good yields without further purification. The sulfonyl chlorides were obtained in oily form and could not be purified further due to a chlorine liability. Sulfonamides as the final products were purified by column chromatography and crystallised to ensure product purity.

Table 5 *Yields and states of products from reactions producing carborane sulfonamides.*

isomer	substitution	OH	OTf	SCN	SO_2Cl	SO_2NH_2
ortho	mono	**55o**• / s˙ / 39*	**57o** / c / 81	**59o** / s / 82	**60o** / o / 82	**61o** / c / 72
meta	mono	**55m** / s / 49	**57m** / o / 84	**59m** / s / 85	**60m** / o / 77	**61m** / s / 64
	di	**62m** / s / 38	**63m** / o / 92	**64m** / s / 86	**65m** / o / 92	**66m** / s / 59
para	mono	**55p** / c / 28	**57p** / o / 82	**59p** / s / 77	**60p** / o / 78	**61p** / s / 74
	di	**62p** / c / 42	**63p** / o / 88	**64p** / s / 77	**65p** / o / 59	**66p** / s / 54

•compound index; ˙state: c = crystalline, o = oil, s = solid; *yield in %

During the last decade, Sharpless-Huisgen cycloaddition reactions[172,173] acquired importance for the rapid merging of two components into one biologically active molecule. For the performance of studies on tissue penetrations by carboranes it seemed useful to combine the cage compounds with known drugs. Thus, the route to an azido derivative from triflate ester was developed contemporaneously. Reaction of the triflate ester with sodium azide carried out under mild conditions proceeded well. However, it gave a mixture of three products, which were difficult to separate. Furthermore, even after successful separation by column chromatography, we could not distinguish between the three products using ^{1}H, ^{13}C and ^{11}B NMR spectroscopy or MS. MS showed *m/z* corresponding to a fragment with formula $C_2B_{10}H_{11}CH_2CH_2CH_2^-$ observed for all three products. Since the starting material and products did not contain any proton signal which could be uniquely assigned to the expected product, we were unable to analyse this mixture by NMR as well.

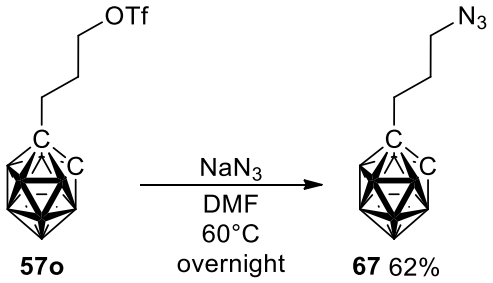

Scheme 27 *Substitution reaction with sodium azide provides a good yield after separation from a mixture of by-products.*

In the meantime, the same compound **67** was independently prepared by Viñas *et al.*[174] and Olejniczak *et al.*[175] under two different pathways (Scheme 28). The first method is an insertion of an alkyne chloride (**68**) into *arachno*-decaborane (**69**) and the second is based on the reaction of lithiated carborane **1o** with 1-bromo-3-chloropropane (**70**) and the subsequent conversion to the product with sodium azide.

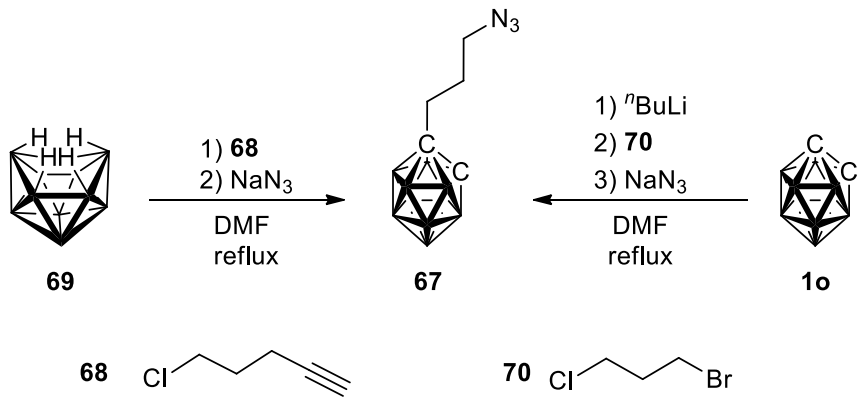

Scheme 28 *Previously published reactions providing the ortho-carborane azide derivative **67**.*

We found an agreement between our ^{1}H NMR experimental data with those in the published articles, for a triplet signal in the range 3.50-3.30 ppm. Unfortunately, in our case, the product exhibiting this signal corresponds to one of the two minor products. This was detected later, when we were able to grow a single crystal of the major product exhibiting a triplet in proton NMR at 4.14 ppm and this unequivocally confirmed the structure of the anticipated azide **67** (Figure 18). Thus, the nature of the product reported by Viñas and Olejniczak, or at least its spectroscopic characterization is dubious. Nevertheless, both groups described successful "click" reactions with alkynes, confirmed from NMR or X-ray structures of the corresponding adducts[174,175]

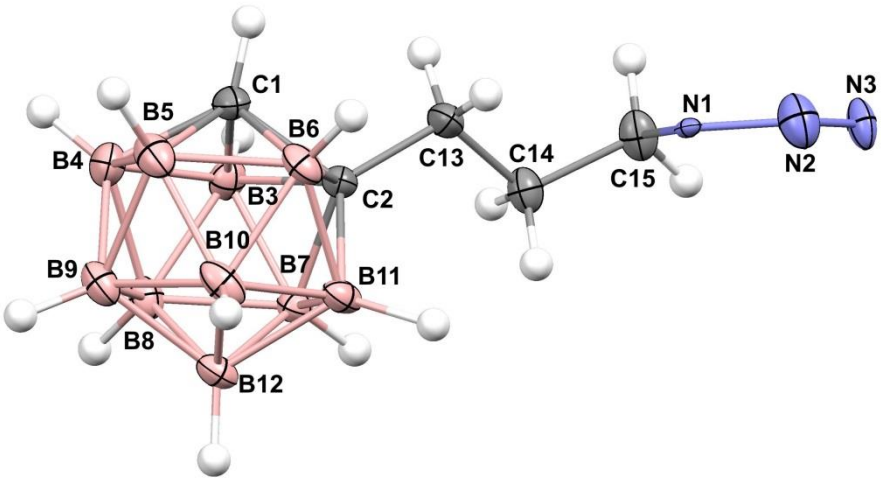

Figure 18 *The compound **67** crystallizes in the monoclinic space group $P2_1/c$ with four molecules within the unit cell. The structure of **67** contains a positional static disorder of the N_3 group and was treated by standard procedures implemented in SHELXL software.*[167] *The*

atoms were split into three positions with occupancy of about 50:30:20. The molecular structure (ORTEP 35% probability level) of ***67*** *is shown with the disorder of N_3 group omitted for clarity. Selected interatomic distances [Å] and angles [°]:C1-C2 1.642(3), C1-B3 1.713(4), C1-B4 1.697(4), C1-B5 1.690(4), C1-B6 1.713(4), N1-C15 1.448(7), N1-N2 1.320(6), N2-N3 1.239(8); C14-C13-C2 114.2(2), C15-C14-C13 112.9(2), N1-C15-C14 106.2(3), N2-N1-C15 117.8(5), N3-N2-N1 123.7(7).*

In summary, we have developed a 5-step synthetic protocol how to prepare sulfonamide derivative of *ortho*-carborane. Obviously, the main advantage of our approach is its versatility and the possibility to apply this protocol to all three isomers of carborane (**1o,m,p**). The isomeric compounds are inaccessible from alkyne-insertion reactions or, as found experimentally, by thermal rearrangement of the products at high temperatures (due to their decomposition). The formation of the respective products is nicely demonstrated by proton NMR, where there is consistent and measurable change in the chemical shift of the methylene protons adjacent to a variety of functional groups (Figure 19). These shifts are a good indication for monitoring the progress of the conversion.

We also observed the formation of pyridinium salt (**56**) during an initial esterification and successfully found a way to avoid this phenomenon.

Finally, we investigated the composition of the mixture of products which forms during the substitution of triflate ester (**57o**) with sodium azide, and we were able, with the support of the X-ray evidence, to identify the proton NMR resonances due to the azide derivative (**67**).[176]

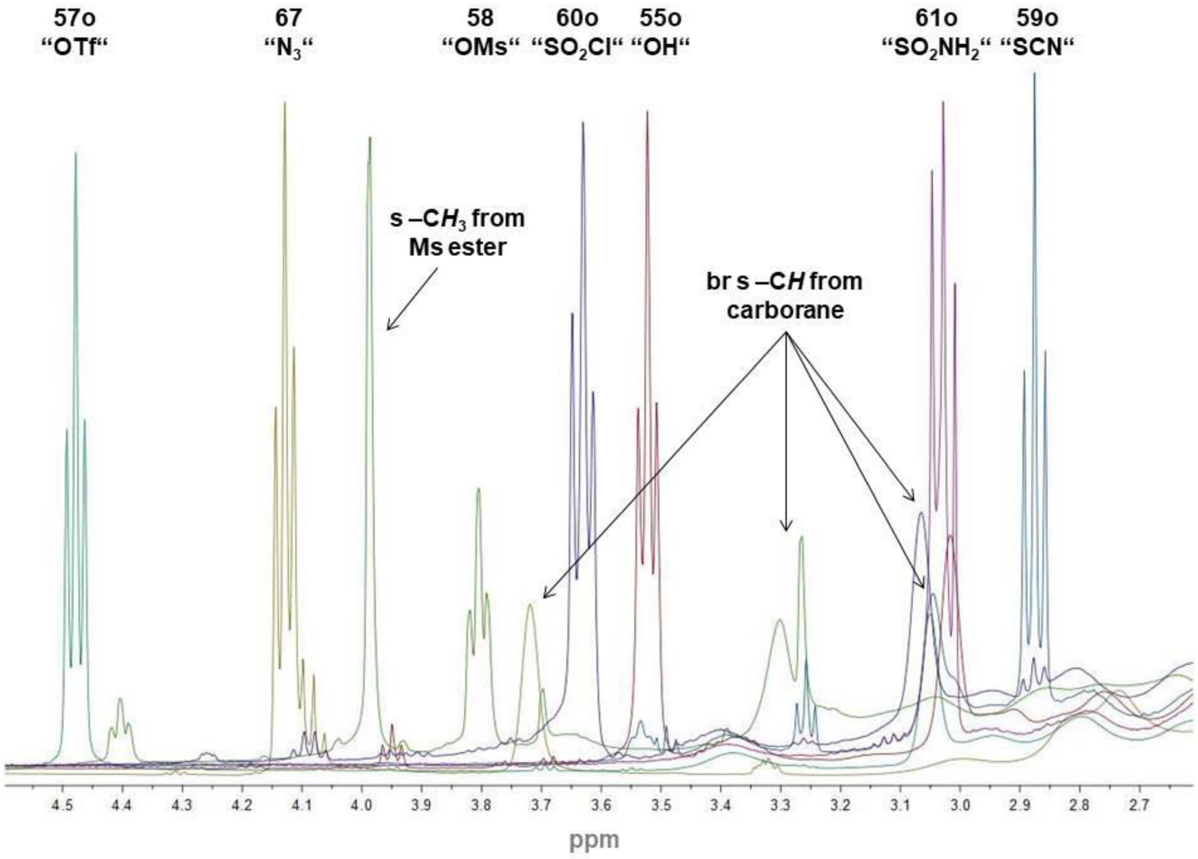

Figure 19 *Superimposed NMR shifts of all ortho-carborane derivatives (**55o**, **57o**, **58**, **59o**, **60o**, **61o** and **67**) (apart from pyridinium salt **56**) are a good evidence of successful reaction conversion.*

2.1.3 DEGRADATION OF CARBORANE CAGE

The chemical stability of the alkyl sulfonamide group in the *closo*-carborane derivatives resembles that of the organic sulfonamide compounds, and, therefore, it withstands attack by strongly acidic or basic reagents with no noticeable decomposition. This feature has been employed to produce a series of substituted eleven vertex *nido*-dicarbollide ions of general formulation $[7\text{-}NH_2SO_2(CH_2)_3\text{-}7,X\text{-}C_2B_9H_{11}]^-$ (**71o** X = 8; **71m** X = 9) and $[7,9\text{-}(NH_2SO_2(CH_2)_3)_2\text{-}7,9\text{-}C_2B_9H_{10}]^-$ (**72**) by using degradation of the cage by excess potassium hydroxide in methanol. The degradation proceeds far more easily than with the parent carborane and can be thus accomplished even in the presence of water in methanol (typically used for quenching these reactions) or with alkaline aqueous solutions. For example, the degradation of *closo*-carborane **61o** to the respective potassium salts of **71o** may be performed using 6% aqueous KOH at 60°C (Scheme 29). The addition of potassium fluoride and prolonged heating at reflux was necessary to remove boron vertices from *closo*-carboranes **61m** and **66m**,

following the procedure developed previously by Fox *et al.*[3] (Scheme 30). These salts can be isolated or converted to sodium salt by metathesis and used in biological assays, or, they can be converted to their triethylammonium salts for better characterisation purposes (potassium or sodium coordinates water, making it difficult to dry them in order to measure appropriate NMR spectra) and for subsequent complexation reactions (Scheme 31). The substitution with alkylsulfonamide groups appreciably increases the water solubility compared to the parent series *nido*-dicarbollide ions.

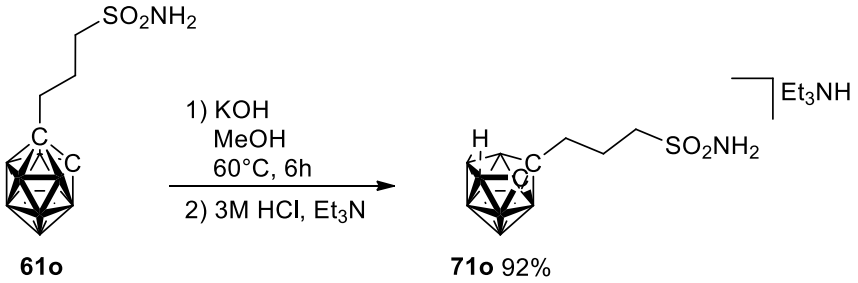

61o **71o** 92%

Scheme 29 *Removal of one boron vertex provides nido-carborane **71o** from ortho isomer **61o** in very good yield.*

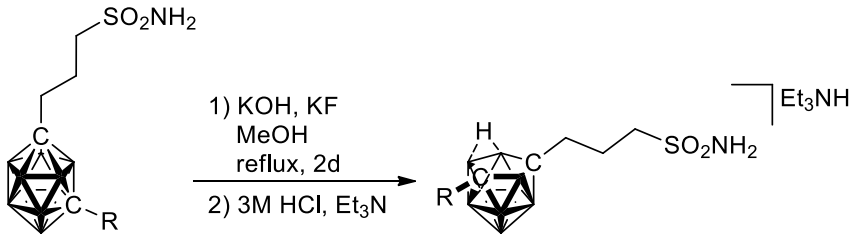

61m R = H
66m R = $(CH_2)_3SO_2NH_2$

71m R = H 74%
72 R = $(CH_2)_3SO_2NH_2$ 68%

Scheme 30 *Removal of one boron vertex provides nido-carboranes **71m** and **72** from meta isomers **61m** and **66m** in very good yields, but only after prolonged heating and in a more basic environment.*

We additionally tried to accomplish insertion reaction of cobalt into a ligand **71m** (Scheme 31). First, the starting *nido* anion was deprotonated to divalent anion **71m**$^-$ in situ using NaH and then we introduced solid cobalt dichloride. Essential here is that all components must be perfectly dried before the reaction. The ambition was to prepare an even more space demanding type of metallacarborane (**73**), but during a pilot experiment, where we observed a corresponding peak on MS, the product decomposed and we were not able to reproduce this reaction again. This type of reaction is well known and has been widely investigated.[4,90,177] It is also known, that the complexation of *nido*-carboranes derived from *ortho*-isomer proceed better than those from the *meta*-isomer. In our case, there must be some kind of an interaction

between $CoCl_2$ and the sulfonamide group. Therefore, we did not succeed to obtain the expected product in this particular reaction.

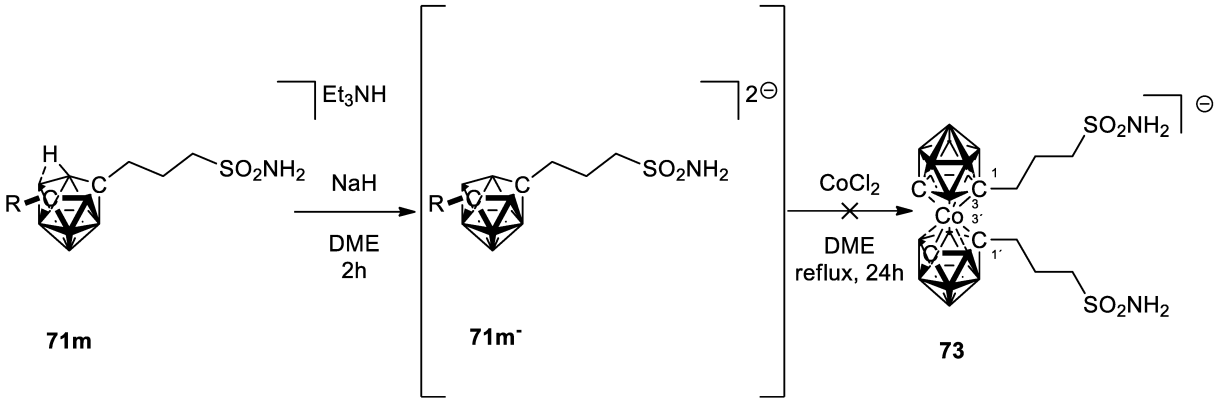

Scheme 31 *Unsuccessful reaction of complexation the cobalt ion with two nido-carborane planes.*

Overall, we have implemented protocols known from organic chemistry on carborane clusters and successfully prepared a series of isomeric *closo*-carborane sulfonamides alongside with their *nido*-congeners. These were the subject of biological studies on *in vitro* and *in vivo* activity and will be discussed in next chapter.

2.1.4 BIOLOGICAL STUDIES

The inhibitory properties of the compounds presented in the previous two sections (see Figure 20 for schematic structures) were tested in *in vitro* using the stopped-flow carbon dioxide hydration assay. In order to assess selectivity, the inhibition of two CA isoforms, the cancer associated CA IX and the widespread CA II, was compared (Table 6). These assays were performed at the Institute of Molecular Genetics by team of Jiří Brynda, Ph.D.

Furthrmore, compounds **51b** and **52b**, as the most potent inhibitors, were tested *in vitro* on malignant cells and for cytotoxicity studies, on distribution penetration into MCSs, pharmacological properties using ADME tests and finally, on *in vivo* antitumour activity. These assays were performed at the Institute of Molecular and Translation Medicine in Olomouc by group of Marián Hajdůch, Ph.D.

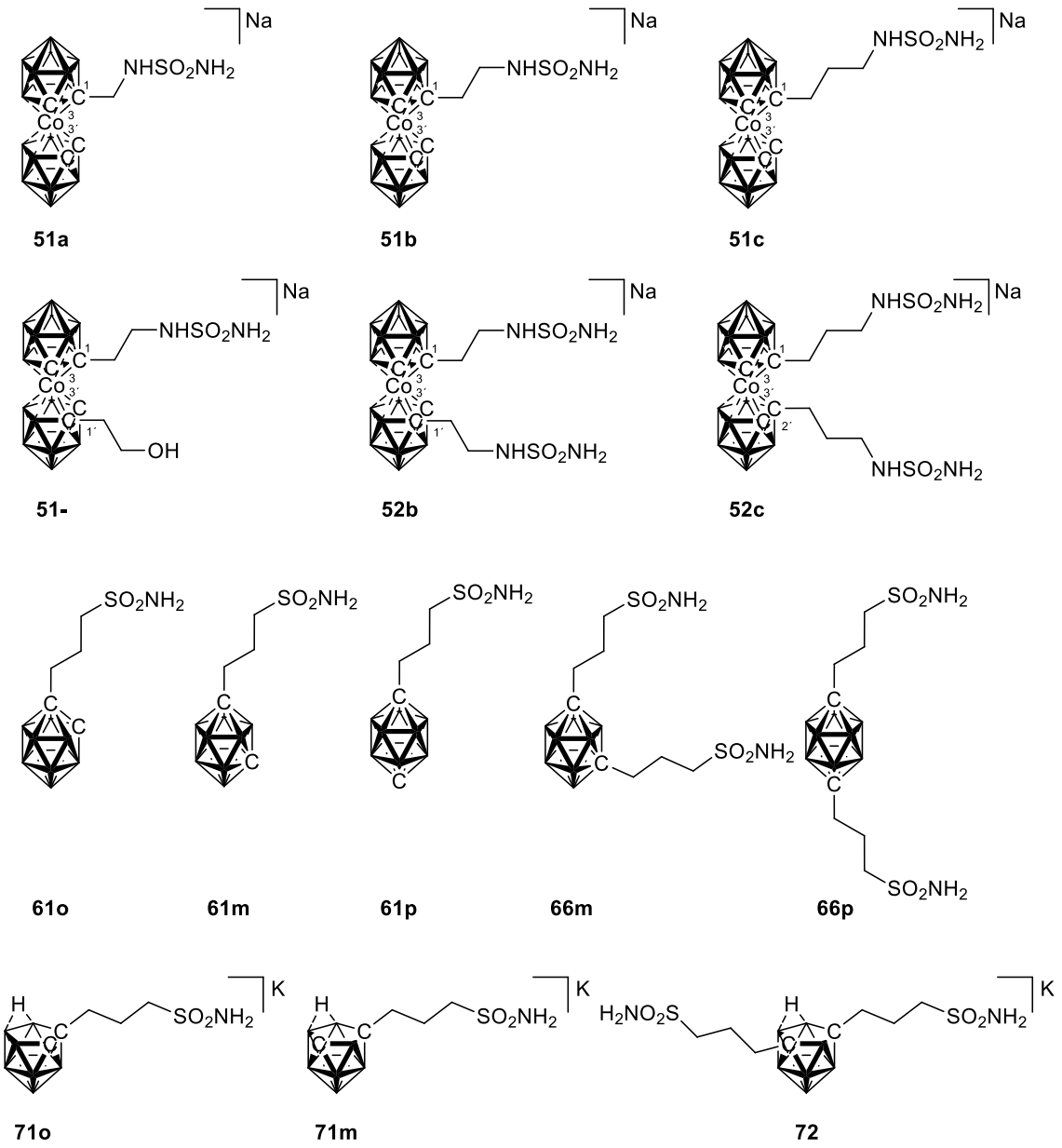

Figure 20 *Graphical representation of prepared cobaltacarborane and closo- and nido-carborane CA IX inhibitors.*

Table 6 *Inhibitory properties and selectivity of compounds summarized in Figure 20.*

Compound	K_i (CA II) [nm]	K_i (CA IX) [nm]	Selectivity index[‡]
51a	5.85 ± 1.20	0.116 ± 0.02	50.5
51b	25.80 ± 10.80	0.063 ± 0.03	410.0
51c	335.90 ± 101.00	0.649 ± 0.09	517.6
51-	23.93 ± 3.08	0.661 ± 0.10	36.0
52b	35.38 ± 3.42	0.560 ± 0.07	63.0

52c	31.72 ± 4.30	0.739 ± 0.08	42.9
61o	622.04 ± 177.40	0.506 ± 0.11	1229.3
61m	253.90 ± 22.83	0.953 ± 0.09	267.3
61p	170.50 ± 16.92	10.536 ± 1.12	16.2
66m	42.45 ± 6.05	0.241 ± 0.03	176.9
66p	42.30 ± 5.14	2.113 ± 0.28	20.0
71o	1546 ± 385.93	1.178 ± 0.12	1312.4
71m	1680 ± 191.90	3.192 ± 0.41	526.3
72	11.67 ± 1.88	2.425 ± 0.23	4.8

[‡]Selectivity index is the ratio between K_i (CA II) and K_i (CA IX)

All cobaltacarborane compounds **51a-c**, **51-** and **52b,c** show high inhibitory activity against CA IX with K_i values in the low nanomolar to subnanomolar range and substantial selectivity toward CA IX over CA II. This activity is further improved when the linking group is elongated by one methylene unit in **51b**, giving a K_i value of 63 pM. At this point, corresponding to an ethylene chain between the metallacarborane cage and sulfamide group, the length of the linker group seems to have reached an optimum for affinity toward the CA IX isoform. Further elongation to a propylene chain length, as in **51c**, leads to a K_i value that is one order in magnitude higher. The presence of a second polar alkylsulfamide or hydroxy group on the cage reduces the *in vitro* activity. A slight drop in K_i values can be also observed between the **52b** and **52c**, however, these two compounds represent different diastereoisomers and thus, the effect would not be directly comparable. The compounds show selectivity for the CA IX isozyme over the cytosolic hCA II with a selectivity index from 42 to 518. Cobaltacarborane compounds have about six orders of magnitude lower K_i values toward CA IX and an almost 28-fold increase in selectivity against the CA IX isozyme compared to the previously[92] explored series of carborane inhibitors.

The inhibitory activity of carborane compounds **61o,m,p**, **66m,p**, **71m,p** and **72** against CA IX ranged from micromolar to low nanomolar K_i values and also the selectivity toward CA IX over CA II differed substantially among compounds. High inhibitory activity against CA IX (with K_i values in the low nanomolar range) was observed for compounds with longer alkyl linker interconnecting sulfonamide moiety with the cluster. The alkyl linker length optimal for CA IX affinity was three atoms. Compounds **61o,m** and **66m** have subnanomolar, and the rest

of carborane compounds have low nanomolar K_i values toward CA IX and a significantly reduced selectivity.

Structure of cobaltacarborane inhibitors in the CA IX active site.

Compounds **51a** and **51b** were selected for structural studies to explore their interaction with the CA IX active site. Compounds were co-crystallized with the CA IX mimic: CA II enzyme containing seven amino acid residue substitutions: A65S, N67Q, E69T, I91L, F130V, K169A, and L203A. This variant is often used in structural studies as it retains the good crystallization properties of CA II while the active site resembles CA IX.[87,178] Two crystal structures were determined at atomic resolution of 1.1 Å and confirmed specific binding of **51a** and **51b** in the active site of CA IX (Figure 21). The structural studies were carried out at the Institute of Organic Chemistry and Biochemistry by team of Pavlína Řezáčová, Ph.D.

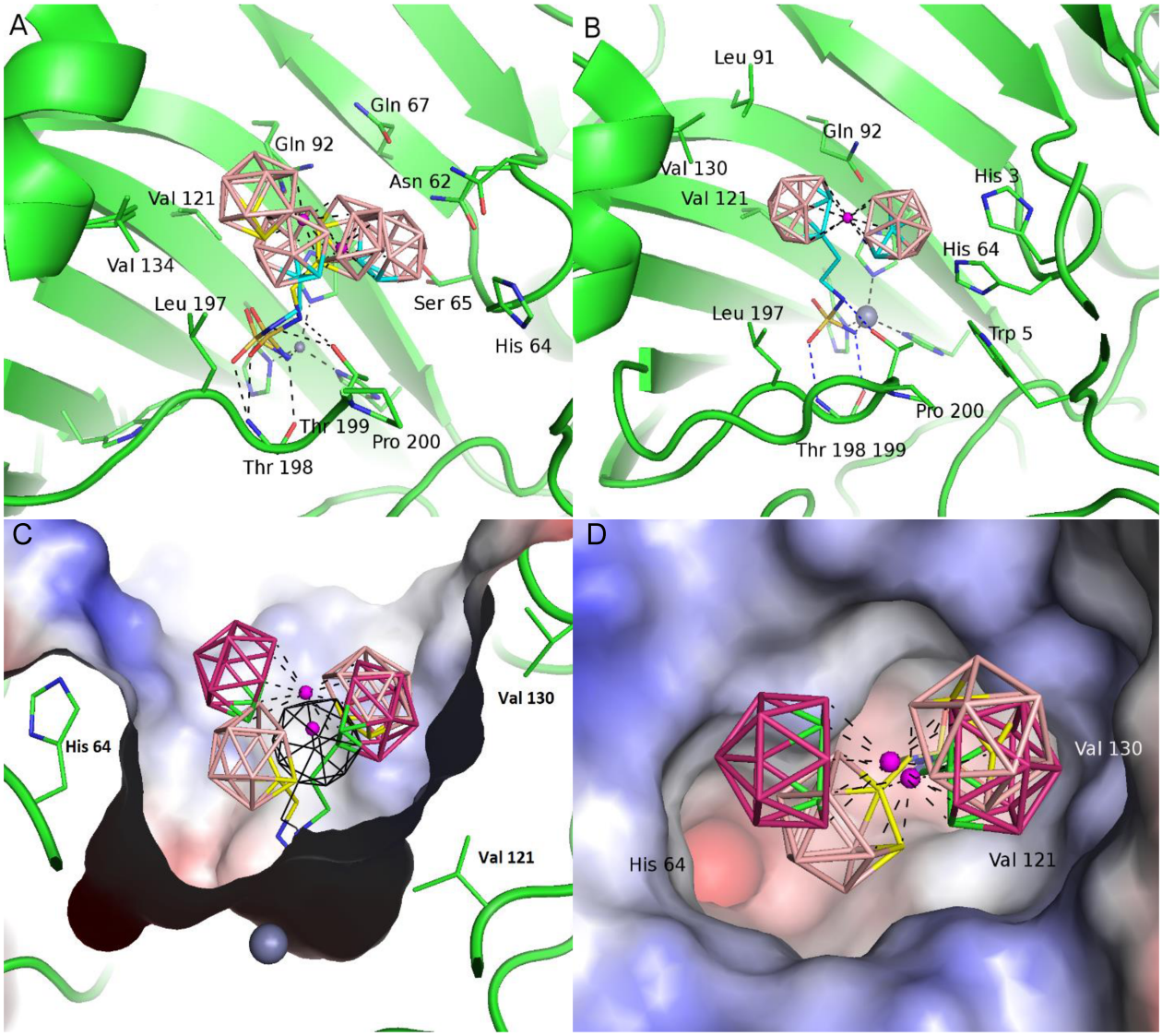

Figure 21 *Structure of compounds **51a** (A) and **51b** (B) bound to the CA IX active site. Compounds are depicted with a stick model and with the cobalt atom shown as maroon spheres.*

*Coordination bonds with the cobalt atom are depicted by black dashed lines and interacting residues highlighted as sticks. Protein is shown in green cartoon representation with interacting residues highlighted as sticks. Top view (C) and side view (D) into the CA IX active site, which is represented by its solvent accessible surface coloured by electrostatic potential (red for negative, blue for positive). Superposition of **51a** (borons coloured light pink, only dominant alternative conformation is shown for clarity), **51b** (boron atoms coloured dark pink). In panel (C), superposed pose of carborane sulfamide inhibitor in CA II (PDB code 4MDG[179]) is showed as black lines.*

The electron density map in the active site of the CA IX indicated that compound **51a** assumes two alternative conformations while **51b** is bound in one single binding mode (Figure 22). The sulfamide moiety is deeply buried in the active site, where it makes polar interactions with the zinc ion and protein residues located at the bottom of the active site cavity (His94, His96 and His119). This binding mode is similar to the typical interactions with the enzyme active site reported for organic sulfamide-containing inhibitors.[180–182] The cobaltacarborane cluster of **51a** occupies two alternative binding sites. The preferred conformation 1 interacts by 84 interatomic contacts with: Asn62, Ser65, Gln67, Leu91, Gln92, His94, Val130, Val134, Leu197 and Thr198-199. Conformation 2 makes 147 interactions with Trp5, Asn62, His64, Ser65, Gln67, Gln92, His94, Leu197, Thr198-199, and Pro200. Cobaltacarborane cluster of the **51b** interacts through 89 interatomic contacts with His3, Trp5, Asn62, His64, Leu91, Gln92, Val121, Val130, Leu197, Thr198-199, and Pro200. Crystal structures explained high inhibitory affinity of compounds **51a** and **51b** by efficient interaction of bulky cobaltacarborane cage with the enzyme active site.

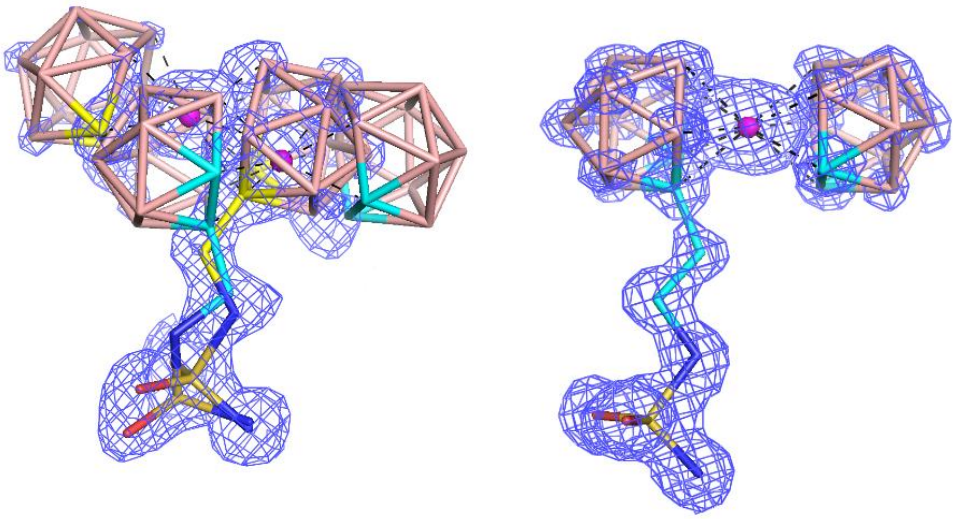

Figure 22 *Compounds **51a** (left) and **51b** (right) bound to the active site of CA IX-mimics. 2Fo-Fc map contoured at 1 σ is shown. Compound **51a** was modelled in two alternative conformations with partial occupancy 0.5 and 0.3, respectively. Compound **51b** was modelled in one conformation with full occupancy.*

Both compounds, **51a** and **51b**, have one dicarbollide ligand of the cobalt bis(dicarbollide) sandwich interacting with hydrophobic pocket formed by Val130 and Val134. However, the compound **51a** has the second dicarbollide part buried within a hydrophilic pocket loop Asn62 – Ser65 located deeper in the enzyme cavity. Due to the longer linker in **51b** the dicarbollide ligand interacts with hydrophilic patch formed by the N-terminal part of protein. Extensive interactions of cages with hydrophobic pocket containing Val130 explains the high selectivity of the compounds toward CA IX. Isoform CA II contains a phenylalanine residue in the position normally occupied by Val130 and this bulky sidechain significantly changes the shape of the active site.

Cobaltacarborane inhibitors preferentially reduce survival of malignant cells *in Vitro.*

Compounds **51a,b,c** and **52b,c** were further tested at the Institute of Molecular and Translation Medicine at Palacký university in Olomouc, under normoxic conditions on a panel of 11 cell lines derived from malignant issues and 2 prototypes of non-malignant fibroblast cell lines using a standard MTT assay (Table 7). The IC_{50} values of most of the compounds varied among the cell lines. Consistent with the proposed mechanism of CA IX inhibition, the compounds showed moderate cytotoxicity in tumour cells regardless of histogenetic origin and drug resistance characteristics. However, the compounds were consistently less cytotoxic in

non-malignant BJ and MRC-5 cells, thus demonstrating a favourable *in vitro* toxicology profile. Interestingly, MDCK cells were not sensitive to cobaltacarborane cytotoxicity regardless of CA IX expression, most likely reflecting their non-malignant and/or non-human origin. Cumulatively, the cytotoxicity data suggest that CA IX inhibitors preferentially reduce the survival of malignant but not non-malignant cell lines, regardless of whether the cells express the target.

Table 7 *Cytotoxicity of compounds against a panel of cell lines.*

compound / cell line	**51a**	**51b**	**51c**	**52b**	**52c**
MRC-5	93±7	98±4	>100	96±7	>100
BJ	>100	>100	>100	>100	>100
CCRF-CEM	85±2	67±3	71±6	69±7	69±1
CEM-DNR	100±0	86±4	44±7	82±2	76±5
K652	99±2	>100	98±2	80±1	75±4
K652-TAX	66±8	74±2	67±3	100±1	99±3
A549	>100	85±3	>100	>100	>100
HCT116	75±4	50±1	52±3	79±1	88±1
HT-29	>100	78±9	>100	>100	>100
HeLa	90±2	>100	>100	97±7	>100
4T1-12B	>100	>100	>100	>100	>100
MDCK-CA IX	>100	>100	>100	>100	>100
MDCK-NEO	>100	>100	>100	>100	>100

IC_{50} (μM) values are presented as mean ± SEM of four independent experiments.

The evaluation of cytotoxicity and/or inhibitory activity of **51b** and **52b**, the time-dependent effect of the compounds on MCSs of CA IX-positive HT-29 and CA IX-negative HCT116 cells (Figure 23) were measured. In parallel, the cytotoxicity of **51b** and **52b** in 2D cultures under normoxic conditions was determined. There was no significant difference in the cytotoxicity of **51b** and **52b** in normoxic 2D cultures following treatment for 3-7 days (Figure 23A), although there was a slight increase in the IC_{50} of **51b** in HT-29 cells between days 3 and 7. To determine the effect of **51b** and **52b** in MCSs, 3-day-old MCSs were treated for 3 to 7

days, and the change in MCS size was recorded. Treatment with both compounds resulted in a time-dependent decrease in MCS size; however, the effect was more pronounced in MCSs of HT-29 cells (Figure 23A). This time-dependent effect of **51b** and **52b** on MCS size was proportional to a time-dependent increase in CA IX expression in MCSs in the absence of inhibitors, particularly in HT-29 cell MCSs (Figure 23B, C).

A

	HCT116				HT-29			
	Day 3		Day 7		Day 3		Day 7	
	2D	MCS	2D	MCS	2D	MCS	2D	MCS
51b	50±1	109±1	49±0	78±2	79±9	>500	52±9	141±39
52b	79±1	125±2	58±2	84±16	>100	>500	>100	59±12

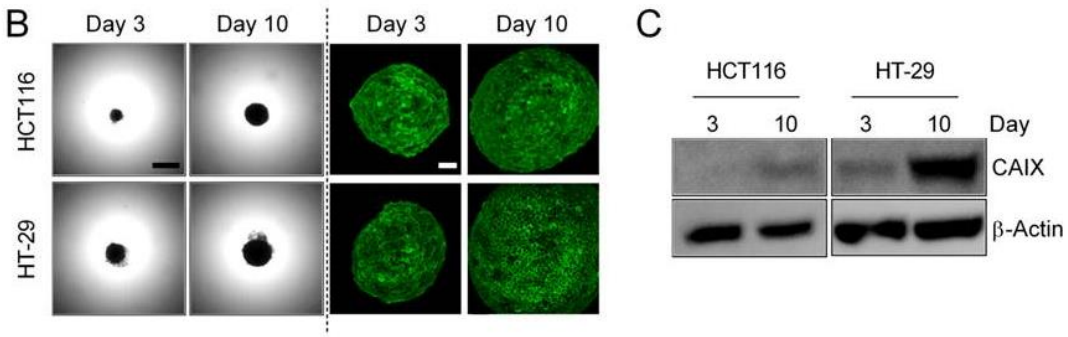

Figure 23 *Effect of **51b** and **52b** in 2D and MCS cultures. (A) IC_{50} values (μM) of **51b** and **52b** in 2D and MCS cultures of HCT116 and HT-29 cells following 3 to 7 days of treatment under normoxic condition. IC_{50} in 2D cultures were determined by MTT cell proliferation assay, whereas, those in MCS cultures were determined based on changes in MCS size over time. Data are mean ± SEM of 3-5 independent experiments. (B) Increase in MCS size results in the upregulation of CA IX (green) expression in MCSs. Objective: 5x, scale bar: 500 μm (brightfield images) and 50 μm (immunostained images). (C) Representative western blots showing a time-dependent increase in the expression of CA IX in MCSs of HCT116 and HT-29 cells. n = 2-3.*

Cobaltacarborane inhibitors affect the intracellular distribution of CA IX.

To determine the interaction of **51b** and **52b** with CA IX in HT-29 cells, the cellular distribution of the compounds was determined by Raman spectroscopy followed by immunofluorescence to measure CA IX expression (Figure 24). The presence of **51b** and **52b** was detected using specific marker bands at 202 cm^{-1} and 193 cm^{-1}, respectively, in Raman maps of treated cells (Figure 24A, B). This marker corresponds to the characteristic vibration

between a cobalt atom and dicarbollide ligands. Immunostaining of HT-29 grown under hypoxic conditions showed that **51b** has a greater effect on CA IX localization compared to cells treated with **52b** and untreated cells (Figure 24C). CA IX was re-distributed from the cell surface to the cytoplasm and nucleus of inhibitor-treated cells. Raman spectroscopy corroborated these results, indicating the presence of more **51b** in the nucleus than cytoplasm of treated cells (Figure 24A, B). On the other hand, **52b** was preferentially present in the cytoplasm, in agreement with the cytoplasmic membrane localization of CA IX upon treatment with **52b** (Figure 24A, B). Quantitative comparisons of Raman intensity showed that the signal intensity for **51b** corresponds to a nearly 25 mM concentration in nuclei and 19 mM in the cytoplasm (Figure 24D). The signal for **52b** corresponds roughly to 5 mM in nuclei and 9 mM in the cytoplasm (Figure 24D), indicating that approximately five-fold more **51b** than **52b** is localized in nuclei and only two-fold more in the cytoplasm.

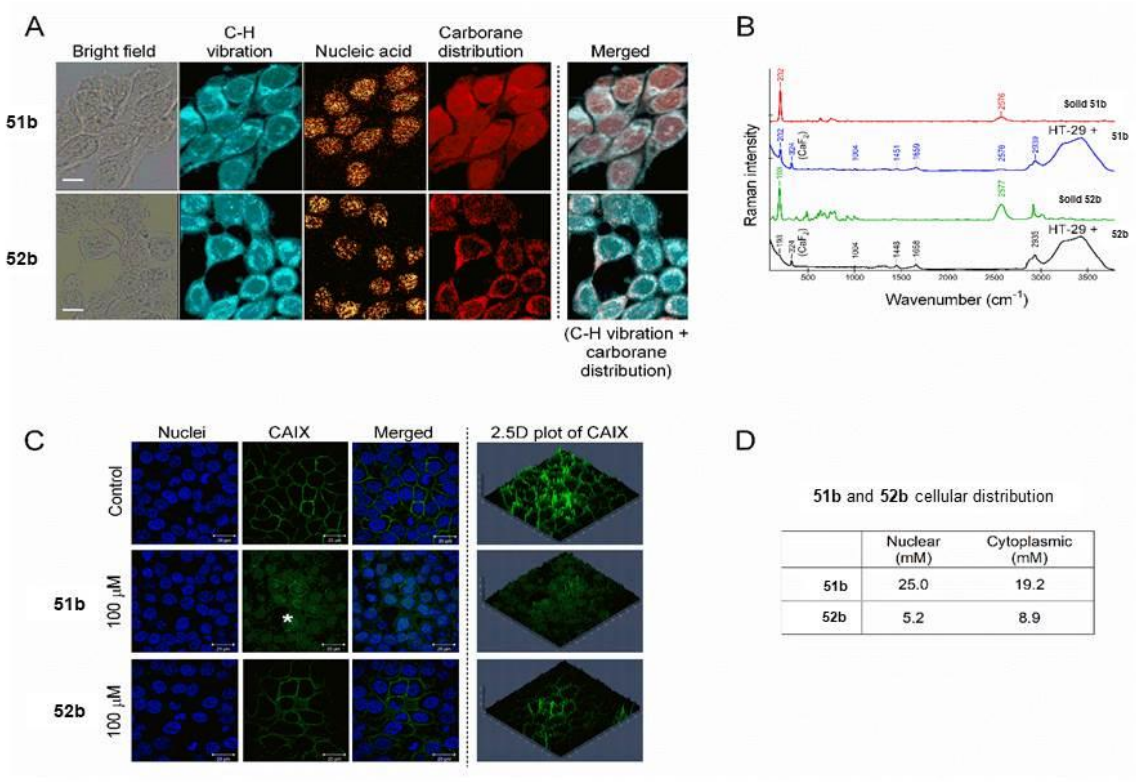

Figure 24 *Raman spectra showing distribution of **51b** and **52b** in HT-29 cells. (A) HT-29 cells treated with 100 µM **51b** and **52**$^{-}$ for 12 hours. From left to right: microscopic bright-field image (scale bar 10 µm); distribution of C-H stretching vibrations at 2800 cm^{-1} - 2950 cm^{-1}; distribution of nucleic acid marker at 790 cm^{-1}; distribution of **51b** and **52b** according to Raman marker bands at 202 cm^{-1} and 193 cm^{-1}, respectively; merged image of C-H vibrations and*

*carborane distribution. (B) Raman spectra of **51b** and **52b** in solid form are shown in red and green, respectively; the typical appearance of **51b** and **52b** Raman marker bands on the background of the HT-29 cell fingerprint are in blue and black, respectively. The band at 324 cm^{-1} corresponds to CaF_2 substrate. (C) Images showing the changes in expression of CA IX in HT-29 cells treated with 100 μM **51b** and **52b** for 12h. (D) The average concentration (mM) of **51b** and **52b** in the nucleus and cytoplasm of HT-29 cells based on Raman measurements.*

Faciliated DOX penetration into MCSs.

As treatment with **51b** affected CA IX distribution in 2D cultures (Figure 24C), our colleagues next followed CA IX expression and distribution in MCSs of HT-29 cells treated with **51b** and **52b** and determined whether CA IX inhibition facilitates the penetration of DOX (Figure 26), a prototypal anticancer molecule with fluorescent properties. Western blot analysis of MCS lysates indicated that both **51b** and **52b** (at 60 μM concentration) significantly downregulated the expression of CA IX in MCSs (Figure 25A). Immunostaining of MCSs showed that **51a** changed the distribution of CA IX in cells (Figure 25B), similar to what was observed in 2D cultures (Figure 24C).

Redistribution of CA IX may affect the composition of the extracellular matrix *via* modulation of matrix metalloproteinases activities,[183] resulting in aberrant penetration of cytotoxic drugs into tissues.[184] To test the hypothesis that **51b** and **52b** affect penetration and/or accumulation of cytotoxic drugs, MCSs were treated with DOX in combination with either **51b** or **52b** and imaged every 10 min for 120 min by light sheet fluorescence microscopy. Treatment with **51b** and **52b** greatly facilitated the accumulation of DOX (Figure 25C, D). As the increased anti-CA IX activity of **51b** is associated with the presence of a methylene sulfamide functional group, the MCSs with DOX in the presence of cobalt bis(dicarbollide) ion, a compound lacking the methylene sulfamide functional group were than treated. This ion did not have a major effect on DOX penetration (Figure 25D). In addition to increasing DOX penetration over time, **51b** affected MCS integrity (Figure 25D). A line plot across the MCS surface at 50 μm depth indicates an increased accumulation of DOX in MCSs treated with **51b** (Figure 25E). Altogether, these data reveal better penetration of DOX in MCSs co-treated with cobaltacarborane CA IX inhibitors and suggest the potential for future synergistic combinations to combat human cancers.

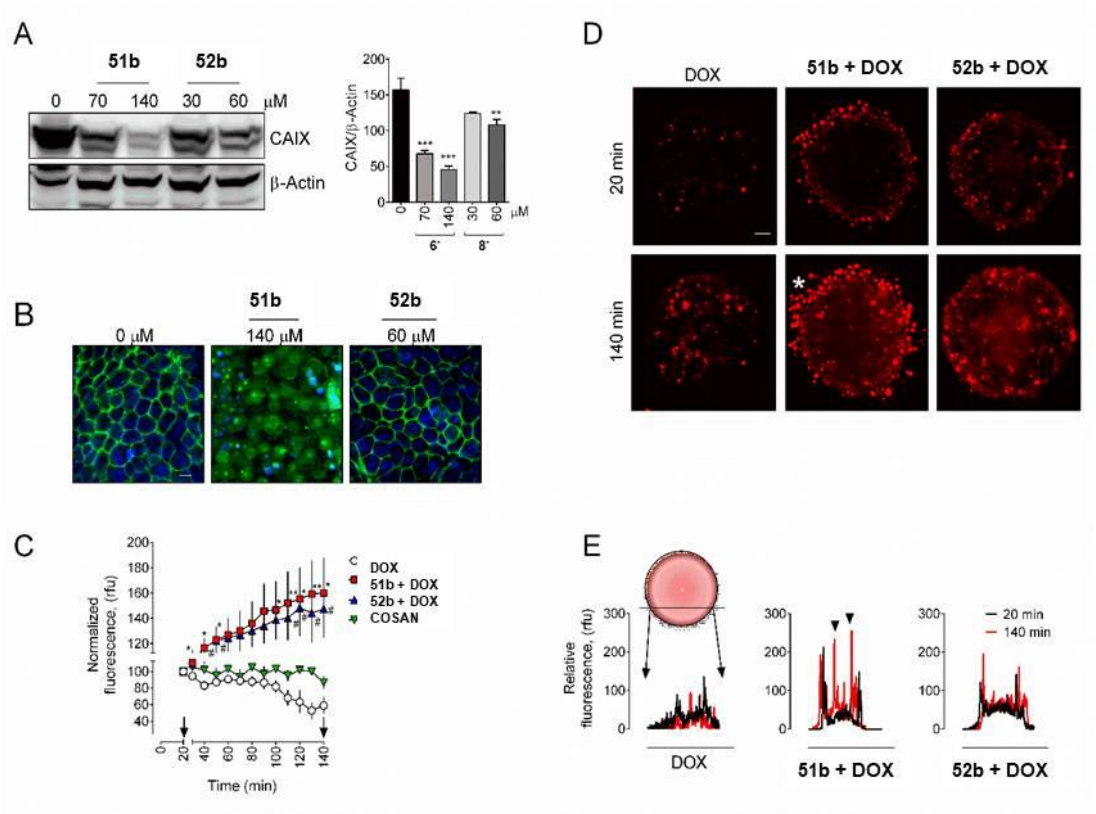

Figure 25 *Effect of **51b** and **52b** on CA IX expression and DOX accumulation in MCSs of HT-29 cells. (A) CA IX expression in MCSs treated with **51b** or **52b** for 3 days with the indicated concentrations. Data are mean ± SEM from 3-5 independent experiments (B) Immunostaining of drug-treated MCSs shows the downregulation of CA IX by **51b**. Images are enlarged sections of the MCS surface. Nuclei are stained blue with Hoechst. 33342. 5x objective, scale bar: 50 µm. (C) Graph showing the rate of DOX accumulation in MCSs treated with DOX only, 430 µM **51b** in combination with DOX (**51b** + DOX), 180 µM **52b** in combination with DOX (**52b** + DOX), and 430 µM cobalt bis(dicarbollide) ion in combination with DOX [cobalt bis(dicarbollide) ion + DOX] 140 min after the beginning of the experiment (120 min of treatment; the treatment period is indicated by arrows). Data are mean ± SEM of at least 2 MCSs per treatment type from 3 independent experiments. The DMSO concentration in treated samples in (A-C) was always below 0.5%. (D) Representative images of DOX accumulation at 50 µm z-plane height in MCSs treated with DOX alone or in combination with **51b** or **52b** at the indicated time points. Note the effect of 6⁻ on MCS integrity (indicated by an asterisk). 5x objective, scale bar: 20 µm. (E) A plot of DOX intensity along the line profile in images from (D) shows increased accumulation of DOX in the interior of MCSs treated with **51b** (indicated by arrowheads).*

Pharmacological properties.

Results from ADME assays revealed that **51b** and **52b** are stable in the presence of plasma proteins and are very slowly metabolized by microsomes (Table 8). This is evident from the low value of intrinsic clearance, which indicates that there is a high probability that the compounds will not be primarily metabolized in the liver. Both **51b** and **52b** bound to plasma proteins with more than 99% affinity. The passive diffusion mechanism for both compounds through the PAMPA membrane was classified as medium compared with other commonly used drugs. The limited intercellular diffusion of **51b** and **52b** may further increase the CA IX/CA II specificity index because intracytoplasmic CA II protein will be less available for the cobaltcarborane inhibitor. The compounds showed poor permeability in MDCK-MDR1 cells, indicating a low potential for penetration through the blood-brain barrier. Furthermore, the low permeability of **51b** and **52b** in Caco-2 cells suggests that the compounds are likely not suitable for oral administration due to their poor absorption through the intestine.

Table 8 *Pharmacological properties of **51b** and **52b** determined by in vitro and in vivo ADME assays.*

Compounds	Metabolism			Permeability			
	in vitro			*in vitro*		*in vivo*	
	Plasma stability (category)	Plasma protein binding (% bound)	Microsomal stability (clearance)	PAMPA		MDR1-MDCK	Caco-2
				Category	%recovery	CNS (-ive/+ive)	Category
51b	Stable	99.8	Low	Medium	86.4	CNS: -ive Efflux ratio: 1.7 Active efflux: No % recovery: 38.1	Low Efflux ratio: 0.8 Active efflux: No % recovery: 20.0
52b	Stable	99.3	Low	Medium	72.7	CNS: -ive Efflux ratio: 14.1 Active efflux: Yes % recovery: 87.3	Low Efflux ratio: 42.0 Active efflux: Yes % recovery: 81.0

The plasma concentration-time profiles of **51b** and **52b** following IP administration to NMRI mice at a maximum tolerated dose (MTD) of 125 mg/kg were determined over 36 hours. The compounds were administered as sodium salts in a vehicle comprising 10% DMSO. Apart from initial symptoms of somnolence following **51b** and piloerection following **51b** and **52b**, there were no visible signs of major toxicity on animal behaviour, appearance, or body weight. The maximum concentrations (C_{max}) of boron and cobalt in serum at the MTD were 661 μM for **51b** at 3 hours and 404 μM for **52b** at 6 hours. The serum half-life ($t_{1/2}$) of **51b** was 4.8h and

15.6h for **52b**. The MTD for repeated dose toxicity delivered once (**51b**) or twice (**52b**) daily for 5 days in two cycles with two days in between cycles was 62.5 mg/kg for both compounds.

Antitumour activity in mouse models of mammary and colorectal tumours.

Next, the *in vivo* antitumour activity of **51b** and **52b** in two mouse models were explored: (i) syngenic mouse mammary tumours of 4T1-12B cells orthotopically transplanted into the mammary glands of Balb/c mice and (ii) human colorectal cancer HT-29 cells xenotransplanted into SCID mice. Treatment with **51b** and **52b** significantly decreased the 4T1-12B tumour size over the first 10 days. A significant effect on tumour size was also observed after 22-32 days of treatment with **51b** compared to vehicle-treated animals (Figure 27A).

Both **51b** and **52b** significantly reduced the tumour size compared to vehicle-treated controls in SCID mice xenotransplanted with HT-29 over the entire period of the experiment (Figure 27B). To better compare these effects, U-104 was included (Figure 26), a reference CA IX inhibitor being evaluated in clinical trials.[185] Interestingly, the effect of U-104 was less than those of **51b** and **52b** in SCID mice. The tumour sizes after 24 days in mice treated with **51b**, **52b** and U-104 were 68%, 75%, and 87% of the vehicle-treated tumours, respectively.

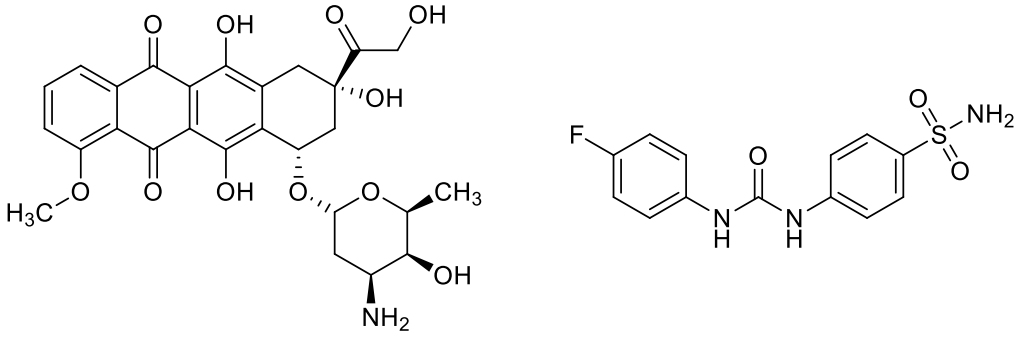

Figure 26 *Structures of doxorubicin (**DOX**) and **U-104**.*

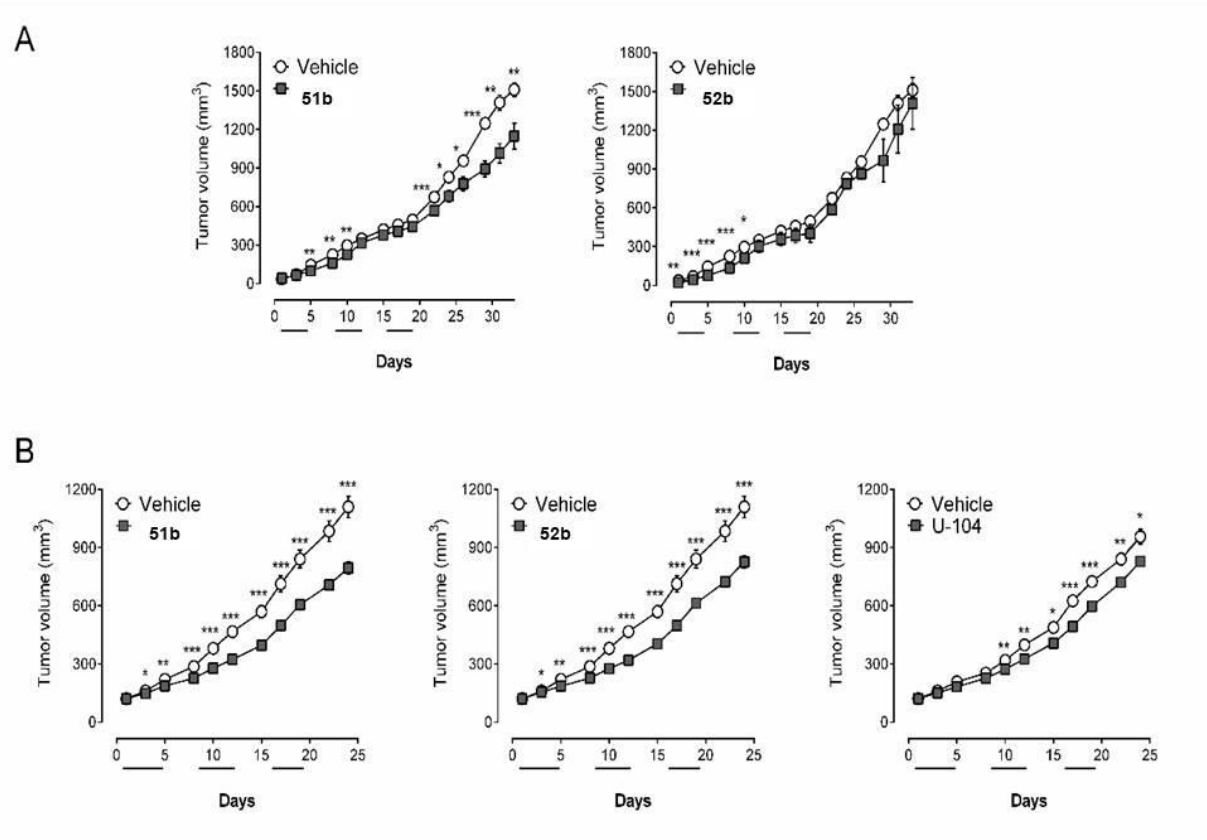

Figure 27 *In vivo antitumour activity of **51b** and **52b**. (A) Graphs showing the effect of **51b** and **52b** on tumour size in female BALB/c mice orthotopically transplanted with 4T1-12B cells over a period of 33 days. (B) Graphs showing the effect of **51b**$^{-}$, **52b** and U-104 over a period of 24 days in female SCID mice bearing subcutaneously transplanted HT-29 cell tumours. Mice were administered **51b** and **52b** twice and once per day, respectively, at a dose of 62.5 mg/kg. U-104 was administered once per day at a dose of 0.76 mg/kg for 3 weeks. Dosing schedules are shown by the black solid lines in the x-axes. Data in (A) and (B) are mean ± SEM of 4 experiments.*

Structure of carborane Inhibitors in the CA IX Active site.

Two compounds with the two of the highest affinity toward CA IX, **61o** and **71o**, were selected for structural studies to explore their interaction with the CA IX active site. The compounds were co-crystallized under the same condition with CA IX mimic, CA II enzyme containing seven amino acid residue substitutions in the active site (same as above A65S, N67Q, E69T, I91L, F130V, K169A, and L203A). Two crystal structures were determined at an atomic resolution of 1.2-1.1 Å and confirmed the specific binding of **61o** and **71o** in the CA IX active site.

The binding conformation of **71o** molecule is extended, with second carbon to sulfur atom in a *trans* position to the nitrogen atom of the sulfonamide group, whereas **61o** displays a

gauche conformation between the second and third carbon atoms in the aliphatic chain and the second carbon atom in chain is in a *trans* position to the O2 atom of the sulfonamide group (see comparison Figure 28 and Figure 29). The hydrophobic carborane clusters interact with the hydrophobic pocket formed by Leu91, Val121, Val131, Val135, Leu141 and Leu198. Adaptation of the sidechains atoms forming the binding pocket is most pronounced on Leu91 and Gln92. One may speculate that the extended conformation of **71o** is caused by dihydrogen bonding[186,187] between the hydrogen of the amino group of Gln92 and a terminal hydrogen atom on a boron vertex of the carborane cage.

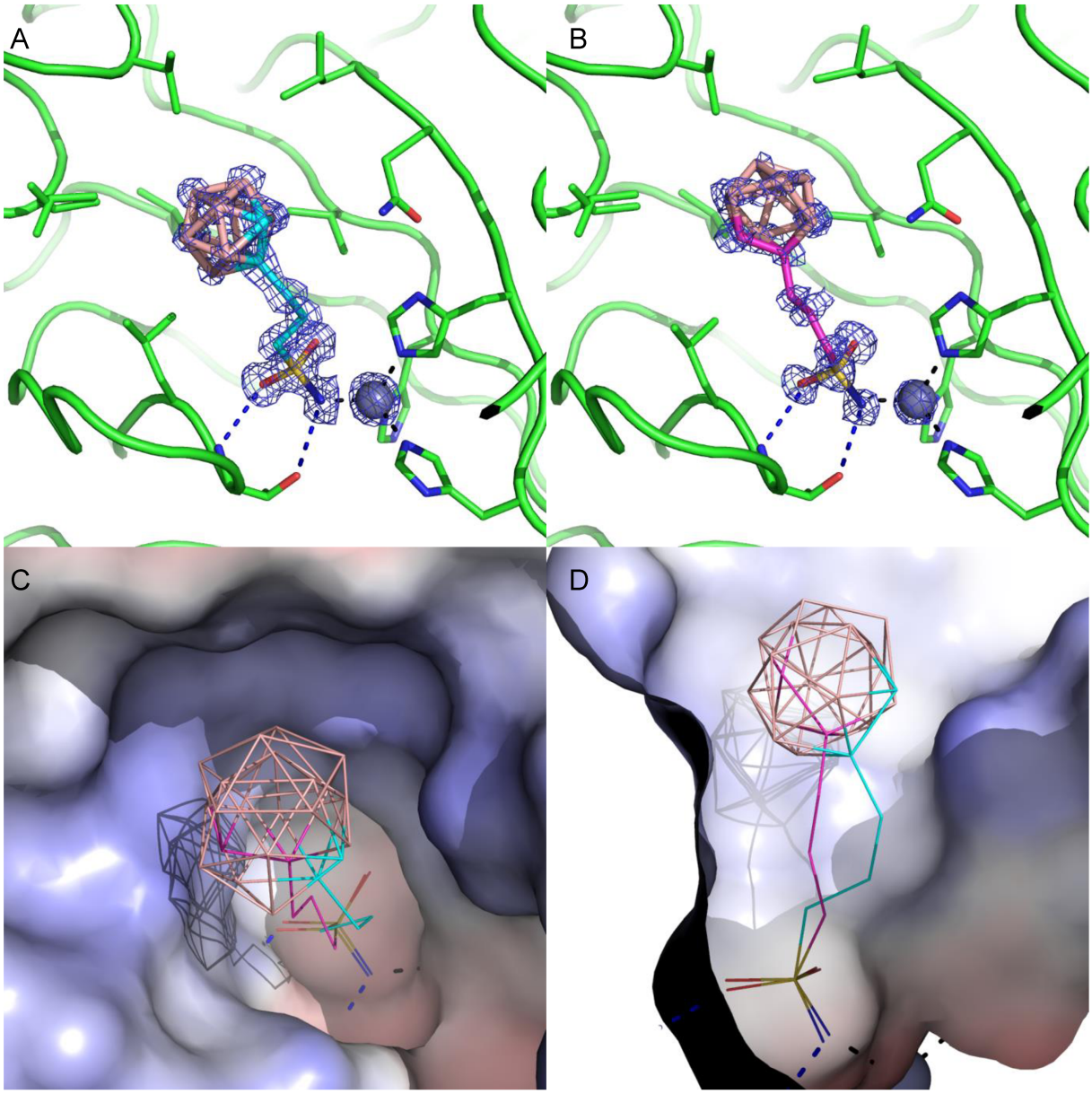

Figure 28 *Structure of compounds **61o** (A) and **71o** (B) bound to the CA IX active site. Compounds are depicted in stick model. Protein is shown in green cartoon representation with interacting residues highlighted as sticks. Top view (C) and side view (D) into the CA IX active site, which is represented by its solvent accessible surface coloured by electrostatic potential*

*(red for negative, blue for positive). Superposition of **61o** (borons coloured light pink, only dominant alternative conformation is shown for clarity), **71o** (boron atoms coloured light pink).*

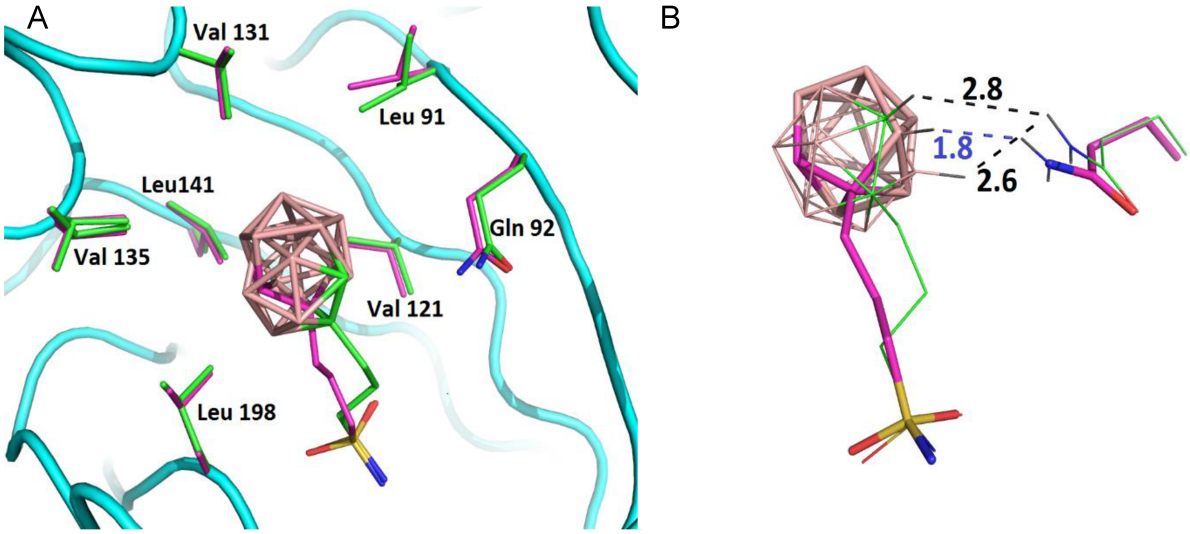

Figure 29 *Detailed comparism of closo- (**61o**) and nido-carborane (**71o**) sulfonamides. In both cases are compounds stacked over each other. A) Overall view on position of inhibitors in CA IX active site. B) Detailed look on positions of **61o** and **71o**. The difference is caused by greater acidity of B-H protons on the open-face of **71o** which is caused by charge delocalisation and leads to formation of a dihydrogen bond B-H-H with Gln92.*[188]

A further nice example of the binding of **66p** in the CA IX mimic active site was determined. One functional sulfonamide group is coordinated to a zinc atom while the other sulfonamide group is reaching out of the cavity into solution. The electron density is equally distributed. Also, further evidence of the formation of dihydrogen B-H-H bond between hydridic B-H vertex and NH_2 group of Gln92 is shown.

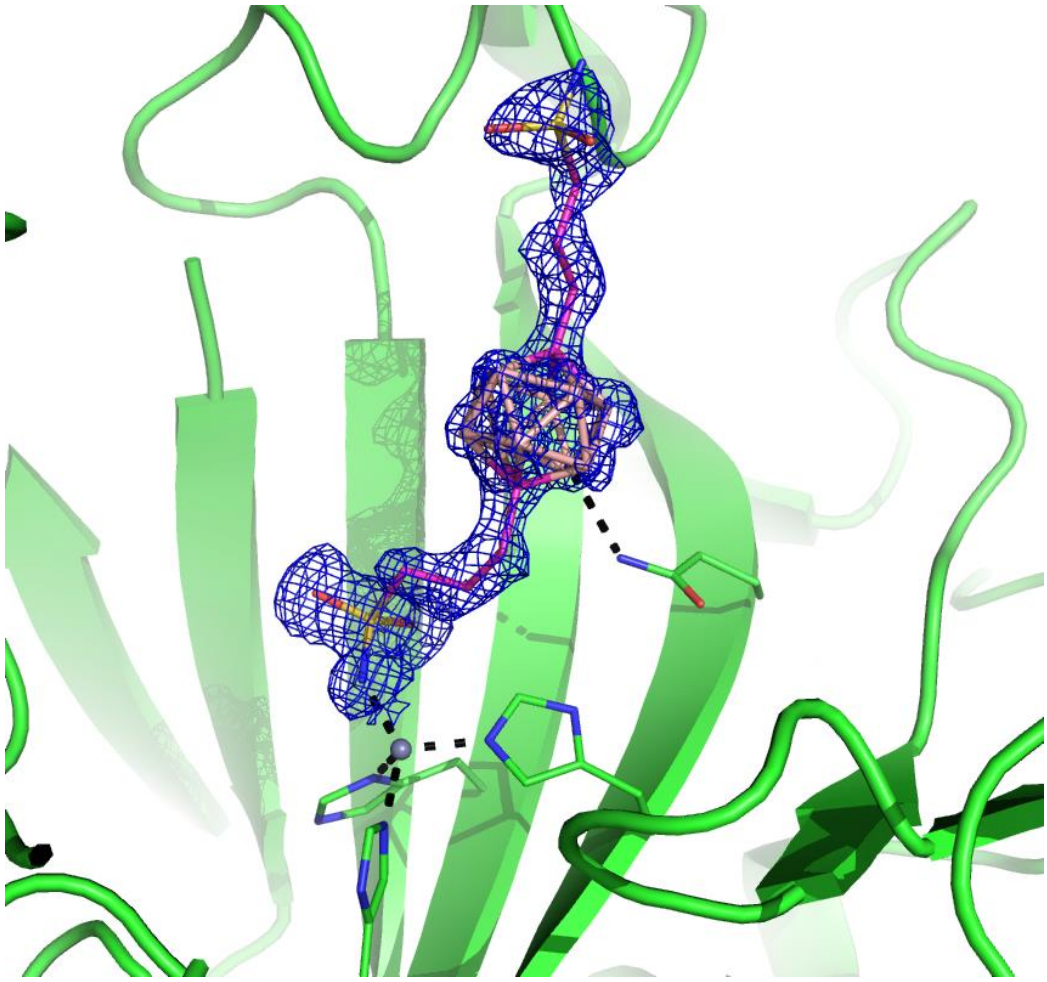

Figure 30 *Closo-carborane sulfonamide derivative (**66p**) coordinated in a mimic CA IX active site is stabilised by formation of a dihydrogen bond with Gln92.*

2.2 DNA INTERCALATORS

To better exploit the knowledge gained from the preparation of amines derived from metallacarboranes,[6] we introduced these amine derivatives with a simple, one-step procedure[189] that was carried out by nucleophilic reaction of the amine derivatives **44b,c** attacking the 3-nitro-1,8-naphthalic anhydride **74** (Scheme 32). These reactions provided good overall yields, after purification by column chromatography and the isolation of products as sodium salts. Reaction with **44a** was excluded, because the methylene connector was considered to be too short.

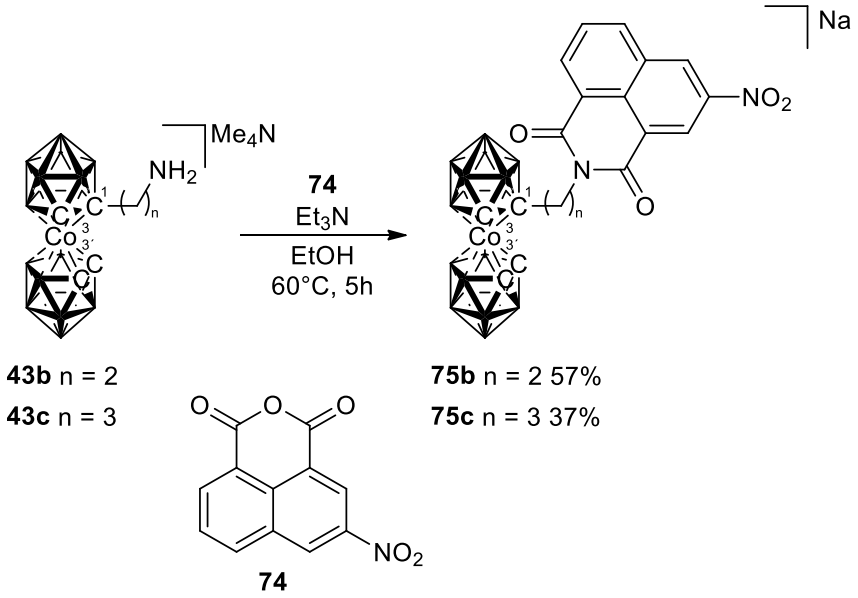

Scheme 32 *Preparation of naphthalimide derivatives 7**5b,c** of metallacarborane.*

We applied the same procedure on diastereoisomeric compound **44b** determined as 1,1´-*anti* (as described in Section 2.1.1) and a mixture of semi- and disubstituted products **76-** and **76** were obtained, respectively. This mixture resulted during all experiment, even when an excess of anhydride **74** was added, or the reaction time at higher temperatures was prolonged. The two products could be separated easily though using column chromatography (Scheme 33).

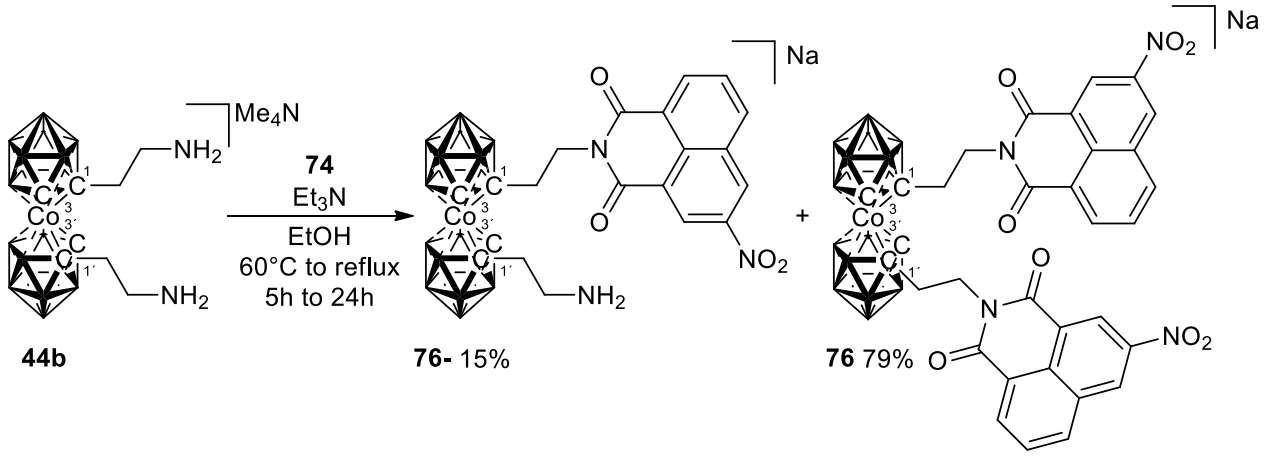

Scheme 33 *Mixture of semi- (**76-**) and disubstituted (**76**) naphthalimide products was obtained every time.*

We also used the well-known Plešek reaction[190] for the synthesis of the ammonium derivatives, in which the nitrogen is connected to the metallacarborane cage *via* a six membered diethylene glycol chain. This reaction forms the dioxanate derivatives of metallacarboranes **3** (cobalt)[190] and **77** (chromium),[17] which, due to strongly hydridic character of the hydrogen at atom at B8, promotes itself by the so-called EINS reaction with 1,4-dioxane producing **78** and **79** under acidic conditions. These species easily undergo cleavage of the ring containing oxonium atom by almost any nucleophile. In our case, the known primary amines **80** and **81** almost quantitatively forms in a very short time when gaseous ammonia[29] is introduced (Scheme 34). To open the dioxanate ring, we also applied an aqueous solution of ammonia (30%), but the reaction needed a longer reaction time at elevated temperature (70°C) and the yields (around 60%) were not as good as the previous method.

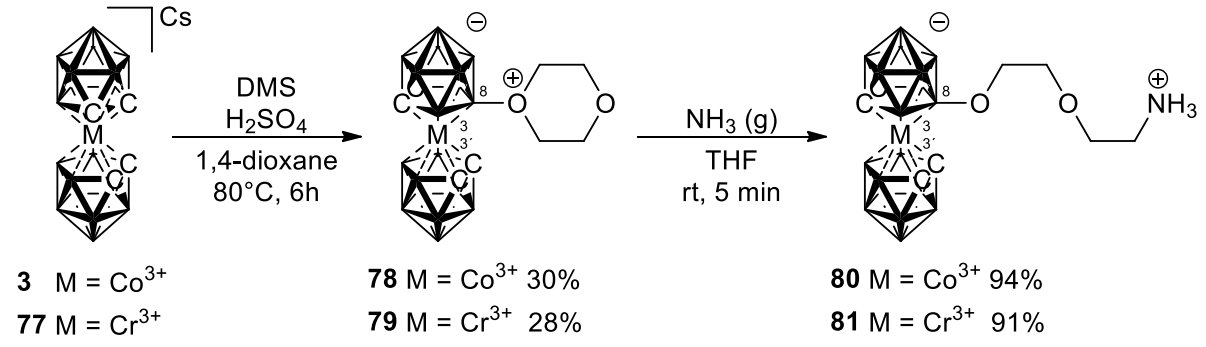

Scheme 34 *Plešek reaction forms zwitterionic dioxanates (**78** and **79**) which can be opened with electrophiles to provide functional groups connected via the diethylene glycol chain to metallacarborane cluster.*

The last two compounds **80** and **81** were then introduced in the same type of reaction with anhydride **74**, which led to the formation of products **82** and **83** in good yield in the case of cobalt metallaacarborane and to lower yields for the chromium metallacarborane.

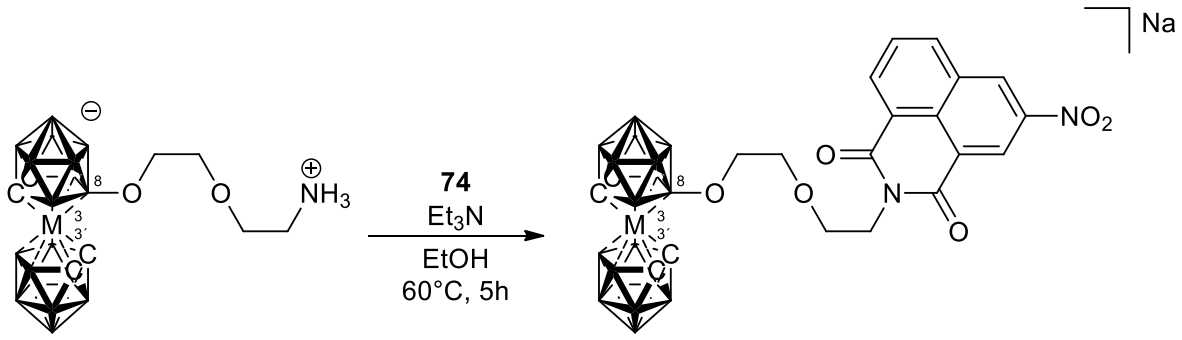

80 M = Co^{3+}
81 M = Cr^{3+}

82 M = Co^{3+} 58%
83 M = Cr^{3+} 20%

Scheme 35 *Preparation of naphthalimide metallacarborane derivatives **82** and **83**.*

The paramagnetic chromium conjugate is one of the prospective labelling systems[188] used in the design and construction of a series of electrochemical labels differing sufficiently in redox potentials, providing a "multi-colour" electrochemical sensing in nucleic acids.[191]

Lastly, the series of metallacarboranes was extended by our colleagues from Lodz, Poland. They prepared amines derived from isomeric carboranes **1o,m,p**[192] and applied the same conditions as shown above. This is graphically depicted in Scheme 36.

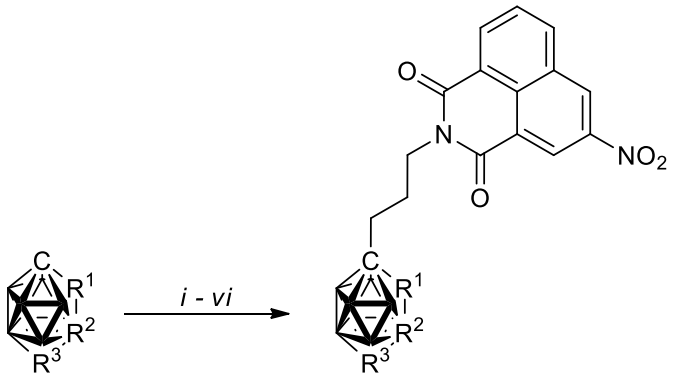

1o
1m
1p

84o R^1 = CH R^2 = BH R^3 = BH
84m R^1 = BH R^2 = CH R^3 = BH
84p R^1 = BH R^2 = BH R^3 = CH

Scheme 36 *Preparation of ortho- **(84o)**, meta- **(84m)** and para-carborane **(84p)** amines and their subsequent reaction with 3-nitro-1,8-naphthalic anhydride **74**, which produces new naphthalimide **84o,m,p**; i. ^{n}BuLi, oxetane, THF, 0°C, ii. CBr_4, PPh_3, DCM, 0°C, iii. NaI, acetone, reflux, iv.Boc_2NH, $Bu_4N^+HSO_3^-$, NaOH, DCM, reflux, v. TFA, DCM, rt, vi. **74**, Et_3N, EtOH, 65°C.*

The work described in this Section was performed during an exchange visit at the Institute of Medical Biology of the Polish Academy of Sciences in Lodz and the biological assays carried out by the Polish team are currently in progress. The biological data are not available yet, but they will be included in a joint paper, which is in preparation.

2.3 TRICARBOLLIDES

As mentioned in Introduction, we chose to investigate tricarbollides as these could offer new hydrophobic and space demanding structures. Our main motivation was to prepare polysubstituted *nido* neutral compounds or/and their metallocenes-like complexes as possible bulky and hydrophobic structural blocks (Section 1.1.3, Scheme 2). The major problem here has been connected with insufficient yields of the initial two-step synthesis of starting *arachno*-6,9-$C_2B_8H_{14}$ (**4**). This reaction was developed by our colleagues in 80's and even after many improvements; yields have remained still low to moderate. The first step corresponds to removal of one boron vertex from *nido*-dicarbollide anion *nido*-7,8-$C_2B_9H_{12}^-$(**2**) and leads to a so-called "Pleškoxide" *nido*-5,6-$C_2B_8H_{12}$ (**85**)[193,194] This is followed by skeletal rearrangement and oxidation leading to the *arachno* structure ("Štíbroxide") (**4**)[195] (Scheme 37) described above.

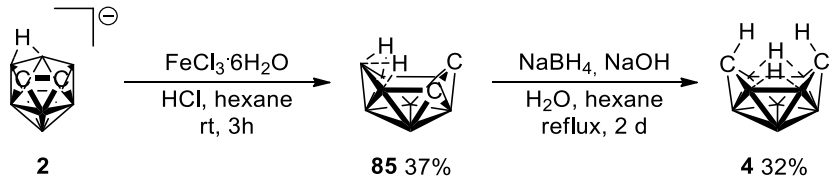

Scheme 37 *Preparation of "Štíbroxid" (4) suitable for SAC reaction in two-step degradation-rearrangement-oxidation cascade.*

Even at different scales and various conditions (time, temperature, ratio of reactants), the yields remained around 30%. Thus, this reaction had to be performed repeatedly to obtain sufficient amounts of compound **4** and to be useful in the SAC reactions. We followed the pathway D shown in Scheme 1 (Section 1.1.3) described previously[34,196] using benzoyl chloride in the presence of proton sponge and prepared tricarbollide derivative with phenyl group 8-Ph-*nido*-7,8,9-$C_3B_8H_{11}$ (**86**) (Scheme 38).

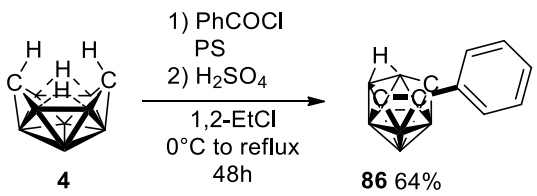

Scheme 38 *Skeletal alkylcarbonation (SAC) with benzoyl chloride provides 8-phenyl tricarbollide **86**.*

This novel reaction was published in 2016[30] and is based on use of alkyl halides as alkylating agents acting at open-face of tricarbollides. This method uses the abstraction of a proton from boron vertices B10 and B11 by sodium hydride followed by a subsequent

alkylation leading to the formation of mono- or dimethylated products. Scheme 39 shows the formation of dimethylated phenyl tricarbollide 8-Ph-*nido*-7,8,9-$C_3B_8H_9$-Me_2 (**87**). The formation of the open-face B-alkyl derivatives is consistent with direct electrophilic attack by the CH_3^+ carbocation at the negative B-B bonded B(10)H-vertex, followed by H(10)-shift to the bridging μ-$H_{10,11}$ position (Figure 31). The X-ray structure of the methylated product **87** was determined (Figure 32).

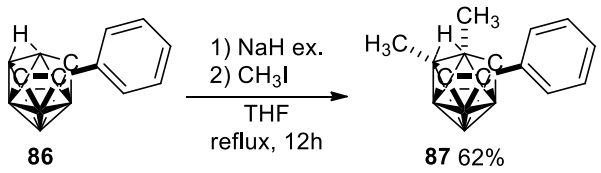

Scheme 39 *Alkylation of tricarbollide **86** on the open face.*

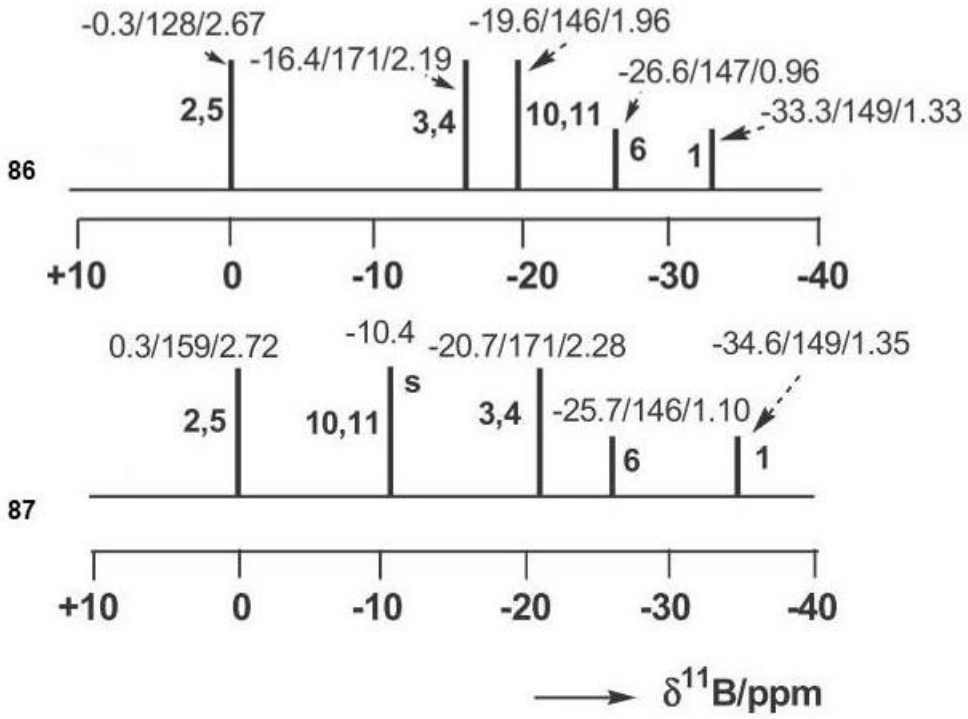

Figure 31 *(top) Stick diagrams inter-comparing the ^{11}B NMR chemical shifts and relative intensities of the B-unsubstituted 8-Ph-nido-7,8,9-$C_3B_8H_{11}$ (**86**) compound (data from ref.*[34]*) Chemical shifts for individual cluster positions are ordered as:$\delta(^{11}B)/^1J_{BH}/\delta(^1H_{cageBH})$. (bottom) Diagrams comparing the ^{11}B NMR shifts and relative intensities for the corresponding disubstituted derivatives 8-Ph-nido-7,8,9-$C_3B_8H_9$-10,11-Me_2 (**87**).*

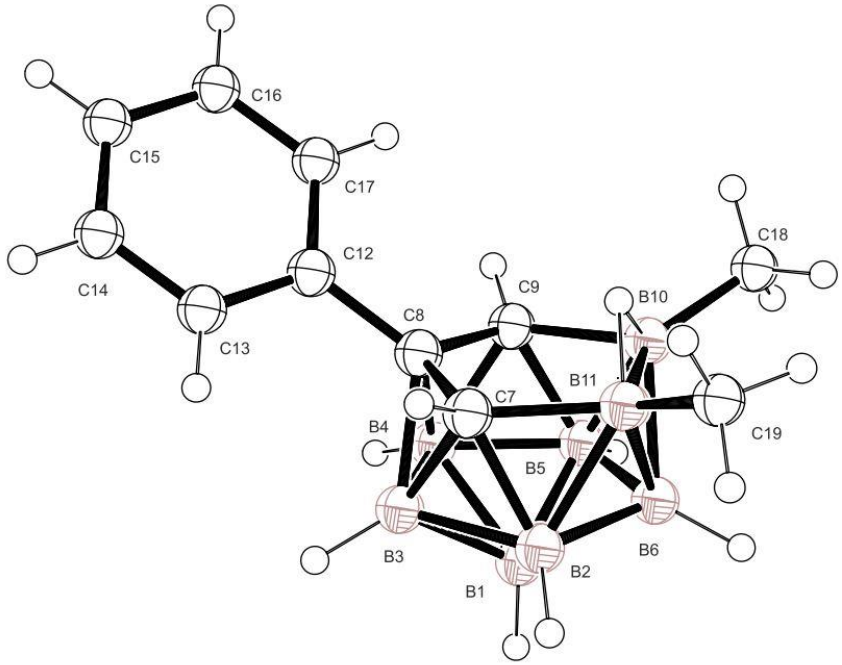

Figure 32 *ORTEP representation of the molecular structure of 8-Ph-nido-7,8,9-$C_3B_8H_9$-10,11-Me_2 (**87**) at 50% probability level. Selected bond lengths (Å) and angles (°): open face: C7-C8 1.527(2), C7-B11 1.672(2), C8-C9 1.525(2), C9-B10 1.666(2), B10-B11 1.872(3); C8-C7-B11 110.18(12), C7-C8-C9 114.47(12), C8-C9-B10 110.21(12), C7-B11-B10 101.85(11), C9-B10-B11 102.17(11); interbelt distances: mean C-B, 1.730(4), mean B-B 1.786(4); lower belt: mean B-B 1.765(4), mean B1-B 1.779(4). The B-H and C-H bond distances and angles fall within usual limits.*

The assumed use of the tricarbollide derivatives was connected with use of tricarbollides as another variety of structural blocks to be introduced into the structures of CA IX inhibitors – giving different interactions and space variability. Eventual incorporations to structures similar to metallocenes, as is indicated in Scheme 40 have been also considered. Nevertheless, due to lack of time, this area remains open.

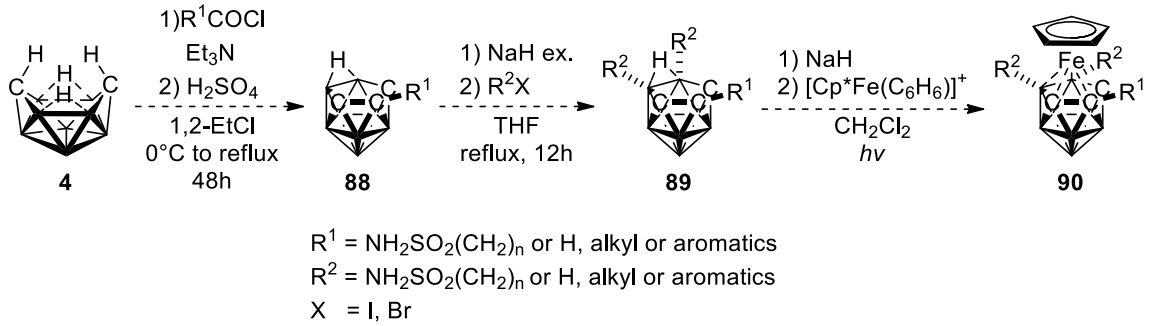

Scheme 40 *Hypothetical synthetic pathways which could provide many variations of CA IX inhibitors.*

2.4 CYCLODEXTRINS

We described the ring-opening reactions of lithiated species in previous paragraphs (Sections 2.1.1 and 2.1.2) and, again, this reaction became our concern here. Thus, in this Section we focus on an oxirane opening reaction[8] with all three isomers of carborane – *ortho*- (**1o**), *meta*- (**1m**) and *para*-carborane (**1p**) (Scheme 41). To briefly recap the problem mentioned in Chapters 2.1.1 and 2.1.2: (*i*) unlike the insertion of acetylene derivatives into the *arachno*-decaborane(14),[10] this method can be applied to all three isomers, (*ii*) in contrast to with metallacarborane chemistry,[5,9] the reaction proceeds very easily even at higher temperatures, i.e. at 0°C,[8,197] and finally, (*iii*) we can tune the ratio between mono- and di-substituted products by adjusting the amount of ^{n}BuLi (one equivalent favours mono-substitution, two or more equivalents favour di-substitution)[5,6,9] or by using a protection-deprotection strategy.[198] Based on our previous experience, we used different amounts of ^{n}BuLi, and obtained mixtures of unreacted starting material, mono- (**91o,m,p**) and disubstituted hydroxyderivatives (**92o,m,p**) which could be then separated by silica gel column chromatography.

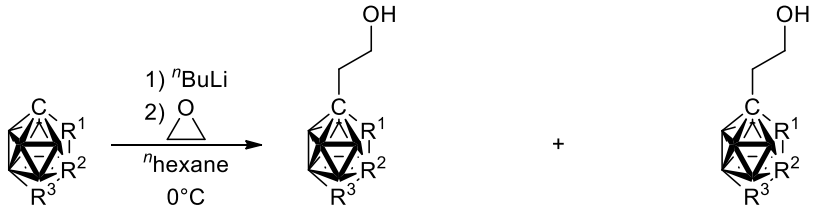

1o **91o** 50% R^1 = CH, R^2 = BH, R^3 = BH **92o** 27% R^1 = $C(CH_2)_2OH$, R^2 = BH, R^3 = BH

1m **91m** 42% R^1 = BH, R^2 = CH, R^3 = BH **92m** 22% R^1 = BH, R^2 = $C(CH_2)_2OH$, R^3 = BH

1p **91p** 45% R^1 = BH, R^2 = BH, R^3 = CH **92p** 12% R^1 = BH, R^2 = BH, R^3 = $C(CH_2)_2OH$

Scheme 41 *Ring-opening reactions with oxirane lead to ethylhydroxy derivatives.*

The oxidation step, using Jones oxidation conditions, was performed based on results from other groups[10,197] as well as on our previous experience,[9] and proceeded as expected to give products (**93o,m,p** and **94o,m,p**) with no starting material remaining (Scheme 42). We did not observe any effect when different acids were used (sulfuric acid or acetic acid). In both cases, all starting material disappeared and only product was formed.

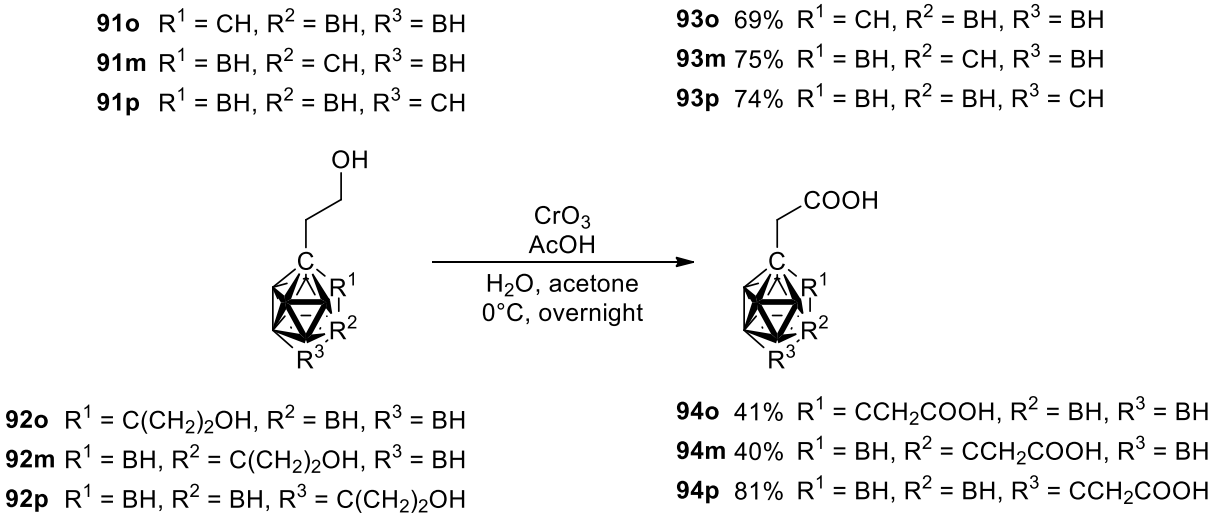

Scheme 42 *Oxidation under Jones conditions lead to a corresponding acid derivatives.*

The carboxymethyl *ortho*-carborane compounds **93o** and **94o** alongside with their isomeric congeners **93m** and **94m** were reported in the early times of carborane chemistry.[197,199] However, only **93o** was partially characterised by ^{1}H and ^{11}B NMR. The rest were characterized only by IR spectra. Compound **93p** was mentioned for the first time in 1976[200] but no report has yet been made for **94p**. We provided in our study on host-guest complexation[201] the improved and simplified synthetic access to the whole series of mono- and disubstituted hydroxyls and carboxylate derivatives of carboranes together with the full characterization of all compounds over the isomeric series by contemporary MS, ^{1}H, ^{11}B and ^{13}C NMR methods along with melting points.

Host-Guest Complexation

The complexation of carboranes with different CD homologues was investigated by ^{1}H NMR spectroscopy, which was possible due to their high solubility at elevated pH (pD) values (pD > 10). ^{1}H NMR titrations were conducted for guests (**93o,m,p** and **94o,m,p**) with α-, β-, and γ-CD in D_2O (Figure 34-36). Spectral changes following the addition of the synthesized carborane derivatives were observed for all CDs as hosts. In particular, we witnessed a pronounced complexation induced shift of the H3 proton (Figure 33), which is located inside the cavity near the secondary hydroxyl rim, signalling the formation of inclusion complexes. With the smallest CD homologue, α-CD, similar chemical shifts were observed for the mono-carboxymethyl carboranes (**93o,m,p**).

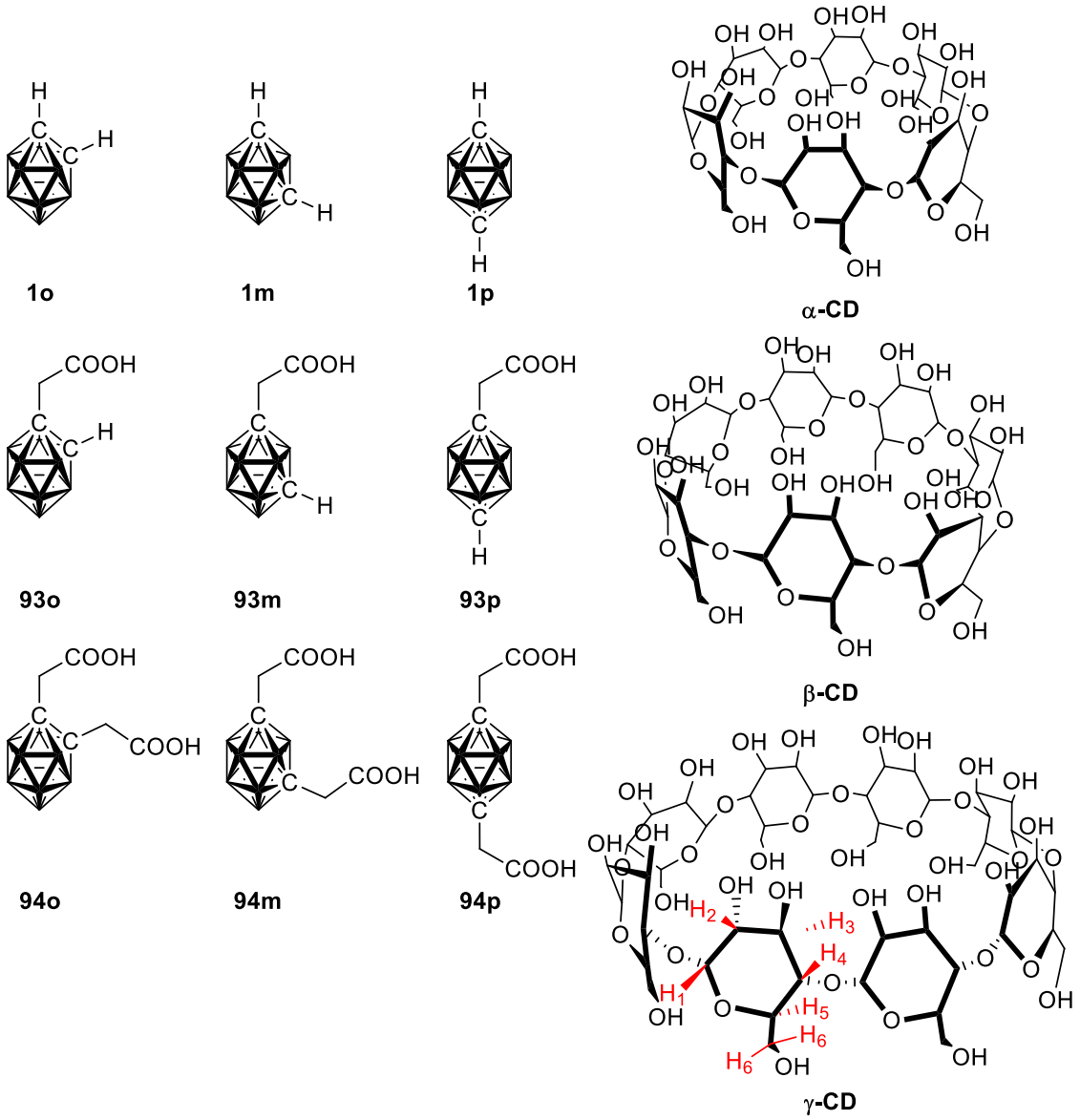

Figure 33 *Representation of studied guest carborane derivatives and host cyclodextrins.*

Larger downfield shifts of proton H3 were obtained for the dicarboxymethyl carboranes (**94o,m,p**), which indicated that these guests might protrude deeper into the cavity of α-CD (Figure 34). For **94m** and **94p**, the distance between the carboxylate groups made it possible that each group can be docked at different CD rims (one at the narrow and one at the wide rim), providing stabilization through hydrogen bonding. In contrast, in **93o**, the carboxymethyl groups are on adjacent carbon atoms and can bind only at one of the two rims, which might hinder the immersion of the carborane core into the cavity. Similarly, **94p** caused large downfield shift of H3 with β-CD (Figure 35). Smaller shifts were observed for γ-CD, which is attributed to its large cavity size and therefore fewer defined contacts between guest and host (Figure 36). All complexes showed a fast exchange within the NMR time scale (ms).

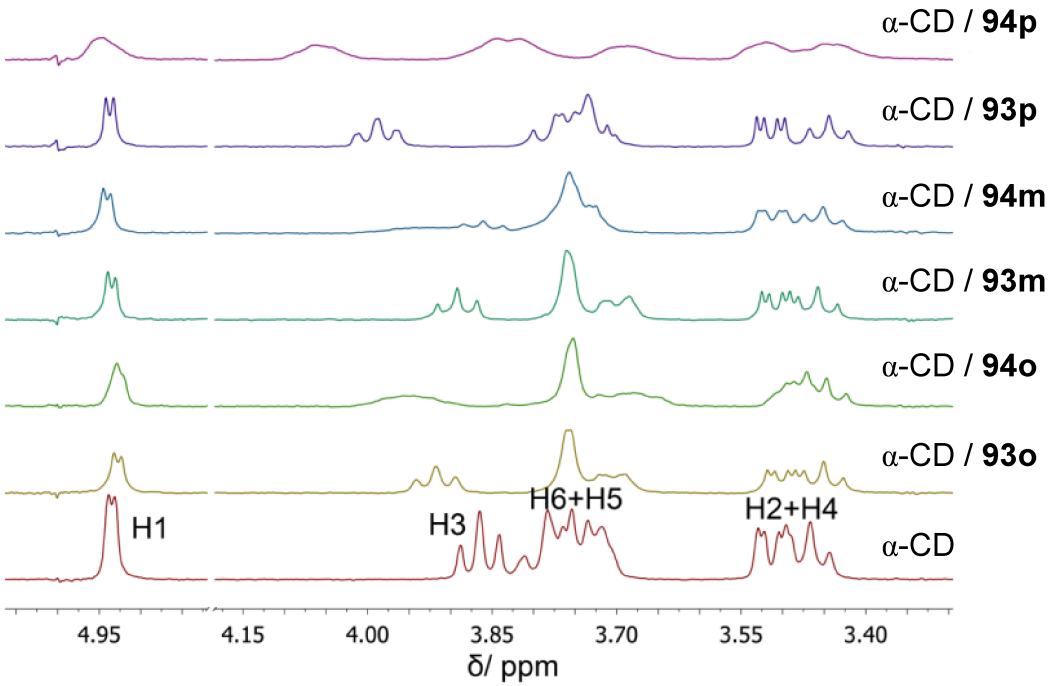

Figure 34 *^{1}H NMR spectra of α-CD with carborane derivatives in D_2O (pD ~ 11).*

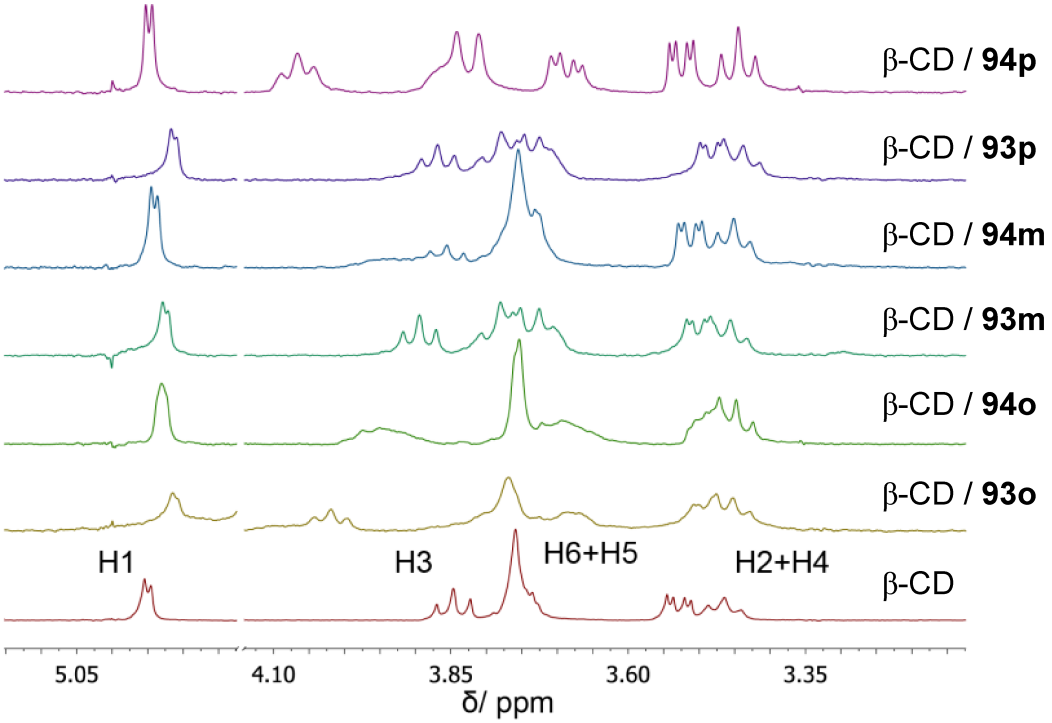

Figure 35 *^{1}H NMR spectra of β-CD with carborane derivatives in D_2O (pD ~ 11).*

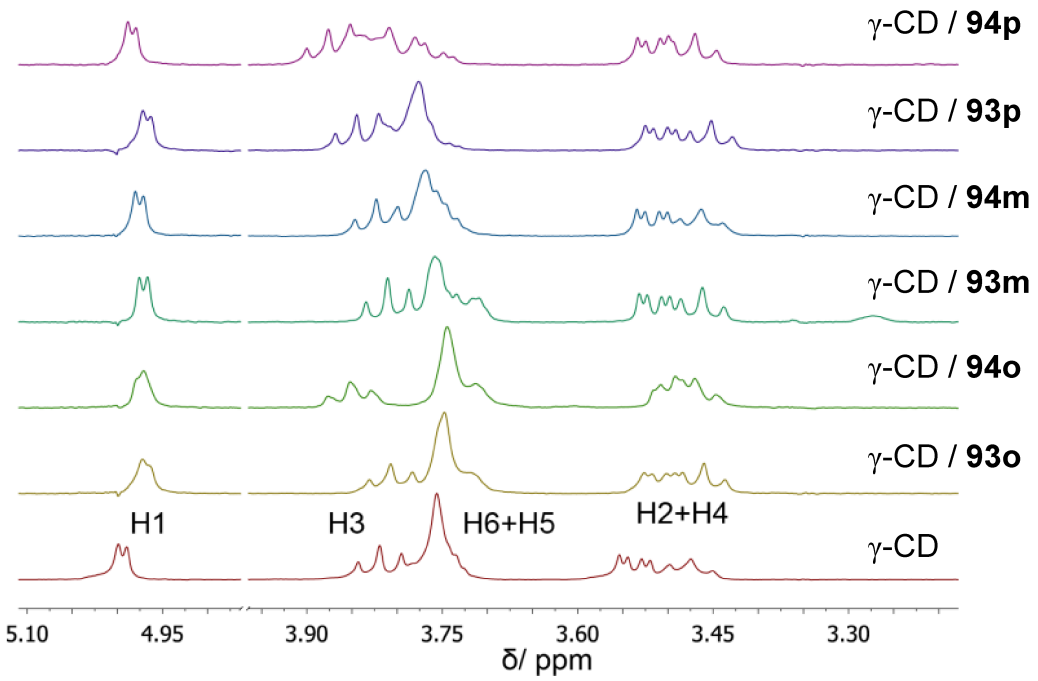

Figure 36 *^{1}H NMR spectra of γ-CD with carborane derivatives in D_2O (pD ~ 11).*

Quantum-chemical calculations were performed in order to further investigate supramolecular host-guest complexes and extract additional structural information. The optimized structures of representative host-guest complexes are shown in Figure 37. It should be noted that different starting geometries were considered for each complex. For example, the position of carboxymethyl group in the case of the mono-carboxymethyl derivatives was varied; as such, the carboxymethyl group was positioned and simulated at the two different rims of the CD.

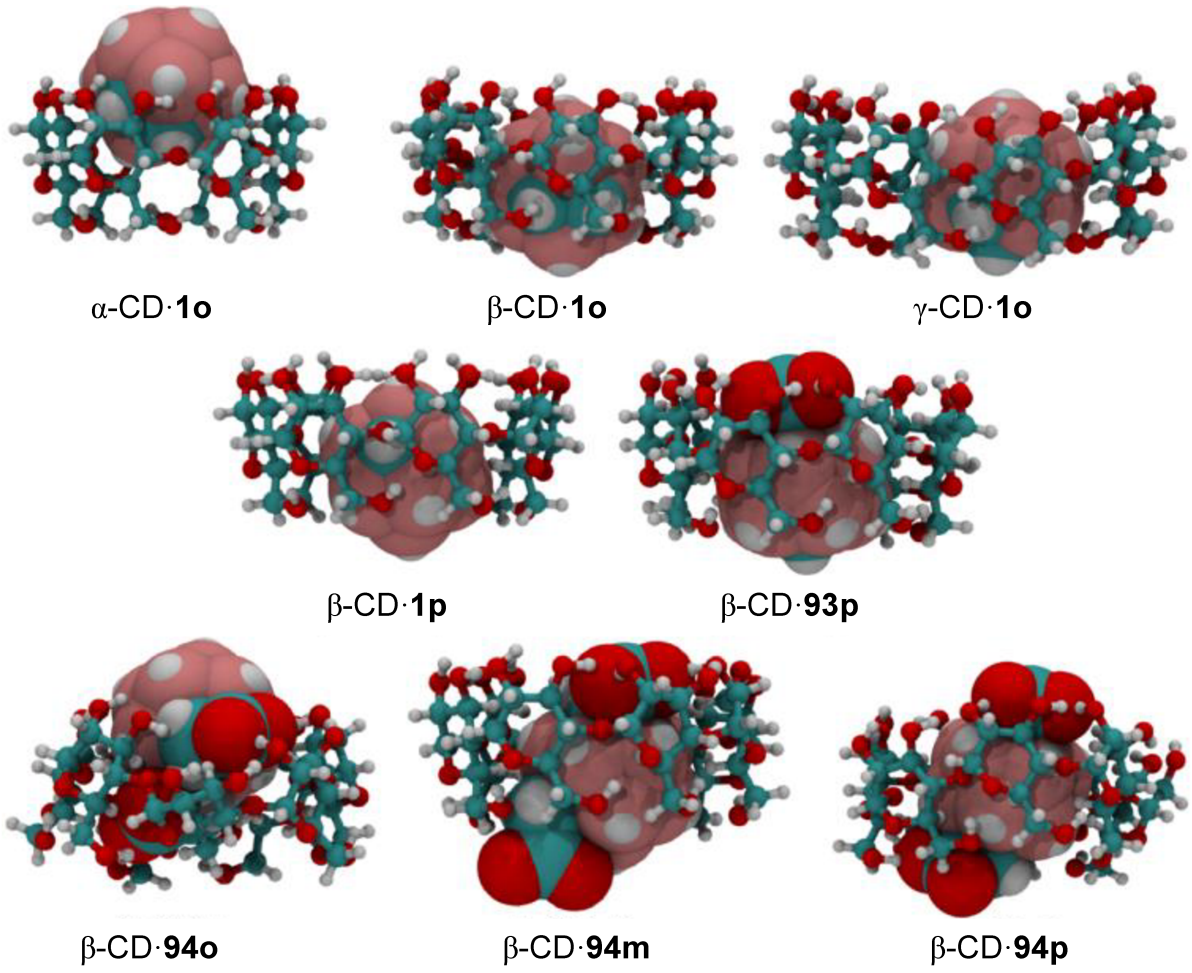

Figure 37 *DFT-optimized (in gas phase, calculated at wB97XD/3-21G*) structures of representative CD·carborane complexes.*

As shown in Figure 37, the carborane residue can partially be encapsulated inside the small cavity of α-CD, while it fits very well inside β-CD, but is too small to fully occupy the cavity of γ-CD. This can be also understood in term of a size match between the carborane moiety (V = 149 Å^3) and the cavity of β-CD (V_{cavity} = 262 Å^3), which provides an ideal packing of the carborane inside β-CD (packing coefficient, *PC*, of 57%; the ideal *PC* is 55%).[202,203] The optimized structure for **1o** with α-CD and β-CD showed that the C-H groups of the carborane unit were located inside the host cavity. For the mono- and dicarboxymethylated carboranes, the structures were mostly determined by the position of the carboxymethyl groups at the hydroxylated rims, which allowed for the formation of hydrogen bonding. For β-CD·**93p** complex, the carboxymethyl groups were found to be docked at the wide rim (the secondary hydroxylate rim). In case of the di-substituted carboranes, the carboxymethyl groups orient to maximize the interactions with both rims.

Indicator displacement experiments[204] have been used to determine the binding affinities of optically transparent and/or sparingly water-soluble, highly hydrophobic guests. We performed such experiments to determine the binding constants of the carborane derivatives to CDs. For this, a dodecaborate-anchor dye,[205] which forms a 1:1 host·dye complex with a high affinity for β-CD and γ-CD, and changes its photophysical properties (here, a red shift in the UV-visible absorption spectrum) upon complexation with CDs, was used as a sensitive reporter pair for indicator displacement applications (Figure 38). The binding constant of the dye to β-CD and γ-CD were reported as 2.7×10^5 and 1.5×10^5 M^{-1}, respectively.[205] It is important to note that the insufficient cavity size of the smallest CD homologues (α-CD) limits the implementation of indicator displacement experiments.[205] So far, no suitable dye has been found that binds to α-CD with a high binding constant associated with changes in its optical properties upon complexation.

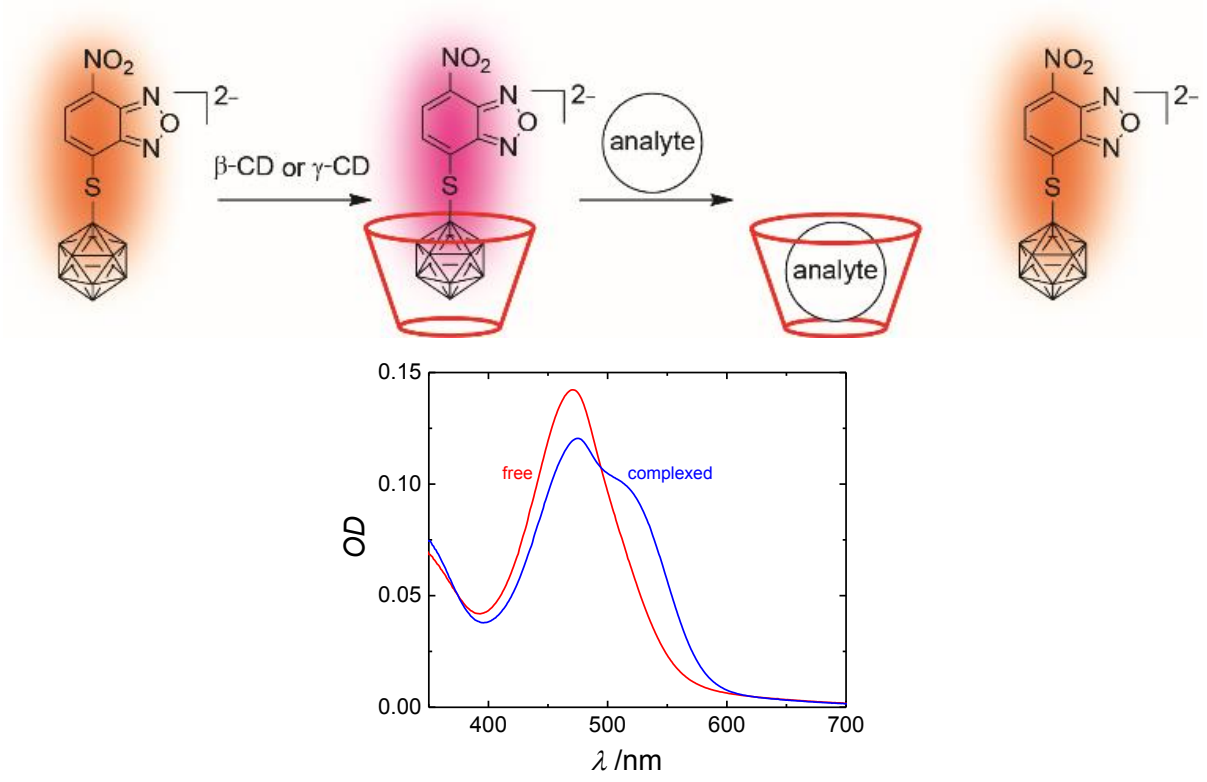

Figure 38 *Schematic illustration of the dye displacement principle: (top) The complexation of the dye with the host (CD) results in a change of its colour (UV−Vis spectrum). Upon the addition of a competitive guest (analyte), the dye is displaced from the host cavity and its original colour is fully restored. (bottom) UV–Vis plot (optical density against wave length) of the dye in the free and complexed form (shown for β-CD).*

Displacement titrations are shown in Figure 39-44, which indicated that all carboranes are able to displace the dye from the CD cavity. The binding constants of carborane derivatives are listed in Table 9. The binding affinity for the *m*- and *p*-carborane isomers has been previously reported and found to decrease with decreasing dipole moment (1830 M^{-1} and 1560 M^{-1}, respectively).[158] The binding constants measured here for the carboranes derivatives were in the range of 10^3-10^4 M^{-1}. These binding affinities fall in the same range as reported for other carborane derivatives by using different methods.[158,159,206] For example, the binding constant for **93m** with β-CD (K_a = 6.4 × 10^3 M^{-1}) is similar to that measured for *m*-carborane carboxylic acid (K_a = 5.6 × 10^3 M^{-1}), which lacks only the methylene group.[206] The **93o** and **94o** derivatives showed a similar binding affinity towards β-CD and γ-CD (~4 × 10^3 M^{-1}). In general, it was found the binding affinity increases from *o*- to *m*- to *p*-carborane with β-CD. It is remarkable that the affinity for the mono-substituted carboranes increases by a factor of 5 from the *o*-substituted to the *p*-substituted derivative. This increase cannot be explained by steric factors. It underlines the necessity to develop proper semi-empirical parameters for docking programs.[207] Presently, boron atoms in clusters are treated as carbon atoms.[208] With such a simplification, differences between the three isomers of carborane cannot be modelled.

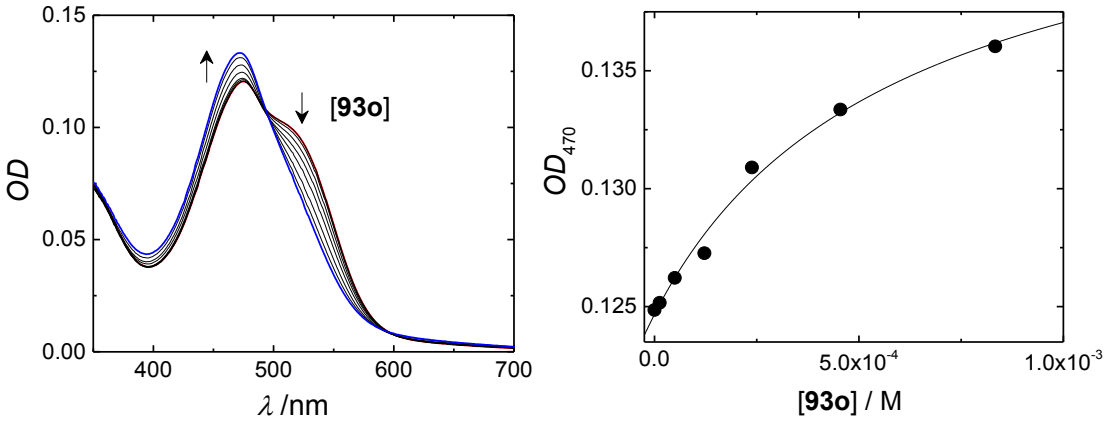

Figure 39 *UV–Vis titration for the competitive displacement of the dye (5 μM) from β-CD (10 μM) by* ***93o****. Left: actual changes in the UV−Vis spectra with increasing concentration of the competitive guest. Right: the fitted data; fitting (black lines) were done by assuming a 1:1 binding model from which the association constants were derived.*

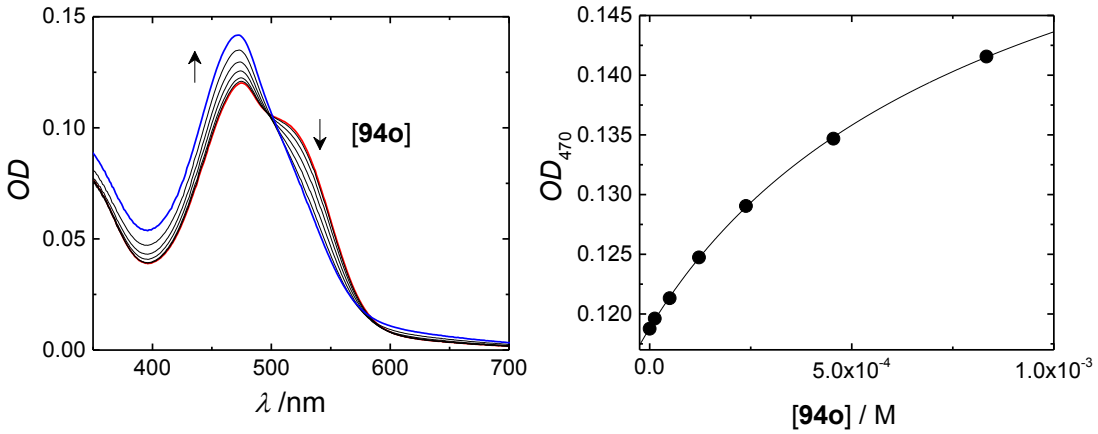

Figure 40 *UV–Vis titration for the competitive displacement of the dye (5 μM) from β-CD (10 μM) by* ***94o****. Left: actual changes in the UV−Vis spectra with increasing concentration of the competitive guest. Right: the fitted data; fitting (black lines) were done by assuming a 1:1 binding model from which the association constants were derived.*

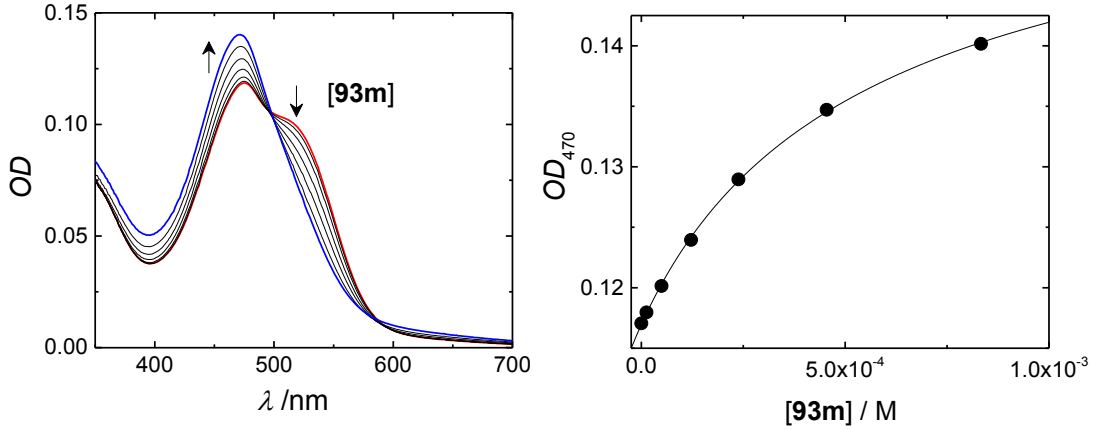

Figure 41 *UV–Vis titration for the competitive displacement of the dye (5 μM) from β-CD (10 μM) by* ***93m****. Left: actual changes in the UV−Vis spectra with increasing concentration of the competitive guest. Right: the fitted data; fitting (black lines) were done by assuming a 1:1 binding model from which the association constants were derived.*

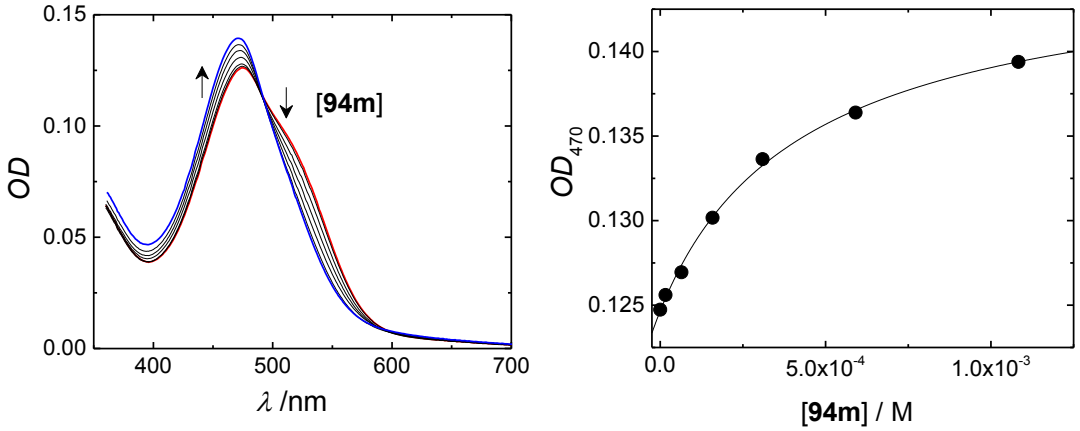

Figure 42 *UV–Vis titration for the competitive displacement of the dye (5 μM) from γ-CD (10 μM) by* ***94m****. Left: actual changes in the UV−Vis spectra with increasing concentration of the competitive guest. Right: the fitted data; fitting (black lines) were done by assuming a 1:1 binding model from which the association constants were derived.*

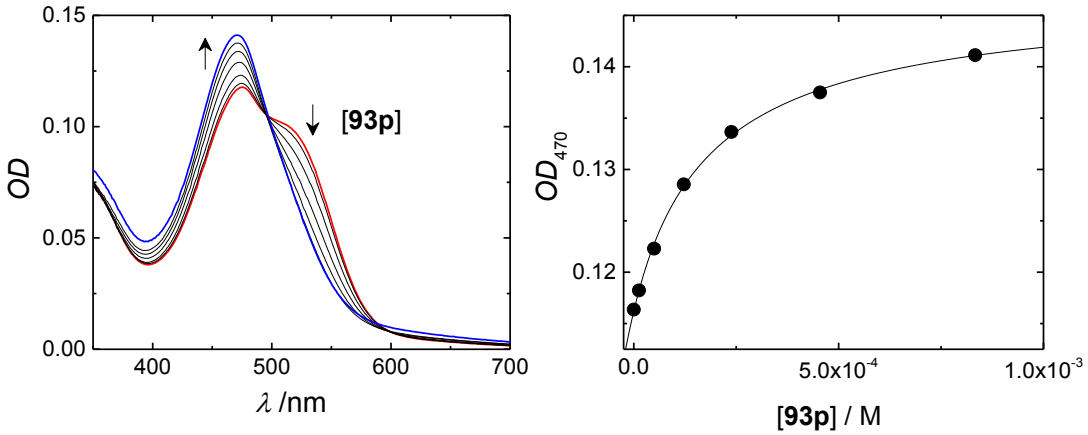

Figure 43 *UV–Vis titration for the competitive displacement of the dye (5 μM) from β-CD (10 μM) by* ***93p****. Left: actual changes in the UV−Vis spectra with increasing concentration of the competitive guest. Right: the fitted data; fitting (black lines) were done by assuming a 1:1 binding model from which the association constants were derived.*

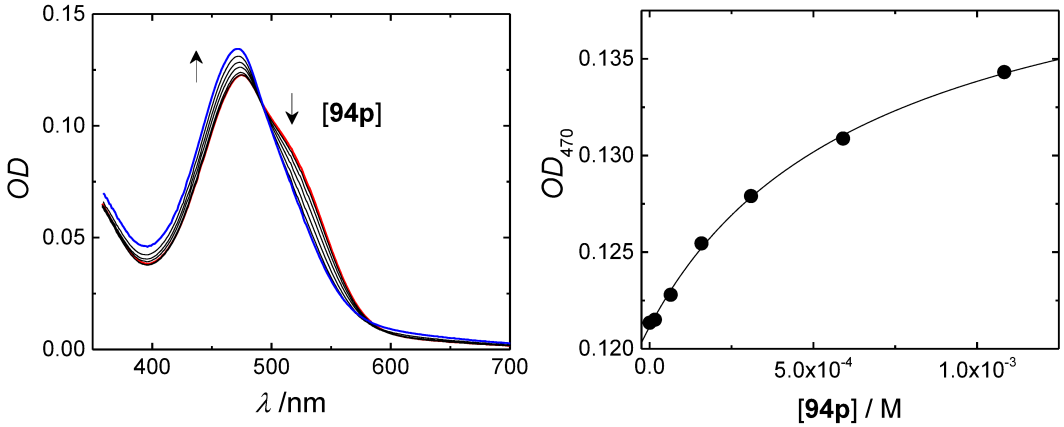

Figure 44 *UV–Vis titration for the competitive displacement of the dye (5 μM) from β-CD (10 μM) by* ***94p****. Left: actual changes in the UV−Vis spectra with increasing concentration of the competitive guest. Right: the fitted data; fitting (black lines) were done by assuming a 1:1 binding model from which the association constants were derived.*

Table 9 *Association constants (K_a / 10^3 M^{-1})[a] of carborane and their derivatives with CDs in aqueous solution.*

	93o	**94o**	**93m**	**94m**	**93p**	**93p**
β-CD	4.1±0.9	3.9±0.2	6.4±0.4	9.9±0.5	20.5±1.5	8.2±0.4
γ-CD	4.3±1.4	4.2±0.7	2.3±0.4	6.0±0.8	8.0±0.9	3.7±0.4

[a]Measured by using indicator displacement titrations at pH = 11.

The calculated binding energies in water, applying the SMD implicit solvation model, indicated that β-CD serves as an ideal host for all the studied guests (Table 10). For the parent carborane isomers, the *o*-carborane showed a preferential binding with β-CD (ΔE = -64 kcal mol^{-1}). On the other hand, α-CD binds the carborane isomers with similar binding energies. Furthermore, the binding energy increased for the mono- and dicarboxymethyl carboranes with all hosts. The monocarboxymethyl carboranes (**93o**, **93m**, and **93p**) showed similar binding affinity towards α- and β-CD. In contrast, the binding of these mono-carboxymethylated carboranes with γ-CD followed the order: **93m** > **93p** > **93o**. The binding energy with di-carboxymethylated carboranes varies depending on the structural isomer and the size of the host. For example, α-CD binds selectively to **94m**, while the larger homologues bind strongly to **94o**. The highest binding energy was obtained for **94p** with β-CD. A directed comparison of the calculated absolute ΔE values with experimental ΔG values is, unfortunately, not possible, but some trends are the same, e.g., **93o** and **94o** showed a similar binding affinity to □β-CD, while **1o** bound more weakly. Indeed, the solubility (hydrophobicity) of the

carboxymethylated-carboranes may differ along the isomers (for *o*, *m* and *p*), such that the hydrophobic effect operates to a different extent.

Table 10 *Calculated binding energies[a] of carboranes and their derivatives with CDs in water[b] (values in the gas phase given in brackets; ΔE/kcal mol^{-1}).*

guest \ host	α-CD	β-CD	γ-CD
1o	-51.4 [-50.3]	-63.6 [-65.0]	-44.7 [-47.1]
93o	-67.7 [-87.6]	-82.1 [-98.7]	-64.0 [-80.6]
94o	-67.4 [-116.8]	-82.7 [-152.8]	-81.2 [-143.2]
1m	-52.2 [-50.4]	-58.7 [-56.7]	-45.7 [-48.3]
93m	-65.4 [-85.2]	-85.0 [-100.3]	-72.5 [-94.0]
94m	-83.5 [-139.1]	-83.3 [-107.7]	-77.1 [-125.5]
1p	-52.4 [-50.3]	-60.8 [-57.6]	-43.2 [-41.4]
93p	-63.8 [-84.6]	-83.1 [-99.4]	-69.3 [-88.1]
94p	-74.1 [-117.5]	-87.4 [-136.4]	-72.2 [-113.4]

[a]Calculated by using Gaussian 09 with the wB97XD/3-21G* method. [b]The SMD solvation model was used for implicit solvent salculations using the gas phase optimized structures.

This work was completed at the Jacobs University in Bremen in cooperation with Khaleel I. Assaf, Ph.D., who performed the DFT calculations, and Prof. Detlef Gabel, Ph.D. and was published in Chemistry - A European Journal in June 2018.[209]

CHAPTER THREE

CONCLUSION

We primarily aimed for the preparation of different carborane and metallacarborane derivatives and at their applicability in medicinal chemistry.

New convenient synthetic routes that enable the introduction of an amino function on the metallacarborane cage connected *via* an aliphatic chain to its carbon sites was published. The new method for C-substitutions offers rich possibilities for optimization of the length of the linker to the metallacarborane cage, and also enables the introduction of a functional group used in the design of active molecules. This has also opened new ways for geometrically predefined disubstitutions (see ref[159]). Asymmetric disubstitutions of metallacarboranes with one zinc binding motif and another arm with terminal NH_2 or OH group offer a background for the further design of drug delivery systems, molecular probes and for tumour imaging.

The inhibitory studies have been carried out within the collaboration between IIC, IOCB and IMG of CAS in Prague and IMTM of Palacký University in Olomouc. As follows from the structural studies, the cobalt bis(dicarbollide) ion provides the desired space-filling properties and introduces additional interactions with the enzyme active site, leading to a dramatic improvement in inhibition efficacy and selectivity for CA IX compared to carboranes with equivalent substitutions. The observed K_i values ranged from nanomolar to subnanomolar and are several orders of magnitude lower than those for equivalent alkylsulfamido-dicarbaboranes.[92] The cobalt bis(dicarbollide) compounds also have two to three-orders-of-magnitude higher inhibition potency than the recently reported metallocene-sulfonamides.[210] Furthermore, the CA IX/CA II selectivity index reached a value of approximately 500 for the best inhibitor of the series, indicating specific inhibition of CA IX. X-ray structural analyses of the cobaltaborane-CA IX mimic complexes revealed that the length of the linker between the sulfonamide anchor and the cluster is important for orientating the ionic cluster for optimal interaction with hydrophobic and hydrophilic pockets in its proximity. Two compounds, **51b** and **52b**, were selected for further studies, including ADME analysis, pharmacokinetics, and antitumour activity experiments. These compounds displayed low *in vitro* and *in vivo* toxicity at MTD dose, and a sufficiently high concentration in serum after administration. The repeated dose of **51b** greatly reduces the tumour size in mice transplanted with 4T1-12B breast cancer cells *in vivo*. Moreover, **51b** and **52b** also reduced tumour size in SCID mice xenotransplanted with HT-29 cells[185] (see ref.[164]).

In parallel to the metallacarborane series, attention was paid to the development of direct methods of sulfonamide substitution at carborane cages that would replace the disadvantageous acetylene insertion reactions into open cage borane precursors (see ref.[165]). During the final two years of this work, the overall synthetic scheme, comprising five steps, was successfully

developed and applied to the synthesis of a series of substituted carboranes. In this case, the hydroxypropyl 1,2-carborane was prepared by the extension of a known procedure, as well as hydroxypropyl and dihydroxypropyl 1,7- and 1,12-carboranes that were subsequently converted to theircorresponding triflate esters and finally to their thiocyanato propyl derivatives. Chlorination of electroneutral carborane, *via* the clean reaction with SO_2Cl_2, produced the desired chlorides in good yield. These chlorides were then smoothly converted to their respective sulfonamides by reaction with aqueous ammonia. The compounds from the 1,2- and 1,7- series were degraded to their respective *nido*-carboranes. Also C,C- disubstituted compounds from *meta*- and *para*- series were synthesized. All compounds were submitted for tests of enzymatic activity at IMG of CAS. As exemplified by the synthesis of *meta*- and *para*-substituted series, which are unavailable from acetylene insertion or from attempted thermal rearrangement of *ortho*- isomers (due to decomposition), our new method is more versatile and opens routes to previously inaccessible isomers of sulfonamidoalkyl substituted species. These methods give a straightforward approach leading to a broad range of boron and carbon substituted isomeric *closo*-carboranes, their respective *nido*-anions. Currently, a joint manuscript is before the submission for evaluation in Chemistry - A European Journal (see ref.[176]), which summarizes synthetic results over the series of *meta*- and *para*- substituted carboranes, K_i values from enzymatic tests and high-resolution synchrotron structures. Carborane families might also offer potential for combined therapy involving BNCT treatment.

In the respect to the carborane area, we have explored reactions of 11-vertex *nido*-tricarbollides with alkylating agents. New open-face alkylation procedures were developed that provide bulky and hydrophobic structural molecular blocks. This study was fully completed and published during 2016 (see ref[30]).

From the medicinal chemistry point of view, the carborane and metallacarborane compounds may represent new types of building blocks potentially useful for the design of biologically active compounds for various targets.

During my collaborative stay at the Institute of Medical Biology of PAS in Lodz, the previously developed knowledge on the synthesis of metallacarborane amines[6] was used in combinations with the syntheses of different types of B-substituted amines (made using the known Plešek reaction[190]) with a focus on two new types of DNA intercalators. Although the chemical part of the manuscript is fully completed, the biological studies are still in progress and the overall results should be published in late 2018 (see ref[211]).

Last, but not least, the studies on cyclodextrin has been published (see ref[209]). ^{1}H NMR spectroscopy and quantum-chemical calculation were used to obtain information on the

complex structures and conformational changes accompanying the inclusion process. Dye displacement titrations were used to determine the binding constants. The preferential binding with β-CD is attributed to the size match between the carborane cage and the cavity of β-CD. Among the di-substituted carboranes isomers, the *p*-carborane showed somewhat greater binding affinity which might reflect the more effective hydrogen bond formation between the substituents of the *p*-carborane and the hydroxyl groups at the rim of CDs.

The author contributed to this work by performing all the synthetic procedures (unless mentioned otherwise in the text), characterisations by MS, ^{1}H, ^{11}B and ^{13}C NMR, IR and m.p. and by NMR and UV-Vis titrations.

APPENDIX ONE

METHODS

General

The caesium salt of cobalt bis(1,2-dicarbollide) (**3**) and isomeric carboranes (**1o,m,p**) were purchased from Katchem Ltd, Czech Republic. This salt was crystallized from hot aqueous ethanol (60%) and dried in vacuum for 4h at 120°C and then 12h at 180°C prior to use. Toluene and DME were dried with sodium diphenyl ketyl and distilled. Other chemicals and solvents were purchased from Aldrich and Lachner, Czech Republic, respectively, and were used without purification. Analytical TLC was carried out on Silufol® (silica gel on aluminium foil, starch as the binder, Kavalier, Czech Republic). Unless otherwise specified, column chromatography was performed on a high-purity silica gel (Merck Grade, Type 7754, 70–230 mesh, 60 Å). All the reactions were performed using the standard vacuum or inert-atmosphere techniques under high-purity argon or nitrogen (99.999%) as described by Shriver[212] although some operations, such as flash chromatography and crystallisation, were carried out in the air.

Melting points

Melting points (m.p.) were determined in sealed capillaries on the BÜCHI Melting Point B-545 apparatus. The majority of the new derivatives was precipitated in the form of the respective Me_4N^+, Me_3NH^+ or Et_3NH^+ salts that are not hygroscopic and do not contain any residual water or solvents. Before measurements of NMR spectra, melting points and elemental analysis the salts were carefully dried in vacuum at 60°C, which ensured consistently good results. The identity of all the reported compounds was also unambiguously proven by their spectral data. Except for compounds **91** – **94**, which were measured in sealed capillaries on a Gallenkamp Melting Point apparatus.

MS

All the carbon mono- and disubstituted species exhibit the respective molecular *m/z* base peaks $[M]^-$ in their electrospray ionisation (ESI^-) mass spectra and $[M]^{2-}$ base peak was observed for the dianionic species. For each particular boron cluster compound, the experimental isotopic patterns were in agreement with the calculated ones (using the mass spectrometric software EXcalibur). The isotopic distribution in the boron plot of all peaks agreed perfectly with the calculated pattern. Mass spectrometry measurements were performed on a Thermo-Finnigan LCQ-Fleet Ion Trap instrument using electrospray (ESI) ionisation. Negative ions were detected. Symplex dissolved in acetonitrile (concentrations approx. 100 ng ml^{-1}) were introduced to the ion source by infusion of 5 μL min^{-1}, source voltage 5.57 kV, tube lens voltage 49.8 V, capillary voltage 10.0 V, drying temperature at 188°C, drying gas flow 8 L min^{-1}, and auxiliary gas pressure 6 Bar. In all cases negative ions corresponding to the

molecular ion were observed with 100% abundance for the highest peak in the isotopic distribution plot. The data presented are for the most abundant mass in the boron distribution plot (100%) and for the peak corresponding to the highest *m/z* value. Compounds **75 – 83** were measured on a CombiFlash PurIon Model Eurus35 (Teledyne ISCO, Lincoln, USA). The ionization was achieved by electrospray ionization in the positive ion mode (ESI+) and negative ion mode (ESI–). The capillary voltage was set to 3.5 kV. The source temperature was 200 °C, and the desolvation temperature was 200 °C. Nitrogen was used as a desolvation gas (flow 35 L/min, purity >99%). Compounds **91** – **94** were measured on a Bruker micrOTOF instrument using electrospray (ESI) ionisation. Negative ions were detected. Samples dissolved in acetonitrile (concentrations approx. 100 μg mL^{-1}) were introduced to the ion source with source voltage 4.5 kV, tube lens voltage 20.0 V, capillary voltage 4.5 kV, drying temperature at 180 °C, drying gas flow 4.0 L min^{-1} and auxiliary gas pressure 0.4 Bar.

NMR

^{1}H, ^{11}B and ^{13}C NMR spectrometry was performed on a Varian Mercury 400Plus instrument and a JEOL 600 MHz instrument. ^{1}H (400 MHz) and ^{13}C NMR (100 MHz) chemical shifts are referred to the residual ^{1}H signal(s) of a deuterated solvent used and are given in ppm. ^{1}H NMR chemical shifts $\delta(^{1}H)$ are given in ppm, coupling constants *J* (H,H) in Hz. ^{11}B NMR (128 MHz) chemical shifts are given in ppm to high-frequency (low field) and to $BF_3 \cdot Et_2O$ as the external reference. Coupling constants $1J$ ($^{11}B–^{1}H$) were measured by resolution-enhanced ^{11}B spectra with a digital resolution of 2 Hz and are given in Hz. The ^{11}B NMR data are presented in the text below in the following format: ^{11}B chemical shifts $\delta(^{11}B)$ (ppm), multiplicity, and coupling *J* ($^{11}B–^{1}H$) constants are given in Hz. The peak assignment is based on $\{^{11}B–^{11}B\}$ COSY NMR spectroscopy and compared with the spectrum of the parent salt **3** (for assignment of the unsubstituted ligand). Only $^{13}C\{1H\}$ NMR resonances are listed; the peak assignment is in full agreement with signal multiplicities observed in coupled ^{13}C NMR experiments.

HPLC

Analytical HPLC was performed on the Merck-Hitachi HPLC system LaChrom 7000 series equipped with a DAD 7450 detector (fixed wavelengths 285, 265, 290 and 308 nm) and an Intelligent Injector L7250. The chromatographic IP-RP procedure based on methods previously reported for the separation of hydrophobic borate anions[213] was applied by using a buffer containing 4.5 mmol/l hexylamine acetate in 58% aqueous CH_3CN for amines and esters, or 53% for hydroxyalkyl derivatives, pH 6.5. Column: RP Separon™ SGX C8, 7 μm (silica

with chemically bonded octyl groups), Tessek Ltd., Prague, Czech Republic. The purity assay was based on the peaks areas present on the chromatograms of the individual compounds, which were recorded at 285 nm.

Elemental analyses

Elemental analyses were performed on Thermo Scientific FlashSmart Organic Elemental Analyzer using V_2O_5 catalyst weighted with the sample for combustion of the samples in oxygen.

UV-Vis

UV-Vis measurements were done on a Varian Cary 4000 UV-visible spectrophotometer. Isothermal titration calorimetry experiments were carried out in water (pH 11) on a VP-ITC from Microcal, Inc., at 25°C. The binding equilibria were studied using a cellular guest (carboranes) concentration of 0.3 mM, to which 5.0 mM CD solution was titrated. Typically, 27 consecutive injections of 10 μL were used. All solutions were degassed prior to titration. The first data point was removed from the data set prior to curve fitting (Origin 7.0 software) according to a one-set-of-sites model. The knowledge of the complex stability constant (K_a) and molar reaction enthalpy ($\Delta H°$) enabled the calculation of the standard free energy ($\Delta G°$) and entropy changes ($\Delta S°$) according to $\Delta G° = -RT \ln K_a = \Delta H° - T\Delta S°$.

IR

Infrared absorption spectra were recorded using a Nicolet 6700 Fourier-transform infrared spectrometer from Thermo Scientific equipped with a ETC EverGlo* source for the IR range, a Ge-on-KBr beam splitter, and a DLaTGS/KBr detector with a smart orbit sampling compartment and diamond window. The samples were placed directly on the diamond crystal, and pressure was added to make the surface of the sample conform to the surface of the diamond crystal.

Crystallography

X-ray Structure Determinations: Single-crystal x-ray diffraction data for **38b** and **40** salts were obtained from Nonius KappaCCD difractometer equipped with Bruker ApexII-CCD detector by monochromated MoKa radiation (λ = 0.71073 Å) at 150(2)K. The structures were solved by direct methods and refined by full-matrix least squares based on F^2 (SHELXS; SHELXL97).[167] The hydrogen atoms were fixed in idealized positions (riding model) and assigned temperature factors $H_{iso}(H) = 1.2\ U_{eq}$(pivot atom). The tetramethylammonium cation in the structure of **38b** appears disordered over several positions forming an unresolvable ball

of electron density. These were refined isotropically with restricted geometry over three positions. For improved overall precision, the contribution of disordered dichlomethane was removed from diffraction data by the PLATON SQUEEZE procedure.

Full-sets of diffraction data for colourless crystals of **56, 60** and **87** were obtained at 150K using an Oxford Cryostream low-temperature device on a Nonius KappaCCD diffractometer with Mo/K_α radiation (λ = 0.71073 Å), a graphite monochromator, and the ϕ and χ scan mode. Data reductions were performed with DENZO-SMN.[214] The absorption was corrected by integration methods.[215] Structures were solved by direct methods (Sir92)[216] and refined by full matrix least-square based on F^2 (SHELXL97).[217] Hydrogen atoms were mostly localized on the difference Fourier map. However, to ensure uniformity of treatment of crystal, all hydrogen were recalculated into idealized positions (riding model) and assigned temperature factors $H_{iso}(H)$ = 1.2 U_{eq} (pivot atom) or of 1.5U_{eq} (methyl). H atoms of the methylene moieties and hydrogen atoms in aromatic rings were placed with C-H distances of 0.97 and 0.93Å, and 1.1 Å for B-H and C-H bonds in the carborane cage. $R_{int} = \sum | F_o^2 - F_{o,mean}^2 | / \sum F_o^2$, $S = [\sum(w(F_o^2 - F_c^2)^2)/(N_{diffrs} - N_{params})]^{1/2}$ for all data, $R(F) = \sum | | F_o | - | F_c | | / \sum | F_o |$ for observed data, $wR(F^2) = [\sum(w(F_o^2 - F_c^2)^2)/(\sum w(F_o^2)^2)]^{1/2}$ for all data.

CA Inhibition Assay.

An Applied Photophysics stopped-flow instrument was used for assaying the CA-catalyzed CO_2 hydration activity in the presence of inhibitors. Phenol red, at a concentration of 0.2 mM, was used as pH indicator at the absorbance maximum of 557 nm, with 20 mM HEPES (pH 7.5) and 20 mM Na_2SO_4. Rates of the CA-catalyzed CO_2 hydration reaction were followed for a period of 30 s, the CO_2 concentration was 8.5 mM. For each inhibitor, at least six traces of the initial 5−10% of the reaction were used for determining the initial velocity. The uncatalyzed rates were determined in the same manner and subtracted from the total observed rates. Stock solutions of inhibitor (10 mM) were prepared in dimethylsulfoxide (DMSO), and dilutions up to 0.01 nM were performed thereafter with DMSO (final concentration of DMSO was at maximum 2.5%). Inhibitor and enzyme solutions were preincubated together for 5 min at room temperature prior to assay, in order to allow for the formation of the E−I complex. The inhibition constants were obtained by nonlinear least-squares methods using an EXCEL spreadsheet. CA isoforms were recombinant and obtained as reported earlier in this chapter.

Protein Cloning, Expression, and Purification

To stabilize CA IX isoform during measurements, 0.0025 % Dodecyl-β-D-maltopyranosid (DDM, Anatrace) was included into the reaction mixture. CA II expression

plasmid (pET-based) was kindly provided by McKenna.[218] CA IX mimic was obtained by introducing mutations A65S, N67Q, E69T, I91L, F131V, K170E, and L204A described in Ref.[218] into the CA II coding region. The mutations were part of a chemically synthesized (Eurofins Genomics, Germany) 600 bp BamHI-HindIII subfragment that was used to replace the wt CA II sequence. Both, wild-type CA II and CA II mimic were expressed in *E.coli* BL21(DE3) and purified as described in the literature.[218]

CA IX was expressed in HEK-293 cells as a construct coding for extracellular part of CA IX comprising of PG and CA domains (residues 38-391). Mutation C174S was introduced according to Alterio et al.[219] The N-terminus consisted of a cleavable leader peptide, His-tag and TEV protease recognition site (MEWSWVFLFFLSVTTGVHSHHHHHHHGTENLYFQ) with amino acid residues SNAAS following the cleavage site. For expression, the whole construct was cloned into a pTT5 vector for expression in human embryonal kidney (HEK) cells. HEK 293 6E cells were cultured in CD 293 medium (Invitrogen) supplemented with 4 mM glutamine and 25 μg/ml G418 at 37°C and 5% CO_2 atmosphere in the spinner with 100 rpm. Eighteen hours prior transfection, HEK 293 cells were transferred into transfection and growth medium Freestyle 293 in a 1l baffled bottle. The seeding density of HEK 293 cells was $0.6x10^6$ cells/ml of media, the volume of the cell suspension was 150 ml. Cells were cultivated for 18 hours at 37°C and 5% CO_2 before transfection by 250 μg plasmid DNA and 250 μl of Lipofectamine 2000 in 10 ml medium Opti MEM-01 (Invitrogen). Cells were incubated 4 h at 120 rpm, 37°C and 5% CO2 atmosphere, and then 150 ml of fresh Freestyle 293 was added to the flask. After 3 days, an additional 200 ml of Freestyle 293 were pipetted into the bottle (swirl speed increased to 150 rpm) and the amount of expressed protein CAIX was determined by ELISA. Nine days later the transfection medium was collected by centrifugation at 4°C, in two steps: 500 g for 10 min and 23000 g for 1h. The final step of cell debris removal was achieved by sterile filtration through a 0.22 μm bottle top filter (Corning). The filtered medium was dialyzed against buffer A (50 mM NaH_2PO_4 pH 8.3; 300mM NaCl) and the sample was loaded onto the column His Trap HP 5 ml (GE Healthcare) equilibrated in buffer A at 4°C. His tagged CA IX was eluted from the column by step gradient 50-500mM imidazole in buffer A. Collected fractions containing CA IX were dialyzed into storage buffer (20 mM HEPES pH 7.5; 100 mM Na_2SO_4).

Protein Crystallization and X-ray Data Collection

For X-ray studies, CA II, comprising amino acid substitutions A65S, N67Q, E69T, I91L, F131V, K170E, and L204A was used as a CA IX mimic.[218] The enzyme was prepared in *E. coli*. Complexes of a recombinant CA IX mimic with compounds **51a**, **51b, 61o, 71 and 70p**

were prepared by addition of a 1.1-fold molar excess of inhibitor (dissolved in DMSO) to a 25 mg/ml protein solution in 50mM Tris pH 7.8. The crystals were prepared using the vapour-diffusion hanging drop at 18°C. Drops containing 2 µl of complex solution were mixed with 1 µl of precipitant solution and equilibrated over a reservoir containing 1 ml of precipitant solution (containing 1.6 M sodium citrate, 50 mM Tris-HCl pH 7.8). For data collection, the crystals were soaked in a reservoir solution supplemented with 20% (v/v) sucrose and stored in liquid N_2. Diffraction data at 100 K were collected using BL14.1 beamline operated by the Helmholtz-Zentrum Berlin (HZB) at the BESSY II electron storage ring (Berlin-Adlershof, Germany).[220] Diffraction data were processed using the XDS suite of programs.[221,222]

Structure Determination, Refinement, and Analyses

The crystal structure of CA IX mimic complexes with compound **51a** was determined by the difference Fourier technique, and the structure of **51b** complex was solved by molecular replacement using the MolRep program,[223] both using the CA II structure (PDB entry 3PO6)[93] as a model. Atomic coordinates of inhibitor molecules were generated by quantum mechanical (QM) optimizations in Turbomole package[224] using density functional theory (DFT) method using the B-LYP functional and the SVP basis set, augmented with empirical dispersion correction.[225] The geometric library for the inhibitors was generated using the Libcheck program. The Coot program[226] was used for inhibitor fitting, model rebuilding, and the addition of water molecules. The refinement was carried out with Refmac5 program[227], with 5% of the reflections reserved for cross-validation.

The structures were first refined with isotropic Atomic Displacement Parameters (ADPs). After addition of solvent atoms and zinc ions, building inhibitor molecules in the active site, and several alternate conformations for a number of residues, anisotropic ADPs were refined for nearly all atoms (with the exception of spatially overlapping atoms in segments with alternate conformations; also oxygen atoms of water molecules with an unrealistic ratio of ellipsoid axes were refined with isotropic ADPs) including atoms in the inhibitor molecules. Compound **51a** was modelled into two alternative conformations with partial occupancy 0.5 and 0.3. Compound **51b** was modelled in one conformation with full occupancy. The quality of the crystallographic model was assessed with MolProbity.[228] All the figures representing structures were created using PyMOL [Schrodinger, LLC (2010) The PyMOL Molecular Graphics System, Version 1.3r1]. Atomic coordinates and structure factors for the crystal structures of **51a** and **51b** complexed with CA IX mimic enzyme were deposited in the PDB with accession codes 5OGP and 5OGN, respectively.

Cell cytotoxicity/proliferation assay

All drug treatment was performed in a standard 37°C humidified 5% CO_2/ 95% air incubator. Cell viability was assayed by a standard MTS cell proliferation assay. The cells were maintained in Nunc/Corning 80 cm^2 plastic tissue culture flasks and cultured in cell culture medium (DMEM or RPMI 1640 supplemented with 10% fetal calf serum, 5 g/L glucose, 2 mM glutamine, 100 U/mL penicillin, 100 µg/mL streptomycin and $NaHCO_3$). Cell suspensions were prepared according to the particular cell type and the expected target cell density (500 – 4,000 cells/well based on cell growth characteristics). Cells were seeded to 384-well destination plates by MultiDrop Combi (Thermo Fisher Scientific, Waltham, MA, USA). Inoculates were pre-incubated for 24 h at 37°C and 5% CO_2 for stabilization. After 24h tested compounds were added to cells by the Echo 550 (Labcyte, USA). Compounds were on the source 384-well LDV plates each in 3 concentrations (10, 1 and 0.1 mM in DMSO). Defined volumes (150 – 5 nl) from defined wells of source plate were transferred by the Echo to defined wells in 384 destination plates (cells). The highest tested concentration of each compound was 50 µM, and the dilution factor was 4. All test compound concentrations were examined in duplicate. On the destination plate (cells) wells with the high (DMSO) and low (ActD and MitC) controls were included. Incubation of the cells with the test compounds was performed for 72h at 37°C in a 5% CO_2 atmosphere at 95 % humidity in the SteriStore (HighResBiosolutions, USA). At the end of the incubation period, the cells were assayed using MTS. Aliquots (4 µl/well) of the MTS stock solution were dispensed to destination plate by BioTek EL 406 (Winooski, VT, USA) and incubated for a further 1–4 h. The optical density (OD) was measured at 490 nm in an EnVision plate reader (Perkin Elmer, Waltham, MA, USA). The IC_{50} value was calculated from the appropriate dose-response curves in Dotmatics (San Diego, CA, USA).

Raman spectroscopy

CaF_2 substrate with fixed cells was placed on a Petri-dish filled with PBS buffer and positioned in a confocal Raman spectrometer WITec Alpha300 R+ (WITec GmbH, Germany) that is coupled with a WITec UHTS300 300 mm focal length lens-based imaging spectrometer (600 grooves/mm grating) and thermoelectrically-cooled detector with back-illuminated CCD chip Marconi 40-11CCD (1024 x 127 pixel format) optimized for VIS spectral region. Bright field images and Raman maps were acquired using Nikon NIR Apo 60x water immersion objective (NA: 1.0). For Raman measurements, samples were excited at 532 nm by a Spectra Physics Excelsior 532-60 laser with 40 mW power. Raman maps of selected cell clusters were done using the piezo stage with raster 3 pixels/µm. Integration of time for each spectrum was

250 ms. Data evaluation was performed using WITec Project Plus software. As an initial step, cosmic rays spikes were removed from the spectral datacube using a built-in procedure. Further evaluation was based on the presence of the specific marker at approximately 200 cm^{-1} in the Raman spectra of **51b** and **52b** carborane, which probably correspond to a stretching mode between the central cobalt atom and the boron cage.[229] Direct comparison of **51b** and **52b** DMSO solutions under identical conditions showed that this marker band is 6.3x stronger in the Raman spectra of **51b** than in **52b**. This fact was taken into account in quantitative comparisons of **51b** and **52b** carborane distribution in cells.

In vitro pharmacology

To measure plasma stability, compounds at a final concentration of 2 μM (DMSO < 0.1%) were incubated with human plasma obtained from the University Hospital, Olomouc, Czech Republic at five different time points (0, 15, 30, 60 and 120 min) at 37°C. The reactions were terminated by adding acetonitrile methanol (2:1) and samples were left at -80°C overnight, followed by centrifugation, lyophilization, and determination by RF-MS as described previously.[230]

Microsomal stability assay with a reaction mixture consisting of compounds (2 μM), 0.5 mg/mL human liver microsomes (ThermoFisher Scientific) and NADPH generating system ($NADP^+$, isocitrate dehydrogenase, isocitric acid, and $MgSO_4$ in 0.1 mol/l K_3PO_4 buffer) was carried out according to the protocol described elsewhere.[231] The assay was performed at 0, 15, 30, and 60 min. intervals. Reactions were terminated using a solution of acetonitrile–methanol (2:1) followed by centrifugation at 3000 rpm for 6 min at 4°C. The supernatant was lyophilized, and the samples were dissolved in a mobile phase containing an internal standard and analyzed by RF-MS as described previously.[230]. The intrinsic clearance was calculated using the formula: $CL_{int} = V*(0{,}693/t_{1/2})$, where V is the volume of incubation in μL related to the weight of microsomal protein in mg per reaction. Half-life values were calculated using the equation $t_{1/2} = 0.693/k$, where k is the slope of the line of the percent compound remaining versus time curve.

The artificial membrane permeability assay (PAMPA) was performed with the Millipore MultiScreen Filter MultiScreen-IP Durapore 0.45 μm plates and receiver plates (Merck Millipore, city, country) according to the manufacturer's protocol.

The protein plasma binding (PPB) assay was carried out using the Rapid Equilibrium Dialysis (Thermo Scientific™, Rockford, USA) according to manufacturer's protocol.[232]

Cell permeability assay was performed on monolayers of Caco-2 and MDR1-MCDK in Transwell® plates were used for transport studies when they had differentiated and the monolayer was intact (determined by checked by Lucifer Yellow Rejection Assay). Prior to the

experiment, the cells were washed with HBBS (Gibco, Waltham, USA) and pre-equilibrated for 1h in HBSS-buffered at pH 7.4. The cells were then treated with carboranes at 10 μM in HBSS for 1h (MDCK) and 2h (Caco-2). After incubation, followed by lyophilization, samples were dissolved in a mobile phase containing internal standard and analyzed on the RF-MS.

The apparent permeability coefficient was calculated according to Eq. 1:

$$P_{app} = \left(\frac{dQ/dt}{C_0 \times A} \right)$$

Where dQ/dt is the rate of permeation of the drug across the cells, C_0 is the donor compartment concentration at time zero and A is the area of the cell monolayer. C_0 is obtained from analysis of the dosing solution at the start experiment.

The efflux ratio was calculated using the following equation (Eq. 2):

$$R = \frac{P_{BA}}{P_{AB}}$$

Where P_{BA} and P_{AB} represent the apparent permeability of test compound from the basal to apical and apical to the basal side of the cell monolayer. The compounds having an efflux ratio of > 2 is considered as having the potential for the P-gp substrate.

The percentage recovery can be useful in interpreting the permeability data (Eq. 3).

$$\%\text{Recovery} = \frac{\text{Total compound in donor and receiver at end of experiment (nmol)}}{\text{Initial compound present (nmol)}} \times 100$$

If the recovery is very low, this may indicate problems with poor solubility, binding of the compound to the plate, metabolism by cells or the accumulation of the compound in the cell monolayer.

Bioanalytics–RF-MS system setup.

The RapidFire RF300 system (Agilent Technologies) was interfaced with a QTRAP 5500 (AB Sciex) mass spectrometer fitted with an electrospray ionization source and running in MRM mode. For a detailed description, see ref.[233] Mass spectrometry was carried out using electrospray ionization in the negative ion mode. Daughter ion peaks were identified using a multiple – reaction monitoring protocol.

Tumour xenografts and drug administration

Human colorectal cancer HT-29 cells were xenotransplanted ($1.5x10^6$ cells/injection) subcutaneously to both sides of the chest of immunodeficient SCID mice (Envigo, Huntingdon, United Kingdom). Mouse breast cancer 4T1 cells were xenotransplanted ($1x10^6$ cells/mice) orthotopically into the seventh mammary fat pad of BALB/c mice (Envigo, Huntingdon, United Kingdom). Animals were randomly enrolled into study groups and treated with compounds

51b, **52b** or U-104 when the optimal tumour size was reached. The compounds were administered intraperitoneally repeatedly on days 1-5, 8-12, and 15-19. Compounds **51b** and U-104 were administered once per day at a dose of 62.5 mg/kg and 38 mg/kg, respectively, whereas, **52b** was administered twice per day at a dose of 62.5 mg/kg. The animals were monitored for an overall period of 24 or 33 days following compound administration. The size of the tumour was recorded using a caliper and the volume was calculated using a modified ellipsoid formula [$(LxW^2)/2$, where L and W denote length and width, respectively). Animals were housed in a Specific Pathogen Free conditions, 12 h light/night regime, and clinically examined on a daily basis for water and food *ad libitum*. All procedures in animals were approved by the Animal Ethics Committee of Faculty of Medicine and Dentistry, Palacký University Olomouc, Czech Republic.

APPENDIX TWO

EXPERIMENTAL DATA

General synthetic procedure for mono- and dialkylhydroxy derivatives 36 - 37.

Procedure A: Reaction in the ratio 1:1.1. Carefully dried (24h at 180°C under reduced pressure) compound **3** (2.28 g, 4.99 mmol) was dissolved in DME (20 ml) under Ar and cooled to approx. -78°C using an acetone/CO_2 (s) bath and the solution was then treated with ^{n}BuLi (2.5 M in hexane, 2.2 ml, 5.35 mmol). The mixture was allowed to warm to room temperature. After cooling again (same conditions as previously), a solution of electrophile (PFA, oxirane or oxetane) in DME (3 ml containing 5.35 mmol of the reagent) was quickly added in one portion from a gas tight syringe. After stirring for an additional 15 min at -78°C, the content of the flask was left to warm to room temperature, gradually changing colour to red. The reaction was quenched by adding 5 ml of MeOH and 0.5 ml of AcOH. The reaction mixture was evaporated and extracted with Et_2O and 3M HCl (3x20 ml), the organic layer was then evaporated and dissolved in minimum volume of MeOH and precipitated with Me_4NCl for preparative purposes. The mixture was then separated using column chromatography (CH_2Cl_2:CH_3CN 4:1, 2x30 cm) giving three bands: first, yellow for parent anion **3**, second, orange for monosubstituted and, third, for disubstituted derivative. The solvent was remved by evaporation and, as before, the mono- and dialkylhydroxy derivatives were extractedwith Et_2O and 3M HCl (3x20 ml). The organic layer was then evaporated and dissolved in a minimum volume of MeOH and precipitated with Me_3NHCl.[5]

Procedure B: Reaction in the ratio 1:2.2. The amount of **3** and the reaction conditions were analogous as in the above experiment, but twofold quantities of ^{n}BuLi (2.5 M in hexane, 4.5 ml, 11.25 mmol) and electroophile in DME solution (11.6 mmol) were used. The reaction mixture was stirred for 40h at room temperature. The products were isolated as described above. None of the starting material, **3**, was observed during the isolation. The ratio of the two isomers of **37** present in the reaction mixture was similar to that observed above. It should be noted that, the red band of **37** was taken in two fractions. The first fraction contained the crude *anti*-isomer. This was further purified by dissolution in aqueous ethanol and precipitation of the crude *anti* **37** Me_3NH. The second fraction provided mixture of *anti*-, *syn*- and *vicinal*-isomers (see later in the text). Further elution with CH_2Cl_2-CH_3CN gave a dark red band which, according to MS (ESI^-), might contain small amount of tri- and tetrasubstituted compounds, but the products were neither isolated nor further characterized.[5]

1-Methylenehydroxy-3,3'-cobalt(III) bis(1,2-dicarbarbollide), trimethylammonium salt, [(1-HO-CH_2-1,2-$C_2B_9H_{10}$)(1′,2′-$C_2B_9H_{11}$)-3,3′-Co]Me_3NH **(36a)**

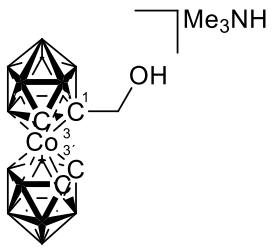

36a

We followed Procedure A. Yield when the reaction was in the ratio 1:1: 0.94 g, 47%. Data corresponds with published results.[5]

1-Ethylenehydroxy-3,3'-cobalt(III) bis(1,2-dicarbarbollide), trimethylammonium salt, [(1-HO-$(CH_2)_2$-1,2-$C_2B_9H_{10}$)(1′,2′-$C_2B_9H_{11}$)-3,3′-Co]Me_3NH **(36b)**

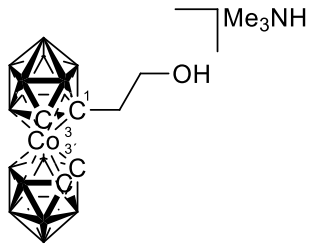

36b

We followed Procedure A. Yield when the reaction was in the ratio 1:1: 50%. Data corresponds with published results.[5]

1-Propylenehydroxy-3,3'-cobalt(III) bis(1,2-dicarbarbollide), trimethylammonium salt, [(1-HO-$(CH_2)_3$-1,2-$C_2B_9H_{10}$)(1′,2′-$C_2B_9H_{11}$)-3,3′-Co]Me_3NH **(36c)**

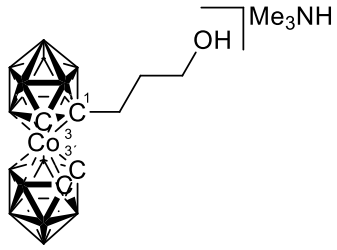

36c

We followed Procedure A. Yield when the reaction was in the ratio 1:1: 54%. Data corresponds with published results.[5]

1,1´-Di(methylenehydroxy)-3,3'-cobalt(III) bis(1,2-dicarbarbollide), trimethylammonium salt, [(1,1´-HO-CH_2-1,2-$C_2B_9H_{10}$)$_2$-3,3´-Co]Me_3NH **(37a)**

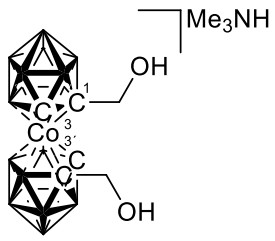

37a

We followed Procedure B. Yield when the reaction was in the ratio 1:2: 40%. Data corresponds with published results.[5]

1,1´-Di(ethylenehydroxy)-3,3'-cobalt(III) bis(1,2-dicarbarbollide), trimethylammonium salt, [(1,1´-HO-$(CH_2)_2$-1,2-$C_2B_9H_{10}$)$_2$-3,3´-Co]Me_3NH **(37b)**

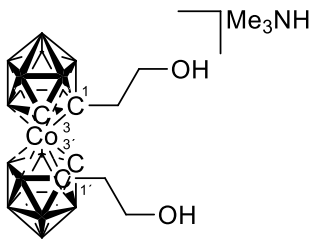

37b

We followed Procedure B. Yield when the reaction was in the ratio 1:2: 56%. Data corresponds with published results.[5]

1,1´-Di(propylenehydroxy)-3,3'-cobalt(III) bis(1,2-dicarbarbollide), trimethylammonium salt, [(1,1´-HO-$(CH_2)_3$-1,2-$C_2B_9H_{10}$)$_2$-3,3´-Co]Me_3NH **(37c)**

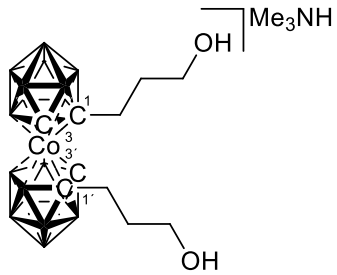

37c

We followed Procedure B. Yield when the reaction was in the ratio 1:2: 50%. Data corresponds with published results.[5]

Separation of *anti*-diastereoisomers from mixtures of dihydroxyderivatives of general formula [(HO-(CH2)$_n$C$_2$B$_9$H$_{10}$)$_2$-3,3'-Co]Me$_3$NH (n= 1-3).

The presence of several isomers of disubstituted species after reactions and their stereochemistry was discussed previously.[5] We searched this time for simpler purification procedures for the main isomers [1,1'-(HO-$(CH_2)_n$-1,2-$C_2B_9H_{10}$)$_2$-3,3'-Co)]$^-$ (**37a-c**) by methods other than tedious chromatography. This could be accomplished by multiple crystallizations of Me_3NH^+ salts from CH_2Cl_2–hexane (adding with a few drops of MeOH to the CH_2Cl_2 dissolution). The 1,1'-substituted (*anti*-) isomer then crystallizes out and the other main (*syn-)* isomer accumulates in the mother liquors. The ease of their separation depends on

the length of the alkyl chain. Two to three crystallizations were therefore necessary to reach a purity better than 99.0% (HPLC analysis)[213] for di(methylenehydroxy), Five to six successive crystallizations for the di(ethylenehydroxy) derivative and about ten crystallizations for the di(propylenehydroxy) derivative.

General synthetic procedure (C) of monosubstituted methanesufonyl and *p*-toluenesulfonate esters 38 - 42.

The corresponding Me_3NH^+ salt 1-alkylhydroxy-1,2-cobalt bis(dicarbollide) (0.80 g, 2.0 mmol) was dried 12h at 80°C and was then dissolved under N_2 in dry CH_3CN (15 ml). Solid Cs_2CO_3 (0.78 g, 2.4 mmol) was added under stirring followed by the addition of *p*-TsCl (or MsCl) in CH_3CN by syringe (4.4 mmol in 2 ml). In the case of tosylate esters, the resulting slurry was stirred and heated at 80°C for 3h, and at 45°C and 4h for the methylsulfonate esters. After cooling, the volatiles were removed under reduced pressure. The solid residue was dissolved rapidly in a smallest volume of methanol, water (5 ml) was then added and the crude product was precipitated by the addition of an excess of aqueous Me_4NCl under vigorous stirring followed by rapid filtration or decantation after standing for 5-10 min. The orange solid was washed with a small volume of water (3x10 ml) and several portions of hexane (3x10 ml) and immediately dried under vacuum at room temperature for 1h, then dissolved in CH_2Cl_2 (eventually with the addition of a small volume of acetone for dissolution), layered with hexane and left to crystallize overnight. The *semi*-crystalline product was decanted, washed with hexane and dried in vacuum for 8h. This procedure furnished essentially pure methanesulfonate or *p*-tosylate esters. For analytical purposes, the esters were quickly purified by liquid chromatography on a silica gel column 1.5x10 cm, and a mobile phase consisting of CH_2Cl_2-CH_3CN (4:1). The collected fractions were immediately evaporated under vacuum and dried for at least 2h. The esters with ethylene and propylene connectors may be stored in dry form under N_2 at room temperature. However, their long-term storage is better accomplished in a fridge.

1-Methylene-methanesulfonate-3,3'-cobalt(III) bis(1,2-dicarbarbollide), tetramethylammonium salt, [(1-CH_3SO_2-OCH_2-1,2-$C_2B_9H_{10}$)(1′,2′-$C_2B_9H_{11}$)-3,3′-Co]Me_4N **(38a)**

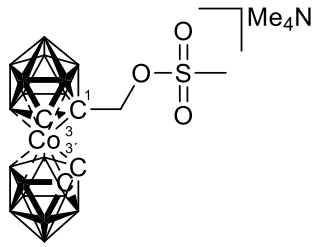

38a

We followed Procedure C. According to HPLC analysis, even after repeated addition of Cs_2CO_3 and MsCl chloride after 6 and 24h and prolonged heating for 48h the reaction led only to 78% conversion. The product was precipitated as the Me_4N^+ salt and twice recrystallized. Using this procedure, the product was isolated only in 86% purity (HPLC assay) with the, main impurity being the hydroxymethyl derivative **36a**. Due to the impossibility of purifying by chromatography (decomposition), this crude product was used for reactions with amines described below. Yield 3.84g (76%), orange solid; R_f (CH_2Cl_2-CH_3CN 4:1) 0.58; mp 63°C; ^{1}H NMR δ_H (400 MHz; acetone-d_6), 5.08 (3H, d, J = 6.6 Hz, SCH_3), 4.21 (1H, s, carborane C*H*), 4.08 (1H, s, carborane C*H*), 3.98 (1H, s, carborane C*H*), 3.45 (12H, s, (CH_3)$_4N^+$), 2.89 (2H, s, CH_2O); ^{11}B NMR δ_B (128 MHz; acetone-d_6; $Et_2O{\cdot}BF_3$), 6.99 (2B, d, J = 116 Hz, B8, 8′), 1.66 (2B, d, J = 137 Hz, B10, 10′), -6.24 (8B, d, J = 125 Hz, B4, 4′, 7, 7′, 9, 9′, 12, 12′), -14.73 (1B, d, J = 153 Hz, B5), -17.27 (3B, d, J = 153 Hz, B5′, 11, 11′), -20.43 (1B, d, J = 189 Hz, B6), -22.86 (1B, d, J = 168 Hz, B6′); ^{13}C NMR δ_C (100 MHz; acetone-d_6), 74.72 (1C, SCH_3), 56.66 (1C, carborane *C*), 56.04 (4C, (CH_3)$_4N^+$), 55.38 (1C, carborane *C*H), 51.53 (1C, carborane *C*H), 50.91 (1C, carborane *C*H), 37.52 (1C, CH_2O); *m/z* (ESI$^-$) 435.55 (M$^-$, 14%), 432.58 (100%), calc. 435.26 and 432.27.

1-Ethylene-methanesulfonate-3,3'-cobalt(III) bis(1,2-dicarbarbollide), tetramethylammonium salt, [(1-CH_3SO_2-$O(CH_2)_2$-1,2-$C_2B_9H_{10}$)(1′,2′-$C_2B_9H_{11}$)-3,3′-Co]Me_4N **(38b)**

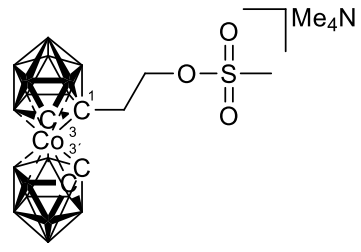

38b

We followed Procedure C. Yield 4.1 g (79%), orange solid; R_f (CH_2Cl_2-CH_3CN 4:1) 0.50; mp 80°C; Analysis found: C, 25.1; H, 7.5 calc. for $CoB_{18}C_{11}H_{40}SO_3N$: C, 25.4; H, 7.8%; ^{1}H NMR δ_H (400 MHz; acetone-d_6), 4.40 (2H, m, CH_2CH_2O), 4.17 (1H, s, carborane C*H*), 3.85 (1H, s, carborane C*H*), 3.77 (1H, s, carborane C*H*), 3.47 (12H, s, (CH_3)$_4N^+$), 3.30 (2H, m, CH_2CH_2O), 3.13 (3H, s, CH_3), 2.88 (2H, m, CH_2CH_2O); ^{11}B NMR δ_B (128 MHz; acetone-d_6; $Et_2O{\cdot}BF_3$), 6.89 (2B, d, J= 140 Hz, B8, 8'), 1.18 (2B, d, J = 144, B10, 10'), -5.71, -6.93 (8B, 4d, overlap, B4, 4′, 7, 7′, 9, 9', 12, 12'), -15.63, -17.56 (4B, 2d, overlap, B5, 5′, 11, 11′), -19.74 (1B, d, overlap, B6), -23.03 (1B, d, J = 162 Hz, B6'); ^{13}C NMR δ_C (100 MHz; acetone-d_6),

70.56 (1C, S*C*H$_3$), 65.28 (1C, carborane *C*), 57.41 (1C, carborane *C*H), 56.01 (4C, (*C*H$_3$)$_4$N$^+$), 53.89 (1C, carborane *C*H), 52.01 (1C, carborane *C*H), 39.25 (1C, CH$_2$*C*H$_2$O), 37.26 (1C, *C*H$_2$CH$_2$O); *m/z* (ESI$^-$) 449.25 (M$^-$,18 %), 446.33 (100 %), calc. 449.28 and 446.29. Crystal for X-ray diffraction study were grown by careful layering of CH_2Cl_2 solution of **38b** (to which few drops of MeOH for complete dissolution) with hexane in a grass tube, leaving it crystallize for several days.

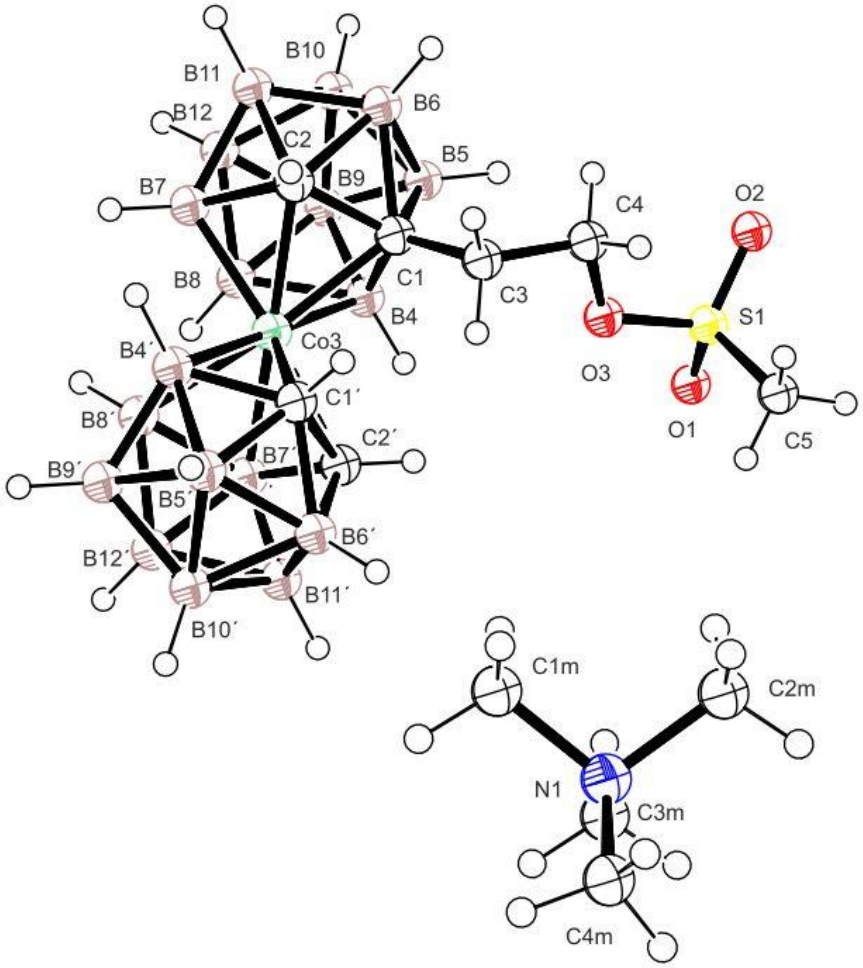

Crystal data for **38b**: $C_7H_{28}B_{18}CoO_3S{\cdot}C_4H_{12}N$, M_r = 520.01, Monoclinic, $P2_1/c$ (No 14), a = 13.1051 (3) Å, b = 17.4222 (4) Å, c = 13.1627 (2) Å, β = 92.068 (1)°, V = 3003.35 (11) Å^3, Z = 4, D_x = 1.150 Mg m^{-3}, red prism of dimensions 0.40 × 0.34 × 0.32 mm, multi-scan absorption correction (μ = 0.66 mm^{-1}), T_{min} = 0.782, T_{max} = 0.818. A total of 24,749 measured reflections (θ_{max} = 27.5°), from which 6897 were unique (R_{int} = 0.033) and 5380 observedaccording to the $I > 2\sigma(I)$ criterion. The refinement converged ($\Delta/\sigma_{max} \leq 0.001$) to R = 0.059 for observed reflections and $wR(F^2)$ = 0.185, *GOF* = 1.09 for 316 parameters and all 6897 re-flections. The final difference map displayed no peaks of chemical significance ($\Delta\rho_{max}$ = 1.59, $\Delta\rho_{min}$ = -0.96

e.Å^{-3}). Crystallographic data for structural analyses are deposited with the Cambridge Crystallographic Data Centre, CCDC deposition no. 1059429.

1-Propylene-methanesulfonate-3,3'-cobalt(III) bis(1,2-dicarbarbollide), tetramethylammonium salt, [(1-CH_3-SO_2-O$(CH_2)_3$-1,2-$C_2B_9H_{10}$)(1′,2′-$C_2B_9H_{11}$)-3,3′-Co] Me_4N **(38c)**

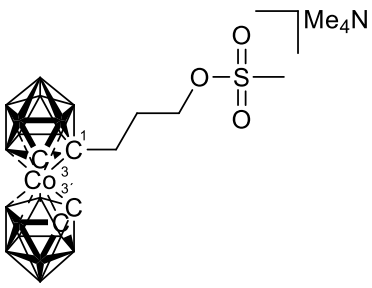

38c

We followed Procedure C. Yield 4.3 g (81%), orange solid; R_f (CH_2Cl_2-CH_3CN 4:1) 0.55; mp 77°C; Analysis found: C, 26.7; H, 7.6 calc. for $CoB_{18}C_{12}H_{42}SO_3N$: C, 27.0; H, 7.9%; ^{1}H NMR δ_H (400 MHz; acetone-d_6), 4.26 (2H, m, $CH_2CH_2CH_2O$), 4.10 (1H, s, carborane C*H*), 3.75 (1H, s, carborane C*H*), 3.67 (1H, s, carborane C*H*), 3.46 (12H, s, $(CH_3)_4N^+$), 3.07 (3H, s, SCH_3), 2.91 (2H, m, $CH_2CH_2CH_2O$), 2.54 (2H, m, $CH_2CH_2CH_2O$); ^{11}B NMR δ_B (128 MHz; acetone-d_6; $Et_2O{\cdot}BF_3$), 6.65 (2B, d, J = 119 Hz, B8, 8′), 0.87 (2B, d, J = 140 Hz, B10, 10′), -5.86 (8B, d, J = 131 Hz, B4, 4′, 7, 7′, 9, 9′, 12, 12′), -15.15 (1B, d, overlap, B5), -17.75 (3B, d, overlap, B5′, 11, 11′), -19.44 (1B, d, overlap, B6), -22.88 (1B, d, J = 150 Hz, B6′); ^{13}C NMR δ_C (100 MHz; acetone-d_6), 68.87 (1C, $CH_2CH_2CH_2O$), 57.88 (1C, carborane *C*), 56.14 (1C, carborane *C*H), 54.00 (1C, carborane *C*H), 51.73 (1C, carborane *C*H), 48.13 (4C, $(CH_3)_4N^+$), 48.04 (1C, SCH_3), 37.04 (1C, $CH_2CH_2CH_2O$), 26.24(1C, $CH_2CH_2CH_2O$); *m/z* (ESI$^-$) 463.51 (M^-, 15%), 460.50 (100%), calc. 463.30 and 460.30.

1-Methylene-*p*-toluenesulfonate-3,3'-cobalt(III) bis(1,2-dicarbarbollide), tetramethylammonium salt, [(1-(4-CH_3-C_6H_4)SO_2-OCH_2-1,2-$C_2B_9H_{10}$)(1′,2′-$C_2B_9H_{11}$)-3,3′-Co]Me_4N **(39a)**

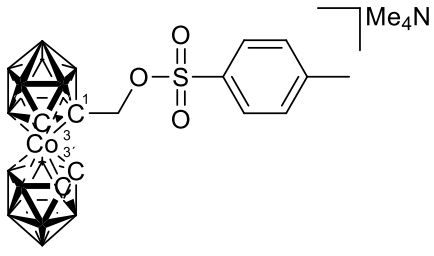

39a

This compound could not be prepared according to the above general procedure. An alternative method was used: The Me_3NH salt of hydroxymethyl derivative **36a**, 105 mg (0.25 mmol) was dissolved in Et_2O (10 ml), and stirred with 1 ml of aqueous 50% CsOH for 10 min. after which time, *p*-TsCl 190 mg (1.0 mmol) dissolved in Et_2O (20 ml) was added and the biphasic system was stirred for 3h. The organic phase was separated and the aqueous phase was extracted by Et_2O-EtOAc (1:1, 3x25 ml). The organic extracts were combined, washed with water (4x20 ml), separated and immediately evaporated under vacuum. The solid residue was dissolved in a mobile phase consisting of CH_2Cl_2-CH_3CN (1:1) and

chromatographed on a silica gel column 1.5x25 cm. The fractions containing the product were combined and evaporated. The product was dissolved in a minimum volume of MeOH and precipitated by aqueous Me_4NCl, separated by decantation, washed with water (3x2 ml), hexane (3x2 ml) and dried under vacuum. The product was crystallized from CH_2Cl_2-hexane; yield 70 mg (47%), orange solid; R_f (CH_2Cl_2-CH_3CN 4:1) 0.60; mp 96°C; ^{1}H NMR δ_H (400 MHz; acetone-d_6), 7.80 (2H, d, J = 8.4 Hz, Ar*H*), 7.51 (2H, d, J = 8.4 Hz, Ar*H*), 4.15 (1H, s, carborane C*H*), 3.96 (1H, s, CH_2O), 3.91 (1H, s, carborane C*H*), 3.57 (1H, s, carborane C*H*), 3.50 (12H, s, (CH_3)$_4N^+$), 2.47 (3H, s, ArCH_3); ^{11}B NMR δ_B (128 MHz; acetone-d_6; $Et_2O{\cdot}BF_3$), 6.91 (2B, d, J = 131 Hz, B8, 8'), 1.47 (2B, d, J = 150 Hz, B10, 10'), -6.21 (8B, 4d, overlap, B4, 4', 7, 7', 9, 9', 12, 12'), -14.51 (1B, d, J = 156 Hz, B5), -17.41 (3B, d, J = 156 Hz, B5', 11, 11'), -20.43 (1B, d, J = 171 Hz, B6), -22.95 (1B, d, J = 171 Hz, B6'); ^{13}C NMR δ_C (100 MHz; acetone-d_6), 146.35 (1C, Ar*C*), 133.43 (1C, Ar*C*), 131.03 (2C, Ar*C*), 128.74 (2C, Ar*C*), 75.05 (1C, *C*H_2O), 69.23 (1C, carborane *C*), 54.83 (4C, Me_4N^+), 51.86 (1C, carborane *C*H) 51.39 (1C, carborane *C*H), 50.94 (1C, carborane *C*H), 21.57 (1C, *CH*$_3$); *m/z* (ESI$^-$) 511.58 (M$^-$, 18 %), 508.33 (100 %), calc. 511.30 and 508.30.

1-Ethylene-*p*-toluenesulfonate-3,3'-cobalt(III) bis(1,2-dicarbarbollide), tetramethylammonium salt, [(1-(4-CH_3-C_6H_4)SO_2-O(CH_2)$_2$-1,2-$C_2B_9H_{10}$)(1′,2′-$C_2B_9H_{11}$)-3,3′-Co]Me_4N **(39b)**

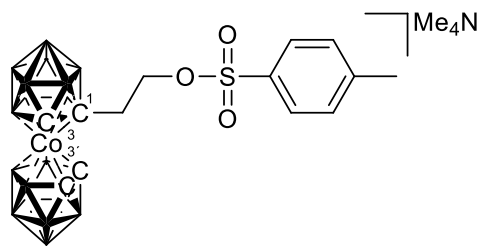

39b

We followed Procedure C. Yield 4.95 g (83%), orange solid; R_f (CH_2Cl_2-CH_3CN 4:1) 0.56; mp 89°C; Analysis found: C, 33.9; H, 7.2 calc. for $CoB_{18}C_{17}H_{44}SO_3N$: C, 34.3; H, 7.4%; ^{1}H NMR δ_H (400 MHz; acetone-d_6), 7.80 (2H, d, J = 7.32 Hz, Ar*H*), 7.50 (2H, d, J = 7.5 Hz, Ar*H*), 4.16 (2H, m, CH_2CH_2O), 3.73 (1H, s, carborane C*H*), 3.56 (1H, s, carborane C*H*), 3.46 (1H, s, carborane C*H*), 3.46 (12H, s, (CH_3)$_4N^+$), 3.05 (1H, m, *CH*$_2$CH$_2$O), 2.71 (1H, m, *CH*$_2$CH$_2$O), 2.47 (3H, s, CH_3); ^{11}B NMR δ_B (128 MHz; acetone-d_6; $Et_2O{\cdot}BF_3$), 6.77 (2B, d, J= 144 Hz, B8, 8'), 1.11, 0.78 (2B, 2d, J = 147 and 149 Hz, B10, 10'), -5.76, -6.99 (8B, 4d, overlap, B4, 4′, 7, 7′, 9, 9', 12, 12'), -15.65, -16.42 (2B, 2d, J =150 and 146 Hz, B5, 11), -17.58 (2B, d, J= 156 Hz, B5', 11'), -19.91 (1B, d, J = 180 Hz, B6), -23.00 (1B, d, J = 169 Hz, B6'); ^{13}C NMR δ_C (100 MHz; acetone-d_6), 146.07 (1C, Ar*C*), 134.08 (1C, Ar*C*), 131.01 (2C, Ar*C*), 128.63 (2C, Ar*C*), 70.88 (1C, *C*H_2O), 64.94 (1C, carborane *C*), 57.29 (1C, carborane *C*H), 56.07 (4C, (*C*H_3)$_4N^+$), 53.95 (1C, carborane *C*H), 51.94 (1C, carborane *C*H), 38.78 (1C, *C*H_2CH$_2$O), 21.58 (1C, *C*H_3); *m/z* (ESI$^-$) 525.17 (M$^-$,15 %), 522.25 (100 %), calc. 522.32 and 525.31.

1-Propylene-*p*-toluenesulfonate-3,3'-cobalt(III) bis(1,2-dicarbarbollide), tetramethylammonium salt, [(1-(4-CH_3-C_6H_4)SO_2-O(CH_2)$_3$-1,2-$C_2B_9H_{10}$)(1′,2′-$C_2B_9H_{11}$)-3,3′-Co]Me_4N **(39c)**

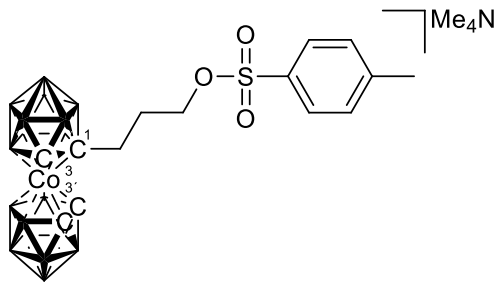

39c

We followed Procedure C. Yield 5.80 g (95%), orange solid; R_f (CH_2Cl_2-CH_3CN 4:1) 0.40; mp 103°C; Analysis found: C, 35.0; H, 7.4 calc. for $CoB_{18}C_{18}H_{46}SO_3N$: C, 35.4; H, 7.6%; ^{1}H NMR δ_H (400 MHz; acetone-d_6), 7.80 (2H, d, *J* = 6.8 Hz, Ar*H*), 7.49 (2H, d, *J* = 7.2 Hz, Ar*H*), 4.06 (2H, m, $CH_2CH_2CH_2O$), 3.77 (1H, s, carborane C*H*), 3.64 (1H, s, carborane C*H*), 3.54 (1H, s, carborane C*H*), 3.45 (12H, s, $(CH_3)_4N^+$), 2.90 (3H, s, ArCH_3), 2.70 (2H, m, $CH_2CH_2CH_2O$), 1.86 (2H, m, $CH_2CH_2CH_2O$); ^{11}B NMR δ_B (128 MHz; acetone-d_6; $Et_2O{\cdot}BF_3$), 6.70 (2B, d, *J* = 125 Hz, B8, 8′), 0.87 (2B, d, *J* = 137 Hz, B10, 10′), -5.90 (8B, d, *J* = 122 Hz, B4, 4′, 7, 7′, 9, 9′, 12, 12′), -15.39 (1B, d, overlap, B5), -17.45 (3B, d, overlap, B5′, 11, 11′), -19.39 (1B, d, overlap, B6), -22.88 (1B, d, *J* = 162, Hz B6′); ^{13}C NMR δ_C (100 MHz; acetone-d_6), 145.88 (1C, Ar*C*), 134.19 (1C, Ar*C*), 130.91 (2C, Ar*C*), 128.60 (2C, Ar*C*), 71.14 (1C, $CH_2CH_2CH_2O$), 57.95 (1C, carborane *C*), 56.03 (1C, carborane *C*H), 53.79 (1C, carborane *C*H), 51.72 (1C, carborane *C*H), 45.55 (4C, $(CH_3)_4N^+$), 36.67 (1C, ArCH_3), 25.19 (1C, $CH_2CH_2CH_2O$), 21.59; *m/z* (ESI$^-$) 539.33 (M^-, 18%), 536.50 (100%), calc. 539.32 and 536.33.

1-Propylene-acetate-3,3'-cobalt(III) bis(1,2-dicarbollide), trimethylammonium salt, [(CH3COO(CH_2)$_3$-1,2-$C_2B_9H_{10}$)(1′,2′-$C_2B_9H_{11}$)-3,3′-Co]Me_3NH **(40)**

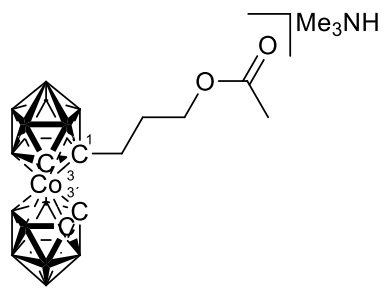

40

This model compound was prepared injecting an excess of AcCl 100 µl (1.33 mmol) to a stirred slurry of Me_3NH **36c** 220 mg (0.5 mmol) and K_2CO_3, 300 mg (2.2 mmol) in 25 ml of CH_3CN-toluene (1:1). The reaction mixture was stirred and heated for 4h at 60°C, then filtered and the filtrate evaporated under in vacuum. The isolation was made according to the general procedure C described above for alkylsulfonyl esters; but the crude product was precipitated from an acidified solution (few drops of 3M HCl) by Me_3NHCl, yield (72%). R_f (CH_2Cl_2-CH_3CN 4:1) 0.45; mp 123°C; ^{1}H NMR δ_H (400 MHz; acetone-d_6), 4.07 (1H, s, carborane C*H*), 4.01 (3H, t, J = 6.0 Hz, OCH_3), 3.72 (1H, s, carborane C*H*), 3.637 (1H, s, carborane C*H*), 3.21 (9H, s, $(CH_3)_3N$), 2.85 (1H, m, $CH_2CH_2CH_2O$), 2.45

(1H, m, $CH_2CH_2CH_2O$), 1.89 (2H, m, $CH_2CH_2CH_2O$), 1.42 (2H, m, $CH_2CH_2CH_2O$); ^{11}B NMR δ_B (128 MHz; acetone-d_6; $Et_2O{\cdot}BF_3$), 6.51 (2B, d, J = 128 Hz, B8, 8′), 0.73 (2B, d, J = 137 Hz, B10, 10′), -5.93 (8B, d, J = 131 Hz, B4, 4′, 7, 7′, 9, 9′, 12, 12′), -14.92 (1B, d, overlap, B5), -16.30 (1B, d, overlap, B5′), -17.89 (2B, d, J = 168 Hz, B11, 11′), -19.22 (1B, d, overlap, B6), -23.15 (1B, d, J = 1620 Hz, B6′); ^{13}C NMR δ_C (100 MHz; acetone-d_6), 171.15 (1C, *C*O), 69.35 (1C, carborane *C*), 64.26 (3C, $(CH_3)_3NH^+$), 61.85 (1C, $CH_2CH_2CH_2OOC$), 57.53 (1C, carborane *C*H), 53.81 (1C, carborane *C*H), 51.73 (1C, carborane *C*H), 46.30 (1C, $CH_2CH_2CH_2OOC$), 37.24 (1C, $COCH_3$), 20.90 (1C, $CH_2CH_2CH_2OOC$); *m/z* (ESI$^-$) 427.50 (M^-, 11%), 424.42 (100%), calc. 427.39 and 424.33. Crystal for X-ray diffraction study were grown by careful layering of CH_2Cl_2 solution of **40** (to which few drops of MeOH for complete dissolution) with hexane in a grass tube, leaving it crystallize for several days.

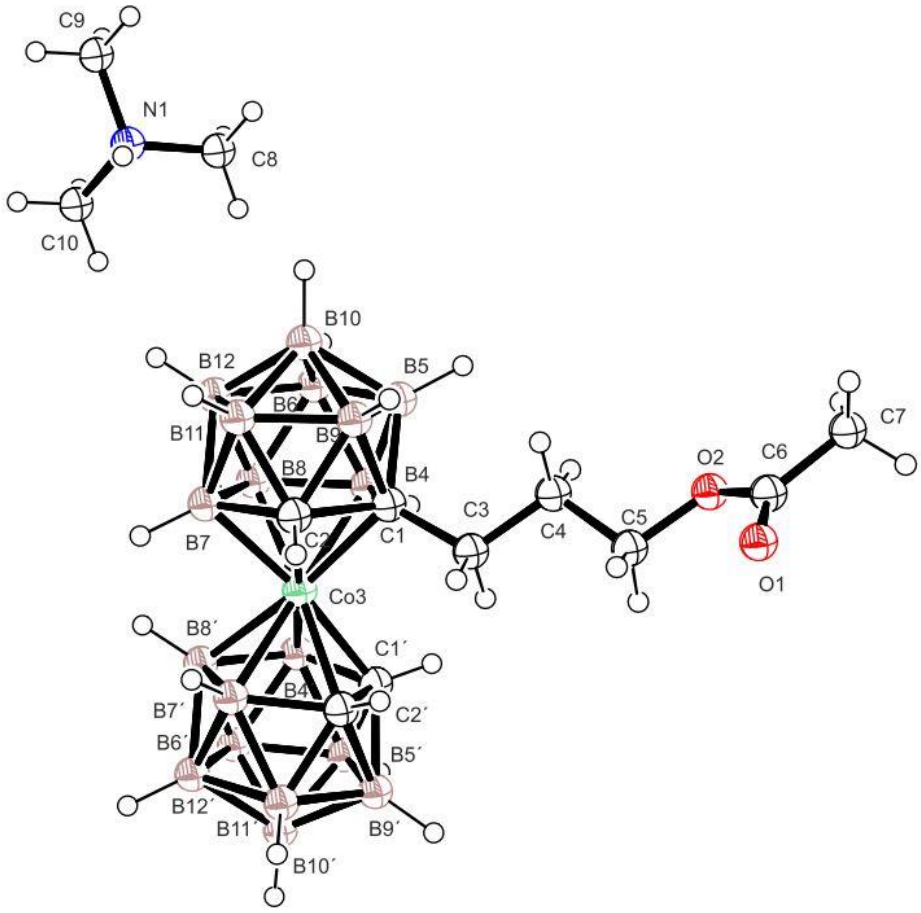

Crystal data for **40**: $C_9H_{30}B_{18}CoO_2{\cdot}C_3H_{10}N$, M_r = 483.96, Triclinic, *P-1* (No 2), a = 7.3101 (2) Å, b = 13.5354 (3) Å, c = 13.6276 (3) Å, α = 88.516 (1)°, β = 87.945 (1)°, γ = 77.235 (1)°, V = 1313.99 (5) Å^3, Z = 2, D_x = 1.223 Mg m^{-3}, red prism of dimensions 0.36 × 0.34 × 0.28 mm, multi-scan absorption correction(μ = 0.67 mm^{-1}), T_{min} = 0.797, T_{max} = 0.834. A total of 16,766 measured reflections (θ_{max} = 27.5°), from which 6028 were unique (R_{int} = 0.015) and 5492 observed according to the $I > 2\sigma(I)$ criterion. The refinement converged ($\Delta/\sigma_{max} \leq 0.001$) to *R*

= 0.026 forobserved reflections and $wR(F^2)$ = 0.071, *GOF* = 1.05 for 327 parameters and all 6028 reflections. The final difference map displayed no peaks of chemical significance ($\Delta\rho_{max}$ = 0.33, $\Delta\rho_{min}$ = -0.26 e.Å^{-3}). Crystallographic data for structural analyses are deposited with the Cambridge Crystallographic Data Centre, CCDC deposition no. 1059432.

1,1′-Di(methylene-methanesulfonate)-3,3'-cobalt(III) bis(1,2-dicarbarbollide), tetramethylammonium salt, [(1,1′-CH_3SO_2-OCH_2-1,2-$C_2B_9H_{10}$)$_2$-3,3′-Co]Me_4N **(41a)**

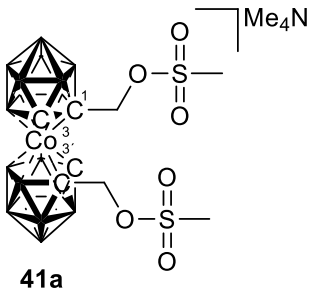

41a

The carefully dried Me_3NH salt of **37a**, 2.48g, (5.58 mmol) was dissolved in dry CH_3CN (75 ml) and then solid Cs_2CO_3 3.64g (11.1 mmol) was added followed by MsCl 1.75 ml (22.2 mmol) by syringe. The reaction mixture was heated to 60ºC and the heating was continued for 24h after which time HPLC analysis showed the presence of ca. 35% of diester in the reaction mixture. Then additional quantities of Cs_2CO_3 3.64 g (11.1 mmol) and MsCl 0.80 ml (10.1 mmol) were added and the addition of the chloride 0.80 ml (10.1 mmol) was repeated after another one day period and the reaction mixture was stirred and heated for another 24h HPLC analysis showed the presence of 56% of diester, along with 35% of monoesterified species and 7% of unreacted starting compound. After cooling, the solids were removed by filtration under nitrogen, washed with CH_3CN (3x5 ml) and discarded. The filtrate was evaporated under vacuum then dissolved in MeOH and precipitated by aqueous Me_4NCl. The solids were rapidly separated by decantation, washed with H_2O (4x5 ml) and dried under vacuum. The solids were dissolved in a mobile phase consisting of mixture of CH_3CN-CH_2Cl_2 (1:4) injected on the top of a silica gel column 2.5x25 cm. The front red band was collected, evaporated and chromatographed once more to remove the rest of monoesterified species. Yield 1.25 g (47%), red solid; R_f (CH_2Cl_2-CH_3CN 4:1) 0.48; mp 59°C; Analysis found: C, 23.5; H, 6.9 calc. for $CoB_{18}C_{12}H_{42}S_2O_6N$: C, 23.6; H, 6.9%; ^{1}H NMR δ_H (400 MHz; acetone-d$_6$), 5.35 (3H, d, *J* = 10.8 Hz, SC*H*$_3$), 5.07 (3H, d, *J* = 11.2 Hz, SC*H*$_3$), 4.39 (2H, s, carborane C*H*), 3.59 (12H, s, (C*H*$_3$)$_4$N$^+$), 2.96 (2H, s, C*H*$_2$O), 2.91 (2H, s, C*H*$_2$O); ^{11}B NMR δ_B (128 MHz; acetone-d$_6$; $Et_2O{\cdot}BF_3$), 9.15 (2B, d, *J* = 137 Hz, B8, 8′), 1.99 (2B, d, *J* = 137 Hz, B10, 10′), -4.38 (6B, d, *J* = 140 Hz, B7, 7′, 9, 9′, 12, 12′), -6.86 (2B, d, *J* = 146 Hz, B4, 4′), -14.01 (2B, d, *J* = 140 Hz, B5, 5′), -16.34 (2B, d, *J* = 143 Hz, B11, 11′), -20.05 (2B, d, *J* = 140 Hz, B6,6′); ^{13}C NMR δ_C (100 MHz; acetone-d$_6$), 73.76 (2C, S*C*H$_3$), 64.13 (2C, carborane *C*), 56.00 (4C, (*C*H$_3$)$_4$N$^+$), 52.36 (1C, carborane *C*H), 37.65 (2C, *C*H$_2$O); *m/z* (ESI$^-$) 543.25 (M$^-$, 17%), 540.42 (100%), calc. 543.25 and 540.26.

1,1′-Di(ethylene-methanesulfonate)-3,3'-cobalt(III) bis(1,2-dicarbarbollide), tetramethylammonium salt, [(1,1'-(CH_3SO_2-O(CH_2)$_2$-1,2-$C_2B_9H_{10}$)$_2$-3,3′-Co]Me_4N **(41b)**

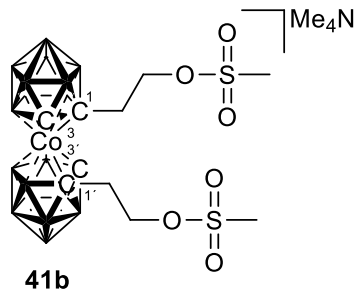

41b

We followed Procedure C. After stirring overnight at 85°C, another portion of 2.0 g Cs_2CO_3, 3.98 g (6.15 mmol) and 0.95 ml (24.1 mmol) of MsCl was added and the slurry was stirred heated for an additional 24h. Isolation was made similarly to **41a**. However, only one chromatographic run was required for removal of a small amount of a monoesterified species from the product. Yield 2.65 g (68%), red solid; R_f (CH_2Cl_2-CH_3CN 4:1) 0.62, mp 105°C; Analysis found: C, 26.2; H, 7.1 calc. for $CoB_{18}C_{14}H_{46}S_2O_6N$: C, 26.2; H, 7.2%; ^{1}H NMR δ_H (400 MHz; acetone-d$_6$), 4.55 (2H, m, CH_2CH_2O), 4.48 (2H, m, $CH_2CH_2'O$), 4.03 (2H, s, carborane C*H*), 3.67 (2H, m, CH_2CH_2O), 3.62 (12H, s, $(CH_3)_4N^+$), 3.29 (6H, s, SCH_3), 3.12 (2H, m, $CH_2'CH_2O$); ^{11}B NMR δ_B (128 MHz; acetone-d$_6$; $Et_2O{\cdot}BF_3$), 8.63 (2B, d, *J*= 128 Hz, B8, 8'), 0.40 (2B, d, *J* = 137, B10, 10'), -3.31, -6.45 (8B, 4d, overlap, B4, 4′, 7, 7′, 9, 9', 12, 12'), -14.63, -15.84 (4B, 2d, overlap, B5,5′, 11, 11′), -19.77 (2B, d, *J* = 125 Hz, B6, 6′); ^{13}C NMR δ_C (100 MHz; acetone-d$_6$), 70.66 (2C, SCH_3), 65.14 (2C, carborane *C*), 56.08 (4C, $(CH_3)_4N^+$), 53.89 (2C, carborane *C*H), 39.33 (2C, CH_2CH_2O), 37.41 (2C, CH_2CH_2O); *m/z* (ESI$^-$) 571.50 (M$^-$,16 %), 568.50 (100 %), calc. 568.29 and 571.28.

1,1′-Di(propylene-methanesulfonate)-3,3'-cobalt(III) bis(1,2-dicarbarbollide), tetramethylammonium salt, [(1,1'-(CH_3SO_2-O(CH_2)$_3$-1,2-$C_2B_9H_{10}$)$_2$-3,3′-Co]Me_4N **(41c)**

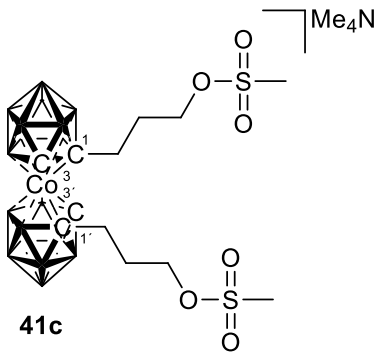

41c

We followed Procedure C. Yield 83%; R_f = 0.37 (CH_2Cl_2:CH_3CN 4:1); ^{1}H NMR δ_H (400 MHz; acetone-d$_6$), 4.25 (2H, t, *J* = 5.8 Hz, $CCH_2CH_2CH_2O$), 4.18 (2H, carborane C*H*), 3.46 (12H, s, $(CH_3)_4N$)), 3.09 (6H, s, SO_2CH_3), 2.76 (2H, m, $CCH_2CH_2CH_2OH$), 2.00 (2H, m, $CCH_2CH_2CH_2OH$); ^{11}B NMR δ_B (128 MHz; acetone-d$_6$; $Et_2O{\cdot}BF_3$), 7.75 (2B, d, *J* = 146 Hz, B8, 8′), 0.11 (2B, d, *J* = 143 Hz, B10, 10′), -5.62 (6B, d, *J* = 137 Hz, B4, 4′, 9, 9′, 12, 12′), -8.09 (2B, d, *J* = 146 Hz, B7, 7′), -14.25 (1B, d, overlap B5), -15.37 (3B, d, overlap, B5′, 11, 11′), -18.86 (2B, d, *J* = 117 Hz, B6, 6′); ^{13}C NMR δ_C (100 MHz; acetone-d$_6$), 70.05 (2C, OSO_2CH_3), 69.40 (2C, carborane *C*), 55.23 (4C, $(CH_3)_4N$), 38.62 (2C, carborane *C*H), 36.30 (2C, $CCH_2CH_2CH_2O$), 30.73 (2C, $CCH_2CH_2CH_2O$), 29.53 (2C, $CCH_2CH_2CH_2O$); *m/z* (ESI$^-$) 599.42 (M$^-$, 20%), 596.67 (100%), calc. 599.50 and 596.50.

1-(Ethylene-methanesulfonate)-1'-(ethylhydroxy)-3,3'-cobalt(III) bis(1,2-dicarbarbollide), tetramethylammonium salt, [(1-(CH_3SO_2-O(CH_2)$_2$-1,2-$C_2B_9H_{10}$)(1'-HO-(CH_2)$_2$-1',2'-$C_2B_9H_{10}$)-3,3′-Co]Me_4N **(41-)**

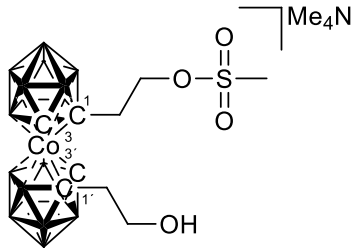

41-

We followed Procedure C. The reaction was monitored by MS every hour. After the disappearance of all the starting material, the reaction proceeded as described in Procedure C. Yield 34%; red solid; R_f = 0.37 (CH_2Cl_2:CH_3CN 4:1); ^{1}H NMR δ_H (400 MHz; acetone-d_6), 4.25 (2H, t, *J* = 5.9 Hz, CCH_2CH_2OS), 4.16 (1H, carborane C*H*), 3.93 (1H, carborane C*H*), 3.47 (12H, s, $(CH_3)_4N$)), 2.76 (2H, m, CCH_2CH_2O), 3.09 (3H, s, SO_2CH_3), 2.68 (4H, m, CCH_2CH_2N, CCH_2CH_2OS); ^{11}B NMR δ_B (128 MHz; acetone-d_6; $Et_2O{\cdot}BF_3$), 6.36 (2B, d, *J* = 138 Hz, B8, 8′), -1.03 (2B, d, *J* = 142 Hz, B10, 10′), -6.69 (8B, d, *J* = 129 Hz, B4, 4′, 7, 7′, 9, 9′, 12, 12′), -12.52 (1B, d, overlap, B5), -16.06 (5B, d, overlap, B5′, 6, 6′, 11, 11′); ^{13}C NMR δ_C (100 MHz; acetone-d_6), 68.88 (1C, carborane *C*), 62.28 (1C, carborane *C*), 66.79 (1C, CCH_2CH_2OS) 55.20 (4C, $(CH_3)_4N$), 54.19 (1C, carborane *C*), 51.80 (1C, carborane *C*H), 44.91 (1C, CCH_2CH_2O), 43.55 (1C, CCH_2CH_2OS), 37.31 (1C, CCH_2CH_2O); *m/z* (ESI$^-$) 493.42 (M^-, 16%), 490.42 (100%), calc. 493.35 and 490.35.

1,1′-Di(ethylene-*p*-toluenesulfonate)-3,3'-cobalt(III) bis(1,2-dicarbarbollide), tetramethylammonium salt, [(1,1'-(4-CH_3-C_6H_4)-SO_2-O(CH_2)$_2$-1,2-$C_2B_9H_{10}$)$_2$-3,3′-Co]Me_4N **(42)**

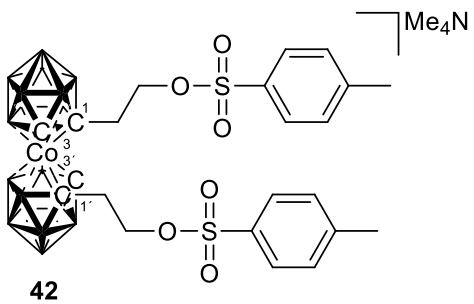

42

The diester **42** was prepared by analogous procedure as that described for **41a,b** reacting Me_3NH**37b**, 476 mg (1.0 mmol) with *p*TsCl 760 mg (4.0 mmol) and Cs_2CO_3 1.4 g (4.4 mmol) at 80^{o}C overnight. The isolation of crude product was made similarly to **41a**. The product was purified by crystallization from CH_2Cl_2-hexane; yield 620 mg (80%), orange-red solid; R_f (CH_2Cl_2-CH_3CN 4:1) 0.60; mp 99°C; ^{1}H NMR δ_H (400 MHz; acetone-d_6), 7.81 (2H, d, *J* = 8.0 Hz, Ar*H*), 7.50 (2H, d, *J* = 8.0 Hz, Ar*H*), 4.19 (2H, m, CH_2CH_2O), 4.10 (2H, m, $CH_2CH'_2O$), 3.66 (2H, s, carborane C*H*), 3.45 (12H, s, $(CH_3)_4N^+$), 2.89 (2H, s, CH_2CH_2O), 2.77 (2H, s, CH'_2CH_2O), 2.47 (6H, s, $ArCH_3$); ^{11}B NMR δ_B (128 MHz; acetone-d_6; $Et_2O{\cdot}BF_3$), 8.39 (2B, d, *J* = 143 Hz, B8, 8′), 0.28 (2B, d, *J* = 146 Hz, B10, 10′), -3.43 (4B, d, *J* = 146 Hz, B7, 7′, 12, 12′), -6.64 (2B, d, *J* = 143 Hz, B4, 4′, 9, 9′), -14.61 (4B, d, overlap, B5,5′, 11, 11′), -19.74 (2B, d, *J* = 168 Hz,

B6, 6´); ^{13}C NMR δ_C (100 MHz; acetone-d_6), 146.07 (2C, Ar*C*), 133.98 (2C, Ar*C*), 131.02 (4C, Ar*C*), 128.62 (4C, Ar*C*), 70.98 (2C, Ar*C*H$_3$), 66.19 (2C, carborane *C*), 58.36 (2C, carborane *C*H), 55.98 (4C, (*C*H$_3$)$_4$N$^+$), 38.18 (2C, CH$_2$*C*H$_2$O), 21.58 (2C, *C*H$_2$CH$_2$O); *m/z* (ESI$^-$) 723.17 (M$^-$, 20%), 720.17 (100%), calc. 723.35 and 720.36.

General method (D) for synthesis of primary amines 43 - 44.

The *p*-toluene- or methanesulfonate esters (4.0 mmol), dried in vacuum at 50°C for 5h, were dissolved under N_2 in a mixture of solvents composed of dry toluene and CH_3CN (5.0 ml, 1:1) in an N_2 flushed Kimberly-Clark bottle equipped with a rubber septum, a Teflon stirring bar and two stainless needles connected to a pressure cylinder with NH_3 and a gas bubbler. Then, the stirred solution was cooled to -78°C (bath temperature) and an excess of ammonia (ca. 2.5 g for monosubstituted, 5.0 g for disubstituted, controlled by weight) was condensed in the flask through a needle, keeping the ammonia gas flowing through the flask. The rubber septum was then replaced with a tight screw-cap and the solution was left to warm to room temperature after which the tube was then placed in an oil bath at 85°C and the reaction mixture was kept under a pressure of ammonia and stirring at this temperature for 48h. The volatiles were removed under reduced pressure. The residue was dissolved in Et_2O, washed with 3M HCl (4x30 ml), the organic phase shaken with water, separated and evaporated to dryness. The product, a strong yellow-orange band, was isolated chromatographically on a silica gel column (2.5x25 cm) using a CH_2Cl_2-CH_3CN 4:1 solvent mixture. The fractions containing the product were evaporated, the resulting solids dissolved in 5% aqueous Na_2CO_3 and the products were precipitated as their Me_4N^+ salt using an excess of aqueous Me_4NCl and collected by filtration, washed with water and dried under vacuum.

1-Aminomethyl-3,3'-cobalt(III) bis(1,2-dicarbarbollide), tetramethylammonium salt, [(1-[H_2N-CH_2-1,2-$C_2B_9H_{10}$)(1',2'-$C_2B_9H_{11}$)-3,3'-Co]Me_4N **(43a)**

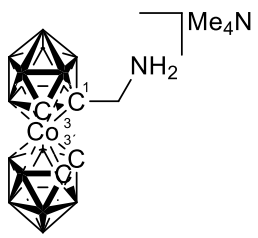

43a

We followed Procedure D. The reaction starting from the ester **38a** and carried out at 60°C, resulted in a green colouration and a mixture of several other products. The methylene amine was separated by repeated chromatography using a mobile phase composed of CH_2Cl_2-CH_3CN (4:1). Collected fractions were analysed by MS. Fractions containing the product were combined and treated with few drops of 10% Na_2CO_3, then precipitated with Me_4NCl and quickly collected, washed with water (3x10 ml) and dried. The product was twice crystallized from CH_2Cl_2(MeOH)-hexane. Yield 0.77 g (18%); ^{1}H NMR δ_H (400 MHz; CD_3CN), 4.35 (1H, d, *J* = 14.4 Hz, *CH*$_2$NH$_2$), 4.09 (1H, s, carborane C*H*), 4.00 (1H,

s, carborane C*H*), 3.88 (1H, s, carborane C*H*), 3.81 (1H, d, *J* = 14.4 Hz, *CH*$_2$NH); ^{11}B NMR δ_B (128 MHz; CD_3CN; $Et_2O{\cdot}BF_3$), 7.15 (2B, d, *J* = 144 Hz, B8, 8'), 2.23, 0.78 (2B, 2d, *J* = 159 and 158 Hz, B10, 10'), -5.65, -6.6, -4.2 (8B, 3d, overlap, B4, 4', 7, 7', 9, 9', 12, 12'), -16.98 (4B, d, *J* = 162 Hz, B5, 5', 11, 11'), -21.58 (1B, d, *J* = 147 Hz, B6), -22.7 (1B, d, *J* = 159 Hz, B6'); *m/z* (ESI$^-$), 356.32 (M$^-$, 10%), 353.32 (100%) calc. 356.30 and 353.31. These data are in agreement with previously reported spectra for this compound prepared by a different procedure.[163]

1-Aminoethyl-3,3-cobalt(III) bis(1,2-dicarbarbollide), tetramethylammonium salt, [(1-H_2N-$(CH_2)_2$-1,2-$C_2B_9H_{10}$)(1',2'-$C_2B_9H_{11}$)-3,3'-Co]Me_4N **(43b)**

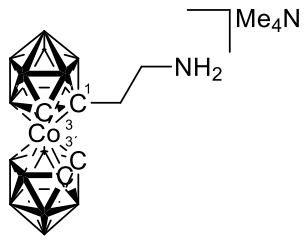

43b

We followed Procedure D. Yield 1.62 g (92%); R_f (CH_2Cl_2-CH_3CN 4:1) 0.96; mp 138°C; Analysis found: C, 27.3; H, 7.9 calc. for $CoB_{18}C_{10}H_{39}N_2$: C, 27.2; H, 8.9%; ^{1}H NMR δ_H (400 MHz; acetone-d_6), 7.8 (2H, br. s, N*H*$_2$), 4.16 (1H, s, carborane C*H*), 3.84 (1H, s, carborane C*H*), 3.71 (1H, s, carborane C*H*), 3.98 (2H, m, $CH_2CH_2NH_2$), 3.41 (2H, m, $CH_2CH_2NH_2$); ^{11}B NMR δ_B (128 MHz; acetone-d_6; $Et_2O{\cdot}BF_3$), 6.99 (2B, d, *J* = 140 Hz, B8, 8'), 1.35, 0.66 (2B, 2d, *J* = 143 and 144 Hz, B10, 10'), -5.60, -7.00 (8B, 4d, overlap, B4, 4', 7, 7', 9, 9', 12, 12'), -15.58, -16.32 (2B, 2d, overlap, B5, 11), -17.45 (2B, d, *J* = 156 Hz, B 5', 11'), -19.67 (1B, d, *J* = 178 Hz, B6), -23.00 (1B, d, *J* = 171 Hz, B6'); ^{13}C NMR δ_C (100 MHz; CD_3CN), 65.50 (1C, carborane *C*), 57.58 (1 C, carborane *C*H), 53.59 (1 C, carborane *C*H), 51.85 (1 C, carborane *C*H), 49.35 (1 C, $CH_2CH_2NH_2$), 37.77 (1C, $CH_2CH_2NH_2$); *m/z* (ESI$^-$) 370.33 (M$^-$, 10%), 367.33 (100%), calc: 370.31 and 367.32.

1-Aminopropyl-3,3-cobalt(III) bis(1,2-dicarbarbollide), tetramethylammonium salt, [(1-H_2N-$(CH_2)_3$-1,2-$C_2B_9H_{10}$)(1',2'-$C_2B_9H_{11}$)-3,3'-Co]Me_4N **(43c)**

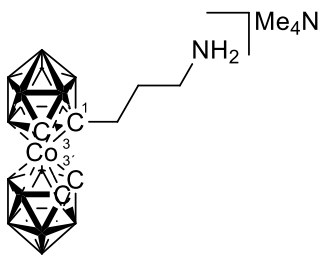

43c

We followed Procedure D. Yield 1.50 g (87 %); R_f (CH_2Cl_2-CH_3CN 4:1) 0.75; mp 115 °C; Analysis found: C, 29.2; H, 9.2 calc. for $CoB_{18}C_{11}H_{41}N_2$: C, 29.0; H, 9.1%; ^{1}H NMR δ_H (400 MHz; acetone-d_6), 7.74 (2H, br. s, N*H*$_2$), 4.03 (1H, s, carborane C*H*), 3.76 (1H, s, carborane C*H*), 3.66 (1H, s, carborane C*H*), 3.82 (2H, d, *J* = 14.4 Hz, $CH_2CH_2CH_2NH_2$), 2.751 (2H, m, $CH_2CH_2CH_2NH_2$), 1.74 (2H, m, $CH_2CH_2CH_2NH_2$); ^{11}B NMR δ_B (128 MHz; acetone-d_6; $Et_2O{\cdot}BF_3$), 6.51 (2B, d, *J* = 149 Hz, B8, 8'), 0.71 (2B, d, *J* = 144 Hz, B10, 10'), -6.02 (8B, 4d, overlap, B4, 4', 7, 7', 9, 9',

12, 12'), -14.70, -16.37 (2B, 2d, overlap, B5, 11), -17.87 (2B, d, J = 190 Hz, B5', 11'), -19.221 (1B, d, J = 177 Hz, B6), -23.12 (1B, d, J = 165 Hz, B6'); ^{13}C NMR δ_C (100 MHz; CD_3CN), 68.71 (1C, carborane *C*), 57.71 (1C, carborane *C*H), 53.82 (1C, carborane *C*H), 51.74 (1C, carborane *C*H), 48.39 (1C, $CH_2CH_2\mathit{C}H_2NH_2$), 41.21 (1C, $CH_2\mathit{C}H_2CH_2NH_2$), 37.57 (1C, $\mathit{C}H_2CH_2CH_2NH_2$); *m/z* (ESI$^-$) 385.42 ($M^-$, 10 %), 381.42 (100%), calc. 385.34 and 381.34.

1,1′-Di(aminoethyl)-3,3'-cobalt(III) bis(1,2-dicarbarbollide), tetramethylammonium salt, $[(1,1'\text{-}(H_2N\text{-}(CH_2)_2\text{-}1,2\text{-}C_2B_9H_{10})_2\text{-}3,3'\text{-}Co]Me_4N$ **(44b)**

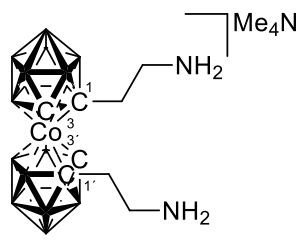

44b

The ester **41b** 2.57 g (4.0 mmol) in 5 ml of CH_3CN/toluene, NH_3 (ca 5.0 g) were reacted in a pressure resistant flask according to general procedure described above, except that the reaction vessel was heated at 45°C for 12h and then additional 48h at 85°C. After free evaporation of ammonia, the solids were removed by filtration, washed with dry CH_3CN and discarded. The solid residue after evaporation was dissolved in mixture of Et_2O and EtOAC (4:1) and extracted with 3M HCl. The aqueous phase was extracted with EtOAc (2x10 ml) and combined organic extracts were evaporated in vacuum. The product was isolated by chromatography on silica gel column (2.5x25 cm) using solvent mixture composed of CH_2Cl_2-CH_3CN (4:1) as the strongest red band; the fractions containing the product were evaporated, the resulting solid was dissolved in 5% aqueous Na_2CO_3 and the product was precipitated in form of their Me_4N^+ salt by an excess of aqueous Me_4NCl, collected by filtration, washed with water (3x15 ml) and dried under vacuum and crystallized from CH_2Cl_2 (with addition of MeOH)-hexane. Yield 75% (1.45 g); red solid; R_f (CH_2Cl_2-CH_3CN 4:1) 0.52; mp 128 °C; Analysis found: C, 29.2; H, 9.2 calc. for $CoB_{18}C_{12}H_{44}N_3$: C, 29.8; H, 9.2%; ^{1}H NMR δ_H (400 MHz; acetone-*d6*) 7.79 (4H, 2 br.s. $CH_2N\mathit{H2}$), 4.202 (2H, s, C*H* carborane), 3.384 (12H, s, $(\mathit{C}H_3)_4N^+$), 3.366 (2H, br. m, CH_2N), 2.977 (2H, m, C-CH_2CH_2); ^{11}B NMR δ_B (128 MHz; acetone-*d6*; $Et_2O{\cdot}BF_3$) 8.20 (2B, d, *J* 147, B8, 8'), -0.34 (2B, br. d, *J* 143, B10, 10'), -3.86 (2B, d, *J* 137, B9, 9'), -4.93 (2B, d, overlap, B4, 4'), -6.24 (2B, d, *J* 152, B7, 7') -8.16 (2B, d, *J* 143, B12, 12'), -12.80 (2B, d, *J* 158, B5, 5'), -15.86 (2B, d, *J* 162, B11, 11'), -20.32 (2B, d, *J* 159, B6, B6'); ^{13}C NMR δ_C (100 MHz; acetone-*d6*) 69.68 (2C, *C* carborane), 55.82 (2C, *C*H carborane), 54.98 (4C, $(\mathit{C}H_3)_4N^+$), 51.46 (2C, $\mathit{C}H_2N$), 32.44 (1C, $\mathit{C}H_2CH_2NH_2$); *m/z* (ESI$^-$) 415.50 (M^-, 10 %), 412.42 (100%), calcd. 415.33 and 412.34.

1,1′-Di(aminopropyl)-3,3'-cobalt(III) bis(1,2-dicarbarbollide), tetramethylammonium salt, [(1,1'-(H_2N-$(CH_2)_3$-1,2-$C_2B_9H_{10}$)$_2$-3,3'-Co]Me_4N **(44c)**

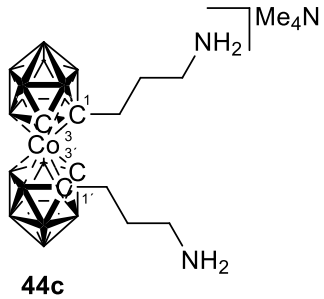

44c

We followed the same procedure as for **44b**. Yield 67%; dark red solid; R_f = 0.68 (CH_2Cl_2:CH_3CN 4:1); ^{1}H NMR δ_H (400 MHz; acetone-d_6), 5.64 (4H, br.s., NH_2), 4.21 (2H, t, *J* = 5.8 Hz, $CCH_2CH_2CH_2N$), 4.02 (2H, carborane C*H*), 3.47 (12H, s, $(CH_3)_4N$)), 2.54 (2H, m, $CCH_2CH_2CH_2N$), 2.36 (2H, m, $CCH_2CH_2CH_2N$); ^{11}B NMR δ_B (128 MHz; acetone-d_6; $Et_2O{\cdot}BF_3$), 6.30 (2B, d, *J* = 138 Hz, B8, 8′), -1.03 (2B, d, *J* = 142 Hz, B10, 10′), -6.69 (8B, d, *J* = 129 Hz, B4, 4′, 7, 7′, 9, 9′, 12, 12′), -12.52 (1B, d, overlap, B5), -16.06 (5B, d, overlap, B5′, 6, 6′, 11, 11′); ^{13}C NMR δ_C (100 MHz; acetone-d_6), 55.19 (4C, $(CH_3)_4N$), 53.92 (2C, carborane *C*), 50.83 (2C, carborane *C*H), 44.87 (2C, $CCH_2CH_2CH_2N$), 43.73 (2C, $CCH_2CH_2CH_2N$), 38.61 (1C, $CCH_2CH_2CH_2N$), *m/z* (ESI$^-$) 441.56 (M^-, 16%), 438.56 (100%), calc. 441.39 and 438.40.

1-Aminoethyl-1′-ethylenehydroxy-3,3'-cobalt(III) bis(1,2-dicarbarbollide), tetramethylammonium salt, [(1-(H_2N-$(CH_2)_2$-1,2-$C_2B_9H_{10}$)(1'-HO-$(CH_2)_2$-1',2'-$C_2B_9H_{10}$)-3,3'-Co]Me_4N **(44-)**

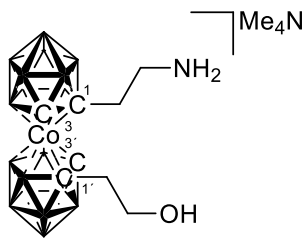

44-

The same procedure as for **44b**. Yield 79%; dark red solid; R_f = 0.37 (CH_2Cl_2:CH_3CN 4:1); ^{1}H NMR δ_H (400 MHz; acetone-d_6), 5.67 (2H, br.s., *NH*$_2$), 4.27 (2H, t, *J* = 5.9 Hz, CCH_2CH_2N), 4.04 (1H, carborane C*H*), 3.94 (1H, carborane C*H*), 3.55 (1H, t, O*H*), 3.47 (12H, s, $(CH_3)_4N$)), 3.38 (2H, m, CCH_2CH_2O), 2.58 (4H, m, CCH_2CH_2N, CCH_2CH_2O); ^{11}B NMR δ_B (128 MHz; acetone-d_6; $Et_2O{\cdot}BF_3$), 6.36 (2B, d, *J* = 138 Hz, B8, 8′), -1.03 (2B, d, *J* = 142 Hz, B10, 10′), -6.69 (8B, d, *J* = 129 Hz, B4, 4′, 7, 7′, 9, 9′, 12, 12′), -12.52 (1B, d, overlap, B5), -16.06 (5B, d, overlap, B5′, 6, 6′, 11, 11′); ^{13}C NMR δ_C (100 MHz; acetone-d_6), 68.88 (1C, carborane *C*), 62.28 (1C, carborane *C*), 61.79 (1C, CCH_2CH_2N) 55.21 (4C, $(CH_3)_4N$), 54.09 (1C, carborane *C*), 50.87 (1C, carborane *C*H), 44.94 (1C, CCH_2CH_2O), 43.78 (1C, CCH_2CH_2N), 37.37 (1C, CCH_2CH_2O), *m/z* (ESI$^-$) 414.66 (M^-, 11%), 411.66 (100%), calc. 414.38 and 411.38.

General procedures (E) for secondary and tertiary amino derivatives 45 - 49.

The methanesulfonate or *p*-toluensulfonate ester (0.33 mmol) was dissolved in dry CH_3CN (10 ml) and then *n*-butylamine, benzylamine or diethylamine (1.0 mmol) was added in excess by syringe. The reaction mixture was stirred at 60°C overnight and analysed. When the starting ester disappeared (HPLC or MS check), the reaction mixture was filtered, the solids

washed with CH_3CN (3x5 ml) and the filtrate evaporated under reduced pressure. The residue was dissolved in a smallest volume of mobile phase (CH_2Cl_2:CH_3CN 4:1) and chromatographed on a silica gel column (1.5x20 cm). The most intense band was collected and volatiles were removed under reduced pressure. Resulting solids were dissolved in 0.5 M Na_2CO_3 in 30% MeOH and the products precipitated as their Me_4N^+ salt by an excess of aqueous Me_4NCl. The products were collected by filtration, washed with water (3x5 ml) and dried under vacuum.

1-*n*-Butyl-aminomethyl-3,3'-cobalt(III) bis(1,2-dicarbarbollide), tetramethylammonium salt, [(1-^{n}C_4H_9-NH-CH_2-1,2-$C_2B_9H_{10}$)(1',2'-$C_2B_9H_{11}$)-3,3'-Co]Me_4N **(45a)**

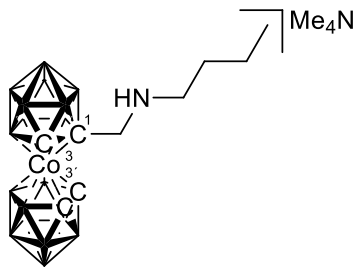

45a

Yield based on the reaction with the ester **38a**: 50 mg (31%). R_f (CH_2Cl_2-CH_3CN 4:1) 0.86; mp 98°C; Analysis found: C, 31.8; H, 9.2 calc. for $CoB_{18}C_{13}H_{45}N_2$: C, 32.3; H, 9.4%; ^{1}H NMR δ_H (400 MHz; CD_3CN), 4.18 (2H, s, carborane C*H*), 4.09 (1H, s, carborane C*H*), 3.87 (2H, m, C*H*$_2$NH), 3.78 (2H, m, NHC*H*$_2$CH$_2$CH$_2$CH$_3$), 2.83(2H, m, NHCH$_2$C*H*$_2$CH$_2$CH$_3$), 1.33 (2H, m, NHCH$_2$CH$_2$C*H*$_2$CH$_3$), 0.89 (3H, t, *J* = 7.6 Hz, NHCH$_2$CH$_2$CH$_2$C*H*$_3$); ^{11}B NMR δ_B (128 MHz; CD_3CN; $Et_2O{\cdot}BF_3$), 6.58 (2B, d, *J* = 131 Hz, B8, 8′), 1.49, 0.80 (2B, 2d, overlap, B10, 10′), -6.31 (8B, d, *J* = 98 Hz, B4, 4′, 7, 7′, 9, 9′, 12, 12′), -17.34 (4B, d, *J* = 143 Hz, B5, 5′, 11, 11′), -21.41 (1B, d, overlap, B6), -22.91 (1B, d, overlap, B6′); ^{13}C NMR δ_C (100 MHz; CD_3CN), 56.71 (1C, *C*H$_2$N), 56.12 (1C, carborane *C*), 55.39 (1C, carborane *C*H), 53.19 (1C, carborane *C*H), 51.58 (1C, carborane *C*H), 49.60 (4C, (*C*H$_3$)$_4$N$^+$), 48.73 (1C, N*C*H$_2$CH$_2$CH$_2$CH$_3$), 30.14 (1C, NCH$_2$*C*H$_2$CH$_2$CH$_3$), 20.47 (1C, NCH$_2$CH$_2$*C*H$_2$CH$_3$), 13.78 (1C, NCH$_2$CH$_2$CH$_2$*C*H$_3$); *m/z* (ESI$^-$) 412.58 (M$^-$, 16%), 409.75 (100%), calc. 412.36 and 409.37.

1-*n*-Butyl-aminoethyl-3,3'-cobalt(III) bis(1,2-dicarbarbollide), tetramethylammonium salt, [(1-C_4H_9-NH-$(CH_2)_2$-1,2-$C_2B_9H_{10}$)(1',2'-$C_2B_9H_{11}$)-3,3'-Co]Me_4N **(45b)**

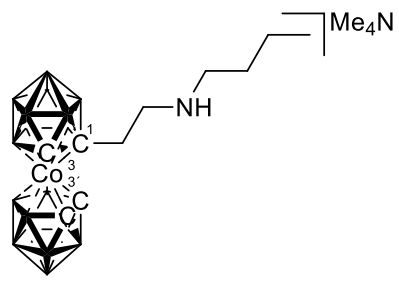

45b

Yield based on the reaction with the ester **39b**: 125 mg (76%). R_f (CH_2Cl_2-CH_3CN 4:1) 0.95; mp 93 °C; Analysis found: C, 33.9; H, 9.5 calc. for $CoB_{18}C_{14}H_{47}N_2$: C, 33.8; H, 9.5%; ^{1}H NMR δ_H (400 MHz; acetone-d_6), 4.07 (1H, s, carborane C*H*), 3.74 (1H, s, carborane C*H*), 3.66 (1H, s, carborane C*H*), 3.46 (12H, s, (C*H*$_3$)$_4$N$^+$), 2.82 (2H, m, CH$_2$C*H*$_2$NH$_2$), 2.54 (2H, m, C*H*$_2$CH$_2$NH$_2$), 2.47 (2H, m, NH$_2$C*H*$_2$CH$_2$CH$_2$CH$_3$), 1.41 (2H,

m, $NH_2CH_2CH_2CH_2CH_3$), 1.33 (2H, m, $NH_2CH_2CH_2CH_2CH_3$), 0.90 (3H, t, J = 6.8 Hz, $NH_2CH_2CH_2CH_2CH_3$); ^{11}B NMR δ_B (128 MHz; acetone-d_6; $Et_2O{\cdot}BF_3$), 6.43 (2B, d, J = 150 Hz, B8, 8′), 0.73 (2B, d, J = 113 Hz, B10, 10′), -6.07 (8B, d, J = 134 Hz, B4, 4′, 7, 7′, 9, 9′, 12, 12′), -14.87 (1B, d, overlap, B5), -16.30 (1B, d, J = 180 Hz, B5′), -17.96 (2B, d, overlap, B11, 11′), -19.72 (1B, d, J = 186 Hz, B6), -23.17 (1B, d, J = 174 Hz, B6′); ^{13}C NMR δ_C (100 MHz; acetone-d_6), 57.79 (1C, carborane *C*), 55.99 (1C, carborane *C*H), 54.24 (1C, carborane *C*H), 51.79 (1C, carborane *C*H), 51.29 (4C, $(CH_3)_4N^+$), 50.16 (1C, $NCH_2CH_2CH_2CH_3$), 40.83 (1C, CH_2CH_2N), 34.28 (1C, CH_2CH_2N), 29.26 (1C, $NCH_2CH_2CH_2CH_3$), 21.09 (1C, $NCH_2CH_2CH_2CH_3$), 14.03 (1C, $NCH_2CH_2CH_2CH_3$); *m/z* (ESI$^-$) 426.50 (M$^-$, 16%), 423.58 (100%), calc. 426.38 and 429.39.

1-*n*-Butyl-aminopropyl-3,3'-3,3'-cobalt(III) bis(1,2-dicarbarbollide), tetramethylammonium salt, $[(1\text{-n-}C_4H_9\text{-NH-}(CH_2)_3\text{-}1,2\text{-}C_2B_9H_{10})(1',2'\text{-}C_2B_9H_{11})\text{-}3,3'\text{-Co}]Me_4N$ **(45c)**

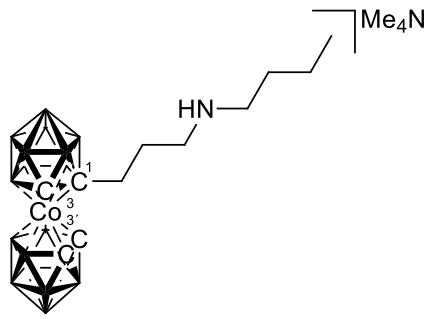

45c

Yield based on the reaction with the ester **39c**: 95 mg (56%). R_f (CH_2Cl_2-CH_3CN 4:1) 0.90; mp 118 °C; Analysis found: C, 30.2; H, 8.7 calc. for $CoB_{18}C_{11}H_{38}N$: C, 30.1; H, 8.8%; ^{1}H NMR δ_H (400 MHz; acetone-d_6), 7.77 (1H, m, N*H*$_2$), 7.68 (1H, m, N*H*$_2$), 4.23 (2H, p, J = 5.2 Hz, $CH_2CH_2CH_2NH_2$), 4.03 (1H, s, carborane C*H*), 3.76 (1H, s, carborane C*H*), 3.63 (1H, s, carborane C*H*), 3.37 (2H, m, $NH_2CH_2CH_2CH_2CH_3$), 2.99 (2H, m, $CH_2CH_2CH_2NH_2$), 2.51 (2H, m, $CH_2CH_2CH_2NH_2$), 1.90 (2H, p, J = 8.4 Hz, $NH_2CH_2CH_2CH_2CH_3$), 1.51 (2H, q, J = 7.6 Hz, $NHCH_2CH_2CH_2CH_3$), 0.96 (3H, t, J = 7.6 Hz, $NH_2CH_2CH_2CH_2CH_3$); ^{11}B NMR δ_B (128 MHz; acetone-d_6; $Et_2O{\cdot}BF_3$), 6.68 (2B, d, J = 150 Hz, B8, 8′), 0.80 (2B, d, J = 146, B10, 10′), -5.79 (8B, d, J = 171 Hz, B4, 4′, 7, 7′, 9, 9′, 12, 12′), -16.34 (2B, d, overlap, B5, 5′), -17.65 (3B, d, overlap, B6, 11, 11′), -23.07 (1B, d, overlap, B6′); ^{13}C NMR δ_C (100 MHz; acetone-d_6), 70.02 (1C, carborane *C*), 57.47 (1C, carborane *C*H), 56.00 (4C, $(CH_3)_4N^+$), 54.13 (1C, carborane *C*H), 51.65 (1C, carborane *C*H), 50.20 (1C, $CH_2CH_2CH_2N$), 49.83 (1C, $NCH_2CH_2CH_2CH_3$), 38.41 (1C, $CH_2CH_2CH_2N$), 33.08 (1C, $CH_2CH_2CH_2N$), 31.72 (1C, $NCH_2CH_2CH_2CH_3$), 21.13 (1C, $NCH_2CH_2CH_2CH_3$), 14.35 (1C, $NCH_2CH_2CH_2CH_3$); *m/z* (ESI$^-$) 440.50 (M$^-$, 18%), 437.50 (100%), calc. 440.40 and 437.40.

1-Benzyl-aminomethyl-3,3'-cobalt(III) bis(1,2-dicarbarbollide), tetramethylammonium salt, [(1-C_6H_5-CH_2NH-CH_2-1,2-$C_2B_9H_{10}$)(1',2'-$C_2B_9H_{11}$)-3,3'-Co]Me_4N **(46a).**

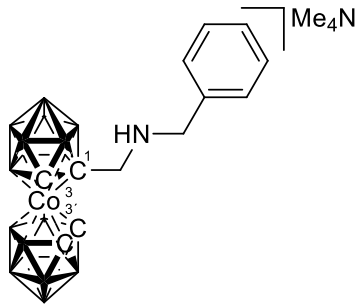

46a

Yield based on the reaction with the ester **38a**: 60 mg (35%); R_f (CH_2Cl_2-CH_3CN 4:1) 0.91; mp 111 °C; ^{1}H NMR δ_H (400 MHz; CD_3CN), 7.31 (2H, d, J = 10.4 Hz, Ar*H*), 7.24 (3H, m, Ar*H*), 4.34 (2H, s, carborane C*H*), 4.09 (1H, s, carborane C*H*), 3.66 (2H, q, J = 12.8 Hz, ArCH_2N), 3.42 (12H, dd, J_{12} = 13.2 Hz, J_{13} = 37.2 Hz, CH_2N), 3.05 (12H, s, (CH_3)$_4N^+$); ^{11}B NMR δ_B (128 MHz; CD_3CN; $Et_2O{\cdot}BF_3$), 5.94 (2B, d, J = 143 Hz, B8, 8′), 0.99 (2B, d, J = 186 Hz, B10, 10′), -6.88 (8B, d, J = 146 Hz, B4, 4′, 7, 7′, 9, 9′, 12, 12′), -13.78 (1B, d, J = 156 Hz, B5), -17.70 (3B, d, J = 156 Hz, B5′, 11, 11′), -20.32 (1B, d, J = 174 Hz, B6), -23.22 (1B, d, J = 165 Hz, B6′); ^{13}C NMR δ_C (100 MHz; CD_3CN), 129.23 (2C, Ar*C*), 129.10 (2C, Ar*C*), 127.78 (1C, Ar*C*), 117.36 (1C, Ar*C*), 58.16 (1C, Ar*C*H_2N), 55.96 (1C, carborane *C*), 54.21 (1C, carborane *C*H), 54.18 (1C, carborane *C*H), 53.93 (4C, (*C*H_3)$_4N^+$), 51.06 (1C, carborane *C*H), 45.53 (1C, *C*H_2N); *m/z* (ESI$^-$) 446.50 (M$^-$, 11%), 443.50 (100%), calc. 446.35 and 443.36.

1-Benzyl-aminoethyl-3,3'-cobalt(III) bis(1,2-dicarbarbollide), tetramethylammonium salt, [(1-C_6H_5-CH_2NH-(CH_2)$_2$-1,2-$C_2B_9H_{10}$)(1′,2′-$C_2B_9H_{11}$)-3,3′-Co]Me_4N **(46b)**

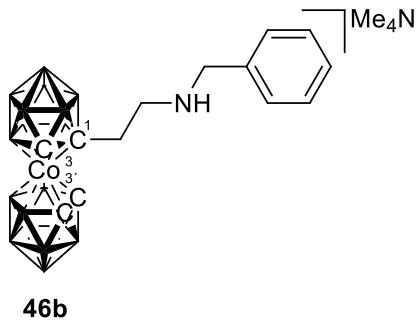

46b

Yield based on reaction with the ester **38d**: 115 mg (66%), orange solid; R_f (CH_2Cl_2-CH_3CN 4:1) 0.69; mp 94 °C; Analysis found: C, 38.6; H, 8.4 calc. for $CoB_{18}C_{17}H_{45}N_2$: C, 38.5; H, 8.5%; ^{1}H NMR δ_H (400 MHz; acetone-d_6), 7.67 (2H, m, Ar*H*), 7.44 (3H, m, Ar*H*), 4.38 (2H, d, J = 4.4 Hz, ArCH_2N), 4.12 (1H, s, carborane C*H*), 3.768 (2H, s, carborane C*H*), 3.45 (12H, s, (CH_3)$_4N^+$), 3.36 (2H, m, CH_2CH_2N), 3.02 (2H, m, CH_2C$H_2$$CH_2$N); ^{11}B NMR δ_B (128 MHz; acetone-d_6; $Et_2O{\cdot}BF_3$), 6.75 (2B, d, J = 134 Hz, B8, 8′), 0.92 (2B, d, J = 137 Hz, B10, 10′), -5.90 (8B, d, J = 122 Hz, B4, 4′, 7, 7′, 9, 9′, 12, 12′), -16.39, -17.51 (4B, 2d, overlap, B5, 5′, 11, 11′), -19.98 (1B, d, J = 139 Hz, B6), -22.65 (1B, d, J = 159 Hz, B6′); ^{13}C NMR δ_C (100 MHz; acetone-d_6), 132.72 (1C, Ar*C*), 131.08 (2C, Ar*C*), 130.13 (1C, Ar*C*), 129.78 (2C, Ar*C*), 67.78 (1C, Ar*C*H_2N), 65.21 (1C, carborane *C*), 57.89 (1C, carborane *C*H), 55.97 (1C, carborane *C*H), 54.54 (1C, carborane *C*H), 52.02 (4C, (*C*H_3)$_4N^+$), 48.92 (1C, CH_2CH_2N), 36.28 (1C, *C*$H_2$$CH_2$N); *m/z* (ESI$^-$) 460.50 (M$^-$, 15%), 457.58 (100%), calc. 460.36 and 457.58.

1-Benzyl-aminopropyl-3,3'-cobalt(III) bis(1,2-dicarbarbollide), tetramethylammonium salt, [(1-C_6H_5-CH_2NH-$(CH_2)_3$-1,2-$C_2B_9H_{10}$)(1′,2′-$C_2B_9H_{11}$)-3,3′-Co]Me_4N **(46c)**

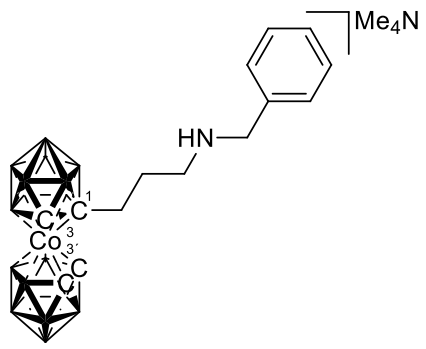

46c

Starting from the ester **38c,** the yield was 130 mg (72%), or alternatively 125 mg (69%) when using **39c** as the starting compound; R_f (CH_2Cl_2-CH_3CN 4:1) 0.65; mp 156 °C; Analysis found: C, 39.6; H, 8.7 calc. for $CoB_{18}C_{18}H_{47}N_2$: C, 39.7; H, 8.6%; ^{1}H NMR δ_H (400 MHz; acetone-d_6), 7.64 (2H, m, Ar*H*), 7.46 (3H, m, Ar*H*), 4.46 (2H, s, ArCH_2N), 4.04 (1H, s, carborane C*H*), 3.78 (1H, s, carborane C*H*), 3.66 (1H, s, carborane C*H*), 3.46 (12H, s, $(CH_3)_4N^+$), 3.28 (2H, m, $CH_2CH_2CH_2$N), 2.94 (2H, m, $CH_2CH_2CH_2N$), 2.55 (2H, m, $CH_2CH_2CH_2N$); ^{11}B NMR δ_B (128 MHz; acetone-d_6; $Et_2O{\cdot}BF_3$), 6.75 (2B, d, *J* = 139 Hz, B8, 8′), 0.87 (2B, d, *J* = 134 Hz, B10, 10′), -5.83 (8B, d, *J* = 134 Hz, B4, 4′, 7, 7′, 9, 9′, 12, 12′), -17.68 (5B, d, overlap, B5,5′, 6, 11, 11′), -23.07 (1B, d, *J* = 132 Hz, B6′); ^{13}C NMR δ_C (100 MHz; acetone-d_6), 132.44 (1C, Ar*C*), 130.98 (2C, Ar*C*), 130.16 (1C, Ar*C*), 129.85 (2C, Ar*C*), 68.88 (1C, ArCH_2N), 59.13 (1C, carborane *C*), 57.95 (1C, carborane *C*H), 55.97 (1C, carborane *C*H), 52.38 (4C, $(CH_3)_4N^+$), 51.84 (1C, carborane *C*H), 48.35 (1C, $CH_2CH_2CH_2N$), 37.72 (1C, $CH_2CH_2CH_2N$), 28.29 (1C, $CH_2CH_2CH_2N$); *m/z* (ESI$^-$) 474.58 (M^-, 17%), 471.67 (100%), calc. 474.38 and 471.39.

1-Diethyl-aminoethyl-3,3'- cobalt(III) bis(1,2-dicarbarbollide), tetramethylammonium salt, [(1-$(CH_3CH_2)_2N$-$(CH_2)_2$-1,2-$C_2B_9H_{10}$)(1′,2′-$C_2B_9H_{11}$)-3,3′-Co]Me_4N **(47b)**

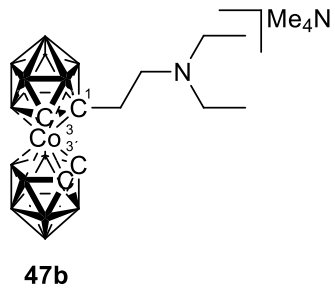

47b

Yield based on the reaction with the ester **39b**: 130 mg (78%). R_f (CH_2Cl_2-CH_3CN 4:1) 0.62; mp 141 °C; Analysis found: C, 33.7; H, 9.5 calc. for $CoB_{18}C_{14}H_{47}N_2$: C, 33.8; H, 9.5%; ^{1}H NMR δ_H (400 MHz; acetone-d_6), 4.16 (1H, s, carborane C*H*), 3.87 (1H, s, carborane C*H*), 3.82 (1H, s, carborane C*H*), 3.45 (12H, s, $(CH_3)_4N^+$), 3.08 (2H, m, CH_2CH_2N), 2.16 (2H, m, CH_2CH_2N), 2.10 (4H, d, *J* = 4.4 Hz, $(NCH_2CH_3)_2$), 1.42 (3H, t, *J* = 7.2 Hz, $(NCH_2CH_3)_2$); ^{11}B NMR δ_B (128 MHz; acetone-d_6; $Et_2O{\cdot}BF_3$), 7.03 (2B, d, *J* = 140 Hz, B8, 8′), 1.33 (2B, d, *J* = 110 Hz, B10, 10′), -5.69 (8B, d, *J* = 141 Hz, B4, 4′, 7, 7′, 9, 9′, 12, 12′), -16.37, -17.68 (4B, 2d, overlap, B5,5′, 11, 11′), -19.91 (1B, d, *J* = 162, B6), -22.76 (1B, d, *J* = 166 Hz, B6′); ^{13}C NMR δ_C (100 MHz; acetone-d_6), 65.07 (1C, carborane *C*), 57.87 (1C, carborane *C*H), 56.05 (1C, carborane *C*H), 54.10 (1C, carborane *C*H), 53.51 (4C, $(CH_3)_4N^+$), 51.97 (1C, CH_2CH_2N), 48.49 (2C,

($NCH_2CH_3)_2$), 34.43 (1C, CH_2CH_2N), 9.31 (1C, ($NCH_2CH_3)_2$); *m/z* (ESI^-) 426.42 (M^-, 16%), 423.58 (100%), calc. 426.38 and 423.39.

1-Diethyl-aminopropyl-3,3'-cobalt(III) bis(1,2-dicarbarbollide), tetramethylammonium salt, $[(1\text{-}(CH_3CH_2)_2N\text{-}(CH_2)_3\text{-}1,2\text{-}C_2B_9H_{10})(1',2'\text{-}C_2B_9H_{11})\text{-}3,3'\text{-}Co]Me_4N$ **(47c)**

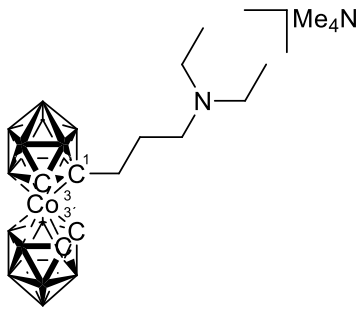

47c

Starting from the ester **38c,** the yield was 130 mg (71%), or alternatively 140 mg (74%) when using **39f** as the starting compound; R_f (CH_2Cl_2-CH_3CN 4:1) 0.53; mp 262 °C; Analysis found: C, 35.2; H, 9.6 calc. for $CoB_{18}C_{15}H_{49}N_2$: C, 35.3; H, 9.7%; ^1H NMR δ_H (400 MHz; acetone-d_6), 4.04 (1H, s, carborane C*H*), 3.74 (1H, s, carborane C*H*), 3.64 (1H, s, carborane C*H*), 3.53 (4H, dd, J_{12} = 6.8 Hz, J_{13} = 14.0 Hz, ($NCH_2CH_3)_2$), 3.39 (12H, s, $(CH_3)_4N^+$), 3.34 (2H, m, $CH_2CH_2CH_2N$), 2.96 (2H, m, $CH_2CH_2CH_2N$), 2.53 (2H, m, $CH_2CH_2CH_2N$), 1.44 (3H, t, J = 6.8 Hz, ($NCH_2CH_3)_2$); ^{11}B NMR δ_B (128 MHz; acetone-d_6; $Et_2O{\cdot}BF_3$), 6.58 (2B, d, J = 109 Hz, B8, 8′), 0.87 (2B, d, J = 134 Hz, B10, 10′), -5.90 (8B, d, J = 134 Hz, B4, 4′, 7, 7′, 9, 9′, 12, 12′), -17.68 (5B, d, overlap, B5,5′, 6, 11, 11′), -23.05 (1B, d, J = 130 Hz, B6′); ^{13}C NMR δ_C (100 MHz; acetone-d_6), 68.68 (1C, carborane *C*), 58.13 (1C, carborane *C*H), 53.95 (1C, carborane *C*H), 53.86 (1C, $CH_2CH_2CH_2N$), 52.77 (2C, ($NCH_2CH_3)_2$), 51.78 (1C, carborane *C*H), 48.78 (4C, $(CH_3)_4N^+$), 37.41 (1C, $CH_2CH_2CH_2N$), 26.46 (1C, $CH_2CH_2CH_2N$), 9.35 (1C, ($NCH_2CH_3)_2$); *m/z* (ESI^-) 440.58 (M^-, 16%), 437.67 (100%), calc. 440.39 and 437.40.

$[(1,1'\text{-}\mu\text{-}(\text{-}CH_2NHCH_2\text{-})(1,2\text{-}C_2B_9H_{10})_2\text{-}3,3'\text{-}Co)]Me_4N$ (**48**)

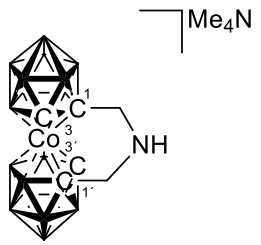

48

The diester **41a** 1.0 g (1.62 mmol) was allowed to react with NH_3 (g) following the above described general conditions with the exception that the reaction mixture was heated at 60°C for 12h and then at 85°C for 36h. HPLC analysis shown almost complete conversion to one product, which could be also be observed by MS as a peak corresponding to *m/z* = 369.5. Solvents were removed under vacuum, and the product purified by column chromatography (CH_2Cl_2-CH_3CN 4:1) as a dark orange band. Solvents were removed under reduced pressure and the product was dissolved in a small volume of methanol, precipitated by aqueous Me_4NCl, collected by filtration and dried; yield 485 mg (68%). The same product was isolated in 33% yield from reaction of 160 mg, (0.26 mmol) of **41a** with potassium phthalimide (140 mg, 1.52 mmol) carried out at 40°C for 12 hours. R_f (CH_2Cl_2-

CH_3CN 4:1) 0.86; mp 82°C; Analysis found: C, 27.2; H, 8.6 calc. for $CoB_{18}C_{10}H_{38}N_2$: C, 27.3; H, 8.7%; ^{1}H NMR δ_H (400 MHz; acetone-d_6), 9.53 (2H, s, N*H*$_2$), 3.57 (1H, s, carborane C*H*), 3.46 (12H, s, (C*H*$_3$)$_4$N$^+$), 3.07 (1H, s, carborane C*H*), 2.28 (2H, s, C*H*$_2$N), 2.07 (2H, s, C*H*′$_2$N); ^{11}B NMR δ_B (128 MHz; acetone-d_6; $Et_2O{\cdot}BF_3$), 7.89 (2B, d, *J* = 100 Hz, B8, 8′), 3.49 (1B, d, *J* = 146 Hz, B10), 0.18 (1B, d, *J* = 140 Hz, B10′), -4.19 (4B, d, *J* = 134 Hz, B7, 7′,12, 12′), -5.93 (1B, d, overlap, B4), -8.62 (4B, d, overlap, B4′, 5, 9, 9′), -15.82 (1B, d, overlap, B5′), -17.18 (3B, d, overlap, B6, 11, 11′), -19.96 (1B, d, *J* = 174 Hz, B6′); ^{13}C NMR δ_C (100 MHz; acetone-d_6), 65.36 (4C, (*C*H$_3$)$_4$N$^+$), 64.92 (1C, carborane *C*) 57.97 (1C, C*C*H$_2$N), 56.60 (1C, carborane *C*H), 55.96 (1C, C*C*H$_2$N), 55.38 (1C, carborane *C*H), 55.00 (1C, carborane *C*H); *m/z* (ESI$^-$) 369.42 (M$^-$, 17%), 366.50 (100%), calc. 369.31 and 366.32.

[(1,1'-μ-(-CH$_2$*n*BuNCH$_2$-)(1,2-$C_2B_9H_{10}$)$_2$-3,3'-Co)]Me_4N (**49**)

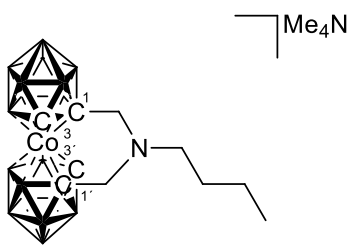

49

The ester **41a** (140 mg, 0.23 mmol) was reacted with *n*-butylamine (5 mL, 50.1 mmol) at 60°C for 12h. The resulting crude product was evaporated and separated by column chromatography (CH_2Cl_2-CH_3CN 4:1). The pure fractions were collected and evaporated and the residue precipitated from aqueous methanol by using Me_4NCl. The pale orange solid was collected and dried under vacuum, yield 50 mg (44%); R_f (CH_2Cl_2-CH_3CN 4:1) 0.35; mp 105°C; Analysis found: C, 33.8; H, 9.1 calc. for $CoB_{18}C_{14}H_{45}N_2$: C, 34.0; H, 9.2%; ^{1}H NMR δ_H (400 MHz; acetone-d_6), 4.14 (2H, s, carborane C*H*), 3.46 (12H, s, (C*H*$_3$)$_4$N$^+$), 3.16 (2H, q, *J* = 14.0 Hz, NCH$_2$CH$_2$C*H*$_2$CH$_3$), 2.87 (2H, s, C*H*$_2$N), 2.84 (2H, s, C*H*$_2$N), 2.45 (2H, t, *J* = 7.2 Hz, NC*H*$_2$CH$_2$CH$_2$CH$_3$), 1.44 (2H, m, NCH$_2$C*H*$_2$CH$_2$CH$_3$), 0.95 (3H, t, *J* = 7.6 Hz, NCH$_2$CH$_2$CH$_2$C*H*$_3$); ^{11}B NMR δ_B (128 MHz; acetone-d_6; $Et_2O{\cdot}BF_3$) 5.32 (2B, d, *J* = 150 Hz, B8, 8′), 0.83 (2B, d, *J* = 143 Hz, B10, 10′), -6.09 (6B, d, *J* = 137 Hz, B7, 7′, 9, 9′, 12, 12′), -8.07 (2B, d, *J* = 143 Hz, B4, 4′), -14.20 (2B, d, *J* = 156 Hz, B5, 5′), -16.96 (4B, d, overlap, B6, 6′,11, 11′); ^{13}C NMR δ_C (100 MHz; acetone-d_6), 76.81 (1C, carborane *C*), 68.05 (1C, carborane *C*H), 65.36 (4C, (*C*H$_3$)$_4$N$^+$), 57.97 (1C, C*C*H$_2$N), 56.60 (1C, carborane *C*H), 55.96 (1C, C*C*H$_2$N), 55.71 (1C, N*C*H$_2$CH$_2$CH$_2$CH$_3$), 55.00 (1C, carborane *C*H), 29.26 (1C, NCH$_2$*C*H$_2$CH$_2$CH$_3$), 20.95 (1C, NCH$_2$CH$_2$*C*H$_2$CH$_3$), 14.11 (1C, NCH$_2$CH$_2$CH$_2$*C*H$_3$); *m/z* (ESI$^-$) 424.50 (M$^-$ 14%), 421.58 (100%), calc. 424.36 and 421.37.

General method (F) for sulfamide derivatives 51 - 52.

The corresponding amines (0.1 mmol) were stirred with inorganic sulfamide (0.5 mmol) in refluxing 1,4-dioxane in the presence of K_2CO_3 (0.2 mmol) as a base for 3-16h (HPLC and

MS monitoring). For the synthesis of the disulfamide derivatives, a ten-fold excess of sulfamine and K_2CO_3 were used. This reaction, tested previously with carborane sulfamides,[92] proceeds with high yields, and, in the case of the ionic cobalt bis(dicarbollide) derivatives, produces only low amounts of side products. Products isolation was achieved by extraction into Et_2O:EtOAc (2:1, 20 ml), washing with diluted 1M HCl (3x10 ml), evaporation with H_2O (10 ml), and precipitation with an excess of aqueous Me_4NCl, washing with H_2O (3x5 ml) and drying. The crude products were purified by liquid chromatography and crystallizations from CH_2Cl_2-hexane and their characterization and purity assays were performed using combinations of HPLC, MS, ^1H, ^{11}B and ^{13}C NMR and standard analytical methods.

Procedure used for conversion to Na^+ salts for biological studies.

50 mg of the Me_4N^+ salt of the respective derivative was dissolved in Et_2O:EtOAc mixture (2:1, 20 ml) and extracted with diluted HCl (2.0 M, 4x20 ml), carefully washed with brine (15 ml), and then with aqueous Na_2CO_3 (2.5%, 20 ml) followed with brine (3-5x20 ml) until pH of the aqueous phase became neutral. The organic layer was carefully separated and the organic solvents were removed under reduced pressure. The Na^+ salts were then dried in vacuum for 2h at room temperature and then 8h at 45°C.

1-Sulfamidomethyl-3,3'-cobalt(III) bis(1,2-dicarbarbollide), tetramethylammonium salt, [(1-NH_2SO_2NH-CH_2-1,2-$C_2B_9H_{10}$)(1′,2′-$C_2B_9H_{11}$)-3,3′-Co]Me_4N **(51a)**

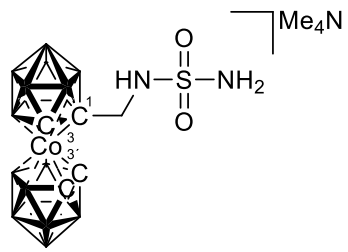

51a

Reaction time 20h.; yield 115 mg (44%); ^1H NMR (400 MHz; CD_3CN) δ_H 5.23 (2H, s, $NHSO_2NH_2$), 5.16 (1H, br, t, CH_2NHSO_2), 4.01, 3.93, 3.91 (3H, 3 br, s, carborane C*H*), 3.86 (2H, d, J = 6.8 Hz, CH_2NH), 3.44 (12H, $(CH_3)_4N^+$); ^{11}B NMR (128 MHz; CD_3CN; $Et_2O{\cdot}BF_3$) δ_B 6.24 (2B, d, J = 153 Hz, B8, 8'), 0.10 (2B, d, J = 143 Hz, B10, 10'), -6.29, -6.86 (8B, 4d, overlap, B4, 7, 4', 7', 9, 12, 9', 12'), -14.35, -16.97 (2B, 2d, J = 152 Hz, overlap, B5, 11), -17.59 (2B, d, J = 159 Hz, B5', 11'), -20.53 (1B, d, J = 171 Hz, B6), -22.72 (1B, d, J = 171 Hz, B6'); ^{13}C NMR (100 MHz; CD_3CN) δ_C 66,47 (1C, carborane *C*), 65.36 (4C, $(CH_3)_4N^+$), 54.88 (1C, carborane *C*H), 52.72 (1C, carborane *C*H), 52.04 (1C, carborane *C*H), 51.05 (1C, CH_2NH); *m/z* (ESI^-) 432.38 (100 %), 436.32 (4 %), calc.: 432.28 (100%), 436.29 (4%).

1-Sulfamidoethyl-3,3'-cobalt(III) bis(1,2-dicarbarbollide), tetramethylammonium salt, [(1-NH_2SO_2NH-$(CH_2)_2$-1,2-$C_2B_9H_{10}$)(1′,2′-$C_2B_9H_{11}$)-3,3′-Co]Me_4N **(51b)**

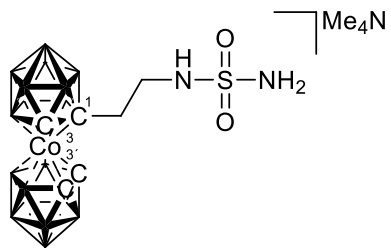

51b

Yield 185 mg (74%); ^{1}H NMR (400 MHz; acetone-d$_6$) δ_H 5.88 (2H, br. s, $NHSO_2NH_2$), 5.71 (1H, br, t, CH_2NHSO_2), 4.08, 3.70, 3.59 (3H, 3 br. s, carborane C*H*), 3.46 (12H, $(CH_3)_4N^+$), 3.22 (2H, m, *J* = 6,4 Hz, CH_2NH), 2.95 (2H, m, CH_2CH_2NH); ^{11}B NMR (128 MHz; acetone-d$_6$; $Et_2O{\cdot}BF_3$) δ_B 6.53 (2B, d, *J* = 146 Hz, B8, 8'), 0.85 (2B, d, *J* = 140 Hz, B10, 10'), -5.33, -6.05, -6.89 (8B, 4d, overlap, B4, 7, 4', 7', 9, 12, 9', 12'), -15.44, -16.37 (2B, 2d, *J* = 161 Hz, B5, 11), -17.82 (2B, d, *J* = 171 Hz, , B5', 11'), -19.72 (1B, d, overlap , B6), -22.98 (1B, d, *J* = 180 Hz, B6'); ^{13}C NMR (100 MHz; acetone-d$_6$) δ_C 67.01 (1C, carborane *C*), 65.34 (4C, $(CH_3)_4N^+$), 57.95 (1C, carborane *C*H), 54.30 (1C, carborane *C*H), 51.87 (1 C, carborane *C*H), 44.85 (1 C, CH_2NH), 40.00 (1 C, CH_2CH_2NH); *m/z* (ESI$^-$) 446.50 (100 %), 449.33 (14 %), calc.: 446.29 (100%), 449.29 (14%). This compound was prepared repeatedly for *in vivo* tests starting from 3 mM of the respective amine and converted to Na^+ salt.

1-Sulfamidopropyl-3,3'-cobalt(III) bis(1,2-dicarbarbollide), tetramethylammonium salt, [(1-NH_2SO_2NH-$(CH_2)_3$-1,2-$C_2B_9H_{10}$)(1′,2′-$C_2B_9H_{11}$)-3,3′-Co]Me_4N **(51c)**

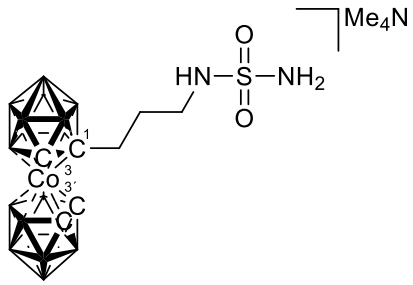

51c

Yield 165 mg (49%); ^{1}H NMR (400 MHz; acetone-d$_6$) δ_H 5.82 (2H, s, $NHSO_2NH_2$), 5.73 (1H, br, t, CH_2NHSO_2), 4.03, 3.71, 3.65 (3H, 3 br. s, carborane C*H*), 3.46 (12H, $(CH_3)_4N^+$), 3.04 (2H, m, *J* = 6,4 Hz, CH_2NH), 2.85 and 2.78 (2H, m, CH_2CH_2NH), 1.82 (2H, 2m, CCH_2); ^{11}B NMR (128 MHz; acetone-d$_6$; $Et_2O{\cdot}BF_3$) δ_B 6.46 (2B, d, *J* = 141 Hz, B8, 8'), 0.56 (2B, d, *J* = 143 Hz, B10, 10'), -6.12, -7.02 (8B, 4d, overlap, B4, 7, 4', 7', 9, 12, 9', 12'), -14.94, -16.37 (2B, 2d, *J*= 177 Hz, B5, 11), -17.84 (2B, d, *J* = 180 Hz, , B5', 11'), -19.25 (1B, d, *J* = 200 Hz, B6), -22.98 (1B, d, *J* = 179 Hz, B6'); ^{13}C NMR (100 MHz; acetone-d$_6$) δ_C 69.53 (1C, carborane *C*), 65.29 (4C, $(CH_3)_4N^+$), 58.03 (1C, carborane *C*), 54.13 (1C, carborane *C*), 51.63 (1C, carborane *C*), 43.72 (1C, CH_2NH), 38.12 (1C, CH_2CH_2NH), 31.55 (1C, CCH_2); *m/z* (ESI$^-$) 460.33 (100 %), 463.33 (12 %), calc.: 460.30 (100%), 463.30 (14%).

1,1′-Di(sulfamidoethyl)-3,3'-cobalt(III) bis(1,2-dicarbarbollide), tetramethylammonium salt, [(1,1'-(NH_2SO_2NH-$(CH_2)_2$-1,2-$C_2B_9H_{10})_2$-3,3'-Co]Me_4N **(52b)**

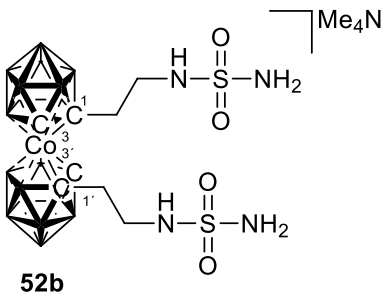

52b

Yield 61%; R_f= 0.64; mp 240-245°C; ^{1}H NMR δ_H (400 MHz; acetone-d$_6$): 5.94 (4H, s, $NHSO_2NH_2$), 5.70 (2H, br, t, CH_2NHSO_2), 3.69 (2H, s, carborane C*H*), 3.46 (12H, $(CH_3)_4N^+$), 3.24 (4H, m. CH_2N), 2.71 (4H, br. t, J = 10.8, CCH_2CH_2); ^{11}B NMR δ_B (128 MHz; acetone-d$_6$; $Et_2O{\cdot}BF_3$): 8.34 (2B, br. d, J = 149 Hz, B8, 8'), -0.09 (2B, br. d, J = 143 Hz, B10, 10'), -3.67 (2B, d, J = 143 Hz, B9, 9'), -4.81 (2B, d, overlap, B4, 4'), -6.48 (2B, d, J = 122 Hz, B7, 7') -8.50 (2B, d, J = 140 Hz, B12, 12'), -14.49 (2B, d, J = 192 Hz, B5, 5'), -16.01 (2B, d, J = 165 Hz, B11, 11'), -19.72 (2B, d, J = 165 Hz, B6, B6'); ^{13}C NMR δ_C (100 MHz; acetone-d$_6$): 68.46 (2C, carborane *C*), 65.42 (4C, $(CH_3)_4N^+$), 59.09 (2C, carborane *C*H), 45.08 (2C, *C*H_2NH), 40.59 (2C, C*C*H_2); *m/z* (ESI$^-$) 571.33 (M$^-$, 10%), 568.33 (100%), calc. 571.31 (16%) and 568.31(100%).

1,2′-Di(sulfamidopropyl)-3,3'-cobalt(III) bis(1,2-dicarbarbollide), tetramethylammonium salt, [(1,2'-(NH_2SO_2NH-$(CH_2)_3$-1,2-$C_2B_9H_{10})_2$-3,3'-Co]Me_4N **(52c)**

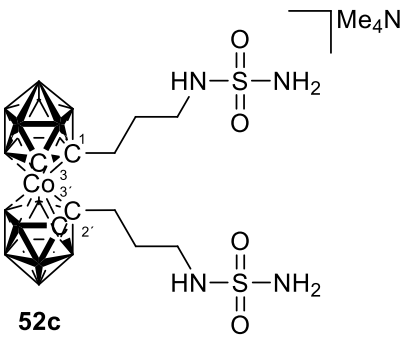

52c

Yield 72%; R_f = 0.53 (CH_2Cl_2:CH_3CN 4:1); ^{1}H NMR δ_H (400 MHz; acetone-d$_6$), 4.06 (2H, br.s., carborane C*H*), 3.46 (12H, s, $(CH_3)_4N$), 3.04 (2H, t, J = 5.6 Hz, $CCH_2CH_2CH_2N$), 2.87 (4H, s, NH_2), 2.59 (2H, t, J = 5.8 Hz, N*H*), 2.15 (2H, m, $CCH_2CH_2CH_2N$), 0.94 (2H, m, $CCH_2CH_2CH_2N$); ^{11}B NMR δ_B (128 MHz; acetone-d$_6$; $Et_2O{\cdot}BF_3$), 7.22 (2B, d, J = 113 Hz, B8, 8′), -0.15 (2B, d, J = 140 Hz, B10, 10′), -5.52 (6B, d, J = 110 Hz, B4, 4′, 9, 9′, 12, 12′), -7.71 (2B, d, J = 140 Hz, B7, 7′), -14.33 (1B, d, overlap B5), -15.63 (3B, d, overlap, B5′, 11, 11′), -18.41 (2B, d, J =108 Hz, B6, 6′); ^{13}C NMR δ_C (100 MHz; acetone-d$_6$), 56.00 (2C, carborane *C*), 55.29 (4C, (*C*$H_3)_4$N), 43.97 (2C, carborane *C*), 31.91 (2C, $CCH_2CH_2CH_2N$), 27.75 (2C, C*C*$H_2CH_2CH_2N$), 14.34 (2C, $CCH_2CH_2CH_2N$); *m/z* (ESI$^-$) 597.61 (19%), 594.59 (100%), calc. 597.32 and 594.32.

1-Sulfamidoethyl-1′-ethylenehydroxy-3,3'-cobalt(III) bis(1,2-dicarbarbollide), tetramethylammonium salt, [(1-(NH_2SO_2NH-$(CH_2)_2$-1,2-$C_2B_9H_{10}$)(1'-HO-$(CH_2)_2$-1',2'-$C_2B_9H_{10}$)-3,3'-Co]Me_4N **(51-)**

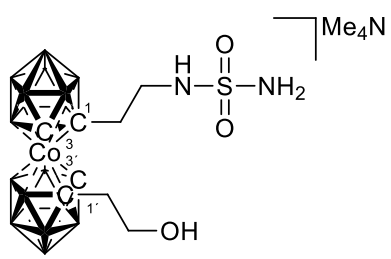

51-

Yield 66%; R_f = 0.36 (CH_2Cl_2:CH_3CN 4:1); ^{1}H NMR δ_H (400 MHz; acetone-d_6), 5.89 (2H, m, CCH_2CH_2N), 3.66 (2H, br.s., carborane C*H*), 3.52 (2H, t, *J* = 5.6 Hz, CCH_2CH_2OH), 3.46 (12H, s, $(CH_3)_4N$), 3.07 (1H, br.s., O*H*), 3.06 (4H, m, CCH_2CH_2), 2.93 (1H, t, J = 5.8 Hz, N*H*), 2.84 (2H, br.s. NH_2); ^{11}B NMR δ_B (128 MHz; acetone-d_6; $Et_2O{\cdot}BF_3$), 8.20 (1B, d, *J* = 150 Hz, B8), 6.03 (1B, d, *J* = 156 Hz, B8′), -0.13 (2B, d, *J* = 140 Hz, B10, 10′), -4.25 (2B, d, *J* = 140 Hz, B4, 7′), -6.05 (4B, d, *J* = 122 Hz, B 9, 9′, 12, 12′), -8.88 (2B, d, *J* = 143 Hz, B4′, 7), -15.99 (4B, d, *J* = 153 Hz, B5, 5′, 11, 11′), -17.98 (2B, d, *J* = 195 Hz, B6, 6′); ^{13}C NMR δ_C (100 MHz; acetone-d_6), 62.10 (1C, CCH_2CH_2O), 61.89 (1C, CCH_2CH_2N), 56.02 (4C, $(CH_3)_4N$), 43.93 (2C, carborane *C*), 38.80 (1C, carborane *C*H), 38.24 (1C, carborane *C*H), 35.14 (1C, CCH_2CH_2N), 31.76 (1C, CCH_2CH_2O); *m/z* (ESI^-) 521.50 (20%), 518.50 (100%), calc. 521.34 and 518.36.

General methods of preparation of carborane sulfonamides 55 - 70:

Alkylating with trimethylene oxide (G or H).

1o(m,p) (10.0 g, 69.44 mmol (G) or 5 g, 34.72 mmol (H)) was dried under vacuum at room temperature for 3h and then dissolved in a dry hexane (40 ml (G) or 20 ml (H)). After cooling down to 0°C the ^{n}BuLi (2.5 M in hexane, 83.33 mmol (G) or 76.38 mmol (H)) was added. Reaction mixture was stirred for additional 30 minutes at room temperature and then was the flask cooled down to 0°C again. Trimethylene oxide (83.33 mmol (G) or 76.38 mmol (H)) was added then dropwise. After few minutes a white precipitate formed. After 5 hours, MeOH (ca. 5 ml) and AcOH (ca. 1 ml) were added. This reaction mixture was evaporated to dryness and then extracted three times with Et_2O (3x20 ml) and H_2O (20 ml). Combined organic layers were extracted with 3M HCl (3x20), dried over $MgSO_4$ and evaporated. Crude product was separated on silica column chromatography (benzene:CH_2Cl_2 2:1).

Activating with triflate ester (I or J).

Dried hydroxy derivative (3.6 g, 18.00 mmol (I) or 3.4 g, 13.03 mmol (J)) was dissolved in dry CH_2Cl_2 (30 ml) and the Tf_2O (3.32 ml, 19.80 mmol (I) or 4.81 ml, 28.66 mmol (J)) in dry CH_2Cl_2 (6 ml) was added dropwise *via* septum (with needle for controlling pressure) at room temperature. The reaction was controlled by TLC (benzene:CH_2Cl_2 2:1) and was quenched with H_2O (30 ml) after disappearing of the starting material (overnight). Reaction mixture was separated and the organic phase was extracted 3 times with H_2O (15 ml) and then dried over $MgSO_4$, filtered and evaporated.

Substitution with potassium thiocyanate (K or L).

Dried triflate ester (2.6 g, 7.64 mmol (K) or 3.0 g, 5.73 mmol (L)) was dissolved in dry acetonitrile (30 ml) and the KSCN (1.48 g, 15.27 mmol (K) or 2.22 g, 22.90 mmol (L)) was added at once at room temperature. Solution changed colour rapidly from light pink to yellow. Reaction was let at this state for another 3 hours and after TLC check (CH_2Cl_2:CH_3CN 5:1) the reaction mixture was evaporated. Crude product was dissolved in H_2O (30 ml) and CH_2Cl_2 (30 ml) and the water phase was extracted 2 more times (30 ml). The organic layer was then dried over $MgSO_4$, filtered and evaporated.

Oxidation and chlorination (M or N).

Dried thiocyanate derivative (1.6 g, 6.48 mmol (M) or 1.65 g, 4.71 mmol (N)) was dissolved in a mixture of AcOH (64.8 mmol (M) or 47.11 mmol (N)) and H_2O (19.44 mmol (M) or 14.22 mmol (N)) and heated up to 50°C. Then the SO_2Cl_2 (0.13 mol (M) or 0.09 mol (N)) was added dropwise and the leaving Cl_2 was trapped in a 1M NaOH in water solution. After addition of all SO_2Cl_2 the reaction mixture was cooled to room temperature and water was added. This water system was extracted with EtOAc three times and the organic layer was then washed with 5% $NaHCO_3$ two times and finally once with brine. The organic layer was then dried over $MgSO_4$, filtered and evaporated.

Amination (O or P).

Sulfonyl chloride derivative (1.4 g, 4.98 mmol (O) or 1.6 g, 4.14 mmol (P)) was dissolved in CH_3CN (20 ml) and cooled to 0°C. Then NH_3 (30% in H_2O, 8ml (O) or 9 ml (P)) was added dropwise and the reaction mixture stirred for one hour at 0°C and then another hour at room temperature. The organic phase was then evaporated and the water phase was extracted with EtOAc (3x20 ml) and the combined organic layers were washed once with brine (20 ml) and then dried over $MgSO_4$, filtered and evaporated. Residue was applied to a silica gel column (CH_2Cl_2:benzene, 1:2) and then recrystallized from CH_2Cl_2 and hexane.

1-Hydroxypropyl-1,2-dicarba-*closo*-dodecaborane, 1-HOC_3H_6-1,2-*closo*-$C_2B_{10}H_{11}$ (**55o**)

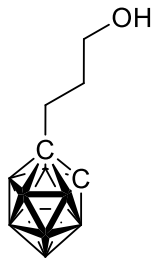

55o

We followed procedure G. Yield 39% (4.34 g) of white solid. m.p.: 65°C; R_f = 0.20 (benzene:CH_2Cl_2 2:1); Analysis found: C, 30.1; H, 9.2 calc. for $B_{10}C_5H_{18}O$: C, 29.7; H, 9.0%; ^{1}H NMR δ_H (400 MHz; CD_2Cl_2), 3.72 (1H, br.s., carborane C*H*), 3.59 (2H, t, *J* = 7.6 Hz, $CCH_2CH_2CH_2OH$), 2.37 (2H, t, *J* = 8.0 Hz, $CCH_2CH_2CH_2OH$), 1.75 (2H, m, $CCH_2CH_2CH_2OH$); ^{11}B NMR δ_B (128 MHz; CD_2Cl_2; $Et_2O{\cdot}BF_3$), -3.56 (1B, d, *J* = 150 Hz, B9), -7.03 (1B, d, *J* = 146 Hz, B12), -10.48 (2B, d, *J* = 153 Hz, B8, 10), -12.55 (2B, d, overlap, B4, 5), -12.98 (2B, d, overlap, B7, 11), -14.09 (2B, d, overlap, B3, 6); ^{13}C NMR δ_C (100 MHz; CD_2Cl_2), 76.84 (1C, carborane *C*), 63.15 (1C, carborane *C*H), 62.53 (1C, $CCH_2CH_2CH_2OH$), 36.03 (1C, $CCH_2CH_2CH_2OH$), 33.36 (1C, $CCH_2CH_2CH_2OH$); *m/z* (ESI$^-$) 205.30 (11%), 202.30 (100%), calc. 205.24 and 202.24.

1-[(Propylpyridinium) triflourmethanesulfonate]-1,2-dicarba-*closo*-dodecaborane, [1-$C_5H_5NC_3H_6$-1,2-*closo*-$C_2B_{10}H_{11}$]SO_3CF_3 (**56**)

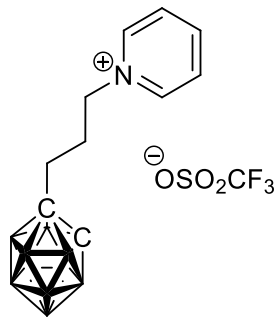

56

1-hydroxypropyl-*o*-carborane (1.0 g, 4.95 mmol) was dissolved in 4 mL of dry DCM and pyridine (0.38 ml, 4.95 mmol) was added. Procedure was then carried out as mentioned above. Yield: 59% (1.20 g) of colourless needles. m.p.: 53°C; R_f = 0.79 (CH_2Cl_2:benzene 1:2); Analysis found: C, 32.1; H, 5.2 calc. for $B_{10}C_{11}H_{22}O_3NSF_3$: C, 32.0; H, 5.4%; ^{1}H NMR δ_H (400 MHz; CD_2Cl_2), 8.97 (2H, d, *J* = 6.0 Hz, $^{py}C_2H$, $^{py}C_6H$), 8.54 (1H, t, *J* = 7.6 Hz, $^{py}C_4H$), 8.10 (2H, d, *J* = 6.4 Hz, $^{py}C_3H$, $^{py}C_5H$), 4.68 (2H, t, *J* = 8.0 Hz, $CCH_2CH_2CH_2N$), 4.17 (1H, br.s., carborane C*H*), 2.52 (2H, t, *J* = 7.7 Hz, $CCH_2CH_2CH_2N$), 2.89 (2H, m, $CCH_2CH_2CH_2N$); ^{11}B NMR δ_B (128 MHz; CD_2Cl_2; $Et_2O{\cdot}BF_3$), -3.61 (1B, d, *J* = 145 Hz, B9), -6.68 (1B, d, *J* = 143 Hz, B12), -10.50 (2B, d, *J* = 150 Hz, B8, 10), -12.88 (6B, d, overlap, B3, 4, 5, 6, 7, 11); ^{13}C NMR δ_C (100 MHz; CD_2Cl_2), 149.22 (1C, aromatic *C*), 145.61 (2C, aromatic *C*), 131.65 (2C, aromatic *C*), 78.82 (1C, carborane *C*), 63.15 (1C, carborane *C*H), 69.82 (1C, $CCH_2CH_2CH_2N$), 38.23 (1C, $CCH_2CH_2CH_2N$), 34.18 (1C, $CCH_2CH_2CH_2N$); *m/z* (ESI$^-$) 266.28 (43%), 264.32 (100%), calc. 266.28 and 264.32.

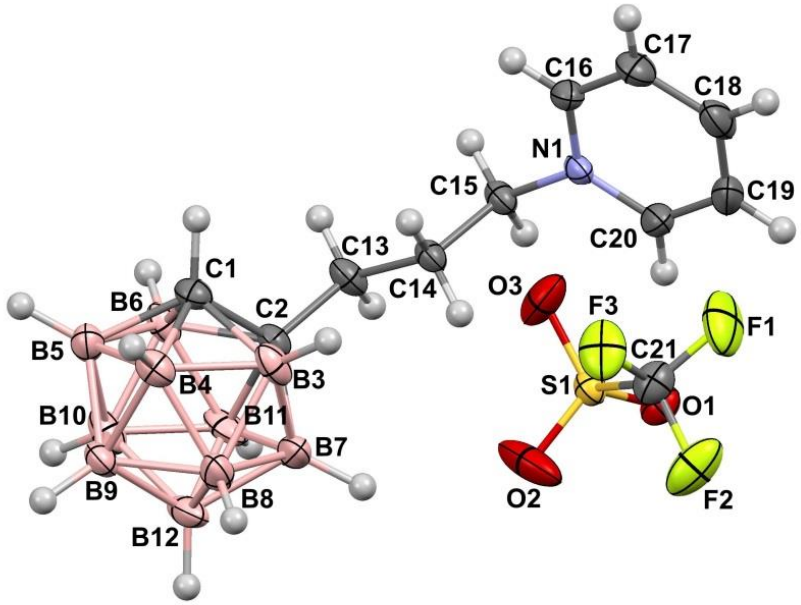

X-ray crystallographic data for **56**: $C_{10}H_{22}B_{10}N{\cdot}CF_3O_3S$, M = 413.45, monoclinic, $P2_{1/c}$, a = 7.1720(6) Å, b = 24.134(2) Å, c = 12.0310(11) Å, β = 100.354(6) °, Z = 4, V = 2048.5(3) Å3, D_c = 1.341 g.cm^{-3}, μ= 0.197 mm^{-1}, T_{min}/T_{max} = 0.933/0.979; -9 ≤ h ≤ 9, -26 ≤ k ≤ 31, -15 ≤ l ≤ 15; 21528 reflections measured (θ_{max} = 27.5 °), 4659 independent (R_{int} = 0.0434), 3414 with I > *2σ(I)*, 275 parameters, S = 1.031, *R1*(obs. data) = 0.0621, *wR2*(all data) = 0.1430; max., min. residual electron density = 0.794, -0.47 eÅ^{-3}.

1-(Triflourmethanesulfonate)propyl-1,2-Dicarba-*closo*-dodecaborane,
1-$CF_3SO_3C_3H_6$-1,2-*closo*-$C_2B_{10}H_{11}$ (**57o**)

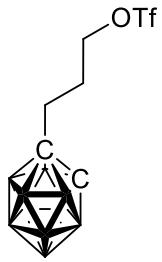

57o

We followed procedure I. Yield: 53% (1.75 g) of white crystalline solid. m.p.: 41°C; R_f = 0.72 (CH_2Cl_2:benzene 1:2); Analysis found: C, 21.9; H, 5.3 calc. for $B_{10}C_6H_{17}O_3SF_3$: C, 21.6; H, 5.1%; ^{1}H NMR δ_H (400 MHz; CD_2Cl_2), 4.54 (2H, t, *J* = 5.2 Hz, $CCH_2CH_2CH_2O$), 3.72 (1H, br.s., carborane C*H*), 2.41 (2H, t, *J* = 8.0 Hz, $CCH_2CH_2CH_2O$), 2.07 (2H, m, $CCH_2CH_2CH_2O$); ^{11}B NMR δ_B (128 MHz; CD_2Cl_2; $Et_2O{\cdot}BF_3$), -3.32 (1B, d, *J* = 150 Hz, B9), -6.63 (1B, d, *J* = 146 Hz, B12), -10.27 (2B, d, *J* = 150 Hz, B8, 10), -12.95 (4B, d, overlap, B4, 5, 7, 11), -13.93 (2B, d, overlap, B3, 6); ^{13}C NMR δ_C (100 MHz; CD_2Cl_2), 118.34 (1C, CF_3), 77.04 (1C, $CCH_2CH_2CH_2O$), 74.99 (1C, carborane *C*), 63.51 (1C, carborane *C*H), 35.20 (1C, $CCH_2CH_2CH_2O$), 30.26 (1C, $CCH_2CH_2CH_2O$); *m/z* (ESI$^-$) *dimer* 539.17 (8%), 535.75 (100%), calc. 539.40 and 535.41.

1-(Mesyloxy)propyl-1,2-dicarba-*closo*-dodecaborane, 1-$CH_3SO_3C_3H_6$-1,2-*closo*-$C_2B_{10}H_{11}$ (**58**)

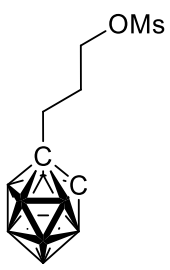

58

We followed procedure I. It was used 50 mg (0.25 mmol) of **55o** in 3 ml of CH_2Cl_2, 30 µl (0.27 mmol) of MsCl and 3 µl (0.03 mmol) of Et_3N. Yield: 72% (50 mg) of the white solid. m.p.: 85°C; R_f = 0.70 (CH_2Cl_2:benzene 1:2); Analysis found: C, 25.9; H, 7.3 calc. for $B_{10}C_6H_{20}O_3S$: C, 25.7; H, 7.2%; ^{1}H NMR δ_H (400 MHz; CD_2Cl_2), 3.99 (3H, s, SC*H*$_3$), 3.82 (2H, t, *J* = 5.6 Hz, $CCH_2CH_2CH_2O$), 3.30 (1H, br.s., carborane C*H*), 2.40 (2H, t, *J* = 7.7 Hz, $CCH_2CH_2CH_2O$), 1.91 (2H, m, $CCH_2CH_2CH_2O$); ^{11}B NMR δ_B (128 MHz; CD_2Cl_2; $Et_2O{\cdot}BF_3$), -4.84 (1B, d, *J* = 159 Hz, B4), -11.62 (5B, d, overlap, B3, 5, 8, 11, 12), -14.23 (2B, d, *J* = 192 Hz, B9, 10), -16.24 (2B, d, *J* = 189 Hz, B2, 6); ^{13}C NMR δ_C (100 MHz; CD_2Cl_2), 76.19 (1C, $CCH_2CH_2CH_2O$), 69.80 (1C, carborane *C*), 69.78 (1C, carborane *C*H), 38.27 (1C, *C*H$_3$), 34.10 (1C, $CCH_2CH_2CH_2O$), 30.58 (1C, $CCH_2CH_2CH_2O$); *m/z* (ESI$^-$) 283.30 (8%), 280.30 (100%), calc. 283.21 and 280.21.

1-(Thiocynate)propyl-1,2-dicarba-*closo*-dodecaborane, 1-$NCSC_3H_6$-1,2-*closo*-$C_2B_{10}H_{11}$ (**59o**)

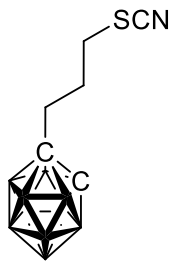

59o

We followed procedure K. Yield: 82% (595 mg) of the white powder. m.p.: 61°C; R_f = 0.28 (CH_2Cl_2:CH_3CN 5:1); Analysis found: C, 29.7; H, 7.2 calc. for $B_{10}C_6H_{17}SN$: C, 29.6; H, 7.0%; ^{1}H NMR δ_H (400 MHz; CD_2Cl_2), 3.74 (1H, br.s., carborane C*H*), 2.95 (2H, t, *J* = 7.2 Hz, $CCH_2CH_2CH_2S$), 2.41 (2H, t, *J* = 8.0 Hz, $CCH_2CH_2CH_2S$), 2.07 (2H, m, $CCH_2CH_2CH_2S$); ^{11}B NMR δ_B (128 MHz; CD_2Cl_2; $Et_2O{\cdot}BF_3$), -3.39 (1B, d, *J* = 150 Hz, B9), -6.70 (1B, d, *J* = 150 Hz, B12), -10.31 (2B, d, *J* = 150 Hz, B8, 10), -12.81 (4B, d, overlap, B4, 5, 7, 11), -13.98 (2B, d, overlap, B3, 6); ^{13}C NMR δ_C (100 MHz; CD_2Cl_2), 111.65 (1C, S*C*N), 74.37 (1C, carborane *C*), 62.29 (1C, carborane *C*H), 36.23 (1C, $CCH_2CH_2CH_2S$), 33.04 (1C, $CCH_2CH_2CH_2S$), 29.67 (1C, $CCH_2CH_2CH_2S$); *m/z* (ESI$^-$) 246.28 (7%), 243.28 (100%), calc. 246.21 and 243.21.

1-(Sulfonylchloride)propyl-1,2-dicarba-*closo*-dodecaborane,

1-$ClO_2SC_3H_6$-1,2-*closo*-$C_2B_{10}H_{11}$ (**60o**)

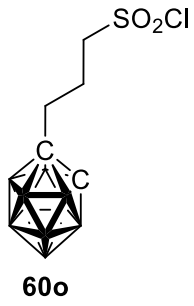

60o

We followed procedure M. Yield: 82% (95 mg) of the yellowish oil. m.p.: <25°C; R_f = 0.43 (CH_2Cl_2:benzene 1:2); Analysis found: C, 21.5; H, 6.4 calc. for $B_{10}C_5H_{17}O_2SCl$: C, 21.1; H, 6.0%; ^{1}H NMR δ_H (400 MHz; CD_2Cl_2), 3.77 (2H, t, *J* = 6.4 Hz, $CCH_2CH_2CH_2S$), 3.75 (1H, br.s., carborane C*H*), 2.45 (2H, t, *J* = 8.0 Hz, $CCH_2CH_2CH_2S$), 2.02 (2H, m, $CCH_2CH_2CH_2S$); ^{11}B NMR δ_B (128 MHz; CD_2Cl_2; $Et_2O{\cdot}BF_3$), -3.32 (1B, d, *J* = 150 Hz, B9), -6.56 (1B, d, *J* = 150 Hz, B12), -10.27 (2B, d, *J* = 150 Hz, B8, 10), -12.95 (4B, d, overlap, B4, 5, 7, 11), -13.93 (2B, d, overlap, B3, 6); ^{13}C NMR δ_C (100 MHz; CD_2Cl_2), 73.82 (1C, carborane *C*), 64.03 (1C, $CCH_2CH_2CH_2S$), 62.39 (1C, carborane *C*H), 35.73 (1C, $CCH_2CH_2CH_2S$), 24.44 (1C, $CCH_2CH_2CH_2S$); *m/z* (ESI$^-$) 286.16 (38%), 284.16 (100%), calc. 286.16 and 284.82.

1-(Sulfonamido)propyl-1,2-dicarba-*closo*-dodecaborane, 1-$H_2NO_2SC_3H_6$-1,2-*closo*-$C_2B_{10}H_{11}$ (**61o**)

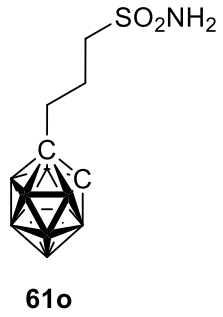

61o

We followed procedure O. Yield: 72% (33 mg) of the colourless crystals. m.p.: 128°C; R_f = 0.10 (CH_2Cl_2:benzene 1:2); Analysis found: C, 22.4; H, 7.1 calc. for $B_{10}C_5H_{19}O_2SN$: C, 22.6; H, 7.2%; ^{1}H NMR δ_H (400 MHz; CD_2Cl_2), 4.85 (2H, br.s., N*H*$_2$), 3.75 (1H, br.s., carborane C*H*), 3.11 (2H, t, *J* = 7.2 Hz, $CCH_2CH_2CH_2S$), 2.41 (2H, t, *J* = 8.0 Hz, $CCH_2CH_2CH_2S$), 2.04 (2H, m, $CCH_2CH_2CH_2S$); ^{11}B NMR δ_B (128 MHz; CD_2Cl_2; $Et_2O{\cdot}BF_3$), -3.42 (1B, d, *J* = 146 Hz, B9), -6.68 (1B, d, *J* = 146 Hz, B12), -10.34 (2B, d, *J* = 153 Hz, B8, 10), -12.83 (4B, d, overlap, B4, 5, 7, 11), -13.98 (2B, d, overlap, B3, 6); ^{13}C NMR δ_C (100 MHz; CD_2Cl_2), 74.22 (1C, carborane *C*), 61.72 (1C, carborane *C*H), 53.82 (1C, $CCH_2CH_2CH_2S$), 35.99 (1C, $CCH_2CH_2CH_2S$), 23.75 (1C, $CCH_2CH_2CH_2S$); *m/z* (ESI$^-$) 267.25 (29%), 265.33 (100%), calc. 267.21 and 265.21.

1-Hydroxypropyl-1,7-Dicarba-*closo*-dodecaborane, 1-HOC_3H_6-1,7-*closo*-$C_2B_{10}H_{11}$ (**55m**)

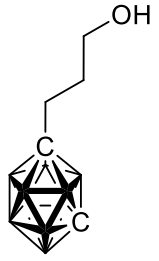

55m

We followed procedure G. Yield: 49% (6.76 g) of the white solid. m.p.: 74°C; R_f = 0.13 (CH_2Cl_2:benzene 1:2); Analysis found: C, 30.3; H, 9.5 calc. for $B_{10}C_5H_{18}O$: C, 29.7; H, 9.0%; ^{1}H NMR δ_H (400 MHz; CD_2Cl_2), 3.54 (2H, t, *J* = 6.0 Hz, $CCH_2CH_2CH_2OH$), 3.02 (1H, br.s., carborane C*H*), 2.07 (2H, t, *J* = 7.3 Hz, $CCH_2CH_2CH_2OH$), 1.64 (2H, m, $CCH_2CH_2CH_2OH$); ^{11}B NMR δ_B (128 MHz; CD_2Cl_2; $Et_2O{\cdot}BF_3$), -5.13 (1B, d, *J* = 162 Hz, B4), -10.35 (1B, d, overlap,

B12), -11.93 (4B, d, overlap, B3, 5, 8, 11), -14.59 (2B, d, J = 192 Hz, B9, 10), -16.24 (2B, d, J = 189 Hz, B2, 6); ^{13}C NMR δ_C (100 MHz; CD_2Cl_2), 76.11 (1C, carborane *C*), 61.95 (1C, $CCH_2CH_2\mathit{C}H_2OH$), 55.82 (1C, carborane *C*H), 33.73 (1C, $CCH_2\mathit{C}H_2CH_2OH$), 33.26 (1C, $C\mathit{C}H_2CH_2CH_2OH$); *m/z* (ESI¯) 205.33 (12%), 202.33 (100%), calc. 205.24 and 202.24.

1-(Triflourmethanesulfonate)propyl-1,7-dicarba-*closo*-dodecaborane,
1-$CF_3SO_3C_3H_6$-1,7-*closo*-$C_2B_{10}H_{11}$ (**57m**)

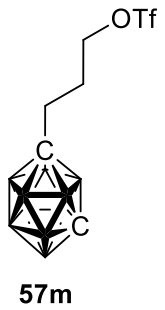

57m

We followed procedure I. Yield: 84% (5.12 g) of the dark pink – brownish oil. m.p.: >25°C; R_f = 0.71 (CH_2Cl_2:benzene 1:2); Analysis found: C, 21.7; H, 5.2 calc. for $B_{10}C_6H_{17}O_3SF_3$: C, 21.6; H, 5.1%; ^{1}H NMR δ_H (400 MHz; CD_2Cl_2), 4.49 (2H, t, J = 6.4 Hz, $CCH_2CH_2C\mathit{H}_2O$), 3.05 (1H, br.s., carborane C*H*), 2.14 (2H, t, J = 8.0 Hz, $CC\mathit{H}_2CH_2CH_2O$), 1.95 (2H, m, $CCH_2C\mathit{H}_2CH_2O$); ^{11}B NMR δ_B (128 MHz; CD_2Cl_2; $Et_2O{\cdot}BF_3$), -5.32 (1B, d, J = 162 Hz, B4), -10.77 (1B, d, overlap, B12), -11.88 (4B, d, overlap, B3, 5, 8, 11), -14.48 (2B, d, J = 174 Hz, B9, 10), -16.24 (2B, d, J = 186 Hz, B2, 6); ^{13}C NMR δ_C (100 MHz; CD_2Cl_2), 119.27 (1C, $\mathit{C}F_3$), 76.15 (1C, $CCH_2CH_2\mathit{C}H_2O$), 69.85 (1C, carborane *C*), 69.81 (1C, carborane *C*H), 34.08 (1C, $CCH_2\mathit{C}H_2CH_2O$), 30.38 (1C, $C\mathit{C}H_2CH_2CH_2O$); *m/z* (ESI¯) 336.12 (10%), 334.12 (100%), calc. 336.18 and 334.18.

1-(Thiocynate)propyl-1,7-dicarba-*closo*-dodecaborane,
1-$NCSC_3H_6$-1,7-*closo*-$C_2B_{10}H_{11}$ (**59m**)

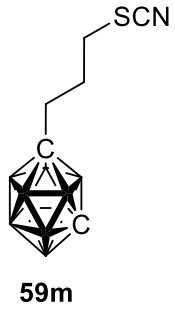

59m

We followed procedure K. Yield: 85% (3.15 g) of the slightly yellow solid. m.p.: 104°C; R_f = 0.67 (CH_2Cl_2:benzene 1:2); Analysis found: C, 29.8; H, 7.4 calc. for $B_{10}C_6H_{17}SN$: C, 29.6; H, 7.0%; ^{1}H NMR δ_H (400 MHz; CD_2Cl_2), 3.05 (1H, br.s., carborane C*H*), 2.89 (2H, t, J = 7.2 Hz, $CCH_2CH_2C\mathit{H}_2S$), 2.12 (2H, t, J = 8.0 Hz, $CC\mathit{H}_2CH_2CH_2S$), 1.98 (2H, m, $CCH_2C\mathit{H}_2CH_2S$); ^{11}B NMR δ_B (128 MHz; CD_2Cl_2; $Et_2O{\cdot}BF_3$), -5.20 (1B, d, J = 159 Hz, B4), -10.88 (1B, d, overlap, B12), -11.91 (4B, d, overlap, B3, 5, 8, 11), -14.52 (2B, d, J = 211 Hz, B9, 10), -16.26 (2B, d, J = 183 Hz, B2, 6); ^{13}C NMR δ_C (100 MHz; CD_2Cl_2), 111.82 (1C, S*C*N), 73.44 (1C, carborane *C*), 70.15 (1C, carborane *C*H), 35.09 (1C, $CCH_2CH_2\mathit{C}H_2S$), 33.35 (1C, $CCH_2\mathit{C}H_2CH_2S$), 30.97 (1C, $C\mathit{C}H_2CH_2CH_2S$); *m/z* (ESI¯) 246.21 (11%), 243.21 (100%), calc. 246.20 and 243.21.

1-(Sulfonylchloride)propyl-1,7-dicarba-*closo*-dodecaborane,

1-$ClO_2SC_3H_6$-1,7-*closo*-$C_2B_{10}H_{11}$ (**60m**)

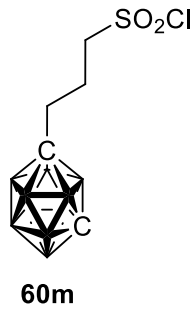

60m

We followed procedure M. Yield: 77% (2.8 g) of the yellowish oil. m.p.: >25°C; R_f = 0.10 (CH_2Cl_2:benzene 1:2); Analysis found: C, 22.0; H, 6.7 calc. for $B_{10}C_5H_{17}O_2SCl$: C, 21.1; H, 6.0%; ^{1}H NMR δ_H (400 MHz; CD_2Cl_2), 3.65 (2H, t, *J* = 7.2 Hz, $CCH_2CH_2CH_2S$), 3.07 (1H, br.s., carborane C*H*), 2.15 (2H, t, *J* = 5.2 Hz, $CCH_2CH_2CH_2S$), 2.10 (2H, m, $CCH_2CH_2CH_2S$); ^{11}B NMR δ_B (128 MHz; CD_2Cl_2; $Et_2O{\cdot}BF_3$), -5.30 (1B, d, *J* = 159 Hz, B4), -10.65 (1B, d, overlap, B12), -11.86 (4B, d, overlap, B3, 5, 8, 11), -14.43 (2B, d, *J* = 171 Hz, B9, 10), -16.26 (2B, d, *J* = 183 Hz, B2, 6); ^{13}C NMR δ_C (100 MHz; CD_2Cl_2), 75.09 (1C, carborane *C*), 64.35 (1C, $CCH_2CH_2CH_2S$), 55.87 (1C, carborane *C*H), 35.06 (1C, $CCH_2CH_2CH_2S$), 24.79 (1C, $CCH_2CH_2CH_2S$); *m/z* (ESI$^-$) 288.14 (16%), 285.14 (100%), calc. 285.16 and 288.16.

1-(Sulfonamido)propyl-1,7-dicarba-*closo*-dodecaborane, 1-$H_2NO_2SC_3H_6$-1,7-*closo*-$C_2B_{10}H_{11}$ (**61m**)

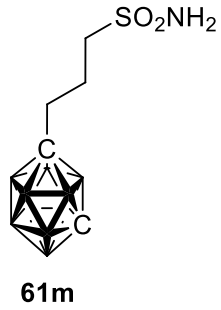

61m

We followed procedure O. Yield: 64% (1.70 g) of the white solid. m.p.: 111°C; R_f = 0.03 (CH_2Cl_2:benzene 1:2); Analysis found: C, 22.3; H, 7.1 calc. for $B_{10}C_5H_{19}O_2SN$: C, 22.6; H, 7.2%; ^{1}H NMR δ_H (400 MHz; CD_2Cl_2), 4.69 (2H, br.s., NH_2), 3.05 (2H, t, *J* = 7.6 Hz, $CCH_2CH_2CH_2S$), 3.03 (1H, br.s., carborane C*H*), 2.14 (2H, t, *J* = 8.0 Hz, $CCH_2CH_2CH_2S$), 1.95 (2H, m, $CCH_2CH_2CH_2S$); ^{11}B NMR δ_B (128 MHz; CD_2Cl_2; $Et_2O{\cdot}BF_3$), -5.25 (1B, d, *J* = 162 Hz, B4), -10.86 (1B, d, overlap, B12), -11.91 (4B, d, overlap, B3, 5, 8, 11), -14.52 (2B, d, *J* = 169 Hz, B9, 10), -16.28 (2B, d, *J* = 186 Hz, B2, 6); ^{13}C NMR δ_C (100 MHz; CD_2Cl_2), 75.13 (1C, carborane *C*), 55.34 (1C, carborane *C*H), 54.32 (1C, $CCH_2CH_2CH_2S$), 35.00 (1C, $CCH_2CH_2CH_2S$), 24.37 (1C, $CCH_2CH_2CH_2S$); *m/z* (ESI$^-$) 268.17 (7%), 265.42 (100%), calc. 268.21 and 265.21.

1-Hydroxypropyl-1,12-dicarba-*closo*-dodecaborane, 1-HOC_3H_6-1,12-*closo*-$C_2B_{10}H_{11}$ (**55p**)

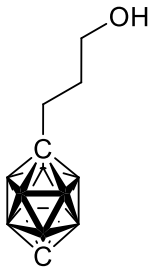

55p

We followed procedure G. Yield: 28% (758 mg) of the white crystals. m.p.: 68°C; R_f = 0.32 (CH_2Cl_2:benzene 1:2); Analysis found: C, 30.4; H, 9.2 calc. for $B_{10}C_5H_{18}O$: C, 29.7; H, 9.0%; ^{1}H NMR δ_H (400 MHz; acetone-d_6), 3.41 (2H, q, J_{12} = 6.0, J_{13} = 12.4 Hz, $CCH_2CH_2CH_2OH$), 3.29 (1H, br.s., carborane C*H*), 1.80 (2H, t, J = 7.6 Hz, $CCH_2CH_2CH_2OH$), 1.40 (2H, m, $CCH_2CH_2CH_2OH$); ^{11}B NMR δ_B (128 MHz; acetone-d_6; $Et_2O{\cdot}BF_3$), -12.56 (5B, d, J = 165 Hz, B2, 3, 4, 5, 6), -15.06 (5B, d, J = 165, B7, 8, 9, 10, 11); ^{13}C NMR δ_C (100 MHz; CD_2Cl_2), 84.73 (1C, carborane *C*), 61.99 (1C, $CCH_2CH_2CH_2OH$), 58.60 (1C, carborane *C*H), 35.64 (1C, $CCH_2CH_2CH_2OH$), 32.70 (1C, $CCH_2CH_2CH_2OH$); *m/z* (ESI$^-$) 336.12 (10%), 334.12 (100%), calc. 336.18 and 334.18. *m/z* (ESI$^-$) 205.34 (11%), 202.34 (100%), calc. 205.24 and 202.24.

1-(Triflourmethanesulfonate)propyl-1,12-dicarba-*closo*-dodecaborane,
1-$CF_3SO_3C_3H_6$-1,12-*closo*-$C_2B_{10}H_{11}$ (**57p**)

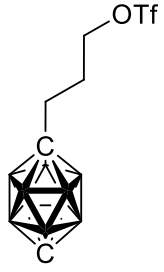

57p

We followed procedure I. Yield: 82% (517 mg) of the dark pink oil. m.p.: >25°C; R_f = 0.82 (CH_2Cl_2:benzene 1:2); Analysis found: C, 21.6; H, 5.3 calc. for $B_{10}C_6H_{17}O_3SF_3$: C, 21.6; H, 5.1%; ^{1}H NMR δ_H (400 MHz; acetone-d_6), 4.60 (2H, t, J = 5.7, $CCH_2CH_2CH_2O$), 3.01 (1H, br.s., carborane C*H*), 1.88 (2H, t, J = 7.5 Hz, $CCH_2CH_2CH_2O$), 1.45 (2H, m, $CCH_2CH_2CH_2O$); ^{11}B NMR δ_B (128 MHz; acetone-d_6; $Et_2O{\cdot}BF_3$), -12.50 (5B, d, J = 164 Hz, B2, 3, 4, 5, 6), -14.99 (5B, d, J = 164, B7, 8, 9, 10, 11); ^{13}C NMR δ_C (100 MHz; CD_2Cl_2), 122.14 (1C, CF_3), 78.36 (1C, $CCH_2CH_2CH_2O$), 70.58 (1C, carborane *C*), 69.75 (1C, carborane *C*H), 35.87 (1C, $CCH_2CH_2CH_2O$), 31.28 (1C, $CCH_2CH_2CH_2O$); *m/z* (ESI$^-$) 336.11 (9%), 334.12 (100%), calc. 336.18 and 334.18.

1-(Thiocynate)propyl-1,12-dicarba-*closo*-dodecaborane,
1-$NCSC_3H_6$-1,12-*closo*-$C_2B_{10}H_{11}$ (**59p**)

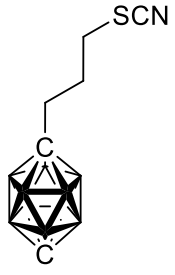

59p

We followed procedure K. Yield: 77% (289 mg) of the slightly yellow solid. m.p.: 86°C; R_f = 0.74 (CH_2Cl_2:benzene 1:2); Analysis found: C, 29.9; H, 7.3 calc. for $B_{10}C_6H_{17}SN$: C, 29.6; H, 7.0%; ^{1}H NMR δ_H (400 MHz; acetone-d_6), 3.35 (1H, br.s., carborane C*H*), 3.03 (2H, t, J = 7.2, $CCH_2CH_2CH_2S$), 1.92 (2H, t, J = 7.3 Hz, $CCH_2CH_2CH_2S$), 1.76 (2H, m, $CCH_2CH_2CH_2S$); ^{11}B NMR δ_B (128 MHz; acetone-d_6; $Et_2O{\cdot}BF_3$), -12.63 (5B, d, J = 165 Hz, B2, 3, 4, 5, 6), -14.99 (5B, d, J = 165, B7, 8, 9, 10, 11); ^{13}C NMR δ_C (100 MHz; CD_2Cl_2),

114.83 (1C, S*C*N), 74.34 (1C, carborane *C*), 71.75 (1C, carborane *C*H), 35.14 (1C, $CCH_2CH_2\mathit{C}H_2S$), 33.73 (1C, $CCH_2\mathit{C}H_2CH_2S$), 31.28 (1C, $C\mathit{C}H_2CH_2CH_2S$); *m/z* (ESI^-) 246.23 (14%), 243.22 (100%), calc. 246.20 and 243.21

1-(Sulfonylchloride)propyl-1,12-dicarba-*closo*-dodecaborane,
1-$ClO_2SC_3H_6$-1,12-*closo*-$C_2B_{10}H_{11}$ (**60p**)

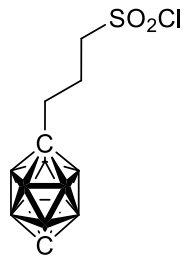

60p

We followed procedure M. Yield: 78% (262 mg) of the yellow oil. m.p.: >25°C; R_f = 0.21 (CH_2Cl_2:benzene 1:2); Analysis found: C, 22.3; H, 6.9 calc. for $B_{10}C_5H_{17}O_2SCl$: C, 21.1; H, 6.0%; ^{1}H NMR δ_H (400 MHz; acetone-d_6), 3.99 (2H, t, *J* = 7.6, $CCH_2CH_2C\mathit{H}_2S$), 3.38 (1H, br.s., carborane C*H*), 2.05 (2H, t, *J* = 5.6 Hz, $CC\mathit{H}_2CH_2CH_2S$), 1.94 (2H, m, $CCH_2C\mathit{H}_2CH_2S$); ^{11}B NMR δ_B (128 MHz; acetone-d_6; $Et_2O{\cdot}BF_3$), -12.71 (5B, d, *J* = 162 Hz, B2, 3, 4, 5, 6), -14.94 (5B, d, *J* = 168, B7, 8, 9, 10, 11); ^{13}C NMR δ_C (100 MHz; CD_2Cl_2), 76.41 (1C, carborane *C*), 65.36 (1C, $CCH_2CH_2\mathit{C}H_2S$), 55.91 (1C, carborane *C*H), 36.74 (1C, $CCH_2\mathit{C}H_2CH_2S$), 30.12 (1C, $C\mathit{C}H_2CH_2CH_2S$); *m/z* (ESI^-) 288.15 (13%), 285.15 (100%), calc. 285.16 and 288.16.

1-(Sulfonamido)propyl-1,12-dicarba-*closo*-dodecaborane,
1-$H_2NO_2SC_3H_6$-1,12-*closo*-$C_2B_{10}H_{11}$ (**61p**)

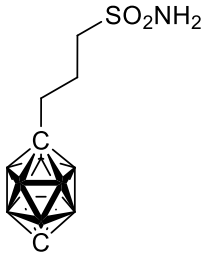

61p

We followed procedure O. Yield: 74% (179 mg) of the white solid. m.p.: 153°C; R_f = 0.14 (CH_2Cl_2:benzene 1:2); Analysis found: C, 22.6; H, 7.4 calc. for $B_{10}C_5H_{19}O_2SN$: C, 22.6; H, 7.2%; ^{1}H NMR δ_H (400 MHz; acetone-d_6), 6.16 (2H, br.s., $N\mathit{H}_2$), 3.33 (1H, br.s., carborane C*H*), 2.97 (2H, t, *J* = 7.6, $CCH_2CH_2C\mathit{H}_2S$), 1.90 (2H, t, *J* = 7.6 Hz, $CC\mathit{H}_2CH_2CH_2S$), 1.73 (2H, m, $CCH_2C\mathit{H}_2CH_2S$); ^{11}B NMR δ_B (128 MHz; acetone-d_6; $Et_2O{\cdot}BF_3$), -12.63 (5B, d, *J* = 162 Hz, B2, 3, 4, 5, 6), -15.01 (5B, d, *J* = 165, B7, 8, 9, 10, 11); ^{13}C NMR δ_C (100 MHz; CD_2Cl_2), 59.02 (1C, carborane *C*), 54.53 (1C, carborane *C*H), 37.15 (1C, $CCH_2CH_2\mathit{C}H_2S$), 30.97 (1C, $CCH_2\mathit{C}H_2CH_2S$), 24.06 (1C, $C\mathit{C}H_2CH_2CH_2S$); *m/z* (ESI^-) 268.42 (7%), 265.42 (100%), calc. 268.21 and 265.21.

1,7-Bis[(hydroxy)propyl]-1,7-dicarba-*closo*-dodecaborane,

1,7-$(HOC_3H_6)_2$-1,7-*closo*-$C_2B_{10}H_{10}$ (**62m**)

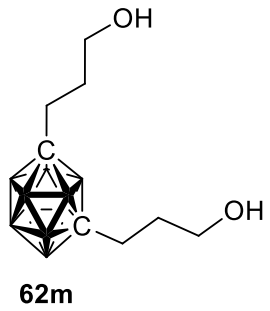

62m

We followed procedure H. Yield: 38% (3.4 g) of the white solid. m.p.: 105°C; R_f = 0.11 (CH_2Cl_2:benzene 1:2); Analysis found: C, 37.3; H, 9.5 calc. for $B_{10}C_8H_{24}O_2$: C, 36.9; H, 9.3%; ^{1}H NMR δ_H (400 MHz; CD_2Cl_2), 3.54 (2H, t, *J* = 6.0 Hz, $CCH_2CH_2CH_2O$), 2.06 (2H, t, *J* = 8.8 Hz, $CCH_2CH_2CH_2O$), 1.62 (2H, m, $CCH_2CH_2CH_2O$); ^{11}B NMR δ_B (128 MHz; CD_2Cl_2; $Et_2O{\cdot}BF_3$), -8.36 (2B, d, *J* = 159 Hz, B9, 10), -12.22 (6B, d, *J* = 156 Hz, B3, 4, 5, 8, 11, 12), -14.52 (2B, d, *J* = 169 Hz, B2, 6); ^{13}C NMR δ_C (100 MHz; CD_2Cl_2), 75.84 (2C, carborane *C*), 62.77 (2C, $CCH_2CH_2CH_2OH$), 32.85 (2C, $CCH_2CH_2CH_2OH$), 30.31 (2C, $CCH_2CH_2CH_2OH$); *m/z* (ESI$^-$) 263.28 (5%), 260.28 (100%), calc. 263.28 and 260.28.

1,7-Bis[(triflourmethanesulfonate)propyl]-1,7-dicarba-*closo*-dodecaborane,

1,7-$(CF_3SO_3C_3H_6)_2$-1,7-*closo*-$C_2B_{10}H_{10}$ (**63m**)

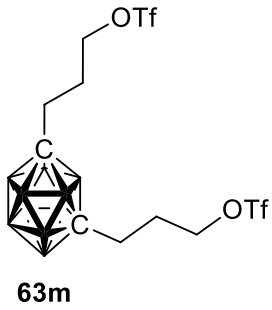

63m

We followed procedure J. Yield: 92% (3.0 g) of the dark pink oil. m.p.: >25°C; R_f = 0.42 (CH_2Cl_2:benzene 1:2); Analysis found: C, 22.9; H, 4.5 calc. for $B_{10}C_{10}H_{22}O_6S_2F_6$: C, 22.9; H, 4.2%; ^{1}H NMR δ_H (400 MHz; CD_2Cl_2), 4.49 (2H, t, *J* = 5.6 Hz, $CCH_2CH_2CH_2O$), 2.14 (2H, t, *J* = 7.6 Hz, $CCH_2CH_2CH_2O$), 1.94 (2H, m, $CCH_2CH_2CH_2O$); ^{11}B NMR δ_B (128 MHz; CD_2Cl_2; $Et_2O{\cdot}BF_3$), -8.22 (2B, d, *J* = 137 Hz, B9, 10), -12.03 (6B, d, *J* = 143 Hz, B3, 4, 5, 8, 11, 12), -14.52 (2B, d, *J* = 157 Hz, B2, 6); ^{13}C NMR δ_C (100 MHz; CD_2Cl_2), 117.24 (2C, CF_3), 77.17 (2C, $CCH_2CH_2CH_2O$), 68.93 (2C, carborane *C*), 36.64 (2C, $CCH_2CH_2CH_2O$), 29.91 (2C, $CCH_2CH_2CH_2O$); *m/z* (ESI$^-$) 527.19 (10%), 524.19 (100%), calc. 527.17 and 524.18.

1,7-Bis[(thiocyanate)propyl]-1,7-dicarba-*closo*-dodecaborane,

1,7-$(NCSC_3H_6)_2$-1,7-*closo*-$C_2B_{10}H_{10}$ (**64m**)

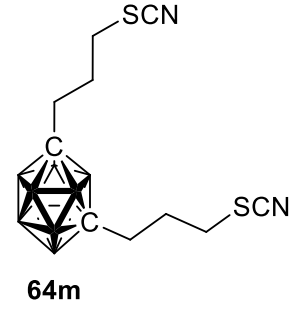

64m

We followed procedure L. Yield: 86% (1.7 g) of the yellowish solid. m.p.: 64°C; R_f = 0.30 (CH_2Cl_2:benzene 1:2); Analysis found: C, 35.3; H, 6.6 calc. for $B_{10}C_{10}H_{22}N_2S_2$: C, 35.0; H, 6.5%; ^{1}H NMR δ_H (400 MHz; CD_2Cl_2), 4.49 (2H, t, *J* = 5.6 Hz, $CCH_2CH_2CH_2S$), 2.14 (2H, t, *J* = 7.6 Hz, $CCH_2CH_2CH_2S$), 1.94 (2H, m, $CCH_2CH_2CH_2S$); ^{11}B NMR δ_B (128 MHz; CD_2Cl_2; $Et_2O{\cdot}BF_3$), -8.22 (2B, d, *J* = 137 Hz,

B9, 10), -12.03 (6B, d, *J* = 143 Hz, B3, 4, 5, 8, 11, 12), -14.52 (2B, d, *J* = 157 Hz, B2, 6); ^{13}C NMR δ_C (100 MHz; CD_2Cl_2), 111.80 (2C, S*C*N), 74.86 (2C, carborane *C*), 35.01 (2C, $CCH_2CH_2\mathit{C}H_2S$), 30.59 (2C, $CCH_2\mathit{C}H_2CH_2S$), 29.96 (2C, $C\mathit{C}H_2CH_2CH_2S$); *m/z* (ESI$^+$) 346.50 (9%), 343.33 (100%), calc. 346.22 and 343.23.

1,7-Bis[(sulfonylchloride)propyl]-1,7-dicarba-*closo*-dodecaborane,
1,7-$(ClSO_2C_3H_6)_2$-1,7-*closo*-$C_2B_{10}H_{10}$ (**65m**)

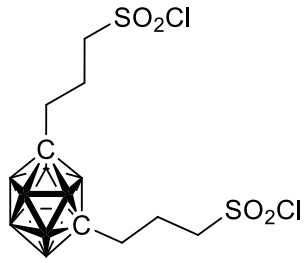

65m

We followed procedure N. Yield: 92% (1.5 g) of the light-yellow oil. m.p.: >25°C; R_f = 0.09 (CH_2Cl_2:benzene 1:2); Analysis found: C, 22.7; H, 5.3 calc. for $B_{10}C_8H_{22}O_4S_2Cl_2$: C, 22.6; H, 5.2%; ^{1}H NMR δ_H (400 MHz; CD_2Cl_2), 3.03(2H, t, *J* = 7.2 Hz, $CCH_2CH_2C\mathit{H}_2S$), 2.27 (2H, t, *J* = 8.0 Hz, $CC\mathit{H}_2CH_2CH_2S$), 2.07 (2H, m, $CCH_2C\mathit{H}_2CH_2S$); ^{11}B NMR δ_B (128 MHz; CD_2Cl_2; $Et_2O{\cdot}BF_3$), -8.20 (2B, d, *J* = 156 Hz, B9, 10), -12.07 (6B, d, *J* = 192 Hz, B3, 4, 5, 8, 11, 12), -14.52 (2B, d, *J* = 180 Hz, B2, 6); ^{13}C NMR δ_C (100 MHz; CD_2Cl_2), 74.32 (2C, carborane *C*), 63.82 (2C, $CCH_2CH_2\mathit{C}H_2S$), 36.87 (2C, $CCH_2\mathit{C}H_2CH_2S$), 25.81 (2C, $C\mathit{C}H_2CH_2CH_2S$); *m/z* (ESI$^-$) 429.24 (13%), 425.13 (100%), calc. 429.13 and 425.13.

1,7-Bis[(sulfonamido)propyl]-1,7-dicarba-*closo*-dodecaborane,
1,7-$(H_2NSO_2C_3H_6)_2$-1,7-*closo*-$C_2B_{10}H_{10}$ (**66m**)

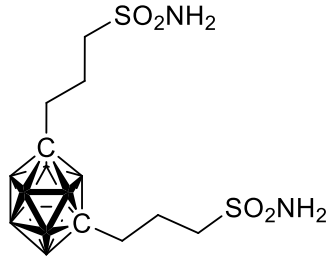

66m

We followed procedure P. Yield: 59% (0.8 g) of the white solid. m.p.: 112°C; R_f = 0.02 (CH_2Cl_2:benzene 1:2); Analysis found: C, 25.1; H, 7.0 calc. for $B_{10}C_8H_{26}O_4S_2N_2$: C, 24.9; H, 6.8%; ^{1}H NMR δ_H (400 MHz; CD_2Cl_2), 4.77 (4H, br.s., NH_2), 3.05 (2H, t, *J* = 6.8 Hz, $CCH_2CH_2C\mathit{H}_2S$), 2.13 (2H, t, *J* = 7.6 Hz, $CC\mathit{H}_2CH_2CH_2S$), 1.92 (2H, m, $CCH_2C\mathit{H}_2CH_2S$); ^{11}B NMR δ_B (128 MHz; CD_2Cl_2; $Et_2O{\cdot}BF_3$), -8.15 (2B, d, *J* = 165 Hz, B9, 10), -12.07 (6B, d, *J* = 156 Hz, B3, 4, 5, 8, 11, 12), -14.57 (2B, d, *J* = 183 Hz, B2, 6); ^{13}C NMR δ_C (100 MHz; CD_2Cl_2), 75.23 (2C, carborane *C*), 52.94 (2C, $CCH_2CH_2\mathit{C}H_2S$), 36.84 (2C, $CCH_2\mathit{C}H_2CH_2S$), 21.85 (2C, $C\mathit{C}H_2CH_2CH_2S$); *m/z* (ESI$^-$) *dimer* 773.33 (17%), 776.33 (100%), calc. 776.46 and 773.46.

1,12-Bis[(hydroxy)propyl]-1,12-dicarba-*closo*-dodecaborane,

1,12-$(HOC_3H_6)_2$-1,12-*closo*-$C_2B_{10}H_{10}$ (**62p**)

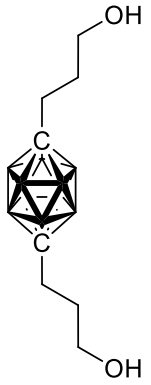

62p

We followed procedure H. Yield: 42% (2.2 g) of the white crystals. m.p.: 153°C; R_f = 0.21 (CH_2Cl_2:benzene 1:2); Analysis found: C, 37.2; H, 9.4 calc. for $B_{10}C_8H_{24}O_2$: C, 36.9; H, 9.3%; ^{1}H NMR δ_H (400 MHz; acetone-d_6), 3.41 (4H, q, J_{12} = 5.6, J_{13} = 11.6 Hz, $CCH_2CH_2CH_2OH$), 1.79 (4H, t, J = 8.0 Hz, $CCH_2CH_2CH_2OH$), 1.39 (4H, m, $CCH_2CH_2CH_2OH$); ^{11}B NMR δ_B (128 MHz; acetone-d_6; $Et_2O{\cdot}BF_3$), -12.80 (10B, d, J = 162 Hz, B2 - 11); ^{13}C NMR δ_C (100 MHz; CD_2Cl_2), 62.00 (2C, carborane *C*), 54.13 (2C, $CCH_2CH_2CH_2OH$), 34.49 (2C, $CCH_2CH_2CH_2OH$), 32.88 (2C, $CCH_2CH_2CH_2OH$); *m/z* (ESI^-) 263.29 (6%), 260.29 (100%), calc. 263.28 and 260.28.

1,12-Bis[(triflourmethanesulfonate)propyl]-1,12-dicarba-*closo*-dodecaborane, 1,12-$(CF_3SO_3C_3H_6)_2$-1,12-*closo*-$C_2B_{10}H_{10}$ (**63p**)

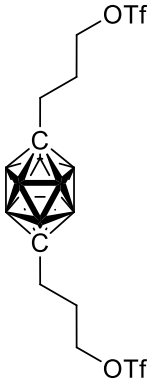

63p

We followed procedure J. Yield: 88% (1.87 g) of the dark pink oil. m.p.: >25°C; R_f = 0.74 (CH_2Cl_2:benzene 1:2); Analysis found: C, 23.2; H, 4.8 calc. for $B_{10}C_{10}H_{22}O_6S_2F_6$: C, 22.9; H, 4.2%; ^{1}H NMR δ_H (400 MHz; acetone-d_6), 4.66 (4H, t, J = 6.4 Hz, $CCH_2CH_2CH_2O$), 1.91 (4H, t, J = 7.4 Hz, $CCH_2CH_2CH_2O$), 1.82 (4H, m, $CCH_2CH_2CH_2O$); ^{11}B NMR δ_B (128 MHz; acetone-d_6; $Et_2O{\cdot}BF_3$), -12.80 (10B, d, J = 162 Hz, B2 - 11); ^{13}C NMR δ_C (100 MHz; CD_2Cl_2), 119.15 (2C, CF_3), 78.93 (2C, $CCH_2CH_2CH_2O$), 69.41 (2C, carborane *C*), 36.82 (2C, $CCH_2CH_2CH_2O$), 30.72 (2C, $CCH_2CH_2CH_2O$); Yield: *m/z* (ESI^-) 527.18 (10%), 524.18 (100%), calc. 527.17 and 524.18.

1,12-Bis[(thiocyanate)propyl]-1,12-dicarba-*closo*-dodecaborane,

1,12-$(NCSC_3H_6)_2$-1,12-*closo*-$C_2B_{10}H_{10}$ (**64p**)

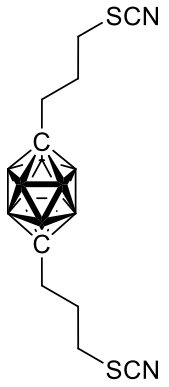

64p

We followed procedure L. Yield: 77% (981 mg) of the light yellow solid. m.p.: 98°C; R_f = 0.37 (CH_2Cl_2:benzene 1:2); Analysis found: C, 35.5; H, 6.7 calc. for $B_{10}C_{10}H_{22}N_2S_2$: C, 35.0; H, 6.5%; ^{1}H NMR δ_H (400 MHz; acetone-d_6), 3.02 (4H, t, *J* = 6.8 Hz, $CCH_2CH_2CH_2S$), 1.92 (4H, t, *J* = 8.0 Hz, $CCH_2CH_2CH_2S$), 1.75 (4H, m, $CCH_2CH_2CH_2S$); ^{11}B NMR δ_B (128 MHz; acetone-d_6; $Et_2O{\cdot}BF_3$), -12.82 (10B, d, *J* = 162 Hz, B2 - 11); ^{13}C NMR δ_C (100 MHz; CD_2Cl_2), 112.14 (2C, S*C*N), 76.39 (2C, carborane *C*), 36.52 (2C, $CCH_2CH_2CH_2S$), 31.83 (2C, $CCH_2CH_2CH_2S$), 30.13 (2C, $CCH_2CH_2CH_2S$); *m/z* (ESI^-) 345.25 (12%), 342.25 (100%), calc. 345.22 and 342.22.

1,12-Bis[(sulfonylchloride)propyl]-1,12-dicarba-*closo*-dodecaborane,

1,12-$(ClSO_2C_3H_6)_2$-1,12-*closo*-$C_2B_{10}H_{10}$ (**65p**)

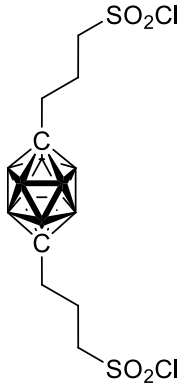

65p

We followed procedure N. Yield: 59% (720 mg) of the yellowish oil. m.p.: >25°C; R_f = 0.22 (CH_2Cl_2:benzene 1:2); Analysis found: C, 22.9; H, 5.7 calc. for $B_{10}C_8H_{22}O_4S_2Cl_2$: C, 22.6; H, 5.2%; ^{1}H NMR δ_H (400 MHz; acetone-d_6), 3.99 (4H, t, *J* = 7.6 Hz, $CCH_2CH_2CH_2S$), 2.02 (4H, t, *J* = 8.0 Hz, $CCH_2CH_2CH_2S$), 1.92 (4H, m, $CCH_2CH_2CH_2S$); ^{11}B NMR δ_B (128 MHz; acetone-d_6; $Et_2O{\cdot}BF_3$), -12.82 (10B, d, *J* = 162 Hz, B2 -11); ^{13}C NMR δ_C (100 MHz; CD_2Cl_2), 76.52 (2C, carborane *C*), 65.22 (2C, $CCH_2CH_2CH_2S$), 37.17 (2C, $CCH_2CH_2CH_2S$), 28.56 (2C, $CCH_2CH_2CH_2S$); *m/z* (ESI^-) 429.24 (12%), 425.16 (100%), calc. 429.13 and 425.13.

1,12-Bis[(sulfonamido)propyl]-1,12-dicarba-*closo*-dodecaborane, 1,12-$(H_2NSO_2C_3H_6)_2$-1,12-*closo*-$C_2B_{10}H_{10}$ (**66p**)

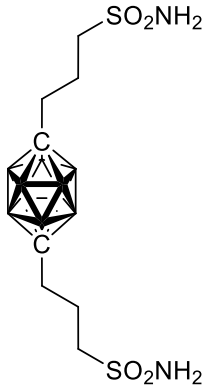

66p

We followed procedure P. Yield: 54% (353 mg) of the white solid. m.p.: 227°C; R_f = 0.02 (CH_2Cl_2:benzene 1:2); Analysis found: C, 25.3; H, 7.2 calc. for $B_{10}C_8H_{26}O_4S_2N_2$: C, 24.9; H, 6.8%; ^{1}H NMR δ_H (400 MHz; acetone-d_6), 6.14 (4H, br.s., N*H*$_2$), 2.96 (4H, t, *J* = 8.0 Hz, $CCH_2CH_2CH_2S$), 1.97 (4H, t, *J* = 8.8 Hz, $CCH_2CH_2CH_2S$), 1.71 (4H, m, $CCH_2CH_2CH_2S$); ^{11}B NMR δ_B (128 MHz; acetone-d_6; $Et_2O{\cdot}BF_3$), -12.85 (10B, d, *J* = 162 Hz, B2 -11); ^{13}C NMR δ_C (100 MHz; CD_2Cl_2), 76.53 (2C, carborane *C*), 53.91 (2C, $CCH_2CH_2CH_2S$), 36.85 (2C, $CCH_2CH_2CH_2S$), 23.28 (2C, $CCH_2CH_2CH_2S$); *m/z* (ESI$^-$) 389.08 (14%), 386.50 (100%), calc. 389.23 and 386.23.

1-(Azido)propyl-1,2-dicarba-*closo*-dodecaborane, 1-$N_3C_3H_6$-1,2-*closo*-$C_2B_{10}H_{11}$ (**67**)

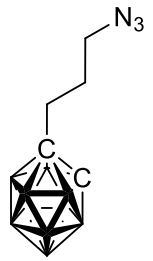

67

Triflate ester (500 mg, 1.5 mmol) and sodium azide (293 mg, 4.5 mmol.) were dissolved in DMF (10 ml) and were stirred overnight at 60°C. The reaction mixture was then diluted with water and extracted with Et_2O (3x20 ml) which was then dried over $MgSO_4$, filtered, concentrated under vacuum and applied to silica gel column (hexane:EtOAc 7:1). m.p.: 36°C; R_f = 0.05 (hexane:EtOAc 5:1); Yield: 62% (212 mg) of the yellowish crystals. Analysis found: C, 26.5; H, 7.7 calc. for $B_{10}C_5H_{17}N_3$: C, 26.4; H, 7.5%; ^{1}H NMR δ_H (400 MHz; CD_2Cl_2), 3.72 (1H, br.s., carborane C*H*), 4.14 (2H, t, *J* = 6.0 Hz, $CCH_2CH_2CH_2N$), 2.36 (2H, t, *J* = 8.0 Hz, $CCH_2CH_2CH_2N$), 1.91 (2H, m, $CCH_2CH_2CH_2N$); ^{11}B NMR δ_B (128 MHz; CD_2Cl_2; $Et_2O{\cdot}BF_3$), -3.47 (1B, d, *J* = 150 Hz, B9), -6.87 (1B, d, *J* = 146 Hz, B12), -10.41 (2B, d, *J* = 150 Hz, B8, 10), -12.79 (4B, d, overlap, B4, 5, 7, 11), -13.98 (2B, d, overlap, B3, 6); ^{13}C NMR δ_C (100 MHz; CD_2Cl_2), 70.58 (1C, carborane *C*), 63.07 (1C, carborane *C*H), 62.53 (1C, $CCH_2CH_2CH_2N$), 36.11 (1C, $CCH_2CH_2CH_2N$), 33.46 (1C, $CCH_2CH_2CH_2N$); *m/z* (ESI$^-$; M-N_3^-) 187.33 (39%), 185.33 (100%), calc. 187.24 and 185.23.

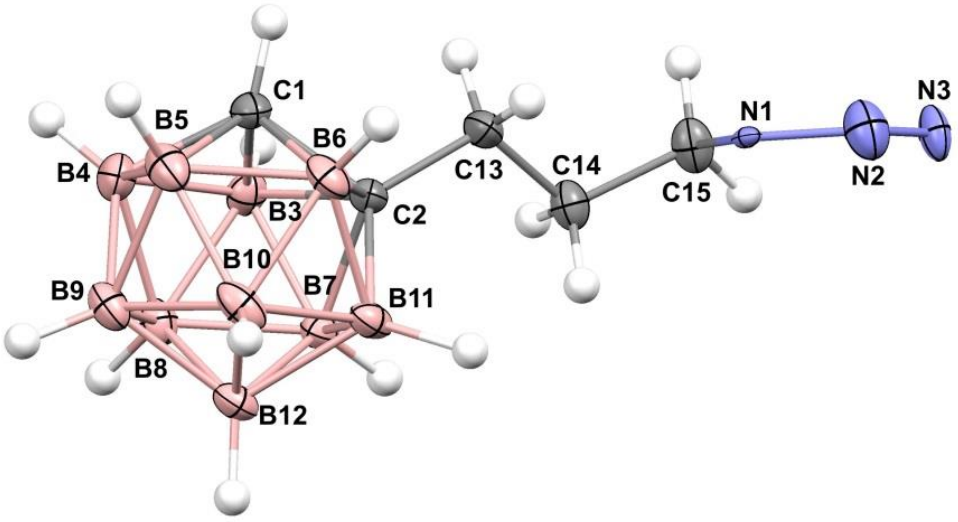

X-ray crystallographic data for **67**: $C_5H_{17}B_{10}N_3$, M = 227.31, monoclinic, $P2_1/c$, a = 12.2918(7) Å, b = 7.6948(4) Å, c = 15.1628(8) Å, β = 110.413(2) °, Z = 4, V = 1344.08(13) Å^3, D_c = 1.123 g.cm^{-3}, μ = 0.057 mm^{-1}, T_{min}/T_{max} = 0.6707/0.7456; $-15 \leq h \leq 15$, $-10 \leq k \leq 9$, $-19 \leq l \leq 19$; 19426 reflections measured (θ_{max} = 27.53 °), 3062 independent (R_{int} = 0.045), 2494 with $I > 2\sigma(I)$, 227 parameters, S = 1.038, *R1*(obs. data) = 0.0831, *wR2*(all data) = 0.2432; max., min. residual electron density = 0.593, -0.824 eÅ^{-3}.

7-(Sulfonamido)propyl-7,8-dicarba-*nido*-undecaborane, triethylammonium salt, [7-NH_2SO_2-$(CH_2)_3$-7,8-*nido*-$C_2B_9H_{11}$]Et_3NH (**71o**)

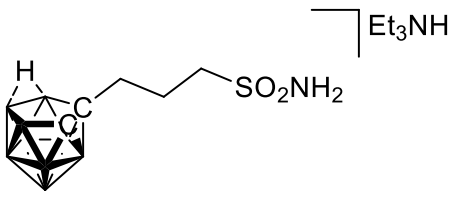

71o

To a **61o** (10 mmol) in MeOH (50 ml) was added KOH (0.40 g, 100 mmol) in several portions under vigorous stirring. The methanol solution was stirred and heated at 60°C for 6h under reflux. Then H_2O (50 ml) was added and the MeOH was evaporated under reduced pressure. The resulting aqueous solution was diluted with H_2O (60 ml) and extracted with Et_2O (2x20 ml) and then by EtOAc (4x25 ml). The EtOAc extracts were combined, H_2O (10 ml) was added and the solvents were evaporated under reduced pressure. Final purification of the products was conducted with liquid chromatography on silica gel column (25x2.5 cm) using CH_2Cl_2-CH_3CN solvent mixture (3:1 to 2:1) for elution. Fractions containing the product (according to NMR) were combined, evaporated under reduced pressure and product was then acidified by another

extraction with 3M HCl and Et_2O (3x20 ml). Finally, the organic layer was evaporated into small volume of water and then precipitated with Et_3N.

m.p. 312-314°C; ^{1}H NMR δ_H (400 MHz, CD_3CN), 5.23 (s, 2H, N*H*$_2$), 4.89 (1H, s, bridging *H*), 4.89 (1H, s, bridging *H*), 3.18 (6H, q, J_{12} = 7.1, J_{13} = 14.7 Hz, N(C*H*$_2$CH$_3$)$_3$), 2.94 (m, 2H, CCH$_2$CH$_2$C*H*$_2$S), 2.30 (s, 1H, carborane C*H*), 1.81 m (2H, CC*H*$_2$CH$_2$CH$_2$S), 1.67 (2H, m, CCH$_2$C*H*$_2$CH$_2$S), 1.15 (9H, t, *J* = 8.0 Hz, N(CH$_2$C*H*$_3$)$_3$); ^{11}B NMR δ_B (128 MHz, CD_3CN, $Et_2O{\cdot}BF_3$) -11.42 (d, 2B, *J* = 34 Hz, B9, 11), -14.32 (1B, d, *J* = 156 Hz, B4), -17.25 (1B, d, *J* = 156 Hz, B6), -18.86 (2B, d, *J* = 186 Hz, B2, 5), -22.22 (1B, d, *J* = 146 Hz, B3), -33.63 (1B, d, *J* = 125 Hz, B10), -37.53 (1B, d, *J* = 137 Hz, B1); ^{13}C NMR δ_C (100 MHz, CD_3CN) 60.14 (1C, carborane *C*), 55.58 (1C, CCH$_2$CH$_2$*C*H$_2$S), 50.49 (3C, N(*C*H$_2$CH$_3$)$_3$), 47.48 (1C, carborane *C*H), 38.39 (1C, C*C*H$_2$CH$_2$CH$_2$S), 26.30 (1C, CCH$_2$*C*H$_2$CH$_2$S) 19.83 (3C, N(CH$_2$*C*H$_3$)$_3$); *m/z* (ESI$^-$), 256.20 (50%), calcd. 256.20. White solid, yield: 2.71 g (92%).

7-(Sulfonamido)propyl-7,9-dicarba-*nido*-undecaborate, triethylammonium salt, [7-NH$_2$SO$_2$(CH$_2$)$_3$-7,8-C$_2$B$_9$H$_{11}$]Et$_3$NH (**71m**)

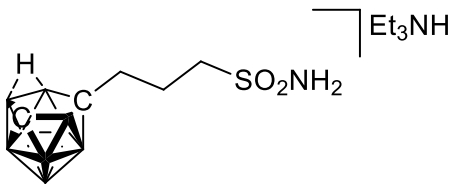

71m

To a **61m** (500 mg, 1.89 mmol) in MeOH (2 ml) was added KOH (1.1 g, 18.9 mmol) and KF (2.2 g, 37.7 mmol) in several portions under vigorous stirring. The methanol solution was stirred and heated at reflux for 2 days under reflux condenser. Then the same procedure as mentioned previously. Yellow honey-like sirup, yield 74%g (1.4). m.p.: >25°C; R_f = 0.31 (CH_2Cl_2:benzene 1:2); Analysis found: C, 37.6; H, 10.5 calc. for $B_9C_{11}H_{35}O_2SN_2$: C, 37.0; H, 9.9%; ^{1}H NMR δ_H (400 MHz; CD_2Cl_2), 5.21 (2H, br.s., N*H*$_2$), 4.95 (1H, s, bridging *H*), 3.20 (2H, t, *J* = 6.8 Hz, CCH$_2$CH$_2$C*H*$_2$S), 3.15 (6H, q, J_{12} = 7.2, J_{13} = 14.8 Hz, N(C*H*$_2$CH$_3$)$_3$), 3.05 (1H, br.s., carborane *H*), 2.04 (2H, t, *J* = 7.6 Hz, CC*H*$_2$CH$_2$CH$_2$S), 1.86 (2H, m, CCH$_2$C*H*$_2$CH$_2$S); 1.21 (9H, t, *J* = 7.9 Hz, N(CH$_2$C*H*$_3$)$_3$); ^{11}B NMR δ_B (128 MHz; CD_2Cl_2; $Et_2O{\cdot}BF_3$), -2.35 (1B, d, *J* = 140 Hz, B8), -5.75 (1B, d, *J* = 131 Hz, B11), -8.05 (1B, d, *J* = 128 Hz, B10), -19.23 (1B, d, *J* = 140 Hz, B6), -22.87 (3B, d, overlap, B2, 4, 5), -35.40 (1B, d, *J* = 147 Hz, B3), -36.57 (1B, d, *J* = 140 Hz, B1); ^{13}C NMR δ_C (100 MHz, CD_3CN) 60.24 (1C, carborane *C*), 55.62 (1C, CCH$_2$CH$_2$*C*H$_2$S), 50.44 (3C, N(*C*H$_2$CH$_3$)$_3$), 47.40 (1C, carborane *C*H), 38.45 (1C, C*C*H$_2$CH$_2$CH$_2$S), 26.15 (1C, CCH$_2$*C*H$_2$CH$_2$S) 21.73 (3C, N(CH$_2$*C*H$_3$)$_3$); *m/z* (ESI$^-$) 257.25 (9%), 255.25 (100%), calc. 257.20 and 255.20.

7,9-Bis[(sulfonamido)propyl]-7,9-dicarba-*nido*-undecaborate, triethylammonium salt, [7,9-($NH_2SO_2(CH_2)_3$)$_2$-7,8-$C_2B_9H_{10}$]Et_3NH (**72**)

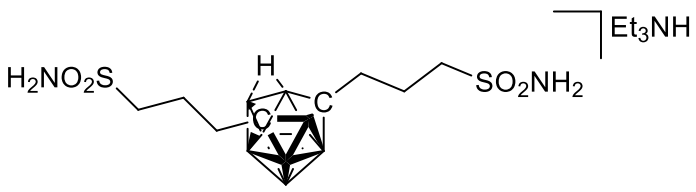

72

The same method as in **71m**. White solid, yield 68% (840 mg). m.p.: 36°C; R_f = 0.25 (CH_2Cl_2:benzene 1:2); Analysis found: C, 32.5; H, 8.7 calc. for $B_9C_{12}H_{38}O_4S_2N_3$: C, 32.0; H, 8.5%; ^{1}H NMR δ_H (400 MHz; acetone-d_6), 6.07 (4H, br.s., N*H*$_2$), 5.94 (1H, s, bridging *H*), 3.18 (6H, q, J_{12} = 7.2, J_{13} = 14.9 Hz, N(C*H*$_2$CH$_3$)$_3$), 3.08 (4H, t, *J* = 6.8 Hz, CCH$_2$CH$_2$C*H*$_2$S), 2.19 (4H, t, *J* = 7.6 Hz, CC*H*$_2$CH$_2$CH$_2$S), 1.78 (4H, m, CCH$_2$C*H*$_2$CH$_2$S) 1.21 (9H, t, *J* = 7.8 Hz, N(CH$_2$C*H*$_3$)$_3$); ^{11}B NMR δ_B (128 MHz; CD_2Cl_2; $Et_2O{\cdot}BF_3$), -8.08 (1B, d, *J* = 149 Hz, B8), -12.14 (6B, d, *J* = 152 Hz, B1, 2, 3, 4, 5, 6), -14.55 (2B, d, *J* = 178 Hz, B10, 11); ^{13}C NMR δ_C (100 MHz, CD_3CN) 60.14 (2C, carborane *C*), 55.58 (2C, CCH$_2$CH$_2$*C*H$_2$S), 50.38 (3C, N(*C*H$_2$CH$_3$)$_3$), 38.42 (2C, C*C*H$_2$CH$_2$CH$_2$S), 27.23 (2C, CCH$_2$*C*H$_2$CH$_2$S), 19.83 (3C, N(CH$_2$*C*H$_3$)$_3$); *m/z* (ESI$^-$) 378.25 (8%), 376.25 (100%), calc. 378.22 and 376.22.

General synthesis of naphthalimide derivatives 75 - 83:

Preparation of dioxanate zwitterions 78 and 79 (Q).

Caesium salt of the metal bis(dicarbollide) (cobalt, **3** or chromium, **77**) (2.19 mmol) was dissolved in 1,4-dioxane (10 ml) and DMS (4.38 mmol) with H_2SO_4 (2.19 mmol) were added. The reaction mixture was then stirred at 80°C for 6h. The precipitate was then removed by filtration and washed with H_2O and benzene. The organic layer was then extracted with H_2O (3x20), dried over $MgSO_4$, filtered and evaporated to dryness.

Ring-opening reaction using gaseous ammonia (R).

Dry zwitterionic compounds **78** or **79** (0.22 mmol) was dissolved in dry THF (5 ml) and NH_3 (g) was bubbled through the solution for 5 minutes. The solvent was then removed under vacuum to give pure products **80** and **81**.

Formation of naphthalimide (S).

A suspension of 3-nitro-1,8-naphthalic anhydride (**74**) (0.29 mmol) in absolute EtOH (3 ml) was treated with Et_3N (0.58 mmol) and solution of the appropriate amine (0.29 mmol) in absolute EtOH (3 ml) was added dropwise. The reaction mixture was stirred for 6h in 60°C under an inert (Ar) atmosphere. Subsequently, the solvents were evaporated to dryness under vacuum and purified by silica gel column chromatography using a gradient elution from 0 to

10% hexane in CH_2Cl_2 (to remove unreacted starting material), and a second column using a gradient elution from 0 to 10% CH_3CN in CH_2Cl_2 to separate the product.

1-(3-Nitro-1,8-naphthalimide)ethyl-3,3'-cobalt(III) bis(1,2-dicarbarbollide), sodium salt, [(1-(3-NO_2-$C_{12}H_5O_2N$)-$(CH_2)_2$-1,2-$C_2B_9H_{10}$)(1′,2′-$C_2B_9H_{11}$)-3,3′-Co]Na **(75b)**

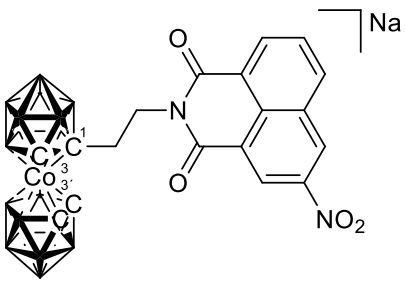

75b

We followed procedure S. Starting from **43b**. Orange solid, yield 57% (74.5 mg). R_f = 0.50 (CH_2Cl_2:CH_3CN 4:1); ^{1}H NMR δ_H (400 MHz, acetone-d_6), 9.38 (1H, d, *J* = 2.0 Hz, Ar*H*2), 9.12 (1H, d, *J* = 2.4 Hz, Ar*H*4), 8.77 (2H, t, *J* = 8.4 Hz, Ar*H*7,Ar *H*6), 8.11 (1H, t, *J* = 8.4, Ar*H*5), 4.41 (2H, m, CCH_2CH_2N), 4.30 (2H, m, CCH_2CH_2N), 4.14 (1H, br s, carborane C*H*), 3.82 (1H, br s, carborane C*H*), 3.70 (1H, br s, carborane CH); ^{11}B NMR δ_B (128 MHz; acetone-d_6; $Et_2O{\cdot}BF_3$), 6.79 (2B, d, *J* = 131 Hz, B8, 8′), 0.86 (2B, d, *J* = 140 Hz, B10, 10′), -6.04 (8B, d, *J* = 119 Hz, B4, 4′, 7, 7′, 9, 9′, 12, 12′), -16.25 (1B, d, *J* = 143 Hz, B5), -17.72 (3B, d, *J* = 162 Hz, B5′, 11, 11′), -19.69 (1B, d, overlap, B6), -22.92 (1B, d, *J* = 186 Hz, B6′); ^{13}C NMR δ_C (100 MHz, acetone-d_6), 136.82 (1C, Ar*C*3), 134.71 (1C, Ar*C*4), 132.16 (1C, Ar*C*7), 130.92 (1C, Ar*C*5), 130.11 (1C, Ar*C*6), 130.02 (1C, Ar*C*2), 126.14 (1C, Ar*C*joined), 125.67 (1C, Ar*C*1), 124.21 (1C, Ar*C*joined), 123.90 (1C, Ar*C*8), 66.38 (1C, CCH_2CH_2N), 57.37 (1C, carborane *C*), 54.20 (1C, carborane *C*H), 51.93 (1C, carborane *C*H), 48.08 (1C, CCH_2CH_2N), 41.83 (1C, carborane *C*H); FT-IR: ν_{max} (cm^{-1}) = 3650-3500 (CH arom), 2921, 2851 (CH alkyl), 2530 (BH), 1703, 1660 (C=O), 1598, 1331 (NO_2), 1540, 1508, 1455, 1402 (C=C); *m/z*: (ESI^-) 592.50 (100%), 593.50 (80%), calcd for $C_{18}H_{30}B_{18}CoN_2O_4$: 593.33.

1-(3-Nitro-1,8-naphthalimide)propyl-3,3'-cobalt(III) bis(1,2-dicarbarbollide), sodium salt, [(1-(3-NO_2-$C_{12}H_5O_2N$)-$(CH_2)_3$-1,2-$C_2B_9H_{10}$)(1′,2′-$C_2B_9H_{11}$)-3,3′-Co]Na **(75c)**

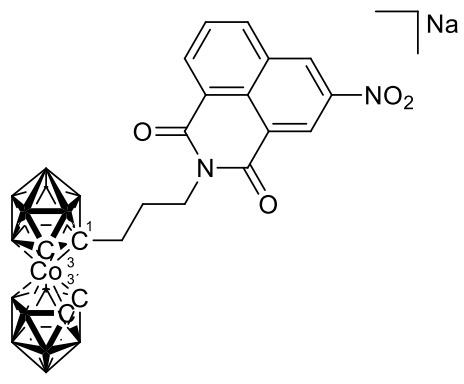

75c

We followed procedure S. Starting from **43c**. Orange solid, yield 37% (36.3 mg). R_f = 0.43 (CH_2Cl_2:CH_3CN 4:1); ^{1}H NMR δ_H (400 MHz, acetone-d_6), 9.33 (1H, d, *J* = 4.0 Hz, Ar*H*2), 9.06 (1H, d, *J* = 2.4 Hz, Ar*H*4), 8.72 (1H, s, Ar*H*7), 8.71 (1H, t, *J* = 3.6 Hz, Ar*H*), 8.08 (1H, t, *J* = 7.6 Hz, Ar*H*5), 4.15 (2H, t, *J* = 6.8 Hz, $CCH_2CH_2CH_2N$), 4.04 (1H, br s, carborane C*H*), 3.68 (1H, br s, carborane C*H*), 3.58 (1H, br s, carborane C*H*),

3.54 (2H, q, $J_{1,2}$ = 7.6, $J_{1,3}$ = 14.8 Hz, CC*H*$_2$CH$_2$CH$_2$N), 2.89 (1H, m, CCH$_2$C*H*$_2$CH$_2$N), 2.53 (1H, m, CCH$_2$C*H*$_2$CH$_2$N); ^{11}B NMR δ_B (128 MHz; acetone-d$_6$; Et$_2$O·BF$_3$), 6.61 (2B, d, *J* = 125 Hz, B8, 8′), 0.83 (2B, d, *J* = 143 Hz, B10, 10′), -5.98 (8B, d, *J* = 137 Hz, B4, 4′, 7, 7′, 9, 9′, 12, 12′), -15.16 (1B, d, overlap, B5), -16.44 (1B, d, overlap, B5′), -17.80 (2B, d, J = 171 Hz, B11, 11′), -19.47 (1B, d, overlap, B6), -23.05 (1B, d, *J* = 143 Hz, B6′); ^{13}C NMR δ_C (100 MHz, acetone-d$_6$), 163.90 (1C, C=O), 163.40 (1C, C=O), 147.09 (1C, Ar*C*3), 136.80 (1C, Ar*C*4), 134.83 (1C, Ar*C*7), 132.07 (1C, Ar*C*5), 130.91 (1C, Ar*C*6), 130.08 (1C, Ar*C*2), 129.97 (1C, Ar*C*joined), 125.56 (1C, Ar*C*1), 124.06 (1C, Ar*C*joined), 123.84 (1C, Ar*C*8), 69.48 (1C, CCH$_2$CH$_2$*C*H$_2$N), 57.94 (1C, carborane *C*), 53.92 (1C, carborane *C*H), 51.81 (1C, carborane *C*H), 48.16 (1C, C*C*H$_2$CH$_2$CH$_2$N), 40.85 (1C, CCH$_2$*C*H$_2$CH$_2$N), 38.35 (1C, carborane *C*H); FT-IR: ν_{max} (cm^{-1}) = 3631-3590 (CH arom), 2920, 2850 (CH alkyl), 2533 (BH), 1701, 1699 (C=O), 1599, 1330 (NO$_2$), 1539, 1507, 1436, 1422 (C=C); *m/z* (ESI$^-$) 605.58 (90%), 606.50 (100%), calcd for C$_{19}$H$_{32}$B$_{18}$CoN$_2$O$_4$: 605.35.

1-(3-Nitro-1,8-naphthalimide)ethyl-1′-aminoethyl-3,3'-cobalt(III) bis(1,2-dicarbarbollide), sodium salt, [(1-(3-NO$_2$-C$_{12}$H$_5$O$_2$N)-(CH$_2$)$_2$-1,2-C$_2$B$_9$H$_{10}$)(1'-NH$_2$-(CH$_2$)$_2$-1',2'-C$_2$B$_9$H$_{10}$)-3,3'-Co]Na **(76-)**

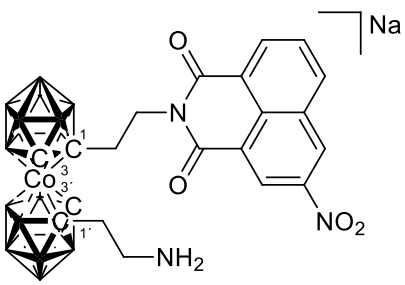

76-

We followed procedure S. 0.37 mmol of **74** and 0.74 mmol of Et$_3$N were used. Red solid, yield 15% (10.3 mg). R_f = 0.41 (CH$_2$Cl$_2$:CH$_3$CN 7:1); ^{1}H NMR δ_H (400 MHz, acetone-d$_6$), 9.37 (1H, s, Ar*H*2), 9.10 (1H, d, *J* = 5.2 Hz, Ar*H*4), 8.74 (2H, t, *J* = 11.2 Hz, Ar*H*7, Ar*H*6), 8.10 (1H, t, *J* = 7.6, Ar*H*5), 5.63 (2H, s, NH$_2$), 4.40 (2H, t, *J* = 7.6 Hz, CCH$_2$C*H*$_2$N), 4.02 (1H, br s, carborane C*H*), 3.85 (1H, br s, carborane C*H*), 3.74 (2H, t, *J* = 10.8 Hz, CCH$_2$C*H*$_2$NH$_2$), 3.54 (2H, m, CC*H*$_2$CH$_2$N), 2.90 (2H, m, CC*H*$_2$CH$_2$NH$_2$); ^{11}B NMR δ_B (128 MHz; acetone-d$_6$; Et$_2$O·BF$_3$), 8.69 (2B, d, *J* = 141 Hz, B8, 8′), 0.01 (2B, d, *J* = 140 Hz, B10, 10′), -3.9d (6B, d, overlap, B4, 4′, 9, 9′, 12, 12′), -8.50 (2B, d, *J* = 140 Hz, B7, 7′), -14.19 (2B, d, *J* = 125 Hz, B5, 5′), -15.89 (2B, d, *J* = 156Hz B11, 11′), -20.24 (2B, d, *J* = 94 Hz, B6, 6′); ^{13}C NMR δ_C (100 MHz, acetone-d$_6$), 163.47 (1C, C=O), 163.07 (1C, C=O), 147.21 (1C, Ar*C*3), (1C, Ar*C*4), 136.79 (1C, Ar*C*7), 134.73 (1C, Ar*C*5), 130.91 (1C, Ar*C*2), 130.06 (2C, Ar*C*6, Ar*Cjoined*), 125.60 (1C, Ar*C*1), 124.19 (1C, Ar*C*joined), 123.90 (1C, Ar*C*8), 62.63 (1C, CCH$_2$*C*H$_2$N), 59.99 (1C, carborane *C*), 58.90 (1C, carborane *C*), 58.82 (1C, carborane *C*H), 57.56 (1C, carborane *C*H), 48.05 (1C, CCH$_2$*C*H$_2$NH$_2$), 43.22 (1C, C*C*H$_2$CH$_2$NH$_2$), 37.59 (1C, CCH$_2$*C*H$_2$N); FT-IR: ν_{max} (cm^{-1}) = 3647-3545 (CH arom), 2922,

2852 (CH alkyl), 2544 (BH), 1704, 1659 (C=O), 1599, 1332 (NO_2), 1539, 1508, 1456, 1423 (C=C); *m/z* (ESI^-) 636.50 (100%), calcd for $C_{20}H_{37}B_{18}CoN_3O_4$: 636.39.

1,1′-Di[(3-nitro-1,8-naphthalimide)ethyl]-3,3'-cobalt(III) bis(1,2-dicarbarbollide), sodium salt, [(1,1'-(3-NO_2-$C_{12}H_5O_2N$)-$(CH_2)_2$-1,2-$C_2B_9H_{10})_2$-3,3'-Co]Na **(76)**

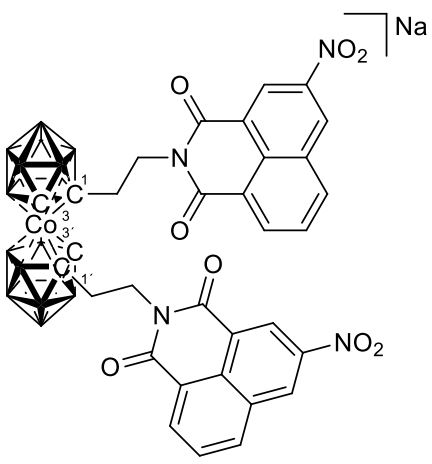

76

We followed procedure S. 0.37 mmol of **74** and 0.74 mmol of Et_3N were used. Red solid, yield 79% (129.8 mg). R_f = 0.43 (CH_2Cl_2:CH_3CN 7:1); ^1H NMR δ_H (400 MHz, acetone-d_6), 9.34 (2H, s, Ar*H*2), 9.05 (2H, s, Ar*H*4), 8.72 (2H, t, *J* = 8.0 Hz, Ar*H*7), 8.68 (2H, t, *J* = 7.8 Hz, Ar*H*6), 8.05 (2H, t, *J* = 7.9, Ar*H*5), 4.36 (4H, m, CCH_2CH_2N), 3.89 (2H, br s, carborane C*H*), 3.51 (4H, m, CCH_2CH_2N); ^{11}B NMR δ_B (128 MHz; acetone-d_6; $Et_2O{\cdot}BF_3$), 8.94 (2B, d, *J* = 177 Hz, B8, 8′), 0.15 (2B, d, *J* = 140 Hz, B10, 10′), -4.13 (6B, d, *J* = 150 Hz, B4, 4′, 9, 9′, 12, 12′), -8.32 (2B, d, *J* = 165 Hz, B7, 7′), -15.14 (4B, d, overlap, B5, 5′,11 11′), -20.51 (2B, d, *J* = 90 Hz, B6, 6′); ^{13}C NMR δ_C (100 MHz, acetone-d_6), 163.45 (2C, C=O), 163.05 (2C, C=O), 147.17 (2C, Ar*C*3), 136.78 (2C, Ar*C*4), 134.68 (2C, Ar*C*7), 132.13 (2C, Ar*C*5), 130.87 (2C, Ar*C*2), 130.03 (4C, Ar*C*joined, Ar*C*6), 125.16 (2C, Ar*C*1), 124.11 (2C, Ar*C*joined), 123.87 (2C, Ar*C*8), 67.80 (2C, CCH_2CH_2N), 59.79 (2C, carborane *C*), 58.81 (2C, carborane *C*H), 37.82 (2C, CCH_2CH_2N); FT-IR: ν_{max} (cm^{-1}) = 3642-3538 (CH arom), 2921, 2850 (CH alkyl), 2549 (BH), 1704, 1660 (C=O), 1600, 1333 (NO_2), 1541, 1508, 1456, 1423 (C=C); *m/z*: (ESI^-) 860.58 (100%), calcd for $C_{32}H_{41}B_{18}CoN_4O_8$: 862.41.

8-Dioxane-3,3'-cobalt(III) bis(1,2-dicarbarbollide), (8-$(CH_2CH_2O)_2$-1,2-$C_2B_9H_{10}$)-1',2'-$C_2B_9H_{10}$)-3,3'-Co **(78)**

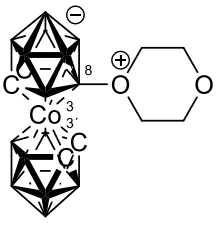

78

We followed procedure Q. Yield 30%. Data correspond to the literature.[190]

8-Dioxane-3,3'-chromium(III) bis(1,2-dicarbarbollide), (8-($CH_2CH_2O)_2$-1,2-$C_2B_9H_{10}$)-1',2'-$C_2B_9H_{10}$)-3,3'-Cr **(79)**

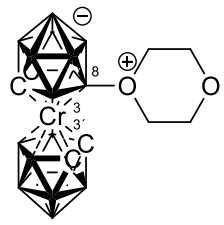

79

We followed procedure Q. Yield 28%. Data correspond to the literature.[17]

8-(Amino)-1,4-diethyleglycolyl-3,3'-cobalt(III) bis(1,2-dicarbarbollide), [(8-(NH_3)-($CH_2CH_2O)_2$-1,2-$C_2B_9H_{10}$)-1',2'-$C_2B_9H_{10}$)-3,3'-Co] **(80)**

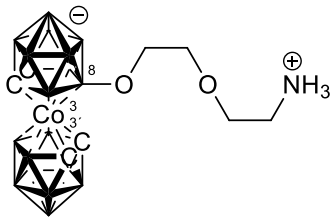

80

We followed procedure R. Yield 94%. Data correspond to the literature.[29]

8-(Amino)-1,4-diethyleglycolyl-3,3'-chromium(III) bis(1,2-dicarbarbollide), [(8-(NH_3)-($CH_2CH_2O)_2$-1,2-$C_2B_9H_{10}$)-1',2'-$C_2B_9H_{10}$)-3,3'-Cr] **(81)**

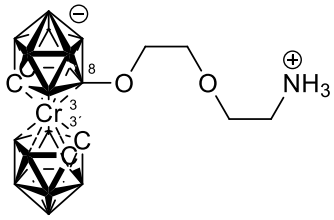

81

We followed procedure R. Brown solid, yield 91% (131 mg). R_f= 0.31 (benzene); Cr^{3+} is a paramagnetic nucleus therefore the NMR spectra are unreliable and are not stated; *m/z*: (ESI^-) 422.2 (81%), 421.2 (100%), calcd for $C_{20}H_{34}B_{21}CrNO_6$: 422.4.

8-(3-Nitro-1,8-naphthalimide)-1,4-diethyleglycolyl-3,3'-cobalt(III) bis(1,2-dicarbarbollide), sodium salt, [(8-(3-NO_2-$C_{12}H_5O_2N$)-$(CH_2CH_2O)_2$-1,2-$C_2B_9H_{10}$)-1',2'-$C_2B_9H_{10}$)-3,3'-Co]Na **(82)**

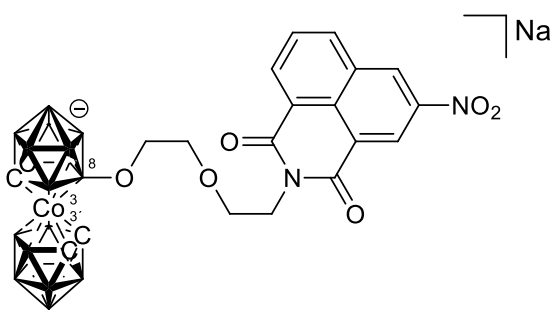

82

We followed procedure S. Yellow solid, yield 58% (7.5 mg). R_f = 0.50 (CH_2Cl_2:CH_3CN 4:1); ^{1}H NMR δ_H (400 MHz, acetone-d_6), 9.28 (1H, d, *J* = 1.8 Hz, Ar*H*2), 9.03 (1H, d, *J* = 2.4 Hz, Ar*H*4), 8.67 (1H, d, *J* = 1.8 Hz, Ar*H*7), 8.66 (1H, s, Ar*H*6), 8.02 (1H, t, *J* = 8.4 Hz, Ar*H*5), 4.36 (2H, t, *J* = 6.6 Hz, OCH_2CH_2N), 4.14 (2H, br s, carborane C*H*), 4.12 (2H, br s, carborane C*H*), 4.36 (2H, t, $J_{1,2}$ = 6.6, $J_{1,3}$ = 12.6 Hz, $BOCH_2CH_2O$), 3.57 (4H, m, $BOCH_2CH_2OCH_2CH_2N$); ^{11}B NMR δ_B (128 MHz; acetone-d_6; $Et_2O{\cdot}BF_3$), 22.17 (1B, s, B8), 3.28 (1B, d, *J* = 128 Hz, B8′), -0.63 (1B, d, *J* = 136 Hz, B10′), -3.43 (1B, d, *J* = 138 Hz, B10), -5.44 (2B, d, *J* = 134 Hz B9, 9′), -8.31 (2B, d, *J* = 141 Hz B12, 12′), -9.04 (4B, d, *J* = 127 Hz B4, 4′, 7, 7′), -18.30 (2B, d, *J* = 155 Hz, B5, 5′), -21.47 (2B, d, *J* = 150 Hz, B11, 11′), -23.06 (1B, d, overlap, B-6), -29.52 (1B, d, *J* = 143 Hz, B6′); ^{13}C NMR δ_C (100 MHz, acetone-d_6), 163.11 (1C, C=O), 162.69 (1C, C=O), 146.36 (1C, Ar*C*3), 136.13 (1C, Ar*C*4), 134.15 (1C, Ar*C*7), 131.33 (1C, Ar*C*5), 130.21 (1C, Ar*C*6), 129.38 (1C, Ar*C*2), 129.24 (1C, Ar*C*joined), 124.59 (1C, Ar*C*1), 123.34 (1C, Ar*C*joined), 123.10 (1C, Ar*C*8), 71.77 (1C, $BOCH_2CH_2O$), 68.51 (1C, OCH_2CH_2N), 67.82 (1C, $BOCH_2CH_2O$), 54.03 (1C, carborane *C*H), 46.52 (1C, carborane *C*H), 39.63 (1C, OCH_2CH_2N); FT-IR: ν_{max} (cm^{-1}) = 3648-3545 (CH aromatic), 3077, 3044, 2923, 2879 (CH alkyl), 2535 (BH), 1705, 1660 (C=O), 1599, 1331 (NO_2), 1540, 1508, 1435, 1422 (C=C); *m/z* (ESI^-) 651.50 (80%), 652.50 (100%), calcd for $C_{20}H_{34}B_{18}CoN_2O_6$: 651.36.

8-(3-Nitro-1,8-naphthalimide)-1,4-diethyleglycolyl-3,3'-chromium(III) bis(1,2-dicarbarbollide), sodium salt, [(8-(3-NO_2-$C_{12}H_5O_2N$)-$(CH_2CH_2O)_2$-1,2-$C_2B_9H_{10}$)-1',2'-$C_2B_9H_{10}$)-3,3'-Cr]Na **(83)**

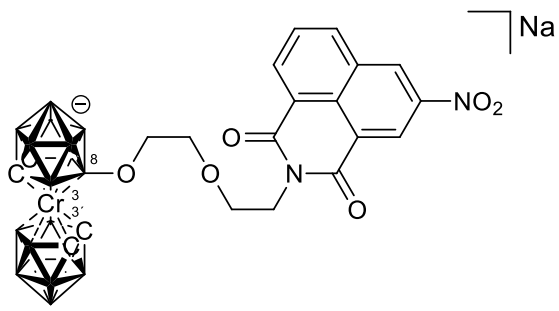

83

We followed procedure S. Brown solid, yield 20% (16.1 mg). R_f=0.45 (CH_2Cl_2:CH_3CN 4:1); Cr^{3+} is a paramagnetic nucleus therefore the NMR spectra is unreliable and is not stated; FT-IR: ν_{max} (cm^{-1}) = 3648-3522 (CH aromatic), 2956, 2922, 2861, 22852 (CH alkyl), 2532 (BH), 1705, 1661 (C=O), 1600, 1333 (NO_2), 1541, 1508, 1456, 1423 (C=C); *m/z*: (ESI^-) 644.67 (90%), 645.67 (100%), calcd for $C_{20}H_{34}B_{18}CrN_2O_6$: 644.36.

Preparation of compounds 4 and 85 - 87.

5,6-dicarba-*nido*-decaborane, *nido*-5,6-$C_2B_8H_{12}$ **(85)**

85

A mixture of $FeCl_3 \cdot 6H_2O$ (120 g) in H_2O (150 ml) and HCl (50 ml) was added dropwise at 0°C to a mixture of anion 7,8-$C_2B_9H_{12}^-$ (**2**) (1M in H_2O) in H_2O (150 ml), HCl (30 ml) and hexane (100 ml). After all material was mixed, the reaction was stirred for additional 4 hours at room temperature and during that period was added three spoons of $FeCl_3 \cdot 6H_2O$. Reaction mixture was then separated and H_2O layer was extracted three times with hexane. Organic layers were combined and washed with 20% Na_2CO_3. The mixture was then dried over $MgSO_4$, filtered and solvent was partially blown away by Ar. The rest was carefully evaporated at 20°C and sublimated at 100°C. It was obtained 6.8 g (37%) of white solid. Data correspond to the literature.[193]

6,9-Dicarba-*arachno*-decaborane, *arachno*-6,9-$C_2B_8H_{14}$ **(4)**

4

A solution of **85** (7.50 g, 0.061 mol) in hexane (75 ml) was added dropwise to a mixture of NaOH (2.44 g, 0.061 mol) and $NaBH_4$ (2.32 g, 0.061 mol) dissolved in EtOH (75 ml) and the reaction mixture was stirred for 2 days at reflux. Reaction mixture was then filtered, washed with hexane and evaporated. The crude product was then extracted with H_2O and the benzene and H_2O layer was acidified and extracted with benzene again. Combined organic layers were evaporated to dryness to give product 4 in 32% yield (2.4 g). Data correspond to the literature.[195]

8-Phenyl-7,8,9-tricaba-*nido*-undecaborane, 8-Ph-*nido*-7,8,9-$C_3B_8H_{11}$ **(86)**

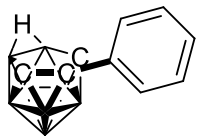
86

A solution containing **4** (250 mg, 2 mmol), PS (900 mg, 4.2 mmol) in 1,2-dichloroethane (30 ml) was cooled to 0°C and PhCOCl (5 mmol) was then added in small portions under stirring during 0.5h. The cooling bath was then removed and the stirring continued for 24h at reflux. The mixture was then treated with conc. H_2SO_4 (2 ml, dropwise) under intensive cooling and shaking at ~ 0°C. The organic layer was carefully separated from the semi-liquid materials sticking on the walls of the reaction flask. The solution thus obtained was then evaporated after adding silica gel (~ 5g). The residual material was mounted onto the top of a column packed with silica gel (2.5x20 cm) which was then eluted with 100% hexane. Combined fractions of R_f = 0.25 were evaporated to dryness to isolate typically 64% of the 8-Ph-7,8,9-$C_3B_8H_{11}$ (**86**) derivative.

8-Phenyl-10,11-dimethyl-7,8,9-tricaba-*nido*-undecaborane, 8-Ph-7,8,9-$C_3B_8H_{11}$-10,11-Me_2 **(87)**

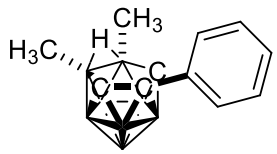
87

Compound **86** (100 mg, 0.5 mmol) was treated with an excess of NaH (72 mg, 3 mmol) and MeI (5 ml) in THF (15 ml) under stirring at reflux temperature for 12h. The mixture was then filtered, the filtrate acidified with several drops of conc. H_2SO_4 and then worked-up by chromatography on silica gel using hexane to isolate the neutral 8-Ph-*nido*-7,8,9-$C_3B_8H_9$-10,11-Me_2 (**87**) (colourless crystals, yield 62%). The compound can be purified by sublimation at 100-150°C (bath).: R_f = 0.41; for $C_{11}H_{20}B_8$ (m.w. 238.76) calcd.55.33% C, 8.44% H, found 55.25% C, 8.35% H. ^{1}H NMR δ_H (400 MHz, acetone-d_6), 7.32 (4H, Ar*H*), 7.25 (1H, Ar*H*), 2.93(2H, br.s., carborane C*H*7, 9), 0.36 (6H, s, B-CH_3), -1.39 (1H, $\mu H_{10,11}$); For ^{11}B NMR spectra see Figure 31; ^{13}C NMR δ_C (100 MHz, acetone-d_6), 129.3 (4C, Ar*C*), 127.7 (2C, Ar*C*), 79.0 (1C, carborane *C*8), 48.1 (2C, carborane *C*H7,9), 1.1 (2C, B-*C*H_3); *m/z*: (ESI$^-$) calcd. 239.23 (100%) and 240.23 (56%), found 239.52 and 240.52.

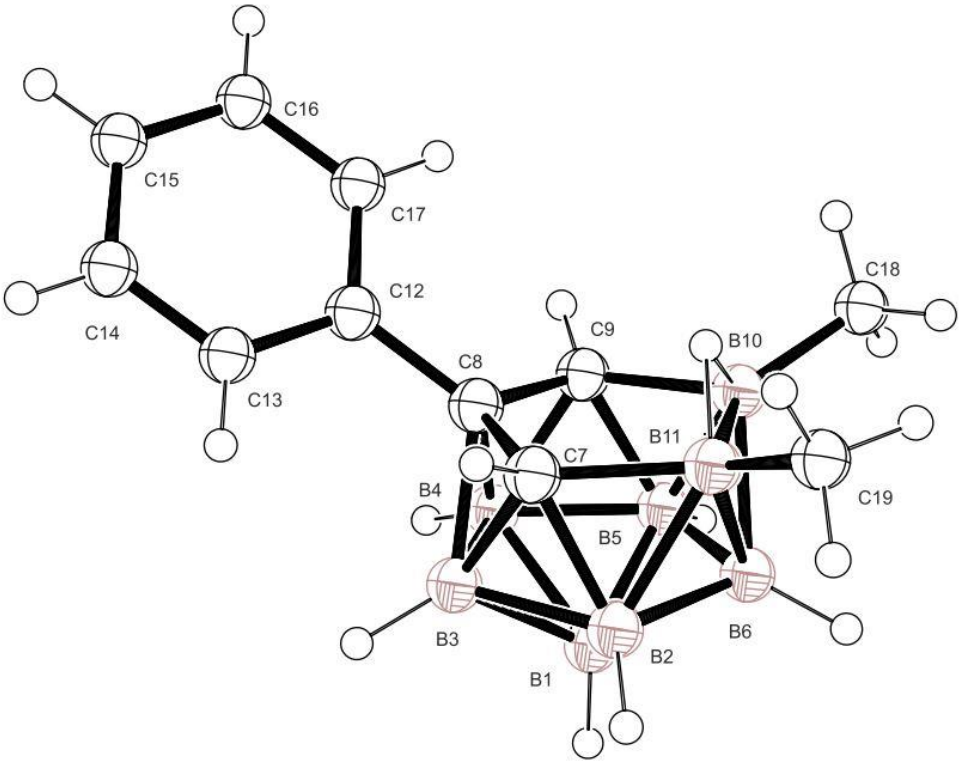

X-ray crystallographic data for **87**: $C_{11}H_{20}B_8$, M = 238.75, monoclinic, $P2_{1/c}$, a = 8.5480(12) Å, b = 15.017(5) Å, c = 12.3510(18) Å, β = 117.453(17)°, Z = 4, V = 1406.9(5) Å^3, D_c = 1.127 g.cm^{-3}, μ= 0.055 mm^{-1}, T_{min}/T_{max} = 0.984/0.994; -11 ≤ h ≤ 11, -19 ≤ k ≤ 19, -15 ≤ l ≤ 16; 22147 reflections measured (θ_{max} = 27.497°), 21961 independent (R_{int} = 0.0523), 2513 with I > $2\sigma(I)$, 180 parameters, S = 1.099, *R1*(obs. data) = 0.0482, *wR2*(all data) = 0.1178; max., min. residual electron density = 0.273, -0.261 eÅ^{-3}. Crystallographic data for structural analyses are deposited with the Cambridge Crystallographic Data Centre, CCDC deposition no. 1471256.

General preparation of compounds 91 - 94.

Alkylation (T).

1o(m,p) (2.13 g, 14.77 mmol) was dried under vacuum at room temperature for 3h and then dissolved in a dry hexane (20 ml). After cooling to 0°C the ^{n}BuLi (2.5 M in hexane, 22.16 mmol) was added. Reaction mixture was stirred for an additional 30 minutes at room temperature and then was the flask re-cooled to 0°C. Ethylene oxide (2.5-3.3 M in THF, 22.16 mmol) was then added dropwise. After few minutes, a white precipitate appeared. After 5 hours, MeOH (ca. 2 ml) and AcOH (ca.0.5 ml) were added. This reaction mixture was separated and the aqueous layer was extracted with Et_2O (3x15 ml). The combined organic layers were dried over $MgSO_4$ and evaporated. Unreacted starting material, mono- and disubstituted product were separated on silica column chromatography (benzene:CH_2Cl_2 2:1).

Oxidation (U or V).

The carborane mono- or disubstituted derivative (96 mg, 0.51 mmol (U) or 167 mg, 0.72 mmol (V)) was dissolved in acetone (5 ml (U) or 8 ml (V)) and cooled to 0°C. Then the mixture of CrO_3 (3.5 mmol (U) or 9.8 mmol (V)) in the AcOH (3 ml (U) or 5 ml (V)) and H_2O (4 ml (U) or 7 ml (V)) was added dropwise and then stirred at room temperature overnight. The mixture was then extracted with Et_2O (3x15) and the combined organic layers were then acidified with 3M HCl and washed with brine. The etheric phase was then dried over $MgSO_4$ and evaporated to give the final product.

1-Hydroxyethyl-1,2-dicarba-*closo*-dodecaborane, 1-$HOCH_2CH_2$-1,2-$C_2B_{10}H_{11}$ (**91o**)

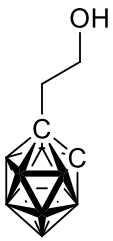

91o

We followed procedure T. Yield: 50% (1.40 g) of colourless glasslike solid. m.p.: 72°C; R_f = 0.27 (benzene:CH_2Cl_2 2:1); ^{1}H NMR δ_H (600 MHz; $CDCl_3$), 3.97 (1H, br.s., carborane C*H*), 3.80 (2H, q, J_{12} = 5.4, J_{13} = 11.4 Hz, CCH_2CH_2OH), 2.49 (2H, t, J = 5.4 Hz, CCH_2CH_2OH); ^{11}B NMR δ_B (192 MHz; $CDCl_3$; $Et_2O{\cdot}BF_3$), -3.11 (1B, d, J = 150 Hz, B9), -6.39 (1B, d, J = 147 Hz, B12), -10.48 (2B, d, J = 150 Hz, B8, 10), -11.94 (2B, d, J = 178 Hz, B4, 5), -12.98 (2B, d, J = 197 Hz, B7, 11), -14.09 (2B, d, J = 154 Hz, B3, 6); ^{13}C NMR δ_C (150 MHz; $CDCl_3$), 73.07 (1C, carborane *C*), 60.78 (1C, carborane *C*H), 60.47 (1C, CCH_2CH_2OH), 39.81 (1C, CCH_2CH_2OH); MS-ESI: *m/z* $[M-1]^-$ 187.2 and 190.2, calc. 187.2 (100%) and 190.2 (2%).

1-Hydroxyethyl-1,7-dicarba-*closo*-dodecaborane, 1-$HOCH_2CH_2$-1,7-$C_2B_{10}H_{11}$ (**91m**)

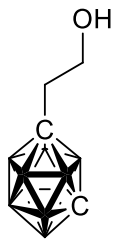

91m

We followed procedure T. Yield: 0.34 g (42%) of white solid. m.p.: 89°C; R_f = 0.21 (benzene:CH_2Cl_2 2:1); ^{1}H NMR δ_H (600 MHz; $CDCl_3$), 3.64 (2H, q, J_{12} = 6.0, J_{13} = 12.6 Hz, CCH_2CH_2OH), 2.93 (1H, br.s., carborane C*H*), 2.21 (2H, t, J = 6.6 Hz, CCH_2CH_2OH); ^{11}B NMR δ_B (192 MHz; $CDCl_3$; $Et_2O{\cdot}BF_3$), -5.12 (1B, d, J = 150 Hz, B4), -10.53 (1B, d, overlap, B12), -11.71 (4B, d, J = 151 Hz, B3, 5, 8, 11), -14.46 (2B, d, J = 166 Hz, B9, 10), -16.16 (2B, d, J = 178 Hz, B2, 6); ^{13}C NMR δ_C (150 MHz; $CDCl_3$), 73.07 (1C, carborane *C*), 61.64 (1C, CCH_2CH_2OH), 55.24 (1C, carborane *C*H), 39.08 (1C, CCH_2CH_2OH); MS-ESI: *m/z* $[M-1]^-$ 187.2 and 190.2, calc. 187.2 (100%) and 190.2 (2%).

1-Hydroxyethyl-1,12-dicarba-*closo*-dodecaborane, 1-$HOCH_2CH_2$-1,12-$C_2B_{10}H_{11}$ (**91p**)

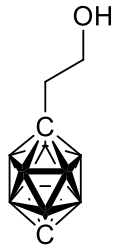

91p

We followed procedure T. Yield 45% (1.24 g) of white solid. m.p.: 90°C; R_f = 0.27 (benzene:CH_2Cl_2 2:1); ^{1}H NMR δ_H (600 MHz; $CDCl_3$), 3.50 (2H, q, J_{12} = 7.2, J_{13} = 13.2 Hz, CCH_2CH_2OH), 2.68 (1H, br.s., carborane C*H*), 2.37 (2H, t, J = 6.6 Hz, CCH_2CH_2OH); ^{11}B NMR δ_B (192 MHz; $CDCl_3$; $Et_2O{\cdot}BF_3$), -13.51 (5B, d, J = 163 Hz, B2, 3, 4, 5, 6), -15.90 (5B, d, J = 166 Hz, B7, 8, 9, 10, 11); ^{13}C NMR δ_C (150 MHz; $CDCl_3$), 81.46 (1C, carborane *C*), 61.41 (1C, CCH_2CH_2OH), 58.79 (1C, carborane *C*H), 41.00 (1C, CCH_2CH_2OH); MS-ESI: *m/z* $[M-1]^-$ 187.2 and 190.2, calc. 187.2 (100%) and 190.2 (2%).

1,2-Bis[(hydroxy)ethyl]-1,2-dicarba-*closo*-dodecaborane, 1,2-$(C_2H_4OH)_2$-1,2-$C_2B_{10}H_{10}$ (**92o**)

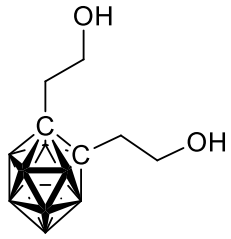

92o

We followed procedure T. Yield: 27% (0.91g) of white solid. m.p.: 98°C; R_f = 0.05 (benzene:CH_2Cl_2 2:1); ^{1}H NMR δ_H (600 MHz; $CDCl_3$), 3.84 (4H, t, J = 7.2 Hz, CCH_2CH_2OH), 2.52 (4H, t, J = 7.2 Hz, CCH_2CH_2OH); ^{11}B NMR δ_B (192 MHz; $CDCl_3$; $Et_2O{\cdot}BF_3$), -5.34 (1B, d, J = 147 Hz, B9), -6.39 (1B, d, J = 147 Hz, B12), -10.97 (4B, d, J = 150 Hz, B7, 8, 10, 11), -11.71 (4B, d, J = 104 Hz, B3, 4, 5, 6); ^{13}C NMR δ_C (150 MHz; $CDCl_3$), 77.07 (2C, carborane *C*), 61.26 (2C, CCH_2CH_2OH), 37.30 (2C, CCH_2CH_2OH); MS-ESI: *m/z* $[M-1]^{2-}$ 230.2 and 233.2, calc. 230.2 (100%) and 233.2 (3%).

1,7-Bis[(hydroxy)ethyl]-1,7-dicarba-*closo*-dodecaborane, 1,7-$(C_2H_4OH)_2$-1,7-$C_2B_{10}H_{10}$ (**92m**)

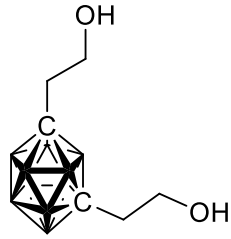

92m

We followed procedure T. Yield: 22% (0.21 g) of colourless crystals. m.p.: 236°C; R_f = 0.09 (benzene:CH_2Cl_2 2:1);); ^{1}H NMR δ_H (600 MHz; $CDCl_3$), 3.63 (4H, t, J = 7.2 Hz, CCH_2CH_2OH), 2.21 (4H, t, J = 7.2 Hz, CCH_2CH_2OH); ^{11}B NMR δ_B (192 MHz; $CDCl_3$; $Et_2O{\cdot}BF_3$), -7.99 (2B, d, J = 167 Hz, B9, 10), -12.07 (5B, d, J = 164 Hz, B3, 4, 5, 8, 11), -13.67 (1B, d, overlap, B12), -14.29 (2B, d, J = 172 Hz, B2, 6); ^{13}C NMR δ_C (150 MHz; $CDCl_3$), 72.97 (2C, carborane *C*), 61.60 (2C, CCH_2CH_2OH), 39.12 (2C, CCH_2CH_2OH); MS-ESI: *m/z* $[M-1]^{2-}$ 230.2 and 233.2, calc. 230.2 (100%) and 233.2 (3%).

1,12-Bis[(hydroxy)ethyl]-1,12-dicarba-*closo*-dodecaborane, 1,12-$(C_2H_4OH)_2$-1,12-$C_2B_{10}H_{10}$ (**92p**)

92p

We followed procedure T. Yield: 12% (0.42 g) of white solid. m.p.: 129°C; R_f = 0.04 (benzene:CH_2Cl_2 2:1); ^{1}H NMR δ_H (600 MHz; $CDCl_3$), 3.50 (2H, t, *J* = 6.0 Hz, CCH_2CH_2OH), 1.96 (2H, t, *J* = 6.6 Hz, CCH_2CH_2OH); ^{11}B NMR δ_B (192 MHz; $CDCl_3$; $Et_2O{\cdot}BF_3$), -13.59 (10B, d, *J* = 164 Hz, B2, 3, 4, 5, 6, 7, 8, 9, 10, 11); ^{13}C NMR δ_C (150 MHz; $CDCl_3$), 76.64 (2C, carborane *C*), 61.55 (1C, CCH_2CH_2OH), 40.00 (1C, CCH_2CH_2OH); MS-ESI: *m/z* $[M-1]^{2-}$ 230.2 and 233.2, calc. 230.2 (100%) and 233.2 (3%).

1,2-Dicarba-*closo*-dodecaboranylacetic acid, 1-CH_2COOH-1,2-$C_2B_{10}H_{11}$ (**93o**)

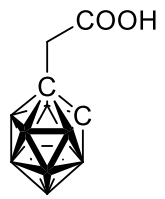

93o

We followed procedure U. Yield: 69% (70.8 mg) of white solid. m.p.: 186°C; R_f = 0.46 (CH_3CN:CH_2Cl_2 20:1); ^{1}H NMR δ_H (400 MHz; $CDCl_3$), 4.39 (1H, br.s., carborane C*H*), 3.31 (2H, s, CCH_2COOH); ^{11}B NMR δ_B (128 MHz; $CDCl_3$; $Et_2O{\cdot}BF_3$), -2.91 (1B, d, *J* = 155 Hz, B9), -5.75 (1B, d, *J* = 148 Hz, B12), -10.08 (2B, d, overlap, B8, 10), -11.42 (2B, d, *overlap*, B4, 5), -13.00 (2B, d, overlap, B7, 11), -13.71 (2B, d, *J* = 90 Hz, B3, 6); ^{13}C NMR δ_C (100 MHz; $CDCl_3$), 170.72 (1C, *C*OOH), 67.38 (1C, carborane *C*), 58.82 (1C, CCH_2COOH), 58.67 (1C, carborane *C*H), MS-ESI: *m/z* $[M-1]^-$ 201.2 and 204.2, calc. 201.2 (100%) and 204.2 (2%).

1,7-Dicarba-*closo*-dodecaboranylacetic acid, 1-CH_2COOH-1,7-$C_2B_{10}H_{11}$ (**93m**)

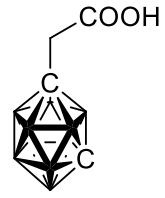

93m

We followed procedure U. Yield: 75% (71.1 mg) of white solid. m.p.: 134°C; R_f = 0.46 (CH_3CN:CH_2Cl_2 20:1); ^{1}H NMR δ_H (400 MHz; $CDCl_3$), 2.97 (1H, br.s., carborane C*H*), 2.93 (2H, s, CCH_2COOH); ^{11}B NMR δ_B (128 MHz; $CDCl_3$; $Et_2O{\cdot}BF_3$), -4.55 (1B, d, *J* = 164 Hz, B4), -10.22 (1B, d, overlap, B12), -11.43 (4B, d, overlap, B3, 5, 8, 11), -14.30 (2B, d, *J* = 173 Hz, B9, 10), -16.07 (2B, d, *J* = 185 Hz, B2, 6); ^{13}C NMR δ_C (100 MHz; $CDCl_3$), 172.82 (1C, *C*OOH), 77.44 (1C, carborane *C*), 45.01 (1C, C*C*H2COOH), 41.97 (1C, carborane *C*H); MS-ESI: *m/z* $[M-1]^-$ 201.2 and 204.2, calc. 201.2 (100%) and 204.2 (2%).

1,12-Dicarba-*closo*-dodecaboranylacetic acid,; 1-CH_2COOH-1,12-$C_2B_{10}H_{11}$ (**93p**)

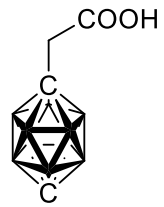

93p

We followed procedure U. Yield: 74% (39.0 mg) of white solid. m.p.: 155°C; R_f = 0.50 (CH_3CN:CH_2Cl_2 20:1); ^{1}H NMR δ_H (600 MHz; $CDCl_3$), 2.68 (1H, br.s., carborane C*H*), 2.58 (2H, d, *J* = 3.6 Hz, CC*H*$_2$COOH); ^{11}B NMR δ_B (192 MHz; $CDCl_3$; $Et_2O{\cdot}BF_3$), -13.37 (5B, d, *J* = 166 Hz, B2, 3, 4, 5, 6), -15.83 (5B, d, *J* = 164 Hz, B7, 8, 9, 10, 11); ^{13}C NMR δ_C (150 MHz; $CDCl_3$), 173.24 (1C, *C*OOH), 76.40 (1C, carborane *C*), 59.00 (1C, carborane *C*H), 43.74 (1C, CCH$_2$*C*H$_2$OH), 29.80 (1C, C*C*H$_2$CH$_2$OH); MS-ESI: *m/z* $[M\text{-}1]^-$ 201.2 and 204.2, calc. 201.2 (100%) and 204.2 (2%).

1,2-Dicarba-*closo*-dodecaboranyl-1,2-diacetic acid, 1,2-$(CH_2COOH)_2$-1,2-$C_2B_{10}H_{10}$ (**94o**)

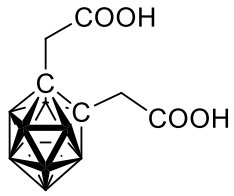

94o

We followed procedure V. Yield: 41% (77.2 mg) of white solid. m.p.: 191°C; R_f = 0.20 (CH_3CN:CH_2Cl_2 10:1); ^{1}H NMR δ_H (400 MHz; $CDCl_3$), 3.30 (4H, d, *J* = 4.0 Hz, CC*H*$_2$COOH); ^{11}B NMR δ_B (128 MHz; $CDCl_3$; $Et_2O{\cdot}BF_3$), -4.84 (2B, d, *J* = 153 Hz, B9, 12), -10.90 (8B, d, *J* = 152 Hz, B3, 4, 5, 6, 7, 8, 10, 11); ^{13}C NMR δ_C (100 MHz; $CDCl_3$), 168.98 (2C, *C*OOH), 73.37 (2C, carborane *C*), 44.97 (2C, C*C*H$_2$COOH); MS-ESI: *m/z* $[M\text{-}1]^{2-}$ 260.2 and 263.2, calc. 260.2 (100%) and 263.2 (3%).

1,7-Dicarba-*closo*-dodecaboranyl-1,7-diacetic acid, 1,7-$(CH_2COOH)_2$-1,7-$C_2B_{10}H_{10}$ (**94m**)

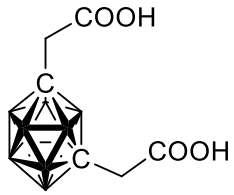

94m

We followed procedure V. Yield: 40% (243.1 mg) of brown solid. m.p.: 138°C; R_f = 0.20 (CH_3CN:CH_2Cl_2 10:1); ^{1}H NMR δ_H (400 MHz; $CDCl_3$), 2.84 (4H, s, CC*H*$_2$COOH); ^{11}B NMR δ_B (128 MHz; $CDCl_3$; $Et_2O{\cdot}BF_3$), -7.33 (2B, d, *J* = 147 Hz, B9, 10), -11.61 (5B, d, *J* = 157 Hz, B3, 4, 5, 8, 11), -13.41 (1B, d, overlap, B12), -14.17 (2B, d, *J* = 172 Hz, B2, 6); ^{13}C NMR δ_C (100 MHz; $CDCl_3$), 170.09 (2C, *C*OOH), 69.14 (2C, carborane *C*), 42.29 (2C, C*C*H$_2$COOH); MS-ESI: *m/z* $[M\text{-}1]^{2-}$ 260.2 and 263.2, calc. 260.2 (100%) and 263.2 (3%).

1,12-Dicarba-*closo*-dodecaboranyl-1,12-diacetic acid, 1,12-$(CH_2COOH)_2$-1,12-$C_2B_{10}H_{10}$ (**94p**)

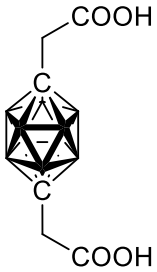

94p

We followed procedure V. Yield: 81% (112.6 mg) of white solid. m.p.: 249°C; R_f = 0.29 (CH_3CN:CH_2Cl_2 10:1); ^{1}H NMR δ_H (400 MHz; $CDCl_3$), 2.51 (4H, s, CC*H*$_2$COOH); ^{11}B NMR δ_B (128 MHz; $CDCl_3$; $Et_2O{\cdot}BF_3$), -13.39 (10B, d, *J* = 167 Hz, B2, 3, 4, 5, 6, 7, 8, 9, 10, 11); ^{13}C NMR δ_C (100 MHz; $CDCl_3$), 169.99 (2C, *C*OOH), 72.80 (2C, carborane *C*), 42.90 (2C, C*C*H$_2$COOH); MS-ESI: *m/z* $[M-1]^{2-}$ 260.2 and 263.2, calc. 260.2 (100%) and 263.2 (3%).

LIST OF ABBREVIATIONS

BNCT	boron neutron capture therapy
CA	carbonic anhydrase
CAIS	carbonic anhydrase inhibitors
CD	cyclodextrin
COSAN	cobalt sandwich anion
DME	dimethoxyethan
DMS	dimethyl sulfide
DOX	doxorubicin
EtOAc	ethyl acetate
HSA	human serum albumin
ITC	isothermal titration calorimetry
MO	molecular orbitals
Ms	mesyl
naph	naphthalimide
NMR	nuclear magnetic resonance
PFA	paraformaldehyde
PNT	proton non-transferring
PS	proton sponge
PT	proton transferring
SAC	skeletal alkylcarbonation
SAR	structure/activity relationship
SMD	solvent model density
THF	tetrahydrofuran
TFA	trifloroacetic acid
Tf	triflate
Ts	tosyl

LEXICON OF BIOLOGICAL TERMS

4T1-12B	cell line is expressing high levels of firefly luciferase to allow non-invasive longitudinal imaging of *in vivo* growth and metastasis of breast cancer.
ADME	is an abbreviation in pharmacokinetics and pharmacology for "absorption, distribution, metabolism, and excretion", and describes the disposition of a pharmaceutical compound within an organism. The four criteria all influence the drug levels and kinetics of drug exposure to the tissues and hence influence the performance and pharmacological activity of the compound as a drug.
BBB	blood brain barrier
BJ	BJ human fibroblast cells were established from normal human foreskin. BJ cells were one of the first cell types to be reprogrammed into induced pluripotent stem (iPS) cells, and are commonly used in human cell reprogramming studies.
BALB/c	is an albino, laboratory-bred strain of the house mouse from which a number of common substrains are derived and are among the most widely used inbred strains used in animal experimentation.
Caco-2	cell line is a continuous cell of heterogeneous human epithelial colorectal adenocarcinoma cells.
HCT116	cells are used in a variety of biomedical studies involving colon cancer proliferation and corresponding inhibitors. The cell line has been used in tumourigenicity studies.
HeLa	is a cell type in an immortal cell line. It is the oldest and most commonly used human cell line. The line was derived from cervical cancer cells taken on February 8, 1951 from Henrietta Lacks. The cell line was found to be remarkably durable and prolific which warrants its extensive use in scientific research.
HT-29	is a human colon cancer cell line used extensively in biological and cancer research. In preclinical research, HT-29 cells have been studied for their ability to differentiate and thus simulate real colon tissue *in vitro*, a characteristic that has made HT-29 useful for epithelial cell research. The cells can also be tested *in vivo via* xenografts with rodents.
in vitro	studies are performed with microorganisms, cells, or biological molecules outside their normal biological context.
in vivo	are those in which the effects of various biological entities are tested on whole, living organisms or cells, usually animals, including humans, and plants, as opposed to a tissue extract or dead organism.

IP Intraperitoneal injection is the injection of a substance into the peritoneum (body cavity).

KB cells are positive for keratin by immunoperoxidase staining. KB cells have been reported to contain human papillomavirus18 (HPV-18) sequences. They are subline of HeLa.

MCSs Spherical aggregates of malignant cells, i.e. multicellular tumour spheroids, may serve as *in vitro* models of tumour micro regions and of an early, avascular stage of tumour growth. The similarities between the original tumour and the respective spheroids include volume growth kinetics, cellular heterogeneity, e.g. the induction of proliferation gradients and quiescence, as well as differentiation characteristics, such as the development of specific histological structures or the expression of antigens.

MDCK Madin-Darby Canine Kidney Epithelial Cells derived by S. H. Madin and N. B. Darby from the kidney tissue of an adult female cocker spaniel.

MDCK-MDR1 cells originate from transfection of MDCK cells with the MDR1 gene, the gene encoding for the efflux protein, P-glycoprotein (P-gp)[2]. It has been found to be a useful predictor of blood brain barrier permeability.

MTT assay is a colourimetric assay for assessing cell metabolic activity. NAD(P)H-dependent cellular oxidoreductase enzymes may, under defined conditions, reflect the number of viable cells present.

MRC-5 MRC-5 (Medical Research Council cell strain 5) is a diploid human cell culture line composed of fibroblasts derived from lung tissue of a 14 week old aborted caucasian male fetus.

NMRI mice are Swiss-type mouse inbred line transferred to the Naval Medical Research Institute. They are used as general purpose model in toxicology, teratology, pharmacology (especially in psychopharmacology for behavioural studies) and physiology.

PAMPA parallel artificial membrane permeability assay is a method which determines the permeability of substances from a donor compartment, through a lipid-infused artificial membrane into an acceptor compartment.

SCID is a severe combined immunodeficiency genetic disorder that is characterized by the complete inability of the adaptive immune system to mount, coordinate, and sustain an appropriate immune response, usually due to absent or atypical T and B lymphocytes.

APPENDIX THREE

LITERATURE

[1] Nekvinda, J. Charles University in Prague, 2012.

[2] Grimes, R. N. Academic Press Publications (Elsevier, Inc.): London- Amsterdam- Burlington- San Diego- Oxford, 2011.

[3] Fox, M. A.; Goeta, A. E.; Hughes, A. K.; Johnson, A. L. *J. Chem. Soc. Dalt. Trans.* **2002**, *11* (10), 2132–2141.

[4] Hawthorne, M. F.; Dunks, G. B. *Science (80-.).* **1972**, *178* (4060), 462–471.

[5] Grüner, B.; Švec, P.; Šícha, V.; Padělková, Z. *Dalt. Trans.* **2012**, *41* (25), 7498.

[6] Nekvinda, J.; Švehla, J.; Císařová, I.; Grüner, B. *J. Organomet. Chem.* **2015**, *798*, 112–120.

[7] Grüner, B.; Šícha, V.; Hnyk, D.; Londesborough, M. G. S.; Císařová, I. *Inorg. Chem.* **2015**, *54* (7), 3148–3158.

[8] Janczak, S.; Olejniczak, A.; Balabańska, S.; Chmielewski, M. K.; Lupu, M.; Viñas, C.; Lesnikowski, Z. J. *Chem. - A Eur. J.* **2015**, *21* (43), 15118–15122.

[9] Nekvinda, J.; Šícha, V.; Hnyk, D.; Grüner, B. *Dalt. Trans.* **2014**, *43* (13), 5106.

[10] Brozek, E. M.; Mollard, A. H.; Zharov, I. *J. Nanoparticle Res.* **2014**, *16* (5).

[11] Plesek, J. *Chem. Rev.* **1992**, *92* (2), 269–278.

[12] Grimes, R. N. *J. Chem. Educ.* **2004**, *81* (5), 657.

[13] Olejniczak, A. B.; Mucha, P.; Gru, B.; Lesnikowski, Z. J. *Organometallics* **2007**, *26* (12), 3272–3274.

[14] Yang, W.; Barth, R. F.; Rotaru, J. H.; Moeschberger, M. L.; Joel, D. D.; Nawrocky, M. M.; Goodman, J. H.; Soloway, A. H. *Int. J. Radiat. Oncol.* **1997**, *37* (3), 663–672.

[15] Tjarks, W.; Barth, R. F.; Rotaru, J. H.; Adams, D. M.; Yang, W.; Kultyshev, R. G.; Forrester, J.; Barnum, B. A.; Soloway, A. H.; Shore, S. G. *Anticancer Res.* **2001**, *21* (2 A), 841–846.

[16] Soloway, A. H.; Barth, R. F.; Gahbauer, R. A.; Blue, T. E.; Goodman, J. H. *J. Neuro-Oncol.* **1997**, *33* (1–2), 9–18.

[17] Białek-Pietras, M.; Olejniczak, A. B.; Tachikawa, S.; Nakamura, H.; Leśnikowski, Z. J. *Bioorganic Med. Chem.* **2013**, *21* (5), 1136–1142.

[18] Valliant, J. F.; Guenther, K. J.; King, A. S.; Morel, P.; Schaffer, P.; Sogbein, O. O.; Stephenson, K. A. *Coord. Chem. Rev.* **2002**, *232* (1–2), 173–230.

[19] Scholz, M.; Hey-Hawkins, E. *Chem. Rev.* **2011**, *111* (11), 7035–7062.

[20] Issa, F.; Kassiou, M.; Rendina, M. *Chem. Rev.* **2011**, *111*, 5701–5722.

[21] Satapathy, R.; Dash, B. P.; Maguire, J. A.; Hosmane, N. S. *Collect. Czechoslov. Chem. Commun.* **2010**, *75* (9), 995–1022.

[22] Leśnikowski, Z. J. *J. Med. Chem.* **2016**, *59* (17), 7738–7758.

[23] Hall, I. H.; Durham, R. W.; Tram, M.; Mueller, S.; Ramachandran, B. M.; Sneddon, L. G. *J. Inorg. Biochem.* **2003**, *93*, 125.

[24] Hall, I. H.; Lackey, C. B.; Kistler, T. D.; Durham, R. W.; Monte Russell, J.; Grimes, R. N. *Anticancer Res.* **2000**, *20* (4), 2345–2354.

[25] Hall, I. H.; Tolmie, C. E.; Barnes, B. J.; Curtis, M. A.; Russell, J. Monte; Finn, M. G.; Grimes, R. N. *Appl. Organomet. Chem.* **2000**, *14* (2), 108–118.

[26] Cígler, P.; Kožíšekek, M.; Řezáčová, P.; Brynda, J.; Otwinowski, Z.; Pokorna, J.; Plešek, J.; Grüner, B.; Dolečková-Marešová, L.; Máša, M.; et al. *Proc. Natl. Acad. Sci.* **2005**, *102* (43), 15394–15399.

[27] Kožíšek, M.; Cígler, P.; Lepšík, M.; Fanfrlík, J.; Řezáčová, P.; Brynda, J.; Pokorná, J.; Plešek, J.; Grüner, B.; Šašková, K. G.; et al. *J. Med. Chem.* **2008**, *51* (15), 4839–4843.

[28] Popova, T.; Zaulet, A.; Teixidor, F.; Alexandrova, R.; Viñas, C. *J. Organomet. Chem.* **2013**, *747*, 229–234.

[29] Kvasničková, E.; Mašák, J.; Čejka, J.; Maťátková, O.; Šícha, V. *J. Organomet. Chem.* **2017**, *827*, 23–31.

[30] Bakardjiev, M.; Holub, J.; Tok, O. L.; Štíbr, B.; Hnyk, D.; Nekvinda, J.; Růžičková, Z.; Růžička, A. *J. Organomet. Chem.* **2016**, *822*, 80–84.

[31] Perekalin, D. S.; Holub, J.; Golovanov, D. G.; Lyssenko, K. A.; Petrovskii, P. V.; Štíbr, B.; Kudinov, A. R. *Organometallics* **2005**, *24* (18), 4387–4392.

[32] Holub, J.; Gruner, B.; Cisarova, I.; Fusek, J.; Plzak, Z.; Teixidor, F.; Vinas, C.; Stibr, B. *Inorg. Chem.* **1999**, *38* (12), 2775–2780.

[33] Grüner, B.; Štíbr, B.; Holub, J.; Císařová, I. *Eur. J. Inorg. Chem.* **2003**, No. 8, 1533–1539.

[34] Bakardjiev, M.; Štíbr, B.; Holub, J.; Padělková, Z.; Ruìšžička, A. *Inorg. Chem.* **2013**, *52* (15), 9087–9093.

[35] Štíbr, B.; Holub, J.; Plešek, J.; Jelínek, T.; Grüner, B.; Teixidor, F.; Viñas, C. *J. Organomet. Chem.* **1999**, *582* (2), 282–285.

[36] Štíbr, B.; Bakardjiev, M.; Holub, J.; Růžička, A.; Padělková, Z.; Olejník, R.; Švec, P. *Chem. - A Eur. J.* **2011**, *17* (47), 13156–13159.

[37] Štíbr, B.; Janoušek, Z.; Jelínek, T.; Heřmánek, S. *Collect. Czechoslov. Chem. Commun.* **987**, No. 52, 103.

[38] Holub, J.; Štíbr, B.; Hnyk, D.; Fusek, J.; Císařová, I.; Teixidor, F.; Viňas, C.; Plzak, Z.; Schleyer, P. v. R. *J. Am. Chem. Soc.* **1997**, No. 119, 7750.

[39] Štíbr, B. *J. Organomet. Chem.* **2005**, No. 690, 2694.

[40] Bakardjiev, M.; Holub, J.; Hnyk, D.; Císařová, I.; Londesborough, M. G. S.; Perekalin, D. S.; Štíbr, B. *Angew. Chemie - Int. Ed.* **2005**, *44* (38), 6222–6226.

[41] Hewett-Emmett, D.; Tashian, R. E. *Mol. Phylogenet. Evol.* **1996**, *5* (1), 50–77.

[42] Nishimori, I.; Minakuchi, T.; Onishi, S.; Vullo, D.; Cecchi, A.; Scozzafava, A.; Supuran, C. T. *J. Enzyme Inhib. Med. Chem.* **2009**, *24* (1), 70–76.

[43] Boone, C. D.; Habibzadegan, A.; Gill, S.; Mckenna, R. *Biomolecules* **2013**, *3* (3), 553–562.

[44] Forster, R. E. In *The Carbonic Anhydrases*; Birkhäuser Basel: Basel, 2000; pp 1–11.

[45] Smith, K. S.; Ferry, J. G. *FEMS Microbiol. Rev.* **2000**, *24* (4), 335–366.

[46] Supuran, C. T.; Scozzafava, A.; Casini, A. *Med. Res. Rev.* **2003**, *23* (2), 146–189.

[47] Keller, H. CRC Press, 2004; Vol. 9.

[48] Scozzafava, A.; Mastrolorenzo, A.; Supuran, C. T. *Expert Opin. Ther. Pat.* **2006**, *16* (12), 1627–1664.

[49] Supuran, C. T. *Nat. Rev. Drug Discov.* **2008**, *7* (2), 168–181.

[50] McKenna, R. *J. Am. Chem. Soc.* **2005**, *127* (10), 3643–3643.

[51] Vullo, D.; Voipio, J.; Innocenti, A.; Rivera, C.; Ranki, H.; Scozzafava, A.; Kaila, K.; Supuran, C. T. *Bioorganic Med. Chem. Lett.* **2005**, *15* (4), 971–976.

[52] Nishimori, I.; Minakuchi, T.; Onishi, S.; Vullo, D.; Scozzafava, A.; Supuran, C. T. *J. Med. Chem.* **2007**, *50* (2), 381–388.

[53] Vullo, D.; Franchi, M.; Gallori, E.; Antel, J.; Scozzafava, A.; Supuran, C. T. *J. Med. Chem.* **2004**, *47* (5), 1272–1279.

[54] Maren, T. H. *Physiol. Rev.* **1967**, *47* (4), 595–781.

[55] Scozzafava, A.; Briganti, F.; Ilies, M. A.; Supuran, C. T. *J. Med. Chem.* **2000**, *43* (2), 292–300.

[56] Supuran, C. T.; Scozzafava, A.; Ilies, M. A.; Briganti, F. *J. Enzyme Inhib.* **2000**, *15* (4), 381–401.

[57] Supuran, C. T.; Scozzafava, A.; Casini, A. *Med. Res. Rev.* **2003**, *23* (2), 146–189.

[58] Keller, H. Supuran, C. T., Scozzafava, A., Conway, J., Eds.; CRC Boca Raton, 2004; Vol. 9.

[59] Maxwell, P. H.; Wlesener, M. S.; Chang, G. W.; Clifford, S. C.; Vaux, E. C.; Cockman, M. E.; Wykoff, C. C.; Pugh, C. W.; Maher, E. R.; Ratcliffe, P. J. *Nature* **1999**, *399* (6733), 271–275.

[60] Semenza, G. *Cancer Metastasis Rev.* **2007**, *26* (2), 223–224.

[61] Thiry, A.; Dogné, J. M.; Masereel, B.; Supuran, C. T. *Trends Pharmacol. Sci.* **2006**, *27* (11), 566–573.

[62] Ratcliffe, P. J.; Pugh, C. W.; Maxwell, P. H. *Nat. Med.* **2000**, *6* (12), 1315–1316.

[63] Trastour, C.; Benizri, E.; Ettore, F.; Ramaioli, A.; Chamorey, E.; Pouysségur, J.; Berra, E. *Int. J. Cancer* **2007**, *120* (7), 1451–1458.

[64] Ord, J. J. et al. *J Urol* **2007**, No. 178, 677–682.

[65] Hutchison, G. J.; Valentine, H. R.; Loncaster, J. A.; Davidson, S. E.; Hunter, R. D.; Roberts, S. A.; Harris, A. L.; Stratford, I. J.; Price, P. M.; West, C. M. L. *Clin. Cancer Res.* **2004**, *10* (24), 8405 LP-8412.

[66] Koukourakis, M. I.; Giatromanolaki, A.; Sivridis, E.; Pastorek, J.; Karapantzos, I.; Gatter, K. C.; Harris, A. L. *Int. J. Radiat. Oncol. Biol. Phys.* **2004**, *59* (1), 67–71.

[67] Potter, C. P. S.; Harris, A. L. *Br. J. Cancer* **2003**, *89* (1), 2–7.

[68] Swinson, D. E. B.; Jones, J. L.; Richardson, D.; Wykoff, C.; Turley, H.; Pastorek, J.; Taub, N.; Harris, A. L.; O'Byrne, K. J. *J. Clin. Oncol.* **2003**, *21* (3), 473–482.

[69] Dorai, T.; Sawczuk, I.; Pastorek, J.; Wiernik, P. H.; Dutcher, J. P. *Cancer Invest.* **2006**, *24* (8), 754–779.

[70] Di Fiore, A.; Pedone, C.; D'Ambrosio, K.; Scozzafava, A.; De Simone, G.; Supuran, C. T. *Bioorganic Med. Chem. Lett.* **2006**, *16* (2), 437–442.

[71] Švastová, E.; Hulíková, A.; Rafajová, M.; Zat'Ovičová, M.; Gibadulinová, A.; Casini, A.; Cecchi, A.; Scozzafava, A.; Supuran, C. T.; Pastorek, J.; et al. *FEBS Lett.* **2004**, *577* (3), 439–445.

[72] Cecchi, A.; Hulikova, A.; Pastorek, J.; Pastoreková, S.; Scozzafava, A.; Winum, J. Y.; Montero, J. L.; Supuran, C. T. *J. Med. Chem.* **2005**, *48* (15), 4834–4841.

[73] Pastorekova, S.; Casini, A.; Scozzafava, A.; Vullo, D.; Pastorek, J.; Supuran, C. T. *Bioorganic Med. Chem. Lett.* **2004**, *14* (4), 869–873.

[74] Supuran, C. T.; Casini, A.; Mastrolorenzo, A.; Scozzafava, A. *Mini Rev. Med. Chem.* **2004**, *4* (6), 625–632.

[75] Garaj, V.; Puccetti, L.; Fasolis, G.; Winum, J. Y.; Montero, J. L.; Scozzafava, A.; Vullo, D.; Innocenti, A.; Supuran, C. T. *Bioorganic Med. Chem. Lett.* **2004**, *14* (21), 5427–5433.

[76] Cecchi, A.; Winum, J. Y.; Innocenti, A.; Vullo, D.; Montero, J. L.; Scozzafava, A.; Supuran, C. T. *Bioorganic Med. Chem. Lett.* **2004**, *14* (23), 5775–5780.

[77] Winum, J.; Innocenti, A.; Nasr, J.; Montero, J.; Scozzafava, A.; Vullo, D.; Supuran, C. Carbonic anhydrase inhibitors: synthesis and inhibition of cytosolic/tumor-associated

carbonic anhydrase isozymes I, II, IX, and XII with N-hydroxys https://www.ncbi.nlm.nih.gov/m/pubmed/15837324/ (accessed Apr 1, 2018).

[78] Winum, J. Y.; Cecchi, A.; Montero, J. L.; Innocenti, A.; Scozzafava, A.; Supuran, C. T. *Bioorganic Med. Chem. Lett.* **2005**, *15* (13), 3302–3306.

[79] Wilkinson, B. L.; Bornaghi, L. F.; Houston, T. A.; Innocenti, A.; Vullo, D.; Supuran, C. T.; Poulsen, S. A. *J. Med. Chem.* **2007**, *50* (7), 1651–1657.

[80] Dubois, L.; Douma, K.; Supuran, C. T.; Chiu, R. K.; van Zandvoort, M. A. M. J.; Pastoreková, S.; Scozzafava, A.; Wouters, B. G.; Lambin, P. *Radiother. Oncol.* **2007**, *83* (3), 367–373.

[81] De Simone, G.; Vitale, R. M.; Di Fiore, A.; Pedone, C.; Scozzafava, A.; Montero, J. L.; Winum, J. Y.; Supuran, C. T. *J. Med. Chem.* **2006**, *49* (18), 5544–5551.

[82] Saczewski, F.; Sławiński, J.; Kornicka, A.; Brzozowski, Z.; Pomarnacka, E.; Innocenti, A.; Scozzafava, A.; Supuran, C. T. *Bioorganic Med. Chem. Lett.* **2006**, *16* (18), 4846–4851.

[83] Abbate, F.; Casini, A.; Owa, T.; Scozzafava, A.; Supuran, C. T. *Bioorganic Med. Chem. Lett.* **2004**, *14* (1), 217–223.

[84] Talbot, D. C. et al. American Association for Cancer Research, 2007; Vol. 13.

[85] Ilies, M.; Supuran, C. T.; Scozzafava, A.; Casini, A.; Mincione, F.; Menabuoni, L.; Caproiu, M. T.; Maganu, M.; Banciu, M. D. *Bioorganic Med. Chem.* **2000**, *8* (8), 2145–2155.

[86] Scozzafava, A.; Menabuoni, L.; Mincione, F.; Supuran, C. T. *J. Med. Chem.* **2002**, *45* (7), 1466–1476.

[87] Pinard, M. A.; Boone, C. D.; Rife, B. D.; Supuran, C. T.; McKenna, R. *Bioorganic Med. Chem.* **2013**, *21* (22), 7210–7215.

[88] Supuran, C. T. *J. Enzyme Inhib. Med. Chem.* **2012**, *27* (6), 759–772.

[89] Lesnikowski, Z. J. *Collect. Czechoslov. Chem. Commun.* **2007**, *72* (12), 1646–1658.

[90] Grimes, R. N. Academic Press, 2011.

[91] Endo, Y.; Iijima, T.; Yamakoshi, Y.; Fukasawa, H.; Miyaura, C.; Inada, M.; Kubo, A.; Itai, A. *Chem. Biol.* **2001**, *8* (4), 341–355.

[92] Brynda, J.; Mader, P.; Šícha, V.; Fábry, M.; Poncová, K.; Bakardiev, M.; Grüner, B.; Cígler, P.; Řezáčová, P. *Angew. Chemie - Int. Ed.* **2013**, *52* (51), 13760–13763.

[93] Mader, P.; Brynda, J.; Gitto, R.; Agnello, S.; Pachl, P.; Supuran, C. T.; Chimirri, A.; Řezáčová, P. *J. Med. Chem.* **2011**, *54* (7), 2522–2526.

[94] Krishnamurthy, V. M.; Kaufman, G. K.; Urbach, A. R.; Gitlin, I.; Gudiksen, K. L.;

Weibel, D. B.; Whitesides, G. M. *Chem. Rev.* **2008**, *108* (3), 946–1051.

[95] Richards, A. D.; Rodger, A. *Chem. Soc. Rev.* **2007**, *36* (3), 471–483.

[96] Jenkins, T. C. *Curr. Med. Chem.* **2000**, *7* (1), 99–115.

[97] Lerman, L. S. *J. Mol. Biol.* **1961**, *3* (1), IN13-IN14.

[98] Becker, H. C.; Nordén, B. *J. Am. Chem. Soc.* **2000**, *122* (35), 8344–8349.

[99] Brana, M. F.; Ramos, A. *Curr. Med. Chem. Agents* **2001**, *1* (3), 237–255.

[100] Berman, H. M.; Young, P. R. *Annu. Rev. Biophys. Bioeng.* **1981**, *10* (1), 87–114.

[101] Martinez, R.; Chacon-Garcia, L. *Curr. Med. Chem.* **2005**, *12* (2), 127–151.

[102] Cholody, W. M.; Kosakowska-Cholody, T.; Hollingshead, M. G.; Hariprakasha, H. K.; Michejda, C. J. *J. Med. Chem.* **2005**, *48* (13), 4474–4481.

[103] De Isabella, P.; Zunino, F.; Capranico, G. *Nucleic Acids Res.* **1995**, *23* (2), 223–229.

[104] Quigley, G. J.; Wang, a H.; Ughetto, G.; van der Marel, G.; van Boom, J. H.; Rich, A. *Proc Natl Acad Sci U S A.* **1980**, *77* (12), 7204–8.

[105] Yu, H.-H.; Kim, K.-J.; Cha, J.-D.; Kim, H.-K.; Lee, Y.-E.; Choi, N.-Y.; You, Y.-O. *J. Med. Food* **2005**, *8* (4), 254–461.

[106] Jain, S. C.; Bhandary, K. K.; Sobell, H. M. *J. Mol. Biol.* **1979**, *135* (4), 813–840.

[107] Li, X.; Lin, Y.; Wang, Q.; Yuan, Y.; Zhang, H.; Qian, X. *Eur. J. Med. Chem.* **2011**, *46* (4), 1274–1279.

[108] Chanh, T. C.; Lewis, D. E.; Judy, M. M.; Sogandares-Bernal, F.; Michalek, G. R.; Utecht, R. E.; Skiles, H.; Chang, S. C.; Matthews, J. L. *Antivir. Res* **1994**, *25*, 133–146.

[109] Andricopulo, A. D.; Müller, L. A.; Cechinel Filho, V.; Cani, G. S.; Roos, J. F.; Corrêa, R.; Santos, A. R. S.; Nunes, R. J.; Yunes, R. A. *Farmaco* **2000**, *55* (4), 319–321.

[110] da Settimo, A.; Primofiore, G.; Ferrarini, P. L.; Ferretti, M.; Barili, P. L.; Tellini, N.; Bianchini, P. *Eur. J. Med. Chem.* **1989**, *24* (3), 263–270.

[111] Lv, M.; Xu, H. *Curr. Med. Chem.* **2009**, *16*, 4797–4813.

[112] Ingrassia, L.; Lefranc, F.; Kiss, R.; Mijatovic, T. *Curr. Med. Chem.* **2009**, *16* (10), 1192–1213.

[113] Banerjee, S.; Veale, E. B.; Phelan, C. M.; Murphy, S. A.; Tocci, G. M.; Gillespie, L. J.; Frimannsson, D. O.; Kelly, J. M.; Gunnlaugsson, T. *Chem. Soc. Rev.* **2013**, *42* (4), 1601.

[114] Kamal, A.; Bolla, N. R.; Srikanth, P. S.; Srivastava, A. K. *Expert Opin. Ther. Pat.* **2013**, *23* (3), 299–317.

[115] Braña, M. F.; Sanz, A. M.; Castellano, J. M.; Roldan, M. C.; Roldan, C. *Eur. J. Med. Chem.* **1981**, *16*, 207–212.

[116] Braña, M. F.; Castellano, J. M.; Moran, M.; de Vega, M. J. P.; Perron, D.; Conlon, D.;

Bousquet, P. F.; Romerdahl, C. A.; Robinson, S. P. *Anti-cancer Drug Des* **1996**, *11*, 297–309.

117 Johnson, C. A.; Hudson, G. A.; Hardebeck, L. K. E.; Jolley, E. A.; Ren, Y.; Lewis, M.; Znosko, B. M. *Bioorganic Med. Chem.* **2015**, *23* (13), 3586–3591.

118 Duke, R. M.; Veale, E. B.; Pfeffer, F. M.; Kruger, P. E.; Gunnlaugsson, T. *Chem. Soc. Rev.* **2010**, *39* (10), 3936.

119 Silvers, W. C.; Prasai, B.; Burk, D. H.; Brown, M. L.; McCarley, R. L. *J. Am. Chem. Soc.* **2013**, *135* (1), 309–314.

120 Long, E. C.; Barton, J. K. *Acc. Chem. Res.* **1990**, *23* (9), 271–273.

121 Xie, L.; Xu, Y.; Wang, F.; Liu, J.; Qian, X.; Cui, J. *Bioorganic Med. Chem.* **2009**, *17* (2), 804–810.

122 Villers, M. A. *Comptes Rendus L Acad. Des Sci. Ser. Ii Fasc. C-Chimie* **1891**, *112*, 536–537.

123 Loftsson, T.; Másson, M.; Brewster, M. E. *J. Pharm. Sci.* **2004**, *93* (5), 1091–1099.

124 Loftsson, T.; Brewster, M. E. *J Pharm Sci* **1996**, *85*, 1017–1025.

125 Buvári-Barcza, Á.; Rohonczy, J.; Rozlosnik, N.; Gilányi, T.; Szabó, B.; Lovas, G.; Braun, T.; Samu, J.; Barcza, L. *J. Chem. Soc. Perkin Trans. 2* **2001**, *0* (2), 191–196.

126 Hedges, A. R. *Chem. Rev.* **1998**, *98* (5), 2035–2044.

127 Additives, F. *World Health Organ. Tech. Rep. Ser.* **1974**, *669* (952), 1–145, back cover.

128 French, D. *Adv. Carbohydr. Chem.* **1957**, *12*, 189–260.

129 Loftsson, T.; Jarho, P.; Másson, M.; Järvinen, T.; Publications, A. *Expert Opin. Drug Deliv. Expert Opin. Drug Deliv* **2005**, *2* (22), 335–351.

130 Frömming, K.-H.; Szejtli, J. Kluwer Academic, 1993; Vol. 30.

131 Szejtli, J. Kluwer Academic, 2013; Vol. 53.

132 Thompson, D. O. *Crit. Rev. Ther. Drug Carrier Syst.* **1997**, *14* (1), 1.

133 Uekama, K. *Chem. Pharm. Bull. (Tokyo).* **2004**, *52* (8), 900–915.

134 Lipinski, C. A.; Lombardo, F.; Dominy, B. W.; Feeney, P. J. *Adv. Drug Deliv. Rev.* **2012**, *64* (SUPPL.), 4–17.

135 Irie, T.; Uekama, K. *J. Pharm. Sci.* **1997**, *86* (2), 147–162.

136 Matsuda, H.; Arima, H. *Adv. Drug Deliv. Rev.* **1999**, *36* (1), 81–99.

137 Uekama, K.; Hirayama, F.; Irie, T. *Chem. Rev.* **1998**, *98* (5), 2045–2076.

138 Marttin, E.; Verhoef, J. C.; Merklus, F. W. H. M. *J. Drug Target.* **1998**, *6* (1), 17–36.

139 Loftsson, T.; Masson, M. *Int. J. Pharm.* **2001**, *225* (1–2), 15–30.

140 Rak, J.; Dejlová, B.; Lampová, H.; Kaplánek, R.; Matějíček, P.; Cígler, P.; Král, V. *Mol.*

Pharm. **2013**, *10* (5), 1751–1759.

[141] Rak, J.; Jakubek, M.; Kaplánek, R.; Matějíček, P.; Král, V. *Eur. J. Med. Chem.* **2011**, *46* (4), 1140–1146.

[142] Loftsson, T.; Brewster, M. E. *J. Pharm. Sci.* **1996**, *85* (10), 1017–1025.

[143] Hirose, K. *J. Incl. Phenom. Macro.* 2001, pp 193–209.

[144] Hiryama, F.; Uekama, K. Duchene, D., Ed.; Editions de Santé, 1987.

[145] LOFTSSON, T.; MÁSSON, M.; BREWSTER, M. E. *J. Pharm. Sci.* **2004**, *93* (5), 1091–1099.

[146] Popielec, A.; Fenyvesi; Yannakopoulou, K.; Lofton, T. *Pharmazie* **2016**, *71* (2), 68–75.

[147] Challa, R.; Ahuja, A.; Ali, J.; Khar, R. K. *AAPS PharmSciTech* **2005**, *6* (2), E329–E357.

[148] Schibilla, F.; Voskuhl, J.; Fokina, N. A.; Dahl, J. E. P.; Schreiner, P. R.; Ravoo, B. J. *Chem. - A Eur. J.* **2017**, *23* (63), 16059–16065.

[149] Voskuhl, J.; Waller, M.; Bandaru, S.; Tkachenko, B. A.; Fregonese, C.; Wibbeling, B.; Schreiner, P. R.; Ravoo, B. J. *Org. Biomol. Chem.* **2012**, *10* (23), 4524.

[150] Cromwell, W. C.; Byström, K.; Eftink, M. R. *J. Phys. Chem.* **1985**, *89* (2), 326–332.

[151] Assaf, K. I.; Gabel, D.; Zimmermann, W.; Nau, W. M. *Org. Biomol. Chem.* **2016**, *14* (32), 7702–7706.

[152] Assaf, K. I.; Ural, M. S.; Pan, F.; Georgiev, T.; Simova, S.; Rissanen, K.; Gabel, D.; Nau, W. M. *Angew. Chemie - Int. Ed.* **2015**, *54* (23), 6852–6856.

[153] Rak, J.; Cigler, P.; Kral, V. *Chemi. List.* **2008**, *102*, 209–212.

[154] Matějíček, P.; Cígler, P.; Procházka, K.; Král, V. *Langmuir* **2006**, *22* (2), 575–581.

[155] Uchman, M.; ɯormǫovič, V.; Tošner, Z.; Matějíček, P. *Angew. Chemie - Int. Ed.* **2015**, *54* (47), 14113–14117.

[156] Rak, J.; Kaplánek, R.; Král, V. *Bioorganic Med. Chem. Lett.* **2010**, *20* (3), 1045–1048.

[157] Goszczyński, T. M.; Fink, K.; Kowalski, K.; Leśnikowski, Z. J.; Boratyński, J. *Sci. Rep.* **2017**, *7* (1), 9800.

[158] Sadrerafi, K.; Moore, E. E.; Lee, M. W. *J. Incl. Phenom. Macrocycl. Chem.* **2015**, *83* (1–2), 159–166.

[159] Vaitkus, R.; Sjöberg, S. *J. Incl. Phenom. Macrocycl. Chem.* **2011**, *69* (3–4), 393–395.

[160] Neirynck, P.; Schimer, J.; Jonkheijm, P.; Milroy, L.-G.; Cigler, P.; Brunsveld, L. *J. Mater. Chem. B* **2015**, *3* (4), 539–545.

[161] Carey, F. A.; Sundberg, R. J. 5th ed.; Springer: New York, 2002.

[162] Olshevskaya, V. A.; Dutikova, Y. V.; Tyutyunov, A. A.; Kononova, E. G.; Petrovskii, P. V.; Sung, D. D.; Kalinin, V. N. *Synlett* **2010**, *2010* (8), 1265–1267.

[163] Grüner, B.; Šícha, V.; Hnyk, D.; Londesborough, M. G. S.; Císařová, I. *Inorg. Chem.* **2015**, *54* (7), 3148–3158.

[164] Grüner, B.; Šícha, V.; Nekvinda, J.; Pospíšilová, K.; Fábry, M.; Pachl, P.; Král, V.; Kugler, M.; Das, V.; Mašek, V.; et al. **2018**.

[165] Holub, J.; Šícha, V.; Nekvinda, J.; Cígler, P.; Pospíšilová, K.; Fábry, M.; Pachl, P.; Král, V.; Štěpánková, J.; Hajdůch, M.; et al. **2018**.

[166] Kalinin, V. N.; Rys, E. G.; Tyutyunov, a a; Starikova, Z. a; Korlyukov, a a; Ol'shevskaya, V. a; Sung, D. D.; Ponomaryov, a B.; Petrovskii, P. V; Hey-Hawkins, E. *Dalton Trans.* **2005**, *0* (5), 903–908.

[167] Sheldrick, G. M. *Acta Crystallogr. Sect. A Found. Crystallogr.* **2008**, *64* (1), 112–122.

[168] Burkard, U.; Effenberger, F. *Chem. Ber.* **1986**, *119* (5), 1594–1612.

[169] Benfodda, Z.; Guillen, F.; Arnion, H.; Dahmani, A.; Blancou, H. *Heteroat. Chem.* **2009**, *20* (6), 355–361.

[170] Suter, C. M. Wiley: New York, 1944.

[171] Tarasov, A. V.; Strikanova, O. N.; Moskvichev, Y. A.; Timoshenko, G. N. *Russ. J. Org. Chem.* **2002**, *38* (1), 87–89.

[172] Kolb, H. C.; Finn, M. G.; Sharpless, K. B. *Angew. Chemie - Int. Ed.* **2001**, *40* (11), 2004–2021.

[173] Rostovtsev, V. V; Green, L. G.; Fokin, V. V; Sharpless, K. B. *Angew. Chemie Int. Ed.* **2002**, *41* (14), 2596–2599.

[174] Couto, M.; Mastandrea, I.; Cabrera, M.; Cabral, P.; Teixidor, F.; Cerecetto, H.; Viñas, C. *Chem. - A Eur. J.* **2017**, *23* (39), 9233–9238.

[175] Matuszewski, M.; Kiliszek, A.; Rypniewski, W.; Lesnikowski, Z. J.; Olejniczak, A. B. *New J. Chem.* **2015**, *39* (2), 1202–1221.

[176] Nekvinda, J.; Holub, J.; Růžička, A.; Brynda, J.; Řezáčová, P.; Grüner, B. **2018**.

[177] Frederick Hawthorne, M. *Acc. Chem. Res.* **1968**, *1* (9), 281–288.

[178] Karioti, A.; Carta, F.; Supuran, C. T. *Curr. Pharm. Des.* **2016**, *22* (12), 1570–1591.

[179] Mader, P.; Pecina, A.; Cígler, P.; Lepšík, M.; Šícha, V.; Hobza, P.; Grüner, B. *Biomed Res. Int.* **2014**, *2014*.

[180] Winum, J. Y.; Scozzafava, A.; Montero, J. L.; Supuran, C. T. *Med. Res. Rev.* **2006**, *26* (6), 767–792.

[181] De Simone, G.; Langella, E.; Esposito, D.; Supuran, C. T.; Monti, S. M.; Winum, J. Y.; Alterio, V. *J. Enzyme Inhib. Med. Chem.* **2017**, *32* (1), 1002–1011.

[182] Di Fiore, A.; Monti, S. M.; Innocenti, A.; Winum, J. Y.; De Simone, G.; Supuran, C. T.

Bioorganic Med. Chem. Lett. **2010**, *20* (12), 3601–3605.

183 Yang, J.-S.; Lin, C.-W.; Hsieh, Y.-H.; Chien, M.-H.; Chuang, C.-Y.; Yang, S.-F. *Oncotarget* **2017**, *8* (47), 83088–83099.

184 Ji, T.; Lang, J.; Wang, J.; Cai, R.; Zhang, Y.; Qi, F.; Zhang, L.; Zhao, X.; Wu, W.; Hao, J.; et al. *ACS Nano* **2017**, *11* (9), 8668–8678.

185 Lou, Y.; McDonald, P. C.; Oloumi, A.; Chia, S.; Ostlund, C.; Ahmadi, A.; Kyle, A.; Auf Dem Keller, U.; Leung, S.; Huntsman, D.; et al. *Cancer Res.* **2011**, *71* (9), 3364–3376.

186 Fanfrlík, J.; Lepšík, M.; Hořínek, D.; Havlas, Z.; Hobza, P. *Phys. Chem. Chem. Phys.* **2006**, *7*, 1100–1105.

187 Pecina, A.; Lepšik, M.; Rezac, J.; Brynda, J.; Mader, P.; Řezáčová, P.; Hobza, P.; Fanfrlík, J. *J. Phys. Chem. B* **2013**, *117* (50), 16096–16104.

188 Fanfrlík, J.; Hnyk, D.; Lepšík, M.; Hobza, P. *Phys. Chem. Chem. Phys.* **2007**, *9* (17), 2085–2093.

189 Ghaneolhosseini, H.; Sjöberg, S. *Acta Chem. Scand.* **1999**, *53* (4), 298–300.

190 Plesek, J.; Hermanek, S.; Cisarova, I.; Plešek, J.; Heřmánek, S.; Franken, A.; Císařová, I.; Nachtigal, C. *Collect. Czechoslov. Chem. Commun.* **1997**, *62* (1), 47–56.

191 Lucarelli, F.; Marrazza, G.; Turner, A. P. F.; Mascini, M. *Biosens. Bioelectron.* **2004**, *19* (6), 515–530.

192 Ghirmai, S.; Malmquist, J.; Lundquist, H.; Tolmachev, V.; Sjöberg, S. *J. Label. Compd. Radiopharm.* **2004**, *47* (9), 557–569.

193 Plešek, J.; Heřmánek, S. *Chem. Ind.* **1971**, 1267.

194 Rietz, R. R.; Schaeffer, R. *J. Am. Chem. Soc.* **1971**, *93*, 1263.

195 Štíbr, B.; Plešek, J.; Heřmánek, S. *Collect. Czechoslov. Chem. Commun.* **1974**, *39* (7), 1805–1809.

196 Štíbr, B.; Bakardjiev, M.; Holub, J.; Růžička, A.; Padělková, Z.; Olejník, R.; Švec, P. *Chem. - A Eur. J.* **2011**, *17* (47), 13156–13159.

197 Churkina, L. A.; Zvereva, T. D.; Shingel, I. A.; Malashonok, L. I.; Ol'dekop, Y. A. *Vestsi Akad. Navuk BSSR, Ser. Khimichnykh Navuk* **1986**, No. 2, 59–64.

198 Gomez, F. A.; Hawthorne, M. F. *J. Org. Chem.* **1992**, *57* (5), 1384–1390.

199 Zakharkin, L. I.; Chapovskii, Y. A.; Brattsev, V. A.; Stanko, V. I. *Zhurnal Obs. Khimii* **1966**, *36* (5), 878–886.

200 Stanko, V. I.; Ovsyannikov, N. N.; Klimova, A. I.; Khrapov, V. V; Shmyrkov, L. G.; Garibov, R. E. *Zhurnal Obs. Khimii* **1976**, *46* (4), 871–878.

201 Nekvinda, J.; Gruner, B.; Gabel, D.; Nau, W. M.; Assaf, K. I. *Chem. - A Eur. J.* **2018**.

[202] Nau, W. M.; Florea, M.; Assaf, K. I. *Isr. J. Chem.* **2011**, *51* (5–6), 559–577.

[203] Assaf, K. I.; Nau, W. M. *Chem. Soc. Rev.* **2015**, *44* (2), 394–418.

[204] Assaf, K. I.; Nau, W. M. *Supramol. Chem.* **2014**, *26* (9), 657–669.

[205] Assaf, K. I.; Suckova, O.; Al Danaf, N.; Von Glasenapp, V.; Gabel, D.; Nau, W. M. *Org. Lett.* **2016**, *18* (5), 932–935.

[206] Ohta, K.; Konno, S.; Endo, Y. *Tetrahedron Lett.* **2008**, *49* (46), 6525–6528.

[207] Gabel, D. *Pure Appl. Chem.* **2015**, *87* (2), 173–179.

[208] Calvaresi, M.; Zerbetto, F. *J. Chem. Inf. Model.* **2011**, *51* (8), 1882–1896.

[209] Nekvinda, J.; Grüner, B.; Gabel, D.; Nau, W. M.; Assaf, K. I.; Gruner, B.; Gabel, D.; Nau, W. M.; Assaf, K. I. *Chem. - A Eur. J.* **2018**.

[210] Salmon, A. J.; Williams, M. L.; Wu, Q. K.; Morizzi, J.; Gregg, D.; Charman, S. A.; Vullo, D.; Supuran, C. T.; Poulsen, S. A. *J. Med. Chem.* **2012**, *55* (11), 5506–5517.

[211] Nekvinda, J.; Rózycka, D.; Rykowski, S.; Wyszko, E.; Gurda, D.; Orlicka-Plocka, M.; Wojcieszak, J.; Kiliszek, A.; Rypniewski, W.; Bachorz, R.; et al. **2018**.

[212] Shriver, D. F.; Drezdzon, M. A. John Wiley & Sons, 1986.

[213] Grűner, B.; Plzak, Z. *J Chromatogr A* **1997**, *789* (1), 497.

[214] Otwinowski, Z.; Minor, W. *Methods Enzymol.* **1997**, *276*, 307–326.

[215] Coppens, P. *Crystallogr. Comput. Copenhagen* **1970**, 255–270.

[216] Altomare, A.; Cascarano, G.; Giacovazzo, C.; Guagliardi, A. *J. Appl. Crystallogr.* **1993**, *26* (pt 3), 343–350.

[217] Sheldrick, G. M. *Göttingen, Ger.* **1997**.

[218] Pinard, M. A.; Boone, C. D.; Rife, B. D.; Supuran, C. T.; McKenna, R. *Bioorganic Med. Chem.* **2013**, *21* (22), 7210–7215.

[219] Alterio, V.; Hilvo, M.; Di Fiore, A.; Supuran, C. T.; Pan, P.; Parkkila, S.; Scaloni, A.; Pastorek, J.; Pastorekova, S.; Pedone, C. *Proc Natl Acad Sci USA* **2009**, *106* (38), 16233 LP-16238.

[220] Mueller, U.; Darowski, N.; Fuchs, M. R.; Förster, R.; Hellmig, M.; Paithankar, K. S.; Pühringer, S.; Steffien, M.; Zocher, G.; Weiss, M. S. *J. Synchrotron Radiat.* **2012**, *19* (3), 442–449.

[221] Kabsch, W. *Acta Crystallogr. Sect. D Biol. Crystallogr.* **2010**, *66* (2), 133–144.

[222] Kabsch, W. *Acta Crystallogr. Sect. D Biol. Crystallogr.* **2010**, *66* (2), 125–132.

[223] Vagin, A.; Teplyakov, A. *Acta Crystallogr. Sect. D Biol. Crystallogr.* **2000**, *56* (12), 1622–1624.

[224] Ahlrichs, R.; Bär, M.; Häser, M.; Horn, H.; Kölmel, C. *Chem. Phys. Lett.* **1989**, *162* (3),

165–169.

225 Jurečka, P.; Černý, J.; Hobza, P.; Salahub, D. R. *J. Comput. Chem.* **2007**, *28* (2), 555–569.

226 Emsley, P.; Lohkamp, B.; Scott, W. G.; Cowtan, K. *Acta Crystallogr. Sect. D Biol. Crystallogr.* **2010**, *66* (4), 486–501.

227 Murshudov, G. N.; Skubák, P.; Lebedev, A. A.; Pannu, N. S.; Steiner, R. A.; Nicholls, R. A.; Winn, M. D.; Long, F.; Vagin, A. A. *Acta Crystallogr. D. Biol. Crystallogr.* **2011**, *67* (Pt 4), 355–367.

228 Chen, V. B.; Arendall, W. B.; Headd, J. J.; Keedy, D. A.; Immormino, R. M.; Kapral, G. J.; Murray, L. W.; Richardson, J. S.; Richardson, D. C. *Acta Crystallogr. Sect. D Biol. Crystallogr.* **2010**, *66* (1), 12–21.

229 Leites, L. A. *Chem. Rev.* **1992**, *92* (2), 279–323.

230 Waters, N. J.; Jones, R.; Williams, G.; Sohal, B. *J. Pharm. Sci.* **2008**, *97* (10), 4586–4595.

231 Edwards, M.; Wong, S. C.; Chotpadiwetkul, R.; Smirlis, D.; Phillips, lan R.; Shephard, E. A. In *Methods in molecular biology (Clifton, N.J.)*; Springer, 2006; Vol. 320, pp 273–282.

232 Jitendra Kumar, S.; Anant, S.; Reema, C. M.; Debarupa, B.; Vikas, S. S. vitro 2012.

233 Wu, X.; Wang, J.; Tan, L.; Bui, J.; Gjerstad, E.; McMillan, K.; Zhang, W. *J. Biomol. Screen.* **2012**, *17* (6), 761–772.